Thesis for the Master's degree in chemistry

Sigurd Øien

Synthesis and characterization of modified UiO-67 metal-organic frameworks

60 study points

DEPARTMENT OF CHEMISTRY
Faculty of mathematics and natural sciences
UNIVERSITY OF OSLO 08/2012

Abstract

This thesis describes the synthesis and characterization of metal-bipyridyl complexes used as linkers in UiO-67, a metal-organic framework made up by zirconium oxide connectors and biphenyl linkers. The materials, functionalized with several different d-metals using three different synthesis strategies, have been characterized with various methods determine the local structure of the functionalization, as well as properties of the bulk material (see graphical abstract, Figure 1).

The term MOF will be used a lot in the thesis, and will generally refer to “porous metal organic framework”, even though high porosity is not strictly required of a material to be called a MOF.

The first part herein presents the motivation and theoretical foundations for this thesis, and a quick overview of the history of MOFs. In particular, the Zr-based UiO MOFs are described in detail. Brief theoretical overviews of the characterization methods are also given.

Part two describes the synthesis and characterization of several metal bipyridine complexes, which were later used as linkers in MOF synthesis, and the syntheses of the MOFs themselves. The syntheses were generally successful, sometimes after method improvement. MOF characterization procedures are also described in this section.

The third part gives an account of the results, and a discussion of these. It is shown that key features of UiO-67 such as crystallinity, stability and porosity are retained even with high loading of metal complexes, as is shown with PXRD, TGA and gas sorption measurements. The synthesis of UiO-67 with metal functionalization on bpy linkers must be chosen to fit the desired properties of the product. In metal modified UiO-67, adding a modulator is necessary for obtaining high porosity.

The position and chemical state of the dopant metals have been pinpointed using a combination of NMR and EXAFS. The results clearly show that the bonding between the framework and the metal complexes occurs as intended.

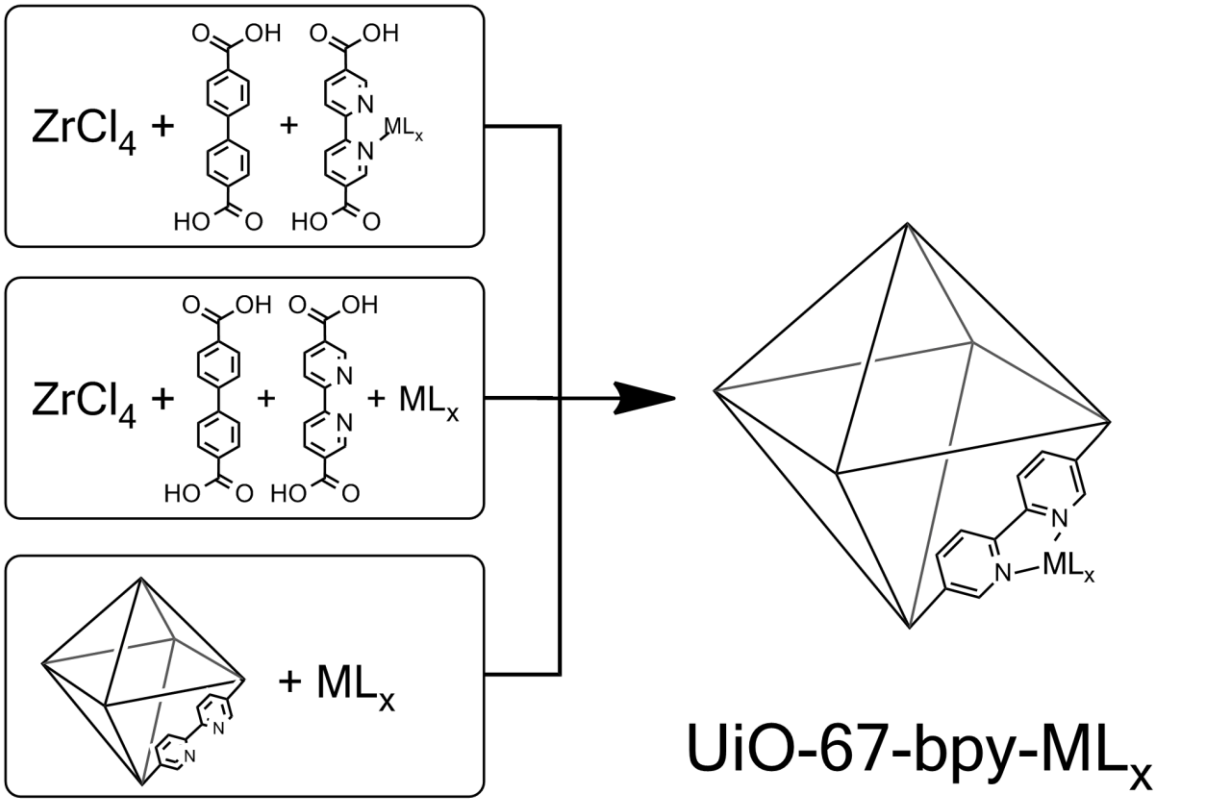

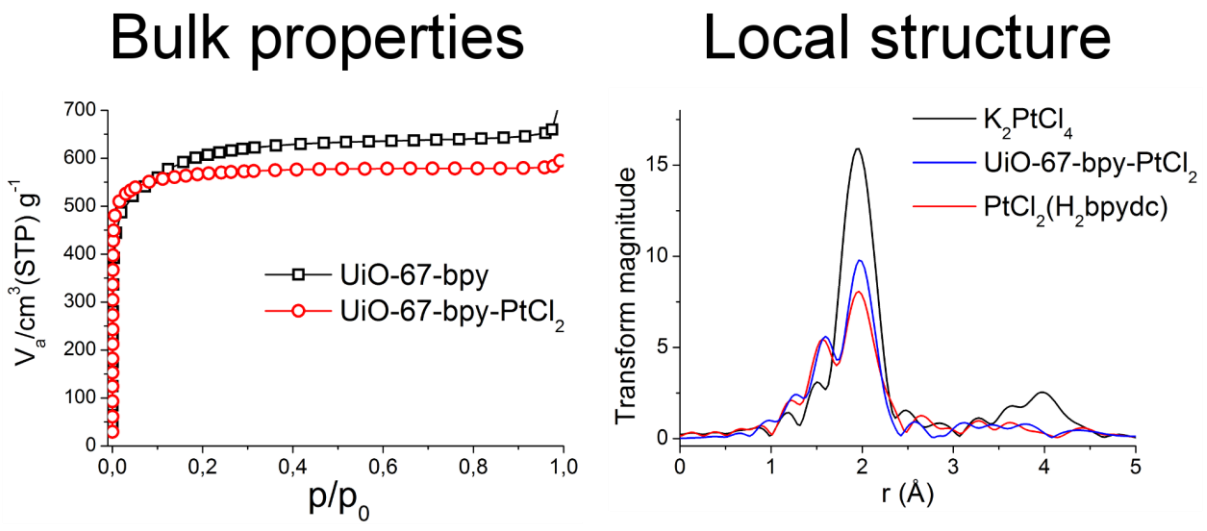

Figure 1. A brief graphical overview of this work, illustrating the three main synthesis procedures investigated (top section), and characterization techniques used to determine bulk properties and local structure of the material (bottom section). The results indicate that bulk properties such as porosity are intact (from adsorption isotherm, left), and the local structure of the functionalization is preserved in the synthesized materials (from EXAFS data, right).

Table of Contents

Foreword

The subject of my Master's thesis work became clear when I first saw the model of UiO-66, a zirconium based Metal-organic framework (MOF) named after the University of Oslo where it was discovered, and published in September 2008[1]. Solid state chemistry had always been a favorite subject, but I had never seen such a beautiful material; complex, but strictly ordered and symmetrical, connecting the realms of organic and inorganic chemistry. As Zhou, Yaghi and Long writes, "On a fundamental level, MOFs epitomize the beauty of chemical structures and the power of combining organic and inorganic chemistry, two disciplines often regarded as disparate."[2]

Recently discovered, MOFs also represent some of the most ground-breaking frontier work in chemistry. Like explorers uncovering unknown landscapes, MOF scientists deploy devious new synthesis and functionalization schemes, and a huge number of different characterization methods, in a race to push the frontiers ever forward. The transition from classroom student to researcher in the catalysis group happened instantaneously, assisted by eager supervisors.

Being a synthetic catalysis chemist, my main goal is to contribute to the development of a robust, versatile solid catalyst. In the solid state, catalyst recovery is easy, and the reusability of the catalyst is potentially energy saving. Due to the porosity and stability, UiO-66 and 67 have the qualities needed for a solid state catalyst. Much of my time in the catalysis group has been spent on large projects, involving several people at the time. Still, the work presented in this thesis is all done by me unless otherwise stated.

I would like to thank my brilliant supervisors, professors Karl Petter Lillerud and Mats Tilset. Both of whom show great passion for chemistry and always are available to an inquisitive student. While always interested in new ideas, they have also (kindly but firmly) pointed out when it was time to put down the spatula and start writing. I would also like to thank Professors Silvia Bordiga and Carlo Lamberti of The University of Torino for their astonishing hospitality during my stay in Torino the summer of 2011, and indispensable contribution to the EXAFS experiments in May, 2012.

Merete H. Nilsen, Søren Jakobsen and Fredrik Lundvall have been very important for this work by providing insight, experience and chemicals.

I'm very happy to have contributed to the research of the catalysis group!

Sigurd Øien

Oslo, September 26th 2012.

Abbreviations

BA:	Benzoic acid
BET:	Brauner, Emmet, Teller. Mathematical model for multilayer adsorption
BFMD:	Bravais, Friedel, Donnay, Harker. Mathematical model for crystal morphology
bpdc:	Biphenyl -4,4'-dicarboxylate (H_2bpdc being the corresponding acid)
bpy:	2,2'-bipyridyl
bpydc:	2,2'-bipyridine-5,5'-dicarboxylate (H_2bpydc being the corresponding acid)
DMF:	N,N-dimethylformamide
EDXS:	Energy Dispersive X-ray Spectroscopy
EtA:	Ethanoic acid, Acetic acid
FCC:	Face Centered Cubic (close packed Bravais lattice)
FTIR:	Fourier Transform Infrared (Spectroscopy)
FWHM:	Full Width at Half Maximum. A measure of peak shape in diffraction
HKUST:	MOFs developed at Hong Kong University of Science and Technology
NMR:	Nuclear Magnetic Resonance.
MIL:	Material from Institut Lavoisier.
MOF:	Porous metal-organic framework
MS:	Mass Spectrometry
PSF:	Post synthetic functionalization
PXRD:	Powder X-Ray Diffraction
pyc:	Isonicotinic acid, pyridine-4-carboxylic acid
tdt:	Toluene-3,4-dithiolate (H_2tdt being the corresponding dithiol)
TGA:	Thermogravimetric Analysis
THF:	Tetrahydrofuran
SBU:	Secondary Building Unit
SEM:	Scanning Electron Microscopy
UiO:	University of Oslo
UV-vis:	Ultraviolet and visible light spectroscopy
ZIF:	Zeolitic Imidazolate Framework

Project description

Title: Synthesis and characterization of modified UiO-67 MOF (metal organic framework).

Supervisors: Karl Petter Lillerud and Mats Tilset.

Main goals:

Develop a standard procedure for the synthesis of UiO-67 made with (non-Zr) metal modifiers.

Characterize the modified samples with PXRD, sorption measurements, TGA and spectroscopic techniques (NMR, UV-vis, IR).

Determine how the material can be stored over extended periods of time, without decomposing.

Secondary goals:

Test the modified UiO-67 as a heterogeneous catalyst in gas and liquid environment.

Compare different synthesis approaches for modified UiO-67.

Synthesize new MOFs, preferably with UiO MOF topology.

Safe job analysis

Date: 11.11.2011	Name of student: Sigurd Øien	Name of supervisors: Karl Petter Lillerud Mats Tilset
Thesis title : Synthesis and characterization of modified UiO-67 MOF		
Toxic chemicals to be used: N,N-dimethylformamide (DMF), zirconium(IV)chloride, lye (NaOH and KOH), Potassium dichromate		
Potentially dangerous equipment: Glass vacuum line		

What can go wrong	**What can be done to prevent this**	**What must be done if an accident occurs**
Spill or intake of toxic chemicals.	Always work according to safety rules of the lab and chemicals in use. Always work in a fume hood. Always wear the appropriate safety equipment.	Necessary safety equipment and first aid kits must be present in all labs. Treat chemical accidents according to MSDS sheets.
Long term exposure to carcinogenic compounds.	DMF and other carcinogenic compounds must always be stored in fume hood or ventilated cupboard. DMF bottles must never be opened outside fume hoods.	If a large DMF spill occurs, the lab is evacuated and HSE-coordinator contacted.
Gas line explosion or implosion.	The line is kept in a fume hood for extra protection. Always wear goggles. The SOP must be followed.	Cuts are treated with compress and elevation of damaged limp. Medical assistance is called if necessary.

1 Introduction

Catalysis is a fundamental part of most branches of chemistry. From the enzymatic activity in all life forms to industrial petrochemical processes, catalysts play a vital role. Naturally, a lot of resources are directed into developing new catalysts for reactions such as water-splitting, CO_2-reduction and C-H bond activation in alkanes; catalysts that would literally change the world.

Metal-organic frameworks are good candidates for heterogeneous catalysis, in the sense that they are crystalline and extremely porous. The versatile organic linker allows for the incorporation of functional groups, and controllability of the pore geometry. This thesis work is merely a small step towards this ambitious goal, exploring ways to functionalize the framework in the most convenient way.

1.1 Metal-organic frameworks

Since the discovery of MOF-5 by Yaghi and coworkers in 1999 (Figure 2), porous metal-organic frameworks (MOFs) have emerged as a hot field of chemical research[3]. This quickly expanding class of crystalline materials displays remarkable properties such as ultrahigh porosity and chemical diversity[4]. These properties, together with the extraordinary degree of flexibility for both the organic and inorganic components of their structures, make MOF materials prime candidates for selective gas adsorption and heterogeneous catalysis[5].

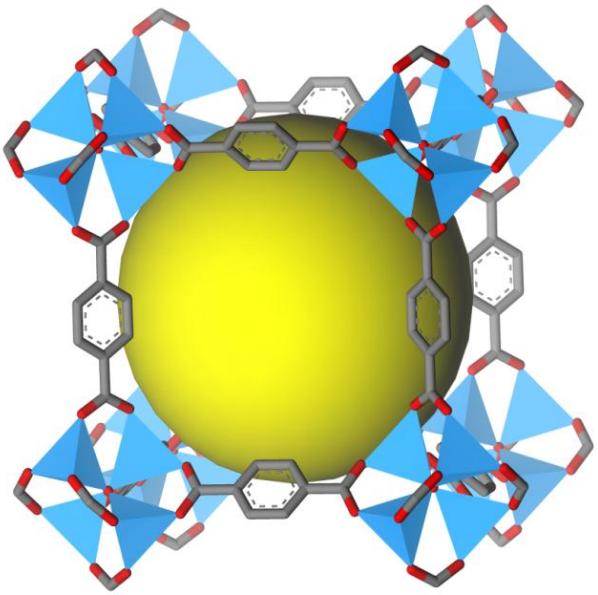

Figure 2. The iconic MOF-5, also called IRMOF-1.

The study of MOFs borders several branches of chemistry. Answers can be found in both traditional organic and inorganic chemistry, or in computational models. To thoroughly characterize a MOF the researcher needs to use and understand several techniques and connect the results to obtain meaningful information.

Some of the long term goals of MOF research is to develop materials for application in catalysis, gas storage or chemical separation, as chemical sensors etc[6]. Since MOFs are relatively expensive to synthesize and the proposed applications are achievable by other more traditional methods, there is a significant pressure on MOF performance in these fields. Catalysts will have to be regio- and enantioselective. Absorbents and sensors will have to be extremely selective and/or energy efficient to compete with existing materials at a cost efficient level.

A lot of money and research hours are being used on MOFs. One may discuss if the motivation behind all this research is a mere fascination over a new class of materials, or pioneering work in a promising field. Stability issues (thermal, chemical and mechanical) severely limit the possible applications for MOFs. Still, they do have several unique properties that may give them the advantage necessary to compete with other materials, namely flexibility, porosity and diversity. MOFs have been made with pore sizes up to 50 Å[7]. The vast amount of possible linker molecules, and ways they (or the metal cluster) can be functionalized may potentially provide tailored MOFs for specific needs. The reported surface areas (up to 10400 m^2/g Langmuir surface area), low densities (down to 220 mg/cm^3), and free inner volume is unparalleled by any other class of crystalline compounds. These record data are obtained from MOF-210[8] (Figure 3).While MOFs are a promising class of materials, a key issue is to improve the stability of MOFs. Not all MOFs are stable in the presence of water or oxygen, and some collapse when guest molecules (most often the solvent from the synthesis) are removed. The fundamental research on MOF formation and decomposition is necessary to provide the information needed for these materials to have commercial applications in the future.

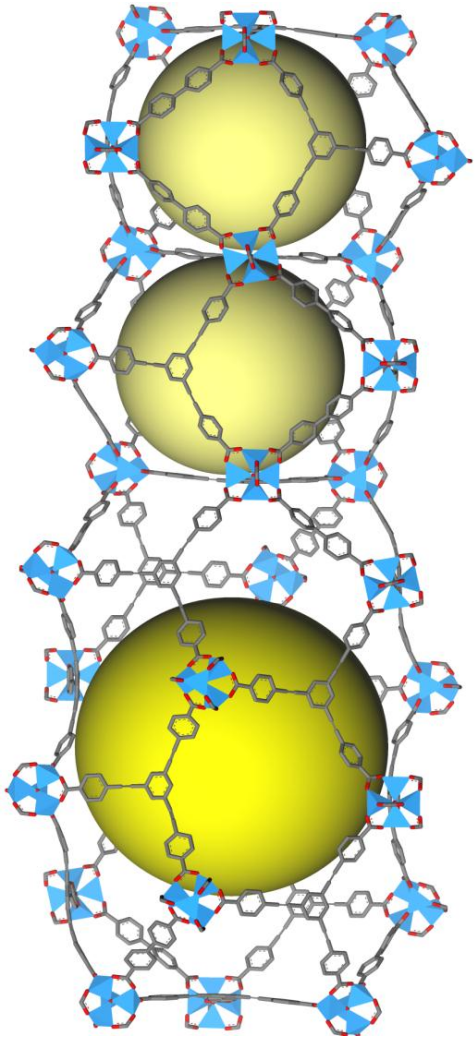

Figure 3. Part of the unit cell of the ultra-porous MOF-210.

1.2 MOF structure

A metal-organic framework is a crystalline compound made out of organic and inorganic secondary building units (SBUs). The SBU model is a simplification, making it easier to classify MOFs, and . In most MOFs the SBUs can be classified into organic *linkers* and metal (or metal ionic) *connectors* (Figure 4). Both the linkers and connectors have a given coordination, thus providing the foundation for the MOF structure. While there is not a generally accepted consensus of what the criteria for a material to be called a MOF is, most agree that there must be some inorganic component bridged by a separate, coordinating organic (carbon-containing) ligand, and a defined crystal structure in two or three dimensions[6].

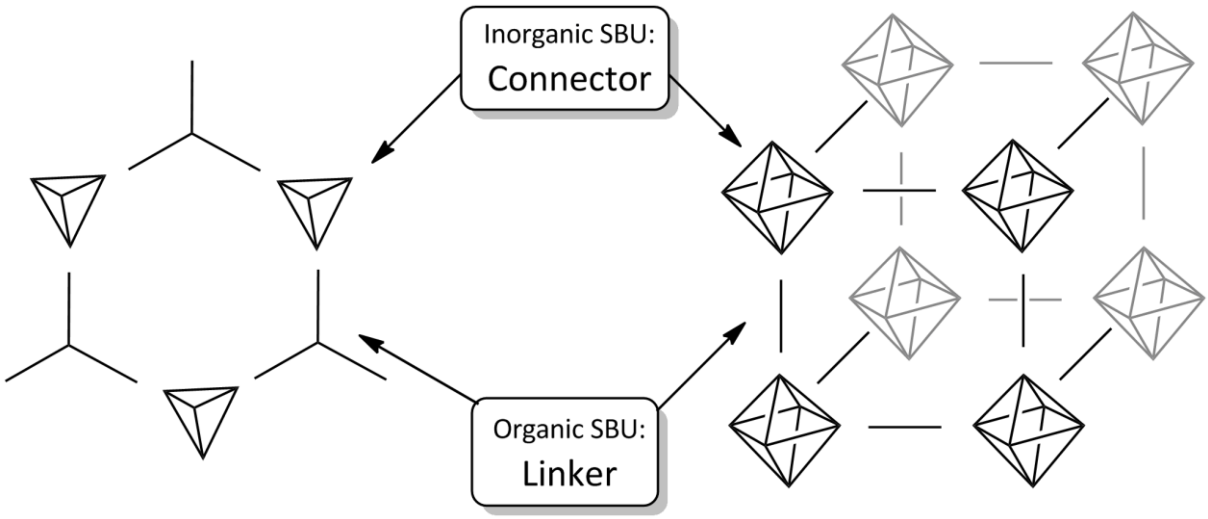

Figure 4. A schematic overview of the general MOF structure.

The linkers are often linear or planar molecules with 2, 3 or 4 functional groups able to form bonds with the connector. This is most commonly carboxylic acids or amines (see Figure 4 for a brief overview). The linkers are usually aromatic because of their stability, rigidity and facile functionalization with halogen-, amine- or alkyl groups, to name a few.

A sub-class of MOFs, Zeolitic imidazole frameworks (ZIFs), is using imidazolate ions as linkers, bonding directly to zinc oxide tetrahedra. The 120 ° angle between the nitrogen atoms in imidazole imitates oxygen in zeolites, giving ZIF analogues to many zeolites[9]. Other examples of M-N coordination bonds are also found with 1,4-pyrimidine and 4,4'-bipyridine.

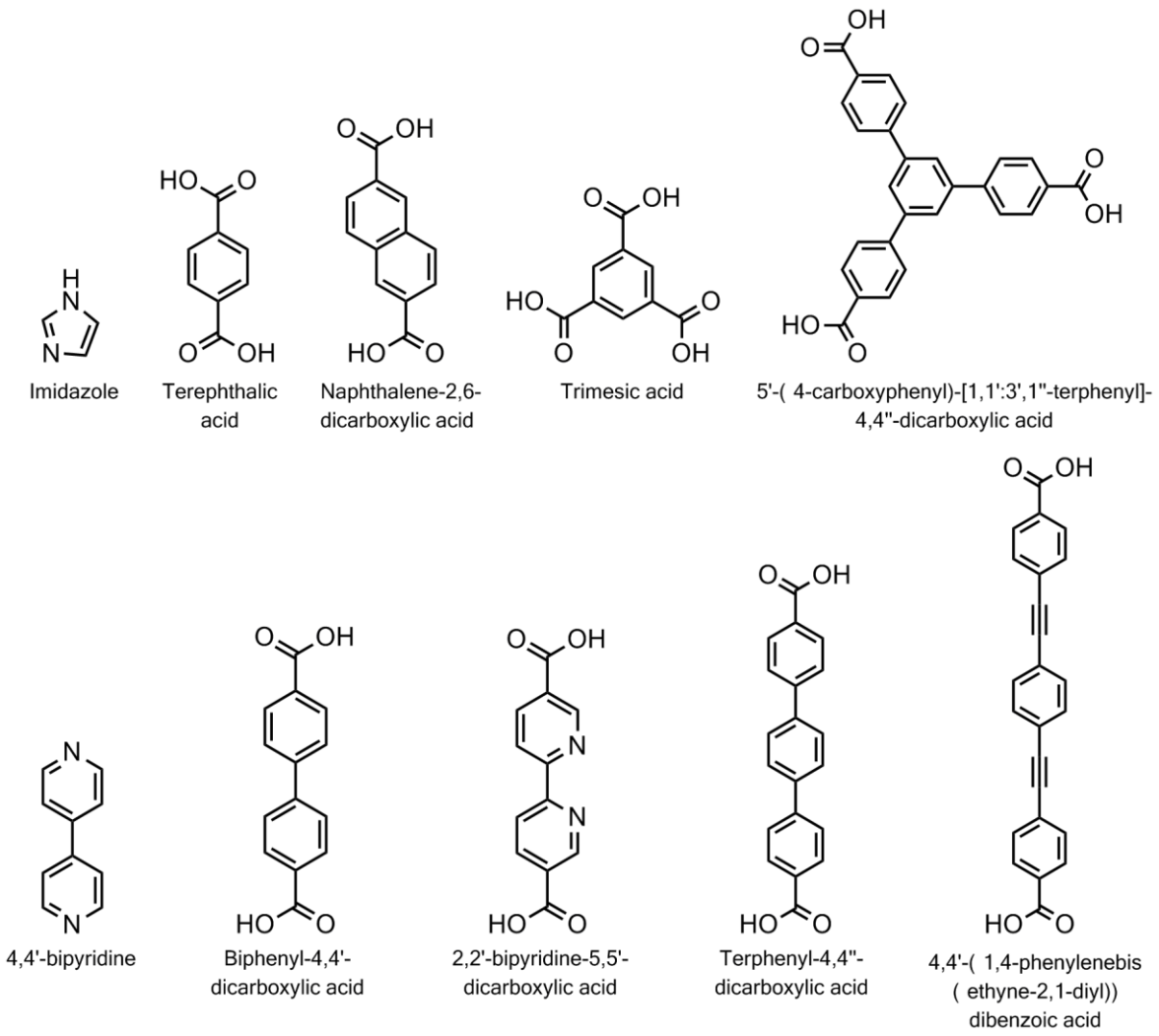

Figure 5. Examples of MOF linkers.

Certain MOFs have two or more different linkers present in the structure in an ordered fashion. $[Cu_2(ndc)_2(dabco)]$ consists of a diatomic Cu-connector, binding to carboxylates (1,4-naphthalene dicarboxylic acid (ndc)) in the a and b directions and to nitrogen lone pairs (1,4-diazabicyclo[2.2.2]octane (dabco)) in the c direction[10].

The connector is usually a small metal oxide cluster, but can also be diatomic or even a single metal atom. The connector is the signature part of the MOF, easily recognizable, and subject for patenting. Researchers in the field are racing to synthesize MOFs with new connectors and solve their structures, to obtain valuable patents and be allowed to name a novel material. Some publications list hundreds of possible connectors found by computational methods[11]. Out of thousands of published MOF structures, some of the most well-known connectors are Zn_4O (MOF-5)[12], Cu^{2+} (HKUST-1)[13], Cr_3O (MIL-101)[14], and also the $Zr_6O_4(OH)_4$ connector of the UiO-series[1] (Figure 6).

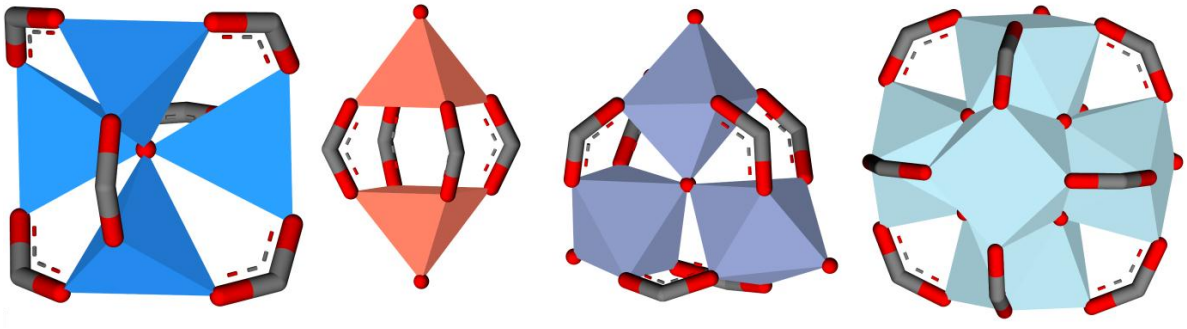

Figure 6. Connectors of MOF-5, HKUST-1, MIL-101 and UiO-66 (not to scale), with carboxylate groups shown to illustrate linker connectivity.

Together, the linker and connector constitute the MOF. The coordinations of the connector and linker make up the three dimensional network of the final material. In the simplest MOFs, with one organic and one inorganic SBU, MOFs tend to adopt high-symmetric crystal structures, like the simple cubic structure of MOF-5 or the FCC structure of UiO-66 and HKUST-1.

MOFs are caught between the two worlds of organic and inorganic porous materials; between polymers and zeolites. They are still called coordination polymers, coordination network solids, and even exclusive names for sub-groups of MOFs. Still, it seems that the scientific community is slowly agreeing on Metal-organic frameworks as a name for three-dimensional crystalline solids consisting of discrete metallic/ionic and organic SBUs. A group has been formed by IUPAC to devise a report called “Coordination polymers and metal–organic frameworks: terminology and nomenclature guidelines”, to resolve nomenclature issues[15].

1.3 MOF discovery and history

Metal organic compounds have a long history, and they are the subject of a whole branch of chemistry. The first metal organic compound to be reported was Zeise's salt, synthesized by William Christopher Zeise in 1825[16]. Materials that fit the modern criteria for MOFs have been known since the discovery of Prussian blue (Hexacyanoferrate) in 1704 (although not characterized until many years later)[17], but such materials are not porous, thus used for other purposes.

The inorganic SBUs $Zn_4O(RCOO)_6$ and $Zr_6O_4(OH)_4(RCOO)_{12}$ were known long before the respective MOFs were discovered ($Zn_4O(RCOO)_6$ since 1954 and $Zr_6O_4(OH)_4(RCOO)_{12}$ from 1996)[18,19], as were all the bi- and polydentate carboxylic acids now used as linkers. One may wonder why these clusters existed for so long before anyone thought to change the carboxylic acid ligand to a diacid. There is no reason to believe that it have been attempted unsuccessfully. After all, most MOFs are synthesized in

simple, solvothermal processes[20]. Perhaps the gap between organic and inorganic chemistry was too wide at the time so that no one had such an idea.

Crystalline metal-organic coordination compounds got more attention in the late 90s, with the discovery of the framework $Cu(4,4'\text{-bpy})_{1.5}NO_3(H_2O)_{1.5}$ by the Yaghi group in 1995[21]. A compound later discovered with layers of ordered metal oxide clusters bound together by terephthalic acid paved the way for the discovery of MOF-5 in 1999[3], the material which set off the hunt for new MOFs and to this day remains the symbol of the entire field. This was the first material which fits the modern criteria for a MOF, with an incredibly high internal surface area, a well-defined crystal structure, porosity in three dimensions and reasonable stability.

MOFs can be classified as network solids, and the study of such structures is often called reticular chemistry (from Latin: Reticulum, meaning "net")[22]. Reticular chemistry is concerned with linking of molecular building blocks (organic molecules, inorganic clusters, dendrimers, peptides, proteins,...) into predetermined structures in which such units are repeated and are held together by strong bonds[23]. And so, any series of MOFs with identical inorganic SBU and same topology are now said to be *iso*reticular, i.e. they have the same network structure. MOF-5 was patented as IRMOF-1 (IsoReticular MOF), along with 15 other MOFS, all with the same Zn_4O connector and linear dicarboxylate linkers[24].

Since these important discoveries, the numbers of known MOF structures and published papers concerning MOFs have exploded. There can be many explanations for this phenomenon: New materials are always exciting and attract a lot of attention in the community; for researchers already familiar with the synthesis and characterization of zeolite-type materials, the transition is fairly easy; and MOFs have promising potential in gas storage and separation that may prove to be profitable in the future.

It is often claimed that MOF research is a growing field, with an exponential growth of the number of published works. Figure 7 shows the growth of publications containing the exact phrase "Metal-organic framework" in the title and/or abstract. The reader should notice that several assumptions have been made. First and foremost "Metal-organic framework" was chosen as the search term because it is exclusive. It is also assumed that the search results from SciFinder[25] give a representative picture of the scientific community as a whole. The data for 2012 is based on the results of a search made on June the 15th 2012 and assuming a constant rate of publications throughout the year.

In the period 2004 to 2012, the statement is valid with almost perfect accuracy (R^2 = 0.9895). In this period, publications about MOFs per year were doubling at a rate of two years and two months.

While it is certainly uplifting to experience growth in ones field of research, these numbers mean nothing unless compared the growth of total publications in chemistry. In 2007, the Chemical Abstracts Service (A division of the American Chemical Society, running SciFinder) published a statistical summary of the CAS database[26]. Figure 7 shows the number of chemistry publications sorted by year of publishing.

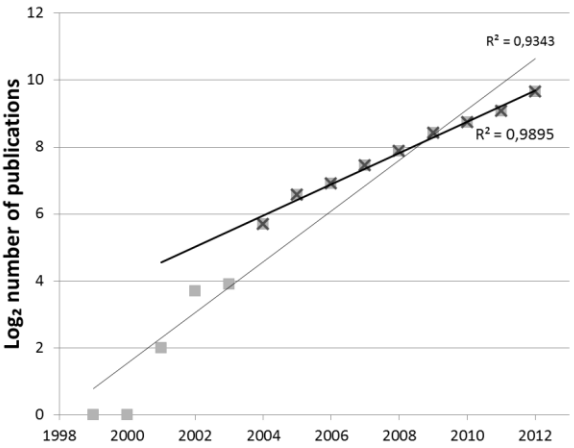

Figure 7. The number of publications containing "Metal-organic framework" in title and/or abstract.

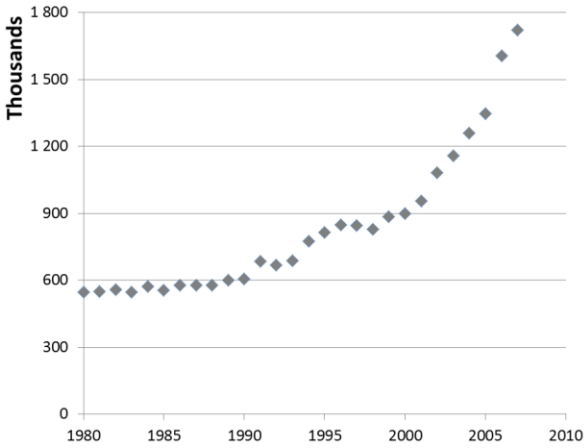

Number of publications in the CAS database, 1980-2007.

Unfortunately, data from after 2007 was not available at the time of writing. The growth after the year 2000 is remarkable in absolute numbers, and may be partly due to the rising of online publications. Nevertheless, even when assuming exponential growth of the number of chemistry publications, the growth rate is significantly less than for MOF publications. It can safely be stated that MOF research is a growing field within chemical research.

1.4 The UiO isoreticular MOF series

The isoreticular series of Zr-MOFs UiO-66, 67 and 68 were first reported by Cavka and coworkers in 2008[1]. It consists of $Zr_6(\mu_3\text{-}O_4)(\mu_3\text{-}OH)_4(CO_2)_{12}$-connectors, bridged by linear organic linkers. These linkers are terephthalic acid, 4,4'-biphenyldicarboxylic acid and 4,4''-p-terphenyldicarboxylic acid, respectively.

The connector (Figure 9) has the ability of reversibly hydrate and dehydrate. In its hydrated form, the six Zr(IV)-ions each have a square antiprismatic coordination to 8 oxygen anions (two oxides, two hydroxides and four carboxylate oxygen), and each antiprism shares one edge with four other antiprisms. Each connector can be seen as a cuboctahedron, having one connection point at each corner. The connectors are arranged in a FCC structure, thus giving one octahedral and two tetrahedral cavities per connector. The space group of the (hydrated) compounds is $Fm\bar{3}m$.

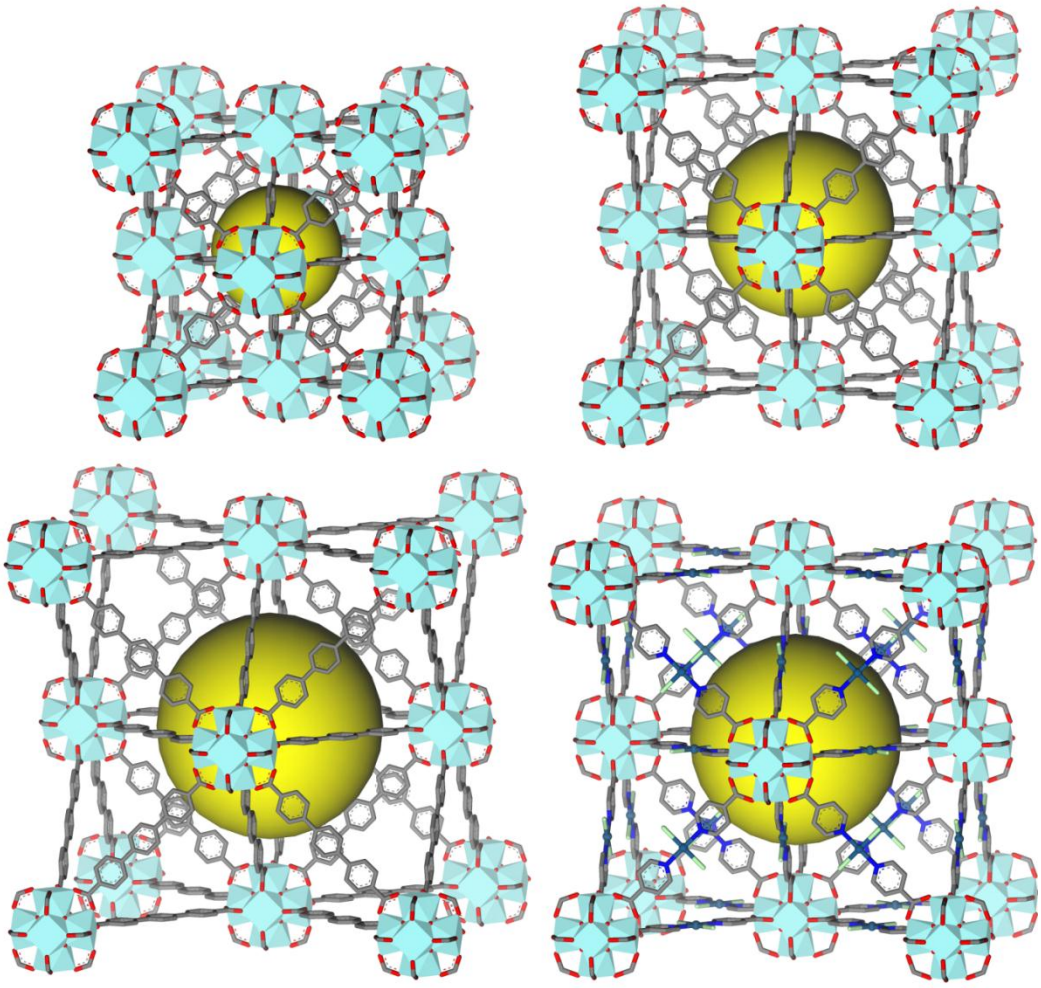

Figure 8. Series of Zr-based UiO-MOFs having the same framework topology, thus being *isoreticular*. From top left: UiO-66, UiO-67, UiO-68 and UiO-70.

Upon activation (removal of solvent by heating the material in vacuum or gas flow), the connector undergoes dehydoxylation, yielding a $Zr_6O_6(COO)_{12}$ stoichiometry. The Zr-ions change to a slightly distorted monocapped trigonal prismatic 7-coordination, but the cuboctahedron 12-coordination of the connector is conserved. This change is fully reversible in UiO-66 and reversible to a certain degree in UiO-67[27]. Figure 9 shows the connector in the two states.

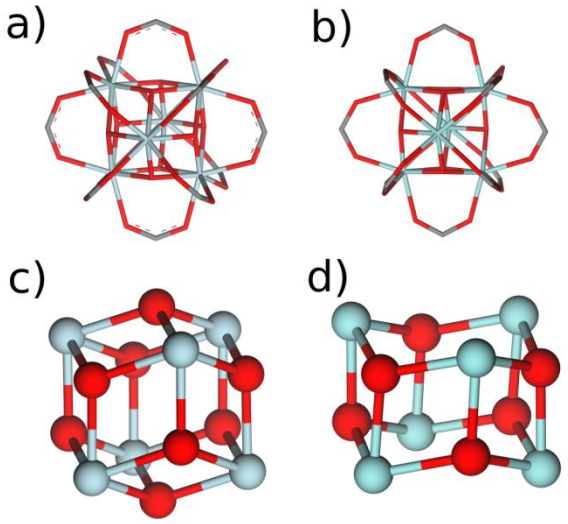

Figure 9. Representations of the UiO-MOF connector. (a) Hydrated, $Zr_6O_4(OH)_4(COO)_{12}$. (b) Dehydrated $Zr_6O_6(COO)_{12}$. (c) Hydrated inner connector, not showing carboxylates, $Zr_6O_4(OH)_4$. (d) Dehydrated inner connector, not showing carboxylates, Zr_6O_6

The UiO MOFs do not decompose upon activation, but retains the crystal structure even in high vacuum. UiO-66 is stable in boiling water[1], while UiO-67 has lower chemical stability with respect to water as evidenced by PXRD during dynamic light scattering (DLS) measurements[28]. UiO-66 and UiO-67 also display high thermal stability, decomposing in air at 375 °C and 450 °C, respectively. It is theorized that the stability of the connector can be explained by the Zr(IV) ion's high affinity for oxygen donor ligands[29,30].

Measured surface areas range from 1100 to 1400 m^2/g for UiO-66 and 1800 to 3000 m^2/g for UiO-67[28,29].

1.5 Proposed synthesis mechanism

The following mechanism was proposed by Nilsen and coworkers at the 34th Annual BZA conference[31]. It is based on an in situ EXAFS study on the crystallization of UiO-66. In contrast to most other MOFs, the isoreticular UiO-series has a significant incubation period before crystallization is observed. This indicates that formation of some intermediate is necessary before crystallization starts. It was assumed that independent zirconium connectors had to be formed before bonding to each other through linkers. However, the EXAFS spectra revealed there is no Zr-Zr interaction before the onset of crystallization.

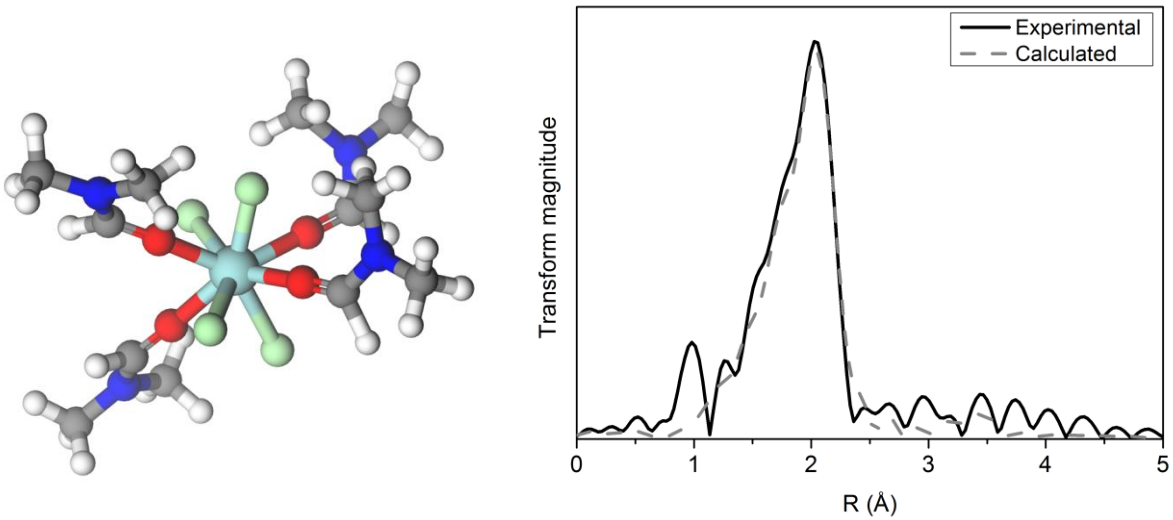

Figure 10. Left: $ZrCl_4(DMF)_4$ complex. Right: The refined EXAFS radial distribution function.

The MOF is formed in a many-step process which starts with the formation of a coordination complex of $ZrCl_4$ and DMF upon solvation. Based on EXAFS radial distribution functions from this stage, it is assumed that Zr adopts a square antiprismatic coordination to 8 oxygen atoms upon solvation:

$$ZrCl_4 + 4\,DMF \rightarrow [ZrCl_4(DMF)_4]$$

The reaction continues with the gradual exchange of chlorides with carboxylate groups from the linker/modifier and hydroxides from water. The exchange is evident from the diminishing Zr-Cl interaction in EXAFS.

$$[ZrCl_4(DMF)_4] + H_2O + H_2bdc \;\leftrightarrow\; [Zr(OH)Cl_2(Hbdc)(DMF)_4] + 2\,HCl$$

Three of these coordination complexes aggregate in a series of reversible steps to give a triangular intermediate:

$$3\,[Zr(OH)Cl_2(Hbdc)(DMF)_4] \leftrightarrow \left[\left(ZrCl(OH)\right)_3(bdc)_3(DMF)_{12}\right] + 3\,HCl$$

These triangular intermediates react to form the connectors. The first diffraction peaks (PXRD), Zr-Zr interaction (EXAFS) and physical precipitation is observed simultaneously at this point (Figure 11). The Zr-Zr interaction becomes steadily more dominating after this, along with diminishing Zr-Cl interaction, until the reaction is complete (Figure 12)

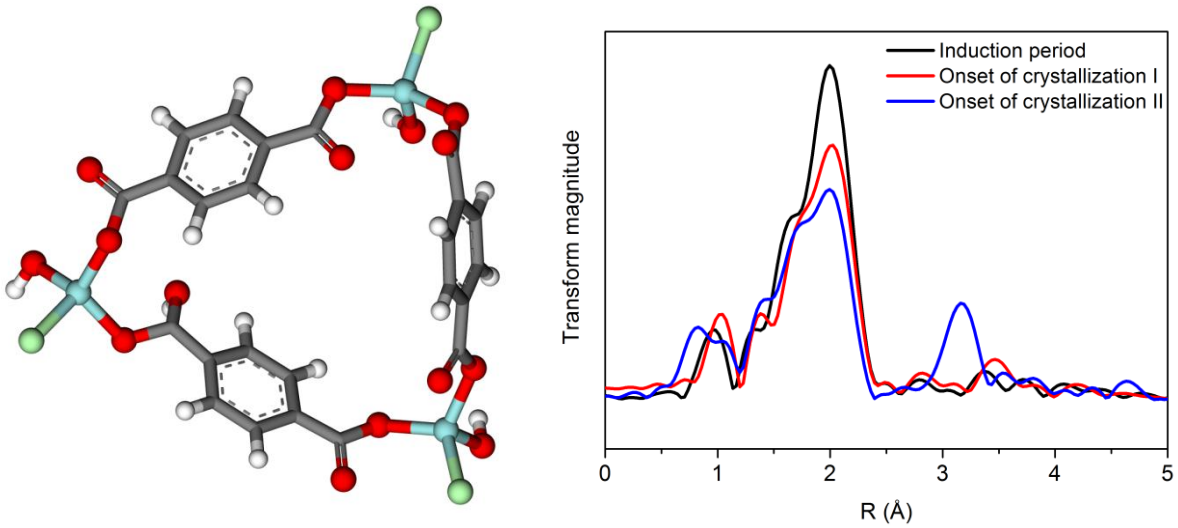

Figure 11. Left: A plausible synthesis intermediate of UiO-66, $[ZrCl_2OH(bpdc)]_3$. Right: EXAFS radial distribution function showing the evolution of the local environment of zirconium before crystallization.

While the proposed mechanism is in agreement with the EXAFS results, the first step does not agree with experimental observations. The addition of $ZrCl_4$ to DMF containing a certain amount of water is extremely exothermic, and HCl vapor is instantaneously emerging from the solution. Anhydrous $ZrCl_4$ is insoluble in anhydrous DMF, suggesting that $ZrCl_4$ monomers need to form a complex with water and/or hydroxide in order to dissolve. The evaporating HCl indicates that a rapid OH^- to Cl^- ligand exchange occurs, to preserve the stoichiometry.

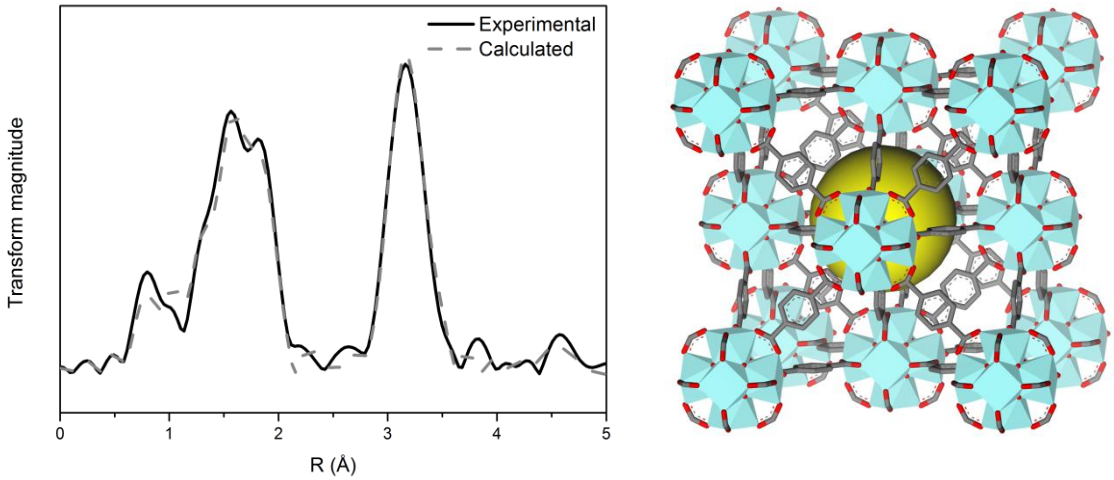

Figure 12. Left: EXAFS radial distribution function of UiO-66 with refinement. Right: Unit cell of final product, UiO-66.

1.6 General aspects of MOF synthesis

Most MOFs are made by some variation of the solvothermal synthesis method[20]. The precursors are dissolved in a solvent that dissolves *both* organic and inorganic solids, and may act as a good ligand. The solution is then subjected to crystallization conditions, meaning mild, near-equilibrium temperatures and concentrations. The reversible formation of coordination and ionic bonds is necessary to obtain crystalline materials, since kinetically formed, amorphous products then have the opportunity to rearrange to the thermodynamically favored product[32]. The formation of MOFs can be seen as a self-assembly process.

The solvothermal approach has several advantages. It is simple to preform (low probability of failure due to faulty preparation), does not require any advanced equipment, and allows homogeneous mixing of the reactants.

A crucial aspect of MOF crystallization is the controlled formation of bonds between connectors and linkers. In the case of carboxylate linkers dissolved in DMF (the synthesis conditions of many MOFs including the UiO series), it is assumed that DMF decompose under acidic conditions to form basic dimethyl amine[33,34]. The carboxylate anion is then free to attack the metal. Figure 13 shows a mechanism suggested by Hausdorf and coworkers, after *in situ* analysis of the by-products of MOF-5 synthesis[35].

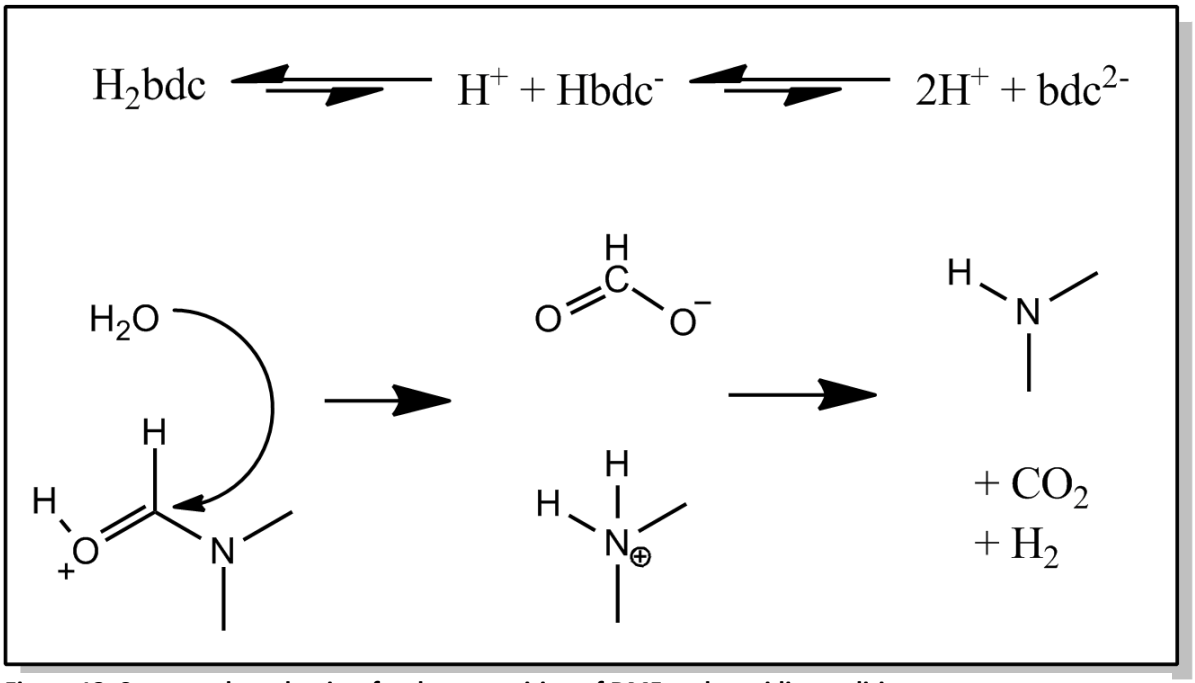

Figure 13. Suggested mechanism for decomposition of DMF under acidic conditions.

1.7 Modulated solvothermal synthesis

Tsurukoa and coworkers has showed that MOF crystal growth can be inhibited by introducing a competing, single-coordinated ligand called a modulator[10]. The MOF $Cu_2(ndc)_2(dabco)$ consists of a diatomic Cu-connector, binding to carboxylates (1,4-naphthalene dicarboxylic acid (ndc)) in the a and b directions and to nitrogen lone pairs (1,4-diazabicyclo[2.2.2]octane (dabco)) in the c direction (Figure 14). Introducing a modulator to the synthesis will slow crystal growth in those directions where the modulator and linker are competing for the same coordination sites.

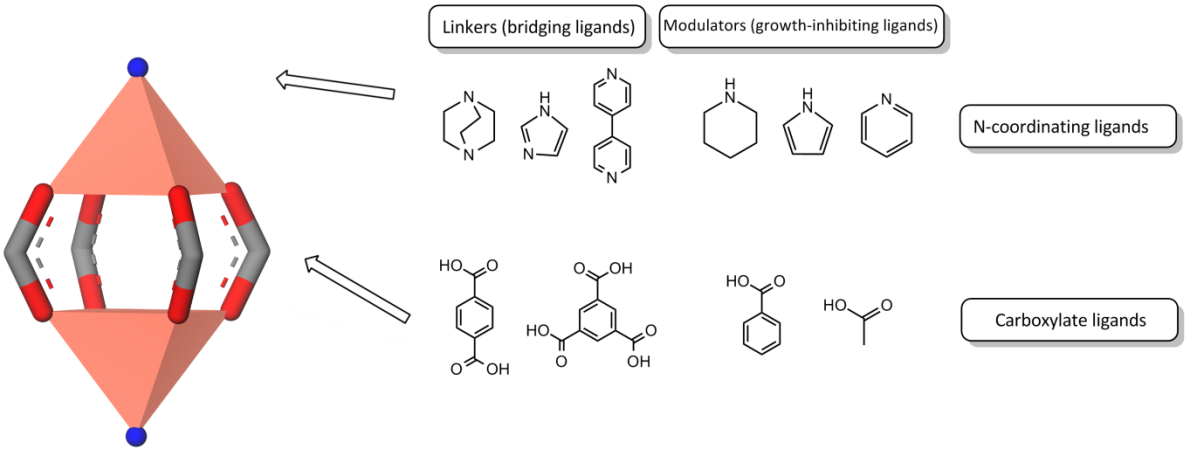

Figure 14. The Cu_2-connector has four carboxylate seats in a plane, and two opposing seats for neutral donor ligands, all perpendicular to each other.

Tsurukoa demonstrated this elegantly by using acetic acid as a modulator for the synthesis of this MOF, creating needle-shaped crystals, whereas the normal synthesis yielded cubic crystals. The growth direction was confirmed by single crystal XRD.

Schaate and coworkers have since utilized this method to improve the synthesis of UiO-67. In the UiO MOFs, all connector sites are equal, and the crystal growth is limited in all directions by the presence of a modulator[28]. This approach yielded larger crystals and greater reproducibility of the synthesis, but yields comparable with unmodulated synthesis. This clearly indicates that seeding is less favorable compared to crystal growth when the modulator is present. By using benzoic acid as a modulator, UiO-68-NH_2 was synthesized. The crystals were large enough to analyze with single crystal XRD.

It has not yet been investigated exactly how the presence of a modulator affects the synthesis mechanism. However, it is observed that fewer crystals are formed, indicating that nucleation is becoming less favorable compared to crystal growth. This leads to larger crystals, the sizes of which are roughly proportional to the concentration of the modulator.

1.8 MOFs as catalysts

Due to their unparalleled porosity and comparability with zeolites and other existing porous catalysts, MOFs were quickly assumed to have a potential role as catalysts for a wide range of reactions[36]. Some MOFs show catalytic activity as an inherent property of the cluster itself, such as HKUST-1 and MIL-101 having accessible Cu(II) and Cr(III) Lewis acid sites, respectively[5]. Examples of catalysis on MOF-encapsulated metal nanoparticles are also known[37].

A third strategy is to incorporate a catalytic site as part of the linker, simply reengineering a known homogeneous catalyst into a heterogeneous one by making it part of the linker. The flexible cavities in MOFs can even be seen as a framework capable of mimicking active sites of enzymes, given the proper functionalization. These approaches has been extensively discussed by (among many others) Lillerud[38] and Kitagawa[39], and lately used with success in UiO-67 by Wang and coworkers[40]. Water oxidation, carbon dioxide reduction, and organic photocatalysis were shown in UiO-67, where a fraction of the linkers (>10 %) were functionalized metal complexes of Ru, Re and Ir, as shown in Figure 15.

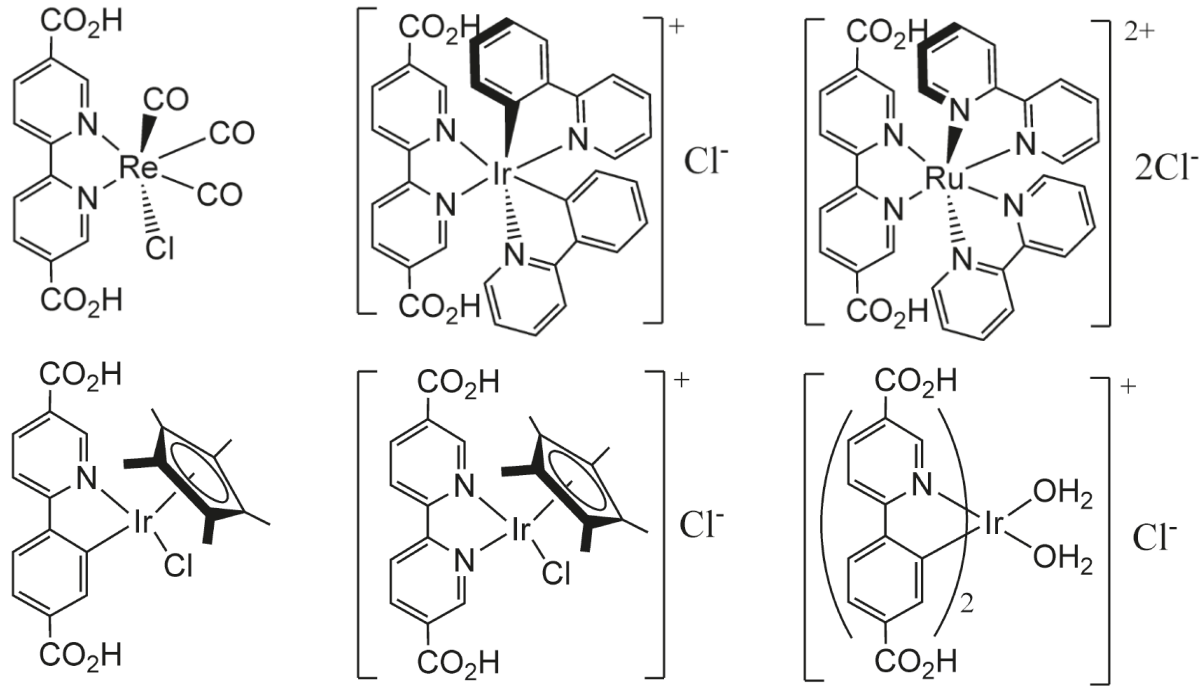

Figure 15: Complexes incorporated into UiO-67 by Wang and coworkers.

1.9 Choice of functionalization

UiO-67 was chosen as the model compound because of its porosity and thermal stability. UiO-66 has the advantage of being stable towards water, but the cavity size limits the number of possible guest molecules in the structure. In addition, the bicyclic linker of UiO-67 offers more ways of functionalization.

One of the main goals of MOF functionalization is to create highly selective adsorbents and/or catalysts. As Wang and coworkers have shown, UiO-67 is a good candidate for the incorporation of known homogeneous catalysts. In this work, platinum was chosen because of the broad expertise on this element at the University of Oslo in both homogeneous catalysis[41,42] and MOFs[43]. Toluene-3,4-dithiolate is a ligand with high affinity for platinum and creates complexes with interesting photochemistry[44]. Copper was chosen for its role in enzyme catalysis and biological transport[45]. It was decided to reproduce Wang's synthesis of $Ru(bpy)_3$ system and the functionalized MOF because of its interesting photocatalytic properties[46]. These three metal centers were also known to bind to soft N-donor ligands such as bipyridine[30].

1.10 Functionalization methods

There are different ways to synthesize MOF with functionalized linkers. This work will focus on the synthesis of functionalized organometallic complexes utilizing 2,2'-bipyridine-5,5'-dicarboxylic acid (H2bpydc) as a chelating ligand. This complex has the ability to act both as a linker in UiO-67 type MOFs, and provide an active seat for catalysis or selective adsorption.

There are three main synthesis pathways for a MOF with functionalized linkers, which will each be described in detail below: functionalized linker synthesis, one pot synthesis and post synthetic functionalization.

In the functionalized precursor synthesis, the functionalized linker is prepared separately by regular organic or organometallic synthesis methods. Then the functionalized linker is used, often along with un-functionalized linker, in MOF synthesis. This approach is generally useful when the linker synthesis require conditions that would decompose the MOF, and gives very good control of the product. However, multi-step linker synthesis can be inefficient, and the linker may not remain intact throughout the MOF synthesis.

In the one pot synthesis method, the precursors for both the MOF synthesis and the functionalized linker synthesis are mixed and used for MOF synthesis. In certain cases, the MOF will form as usual, while the linker is functionalized at the same time, due to selective ligand coordination. This has the

potential to be the most efficient method, but the added reactants could also compromise the quality of the product.

Post-synthetic functionalization (or modification) refers to all synthetic alterations of a synthesized MOF and is analogous to performing the linker functionalization while it is attached to the framework. This could be reactions between the solid framework and liquid or gas phases of functionalization agent.

1.11 UiO-67 synthesis strategy

UiO-67 is generally synthesized by a solvothermal process in a glass flask. In order to develop a good method for the synthesis of functionalized UiO-67, many different approaches had to be tried out. The regular synthesis without modulator was compared to one with modulators based on the work of Schaate and coworkers[28]. Acetic acid and benzoic acid was used in different concentrations to investigate if metal functionalized UiO-67 follows the same trends as regular UiO-67 in respect to crystal nucleation and growth. Regarding reaction vessel, only regular glassware was used, such as Erlenmeyer flasks. Studies by Schoenecker and coworkers (on UiO-66) suggest that crystal nucleation and growth occurs in solution, reporting no correlation between reactor material or volume/surface ratio and product quality[47].

As for the functionalization itself, the three methods discussed in the previous section was compared: Synthesis with pre-functionalized linkers, one pot synthesis and post synthetic functionalization of an empty framework.

Many parameters had to be taken into account in the development of the synthetic procedures, such as synthesis cost, complicity and reproducibility, and the yield and quality of the final product.

1.12 Organic and organometallic synthesis

Organic and metallic organic synthesis plays a vital role in MOF chemistry. Most importantly, metal-ligand bonds between linkers and connectors are a necessary prerequisite for formation of MOFs. Organic and metal organic linkers, often complicated with multiple functional groups, had to be synthesized.

2,2'-bipyridine 5,5'-dicarboxylic acid (H_2bpydc) is a good base compound for metal-organic synthesis, since 2,2’-bipyridyls chelate to many d-metal ions, creating planar 5-membered chelate rings. This dicarboxylic acid can be prepared by oxidizing 5,5’-dimethyl-2,2’-bipyridyl under harsh conditions. H_2bpydc can then be used to prepare various d-metal complexes of the acid, analogous to bpy complexes described in the literature[48].

The demand for linker molecules is steadily increasing, and all but the most common linkers are very expensive. By July 2012, 2,2'-bipyridine-5,5'-dicarboxylic acid cost 1200 NOK per gram at Sigma-Aldrich. By comparison, 25 grams of 5,5'-dimethyl-2,2'-bipyridyl (which is easily oxidized to the acid) cost 2040 NOK, or just 5 % of the price (per mole). Reported methods for the oxidation reaction give yields close to 100 %[49].

1.12.1 Synthesis of 2,2'-bipyridine-5,5'-dicarboxylic acid

The oxidation of 5,5'-dimethyl-2,2'-bipyridyl was carried out as described by Lundvall[50] and Jakobsen[49], in which the methyl groups are oxidized to acid groups by dichromate under acidic conditions. The reaction is executed with care, since potassium dichromate is extremely toxic and carcinogenic. Dichromate is reduced as shown in the following half reaction:

$$\mathrm{Cr_2O_7^{2-} + 14\,H^+ + 6\,e^- \rightarrow 2\,Cr^{3+} + 7\,H_2O} \qquad [+\,1{,}23\ \mathrm{V}]$$

When reacting with the methyl groups (simplified), we get the following total reaction:

$$-CH_3 + Cr_2O_7^{2-} + 8\,H^+ \rightarrow -COOH + 2\,Cr^{3+} + 5\,H_2O$$

It is evident that two molar equivalents of dichromate is needed in respect to 5,5'-dimethyl-2,2'-bipyridyl to complete the reaction, but it is customary to add a small excess to ensure full conversion.

1.12.2 Synthesis of platinum complexes

The synthesis of $PtCl_2(H_2bpydc)$ was carried out as described by Jakobsen and coworkers[51].

$$K_2PtCl_4 + H_2bpydc \xrightarrow[\Delta]{HNO_{3(aq)}} PtCl_2(H_2bpydc) + 2\,KCl$$

The synthesis of $PtCl_4(H_2bpydc)$ was first attempted under acidic conditions, identical to the synthesis of $PtCl_2(H_2bpydc)$. However, this method gave very poor conversion (<10%), even when higher concentrations and longer reaction time was used. Another method, changing to basic conditions was attempted, which gave full conversion and acceptable yields (>60%). KNO_3 is added to prevent platinum from reducing.

$$K_2PtCl_6 + H_2bpydc \xrightarrow[\Delta]{KOH_{(aq)},\ KNO_{3(aq)}} PtCl_4(H_2bpydc) + 2\,KCl$$

The synthesis of $Pt(tdt)(H_2bpydc)$ was carried out as described by Geary and coworkers[52].

$$PtCl_2(H_2bpydc) + H_2tdt \xrightarrow{KOH_{(aq)}} Pt(tdt)(H_2bpydc) + 2HCl$$

1.12.3 Synthesis of ruthenium complexes

The synthesis of [cis-Ru(bpy)$_2$]Cl$_2$ was carried out as described by Sullivan and coworkers[53].

$$RuCl_3 \cdot xH_2O + 2\ bpy \xrightarrow[\Delta]{LiCl,DMF} [cis - Ru(bpy)_2]Cl_2$$

It is possible that the oxidation state of ruthenium changes during this reaction, due to the stability of the low-spin d^6 Ru^{2+} ion. Decomposition products of DMF can act as reducing agents for some metal ions[54]. However, it does not *need* to be reduced, as the ion [cis-RuCl$_2$(bpy)$_2$]$^+$ is also known.

The synthesis of [Ru(bpy)$_2$(H$_2$bpydc)]Cl$_2$ was carried out as described by Xie and coworkers[55].

$$[cis - Ru(bpy)_2]Cl_2 + H_2bpydc \xrightarrow[\Delta]{H_2O,\ EtOH} [Ru(bpy)_2(H_2bpydc)]Cl_2$$

1.12.4 Synthesis of copper complexes

The synthesis of CuCl$_2$(H$_2$bpydc) was carried out in a method analogous to that described by Goddard and coworkers[56], differing in that the 3,3'-dicarboxylic acid was the target of their studies. While bpy complexes with Cu^{2+} is known, it is a harder metal center, and thus tends to form bonds with carboxylate oxygen like those found in HKUST-1. Still, the reported synthesis was simple, and it was decided to try it.

$$CuCl_2 \cdot 2H_2O + H_2bpydc \xrightarrow{H_2O} CuCl_2(H_2bpydc)$$

1.13 Methods of characterization

Many methods of characterization have been utilized in this work. The purpose was not only to characterize the bonding between the framework and the functionalization metal, but also to make sure that the crystallinity and adsorption properties of the bulk material were not compromised. Evaluations of crystallinity in this work was based on a qualitative evaluation of combined results from PXRD, sorption measurements, physical appearance and spectroscopic techniques

While it is usually straightforward to characterize these compounds isolated, it is difficult to pinpoint the exact location of the metal in the synthesized MOF. And even if the chemical environment is known, it is not easily determined whether functionalized linkers are randomly distributed throughout the material, if there is a concentration gradient of functionalized linker from center to surface of the crystals, or if there is some order in which the functionalized linkers are arranged.

PXRD gives the crystal structure of the material, but functionalizations that are incorporated into the symmetry of the material are invisible in the diffraction pattern. EDXS shows if elements are present

in the sample, but does not reveal the surrounding environment of these elements. To know if the functionalization was retained throughout the synthesis, solid state NMR spectroscopy and EXAFS were performed., the latter demonstrated by Bloch and coworkers by using EXAFS to characterize the local structure on $PdCl_2(H_2bpydc)$ in MOF-253[57].

1.13.1 PXRD

When radiation (photons or moving particles with suitable wavelengths) is directed through a crystallite, it interacts with the regular arrays of electron densities in the crystal lattice, causing it to scatter in many directions[58]. The intensities of these reflections are plotted as a function of the scattering angle (θ) to give a diffraction pattern. When diffracting radiation in a single crystal, two angular dimensions (called Ω and ϕ) are added for the orientation of the crystal, giving a three-dimensional pattern. Diffractometers are equipped with a two-dimensional detector, so such a pattern is recorded as a set of two-dimensional patterns in geometric relation to each other.

The peaks are read as intensities of certain reflections, related to the crystal lattice dimensions via the Laue and Bragg equations. The Bragg equation, $n\lambda = 2d_{h,k,l}\sin\theta$, directly relates the distance between Miller planes and the scattering angle. In single crystal X-ray diffraction, intensities and scattering angles are combined to make an electron density map and solving the structure through various refinements.

Powder X-ray Diffraction (PXRD) is the diffraction obtained from a powder consisting of small, randomly oriented crystals, or a bulk material consisting of multiple crystallites. It is analogous to recording a single crystal pattern with the incident beam coming from every possible direction. Thus, a one-dimensional pattern obtained is void of information about the crystallite orientation.

PXRD is still a powerful tool, especially for compounds with high symmetry crystal structures. From a diffraction pattern, unit cell parameters and space group can be determined. This can in some cases, together with elemental analysis, information about precursors and other analytical results, be enough for structure determination of unknown compounds, as was the case for UiO-66[1].

From the Bragg equation, it is apparent that a perfect crystal will give a pattern with infinitely thin peaks and no noise. Peak broadening and noise occurs from crystal defects and amorphous phases in the sample itself, sample preparation factors and instrument inaccuracy, among other factors. This makes it hard to use a PXRD pattern to quantitatively evaluate the crystallinity of the sample. The pattern can still be used as a supplement to other techniques when determining the sample quality.

The number of counts per second (cps), signal-to-noise ratio and FWHM values can be used to qualitatively evaluate the crystallinity of the sample.

Diffraction patterns of pure UiO-67 show clearly discernible peaks for all allowed reflections (Figure 16). Having space group $Fm\bar{3}m$, only reflections from Miller planes where h,k,l are all even or all odd are allowed. Diffraction from other planes are cancelled out by destructive interference, thus labeled *forbidden*.

Since the size of most UiO-67 crystals are in the range 10 – 1000 nm and are thus too small to collect a single crystal diffraction pattern, PXRD is the natural way to characterize the material. The powder can be mounted in disk shaped sample holders, in capillaries or as a thin layer on a glass plate. The last method was chosen because capillary PXRD is very time-consuming, and there was rarely enough of each sample to fully fill the disk shaped sample holders.

PXRD was primarily used as a quick, easy and non-destructive way to determine if the desired phase was present in the product, and if crystalline impurities were present. Known crystalline phases are recognized instantaneously, and the presence of foreign crystalline (and semi-crystalline) pollutants is easily discovered. PXRD also give an indication on the amount of solvent absorbed in the MOF, as this alters the electron density of the pores and shifts the ratios of specific peaks.

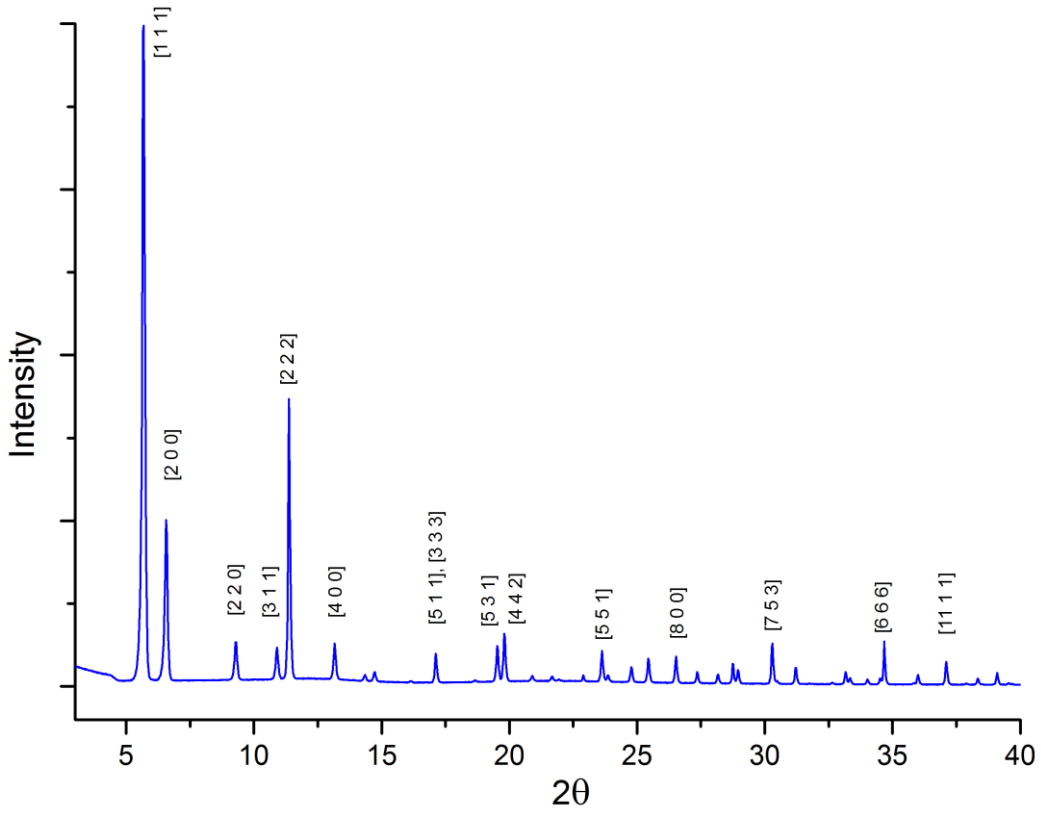

Figure 16. A diffraction pattern of UiO-67, with indices of the most prominent peaks.

PXRD patterns are affected by several factors, such as crystallite size, concentration of defects and amorphous byproducts. Low FWHM values and high signal-to-noise ratio in a pattern indicates large crystallites and low concentrations of defects and amorphous phases.

1.13.2 Gas sorption measurements

A key ability of MOFs is their high free internal volume and surface area. The vast possibilities arising from the many different linkers and connectors give tunable pore sizes, topology and internal pore chemistry[6].

Molecules and atoms can attach to surfaces in two ways: In physiosorption, a Van der Waals-interaction creates an attraction between the surface and the adsorbent. In chemisorption, the adsorbent forms one or more bonds with the surface, usually by attaching to sites where the adsorption enthalpy is minimized[59]. The ratio between occupied sites and available sites is called fractional coverage, θ.

In an adsorption measurement instrument, a series of pressure measurements are made on a cell containing the sample kept at constant temperature, creating an isotherm. This isotherm is plotted as adsorbed volume of standard state nitrogen (0°C, 1.0 atm) per mass of sample (V_a (cm^3(STP) g^{-1}) against relative pressure (p/p_0). Since free gas and adsorbed gas are in dynamic equilibrium, the data from such measurements together with a mathematical model of adsorption can be used to estimate the internal volume and surface area of the material.

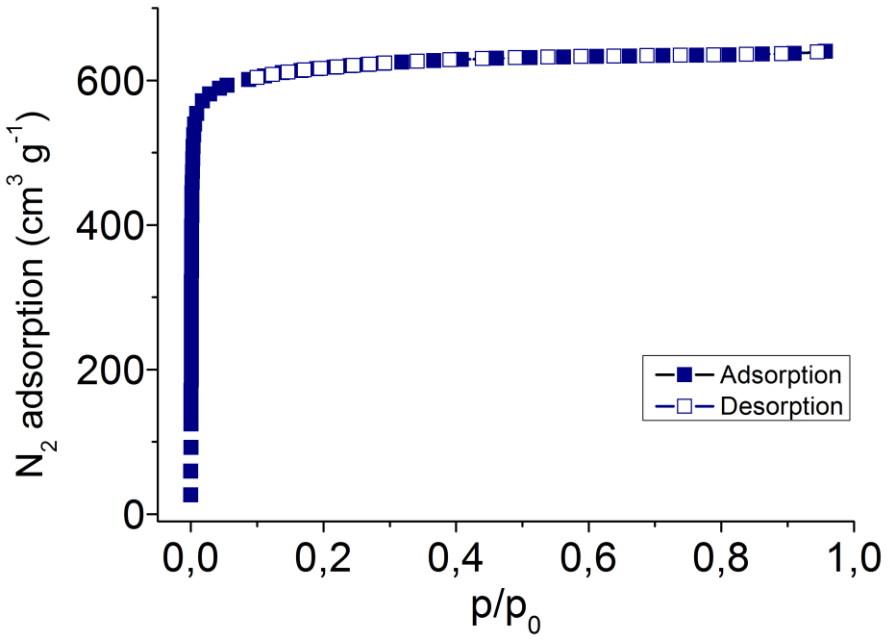

Figure 17. A typical adsorption/desorption isotherm of UiO-67.

The two most widely used isotherms for adsorption are the BET and Langmuir isotherms, and both methods are used in MOF publications. The Langmuir isotherm is a model of single-layer adsorption on microscopically flat surfaces (Langmuir himself experimented on glass, platinum and mica surfaces)[60], and given the very non-flat pore geometry of MOFs it may produce incorrect estimates of surface area for such materials.

The BET isotherm, named after the inventors Stephen Brauner, Paul Emmet and Edward Teller, is a model of multilayer adsorption derived from Langmuir's theory[61]. In a combined experimental and computational study, Walton and coworkers have found very good agreement between BET surface areas from isotherms obtained experimentally and by simulation, and purely geometrical calculations of surface area from the crystal structure. Their conclusion is that BET surface area obtained with nitrogen adsorption at 77 K is remarkably accurate for many MOF materials, even when the dominating adsorption mechanism is pore-filling rather than layering[62]. This method was used, since reported surface areas should be as realistic as possible.

The BET equation is $\frac{p}{V_a(p_0-p)} = \frac{1}{V_m c} + \frac{c-1}{V_m c}\frac{p}{p_0}$, where V_m is the volume required to form a complete monolayer of adsorbent and c is the BET constant. $c = e^{\frac{\Delta H_{ads,1} - \Delta H_l}{RT}}$, the enthalpy terms being the adsorption enthalpy of the first monolayer and the condensation enthalpy. Plotting $\frac{p}{V_a(p_0-p)}$ against $\frac{p}{p_0}$ should give a straight line intercepting the y axis at $\frac{1}{V_m c}$ and with $\frac{c-1}{V_m c}$ as the slope[61]. This model is usually fitted to a region of the adsorption isotherm where the formation of the monolayer is assumed to occur ($0.05 < \frac{p}{p_0} < 0.3$), and the surface area can be derived by applying the cross-sectional area of the adsorbent (σ_0 = 16,2 Å^2 for N_2) using $A_{BET} = v_m \sigma_0 N_{AV}$. However, since MOFs are porous materials, the monolayer will usually have formed in the pores before reaching this pressure range. The most accurate results are in fact obtained by applying the BET theory over the

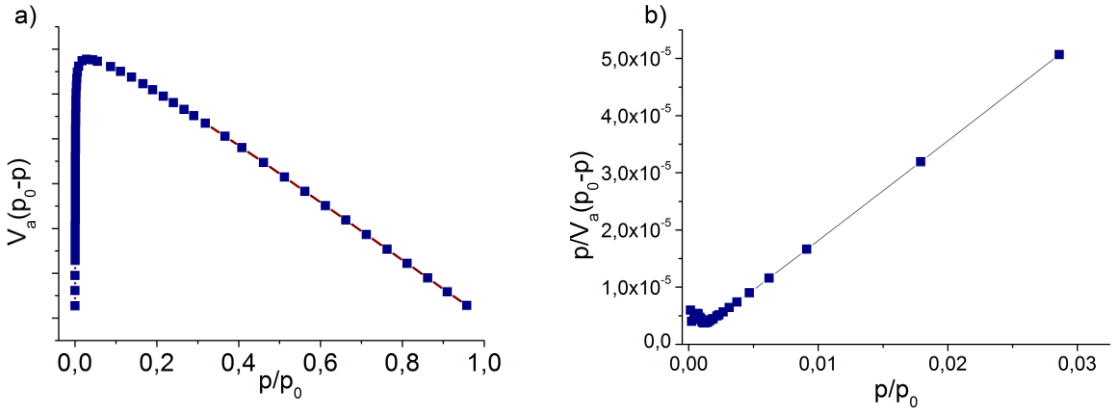

Figure 18. Representations of the adsorption isotherm plotted against p/p0. (a) is used to determine which pressure region to use, and (b) is the linear region of the BET isotherm.

pressure range identified by established consistency criteria. Walton describes these consistency criteria as (1) In the region, values of $V_a(p_0 - p)$ should increase with $\frac{p}{p_0}$, and (2) c should be positive. Criterion (1) is met when the relative pressure starts to rise significantly with each new dosing of adsorbent, i.e. when the adsorption isotherm reaches a plateau (see figure 10).

While theoretical calculation of internal surface areas in MOFs is a relatively new field, it is argued that the solvent accessible Connolly surface area (with the solvent being the adsorbent gas) is the most realistic approximation[63]. The surface areas in this work were calculated using the Atom volumes and surfaces module of the Materials studio software, wherein a probe molecule of a defined size is rolled over the Connolly surface[64]. Table 1 shows the theoretical surface areas for UiO-66 and 67 using this method:

Table 1. Calculated surface areas of UiO-66 and 67.

	UiO-66	UiO-67
Connolly surface	2379 m^2/g	3104 m^2/g
Solvent surface area	1098 m^2/g	2810 m^2/g
Accessible solvent surface area	429 m^2/g	2802 m^2/g

The accessible surface area of UiO-67 seem to agree reasonably well with measured BET surface areas (3000 m^2/g), but is clearly too low for UiO-66 (measured to 1400 m^2/g)[28]. A reason for this could be that UiO-66 has very narrow channels, which could be counted as inaccessible by the model. Either way, the deviations between theoretical and measured values could indicate shortcomings in the models.

One of the key abilities of MOFs is their adsorption capacity. A candidate MOF for industrial application should have high accessible surface area, and be stable without the presence of solvent in the pores. Standard sorption measurement gives the specific surface area of the MOF, in BET or Langmuir surface area. The residue can be analyzed by PXRD to check if the crystallinity is still intact, or if the structure collapses when guest molecules are removed.

Sorption measurements were used to investigate how different synthesis and functionalization methods affect surface area and stability upon high-vacuum activation.

1.13.3 SEM and EDXS

In a scanning electron microscope (SEM), an incident electron beam is fired from an electron gun, focused by an electromagnetic condenser lens and directed towards the sample. Electrons are then

re-emitted from the sample, directly from the sample surface as *backscattered* electrons, or as ionization products of the incident beam as *secondary* electrons. These electrons are detected, and used to create an image of the sample. In addition, ionization creates characteristic X-rays which can be detected and used to determine the elemental composition of the sample, called Energy-Dispersive X-ray Spectroscopy (EDXS)[58].

The size and morphology of crystals in the size range 10-1000 nm are too small to determine morphology and size distribution by optical microscopy, and have thus been analyzed with SEM.

SEM was used to determine the degree of agglomeration, along with crystal size and morphology. The EDXS is used to determine the presence of metals and chlorine and get estimates on their concentration in relation to zirconium.

EDXS spectra show some variation in the results, due to sample preparation issues (sample thickness varies) and noise. This makes it necessary to view the results with some skepticism, especially the elements that are present in low concentrations.

1.13.4 TGA

Thermogravimetric analysis is heating a sample in a reactor while on a very fine scale, plotting temperature and sample weight against time. Some instruments will also report heat flow, thus giving information whether changes in the sample are endothermic or exothermic. The gas flow through the reactor can be controlled, and the effluent gas can be monitored with GC and/or MS.

TGA is a very useful tool when analyzing MOFs, since it shows sample decomposition temperature in different atmospheres, amount of solvent in the sample and information about the thermodynamics of each step. Coupled with MS, the ratio between guest solvent(s) and absorbed water, plus decomposition products can be determined.

TGA was used to test solvent loading and thermal stability of the MOFs in different atmospheres.

1.13.5 MS

Mass spectrometry is the common name for a wide range of analysis techniques that gives information about the mass of chemical compounds. This is achieved by vaporizing and ionizing the sample, and to separate these ions according to their mass to charge ratio[65].

1.13.6 EXAFS

Electrons occupying atomic orbitals can be excited by electromagnetic radiation at energies above the ionization energy of that orbital. These energies, also called absorption edges, are measured in X-

ray Absorption Spectroscopy (XAS). The XAS is obtained by regular transmission spectroscopy of a sample pellet, using an X-ray source with an accurate monochromator to scan the desired region of the X-ray spectrum. The atom of which absorption edge is measured is called the central atom.

Extended X-ray absorption fine structure (EXAFS) is the oscillating part of the X-ray Absorption Spectrum (XAS) that extends to about 1000 eV above an absorption edge of a particular element of a sample. Being a very sensitive technique, EXAFS requires a very high photon flux to obtain enough information. It is therefore usually performed at synchrotrons.

The EXAFS oscillations occur due to interference with neighboring atoms of the adsorption edge being measured. Simply put, the oscillating part of the spectrum is extracted and Fourier transformed using the EXAFS equation, to yield radial distribution functions. The functions can be plotted in real and imaginary space, giving information about the distance between the central atom and neighboring atoms, and their multiplicity.

1.13.7 NMR

Nuclear Magnetic Resonance (NMR) is a very powerful technique for characterization and determination of purity, especially in organic chemistry.

Many atomic nuclei have an odd number of protons and/or neutrons, thus having an intrinsic magnetic moment, or spin. When subjected to a magnetic field, an energy gap is induced between the spin states: $\Delta E = \hbar \gamma B_0$, where B_0 is the applied magnetic field and γ is the magnetogyric ratio, unique to each nucleus. The ratio between spins in the different energy states (α and β) are given by the Boltzmann distribution $\frac{N_\beta}{N_\alpha} = e^{\frac{-\Delta E}{kT}}$. Short pulses of radio frequency radiation are directed at the sample, causing the spin states to resonate between the states when the photon energy matches the energy gap ΔE. The interaction can be measured and can be transformed to an NMR spectrum.

The magnetogyric ratio is influenced by electrons shielding the nucleus, which in turn results from the neighboring chemical environment of the atom. Thus, chemically different nuclei have different distributions between spin states, affecting the resonance. This results in different chemical shifts on the NMR spectrum.

NMR is usually performed in solution, providing free rotation for the dissolved molecules. 1H-NMR is very useful in the characterization of functionalized bipyridine linkers, as the coordinated metal changes the chemical shift of neighboring protons.

NMR can also be used on solid samples such as MOFs. The immobility of the sample is compensated by magic angle spinning (MAS) of the sample during the experiment. Solid state ^{1}H-NMR was in this work used to characterize metal-functionalized MOFs. By comparing the chemical shift of bipyridine alpha-protons in functionalized and un-functionalized MOFs it should be possible to determine if the functionalization is indeed where anticipated.

1.13.8 FTIR spectroscopy

The energy of most molecular vibrations corresponds to that of the infrared region of the electromagnetic spectrum. The infrared spectrum spans photon wavelengths from 750 nm to 1 mm, but infrared spectra are usually labeled cm^{-1}. A sample is subjected to infrared light, and the absorbed wavelengths give information about bonds in the sample. In Fourier transform IR spectroscopy, an interference pattern is generated by combining two beams containing the whole frequency range, one of which transmitted through the sample. This *interferogram* is then Fourier transformed into a spectrum[65].

1.13.9 UV-vis spectroscopy

The radiation energy in the UV-visible region of the electromagnetic spectrum corresponds to transitions between electronic energy levels. In the range from 200 – 700 nm, excitation of electrons from p- and d-orbitals, π-orbitals and conjugated π-systems gives rise to informative spectra[65].

2 Experimental

This section describes the synthesis and characterization of linkers and MOFs. The functionalizations investigated in this work are shown in Figure 19. All organic syntheses will be describes in this section, as will representative examples of MOF syntheses of the three methods described. For a full description of all MOF syntheses and characterization raw data, see the appendix, pages 104 to 145.

2.1 General synthesis remarks

All chemicals obtained commercially were used without further purification, with the exception of DMF.

DMF (≥99.5 %, Merck) was purified using a MBraun MB-SPS-800 encapsulated solvent purification system. Tap water was distilled in a GFL 2002 distillatory. Solvents and 2-propanol (≥99.8 %, Sigma-Aldrich) and acetone (≥99.8 %, Sigma-Aldrich) were used as received.

Acids H_2SO_4 (98 %, VWR), HNO_3 (65 %, VWR), HCl (37 %, VWR), glacial acetic acid (100 %, VWR) and benzoic acid (≥99,5 %, SMPC) were used as received.

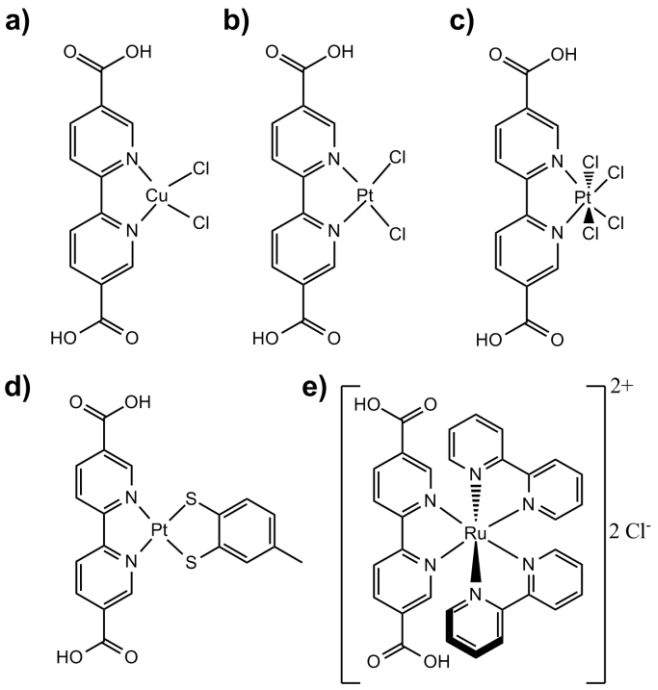

Figure 19. Functionalized linkers used in this work. (a) $CuCl_2(H_2bpydc)$. (b) $PtCl_2(H_2bpydc)$. (c) $PtCl_4(H_2bpydc)$. (d) $Pt(tdt)(H_2bpydc)$. (e) $[Ru(bpy)_2(H_2bpydc)_2]Cl_2$.

The reagents 2,2'-bipyridyl (reagent grade, Fluka), 5,5'-dimethyl-2,2'-bipyridine (98 %, Sigma-Aldrich), toluene-3,4-dithiol (>90%, Sigma-Aldrich), LiCl (reagent grade, Sigma-Aldrich), KOH (>99%, Sigma-Aldrich), KNO_3 (>99%, Sigma), K_2Cr_2O7 (≥98.5 %, Sigma), $CuCl_2{\cdot}2H_2O$ (>99%, Sigma-Aldrich), $ZrCl_4$ (≥99,5 % anhydrous, Sigma-Aldrich), $RuCl_3{\cdot}xH_2O$ (>98 %, Fluka), K_2PtCl_4 (>99%, Sigma-Aldrich) and $Na_2PtCl_6{\cdot}6H_2O$ (>98%, Strem chemicals) were used as received. Sigma-Aldrich defines "reagent grade" as ≥95 %.

Trans-Pt $Cl_2(Hpyc)_2$ was synthesized by Fredrik Lundvall. Para-terphenyl 4,4''-dicarboxylic acid (H_2tpdc) was synthesized by Søren Jakobsen, as described in literature[66].

2.2 Linker synthesis

2.2.1 Synthesis of 2,2'-bipyridine-5,5'-dicarboxylic acid (H_2bpydc)

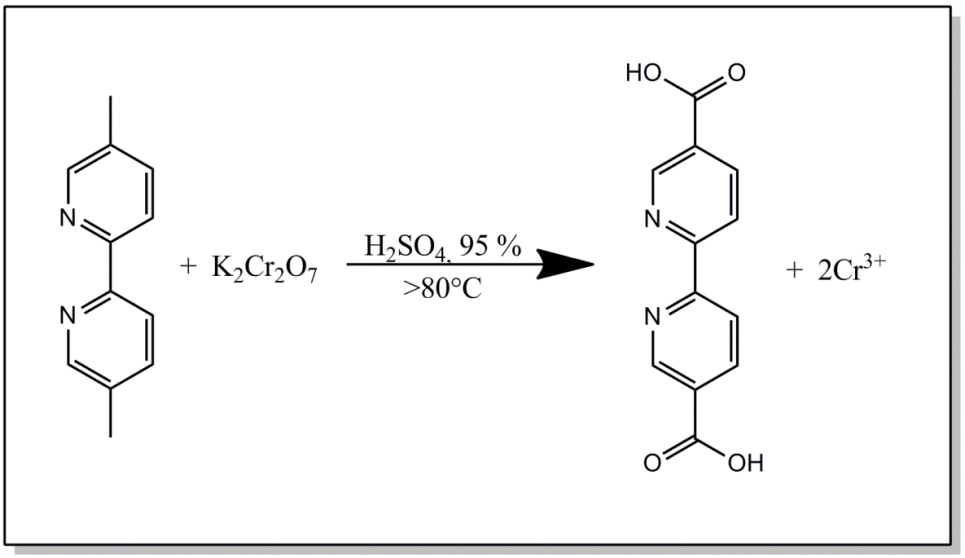

Figure 20. Synthesis of 2,2'-bipyridine 5,5'-dicarboxylic acid (H_2bpydc), reaction overview.

5,5'-dimethyl-2,2'-bipyridyl (5.00 g, 27.1 mmol)was dissolved in 125 mL concentrated sulfuric acid in a 250 mL round bottom flask. Potassium dichromate (24.0 g, 81.6 mmol) was added over approximately 30 minutes. The reaction is very exothermic, and thus the reaction vessel was cooled by an ice bath if the temperature exceeded 80°C in order to prevent further oxidation and unwanted byproducts. When the reaction was complete, the contents of the flask were poured into a 1 L beaker filled with ice and water. The crude product was isolated by filtration, washed five times in 100 mL portions of cold water and once in 100 mL acetone. The product was dried in air at 60°C. The final product weight was 6.24 g (Yield: 94.0 %)

The syntheses were repeated several times and gave high yields of 85 - 94 %. The product was identified by ^{1}H-NMR (300 MHz, DMSO-d6) δ 13.52 (s, 2H), 9.20 (dd, *J* = 2.2, 0.8 Hz, 2H), 8.58 (dd, *J* = 8.2, 0.9 Hz, 2H), 8.45 (dd, *J* = 8.3, 2.2 Hz, 2H). This is in perfect agreement with previously reported spectra of the same compound. See appendix (page 93) for spectrum with assignments.

2.2.2 Synthesis of $PtCl_2(H_2bpydc)$

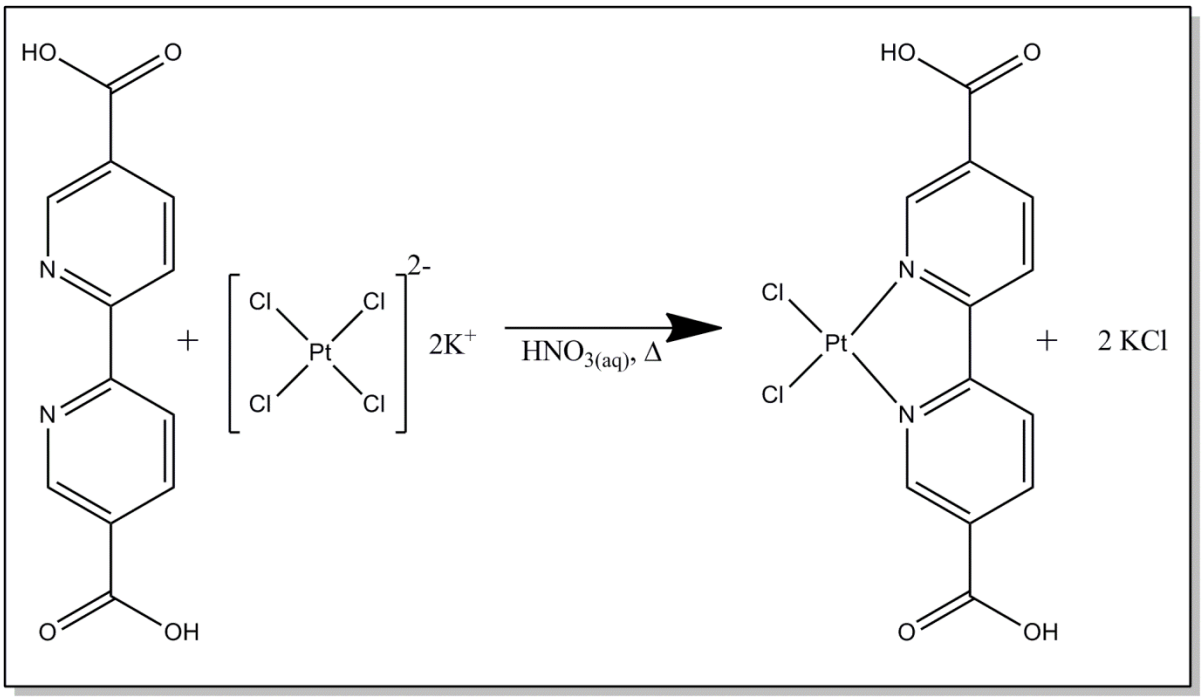

Figure 21. Synthesis of $PtCl_2(H_2bpydc)$, reaction overview.

K_2PtCl_4 (1005 mg, 2.42 mmol) and 65 % HNO_3 (2.0 mL, 29 mmol) were dissolved in 200 mL water in a 250 mL round bottom flask. H_2bpydc (505 mg, 2.07 mmol) was added, but was only suspended in the solution due to its poor solubility in acidic solution. The reaction was heated and stirred under reflux for 40 hours. The precipitated red powder was isolated by filtration and washed three times with water and once with 2-propanol. The powder was dried in air at 60° C, where it changed color to dark brown. It regained the red color upon rehydration and dissolved readily in hot DMF and DMSO, creating a clear, yellow solution. The final product weight was 800 mg (Yield in respect to starting H_2bpydc: 76.8 %)

The synthesis was repeated several times, and gave yields in the range 70 – 77 %. The product was identified by ^1H NMR spectra, which display typical ^{195}Pt coupling satellites as a broadening of the α-proton peak base. The acidic protons are barely visible, but can be observed as a very broad singlet. ^1H NMR (300 MHz, DMSO-d6) δ 14.27 (s, 2H), 10.02 (d, J = 1.7 Hz, 2H), 8.94 – 8.69 (m, 4H). The data is in perfect agreement with previously reported spectra. See appendix (page 95) for spectra with assignments.

2.2.3 Synthesis of $PtCl_4(H_2bpydc)$

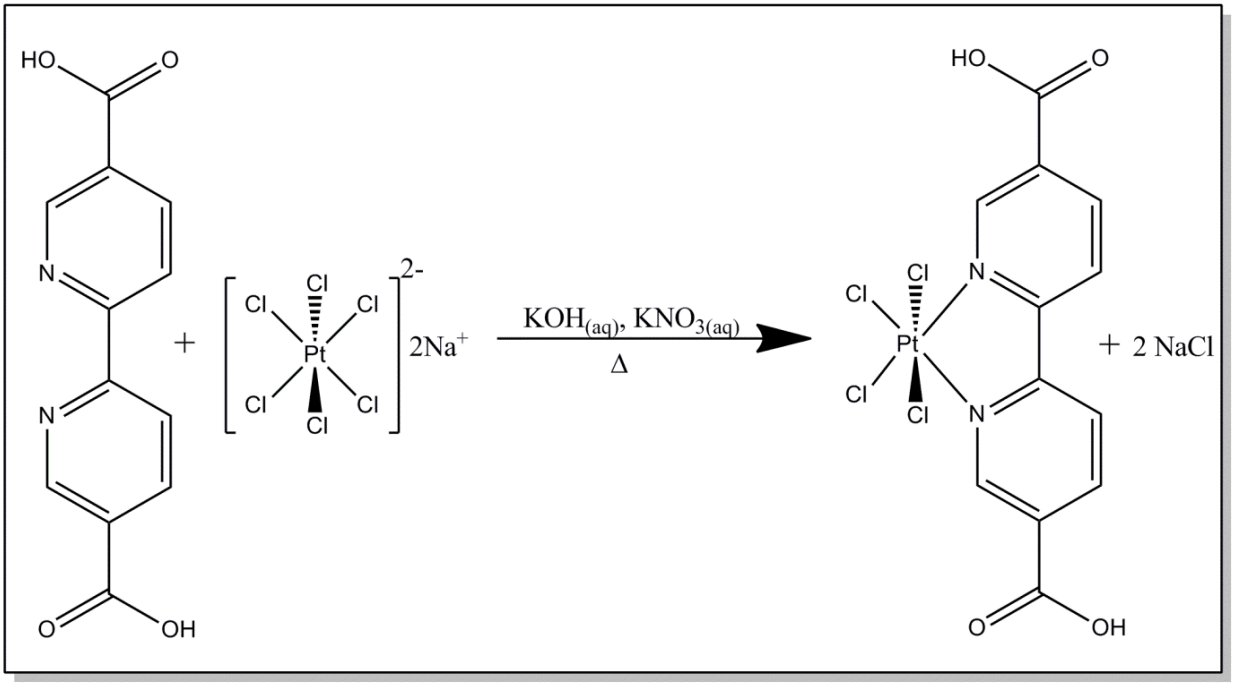

Figure 22. Synthesis of $PtCl_4(H_2bpydc)$, reaction overview.

$Na_2PtCl_6 \cdot 6H_2O$ (600 mg, 1.07 mmol), KNO_3 (1.00 g, 9.89 mmol) and KOH (90 mg, 1.38 mmol) were dissolved in 45 mL water in a 50 mL round bottom flask. H_2bpydc (250 mg, 1.03 mmol) was added, but was only suspended in the solution due to its poor solubility even in basic aqueous solution. The reaction was heated and stirred under reflux for four days. The precipitated yellow powder was isolated by filtration and washed three times with water and once with 2-propanol. The powder was dried in air at 60° C. The final product weight was 366 mg, or a yield of 61.5 % in respect to starting H_2bpydc.

The product was identified by ^{1}H NMR spectra, which display typical ^{195}Pt coupling satellites as separate peaks on both sides of the α-proton peak. The product was of acceptable purity, but shows traces (3-4%) of $PtCl_2(H_2bpydc)$, indicating that some of the platinum had been reduced. The acidic protons are not visible in the spectra, due to peak broadening. ^{1}H NMR (300 MHz, DMSO-d6) δ 9.97 – 9.83 (m, 2H), 9.19 (d, J = 8.5 Hz, 2H), 9.00 (d, J = 8.4 Hz, 2H). The 1H-NMR spectrum for this compound is not reported in the available literature, but the spectrum is similar to that of $PtCl_2(H_2bpydc)$. See appendix (page 96) for spectrum with assignments.

2.2.4 Synthesis of Pt(tdt)(H_2bpydc)

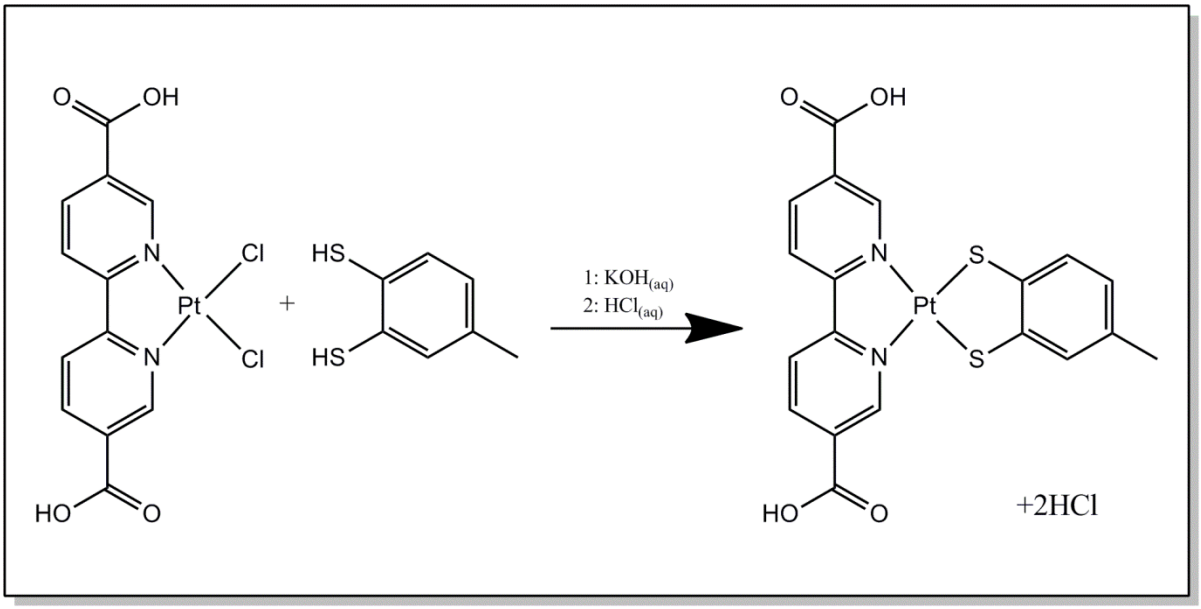

Figure 23. Synthesis of Pt(tdt)(H_2bpydc), reaction overview.

$PtCl_2$(H_2bpydc) (106 mg, 0.208 mmol) and H_2tdt (34 mg, 0.22 mmol) were dissolved in small amounts of 10 mL 0,1 M KOH in a 25 mL round bottom flask and stirred at ambient conditions for 24 hours. The solution gradually turned from yellow to dark purple. 0.1 M HCl was added drop wise, and a blue-black precipitate was formed. This powder was isolated by filtering, washed with water and dried in air. The synthesis gave poor yield (17% in respect to starting $PtCl_2$(H_2bpydc)), and the final product weight was 21 mg.

The product was identified by ^{1}H NMR, which display typical ^{195}Pt coupling satellites as a broadening of the α-proton peak base (δ 9.51). The acidic protons are barely visible, but can be observed as a very broad singlet. A small impurity (7 %) of unreacted H_2bpydc is present, indicating that the Pt-N coordination bonds are weakened in basic aqueous solution, in agreement with Søren Jakobsens research on similar compounds[49]. ^{1}H NMR (300 MHz, DMSO-d6) δ 14.20 (s, 2H), 9.51 (m, 2H), 8.76 (m, 2H), 8.67 (m, 2H), 7.11 (d, J = 7.9 Hz, 1H), 7.04 (s, 1H), 6.56 (d, J = 7.9 Hz, 1H), 2.21 (s, 3H). This is a reasonable agreement with reported data[52], considering different NMR solvents: ^{1}H NMR (300 MHz, D_2O-NaOD): δ 8.68 (2H, t), 8.16 (2H, d), 7.65 (2H, tt), 6.80 (1H, d), 6.71 (1H, s), 6.56 (1H, d), 2.22 (3H, s). See appendix (page 97) for spectrum with assignments.

2.2.5 Synthesis of [cis-Ru(bpy)$_2$]Cl$_2$

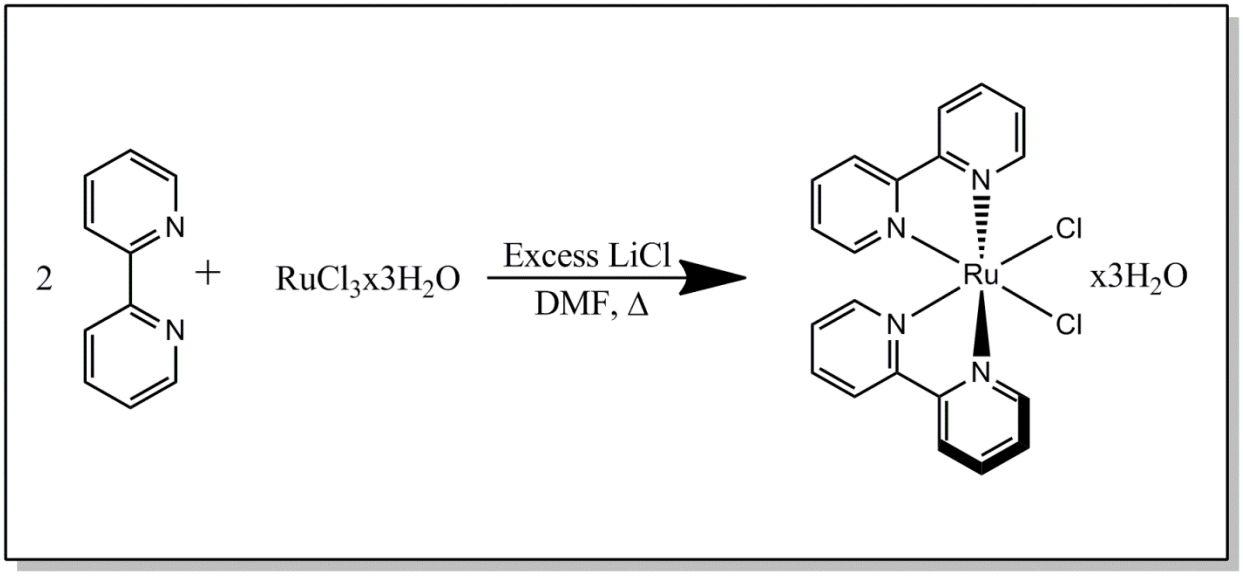

Figure 24. Synthesis of [cis-Ru(bpy)$_2$]Cl$_2$, reaction overview.

$RuCl_3 \cdot xH_2O$ (780 mg, 2.98 mmol), bpy (936 mg, 6.0 mmol), and LiCl (863 mg, 20.4 mmol) were heated and stirred under reflux in DMF (10 mL) for 8 hours. The reaction mixture was cooled to room temperature and 25 mL of reagent grade acetone was added, and a red-black precipitate was formed. Filtering yielded a red to red-violet solution and a dark red-black microcrystalline powder. The powder was washed three times with 20-mL portions of water followed by three 25-mL portions of THF and then dried in air at 60°C. The yield was 288 mg, or (Yield : 20 % based on starting amount of $RuCl_3 \cdot xH_2O$).

The product was identified by ^{1}H NMR. ^{1}H NMR (300 MHz, DMSO-d6) δ 9.97 (d, *J* = 5.2, 2H), 8.64 (d, *J* = 8.1 Hz, 2H), 8.50 – 8.45 (m, 2H), 8.06 (m, 2H), 7.76 (m, 2H), 7.68 (m, 2H), 7.51 (d, *J* = 5.8 Hz, 2H), 7.10 (m, 2H). This agree to some degree with previously reported data[67] (^{1}H NMR(CD_3CN) δ 8.63 – 8.53 (m, $H_{3,3'}$), 8.15 – 7.95 (m, $H_{6,6'}$), 7.75 – 7.68 (m, $H_{5,5'}$), 7.43 – 7.29 (m, $H_{4,4'}$)), with the exception of the high-shift peak at 9.97 ppm. The C_2 molecular symmetry means the protons occupying the same positions in each bpy are equivalent, but the protons occupying equivalent positions in each pyridine fragment are not.

See appendix (page 99) for spectrum with assignments.

2.2.6 Synthesis of $[Ru(bpy)_2(H_2bpydc)]Cl_2$

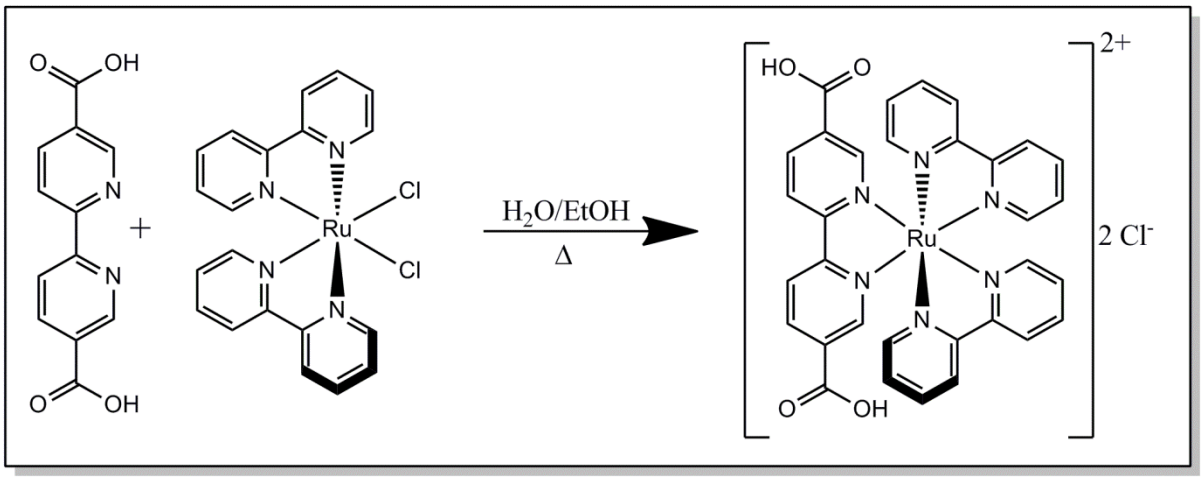

Figure 25. Synthesis of $[cis\text{-}Ru(bpy)_2(H_2bpydc)]Cl_2$, reaction overview.

The reaction was carried out as described by Xie and coworkers[55].

$[cis\text{-}Ru(bpy)_2]Cl_2$ (160 mg, 0.33 mmol) and 2,2'-bipyridine-5,5'-dicarboxylic acid (101 mg, 0.42 mmol) were added to a 20 mL mixture of ethanol and water in equal volumes, refluxed for 12 hours, then concentrated using a rotavapor. The resulting viscous red-black liquid was dried in air at 60°C. After two days an amorphous red-black powder was recovered. The yield was 167 mg, or 69 % based on starting $[cis\text{-}Ru(bpy)_2]Cl_2$.

The product was identified by ^{1}H NMR (300 MHz, DMSO-d6) δ 8.85 – 9.00 (m, 6H), 8.47 (m, 2H), 8.32 – 8.12 (m, 4H), 8.01 (m, 2H), 7.91 – 7.73 (m, 4H), 7.68 – 7.48 (m, 4H). The result is in good agreement with previously reported data[40]: 1H NMR (400 MHz, DMSO-d6) δ 8.99 (d, 2H), 8.89 (m, 4H), 8.53 (d, 2H), 8.20 (m, 4H), 7.99 (s, 2H), 7.84 (d, 2H), 7.78 (d, 2H), 7.59 (t, 2H), 7.49 (t, 2H).

See appendix (page 100) for spectrum with assignments.

2.2.7 Synthesis of $CuCl_2(H_2bpydc)_x$

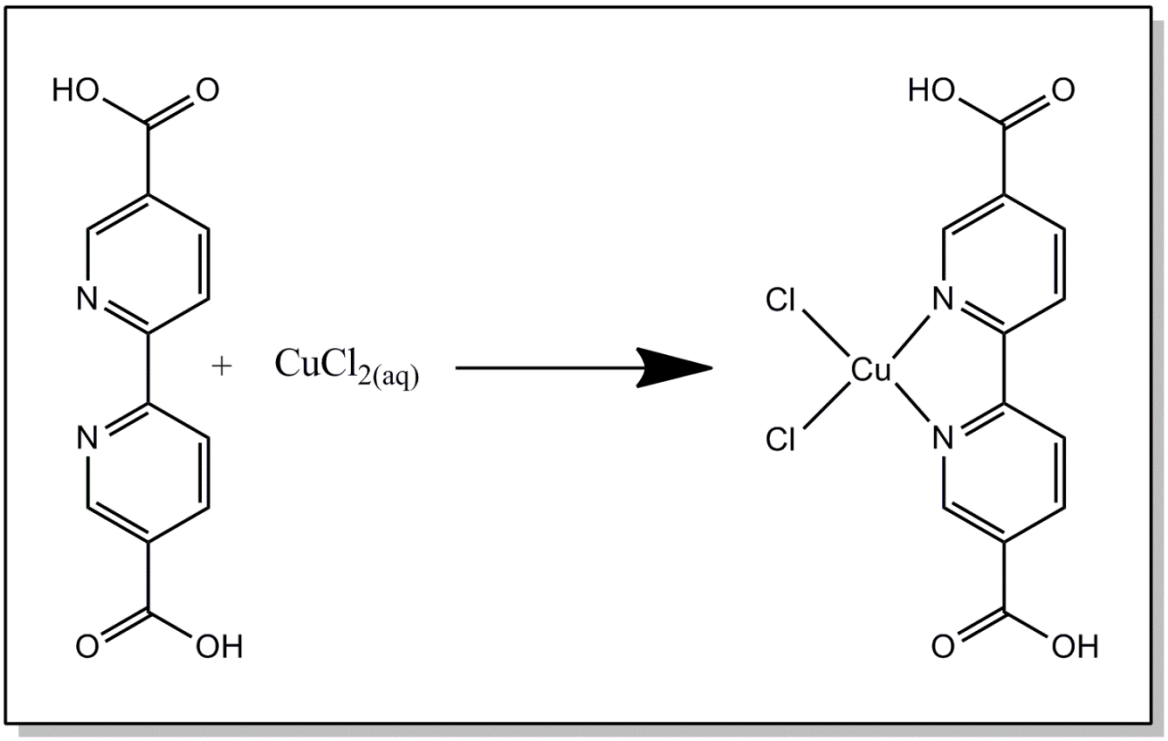

Figure 26. Synthesis of $CuCl_2(H_2bpydc)$, reaction overview.

The reaction was carried out in a method analogous to that described by Goddard and coworkers[56], differing in that the 3,3'-dicarboxylic acid was the target of their studies.

H_2bpydc (505 mg, 2.07 mmol) and $CuCl_2 \cdot 2H_2O$ (365 mg, 2.09 mmol) were dissolved in water in separate beakers, the former in a minimal concentration of KOH. The solutions were combined, and a green precipitate formed immediately. A small amount of 0.1 M HCl was added to acidify the solution. The precipitate was filtered, washed with water and dried in air at 60° C. The yield was 410 mg, or 52.3 % based on starting H_2bpydc.

^1H NMR in basic D_2O was carried out, but no meaningful spectrum was obtained. Only distorted peaks in the HOD and aromatic region were observed. This severe broadening of the peaks occurs as a result of paramagnetic broadening from the d^9 Cu^{2+} ion. The compound was insoluble in DMSO, even when heated, but soluble in DMF.

A PXRD pattern was acquired, and matched neither of the starting materials. It was then assumed that the desired product was formed, and it was used successfully in MOF synthesis. By slow evaporation, single crystals of sufficient size for single crystal XRD were recovered. However, due to instrument malfunction, no pattern has yet been recorded. The compound was also characterized with EXAFS. Due to the inconclusive characterization, the compound is named $CuCl_2 \cdot$(H2bpydc).

2.3 Synthesis of UiO-67

The following text is a detailed description of the general synthesis procedure, followed in all of the MOF syntheses. Illustrating examples will be presented for each of the three main methods used. The specific synthesis procedures for all the compounds are found in the appendix, pages 104 to 145.

$ZrCl_4$ and water are dissolved in DMF. Heating and stirring is necessary to get a clear solution. Upon addition of $ZrCl_4$ to DMF, a cloud of HCl vapor immediately emerging from the solution is often observed.

When a clear solution is obtained, a large amount (usually 5 or 30 molar equivalents with respect to $ZrCl_4$) of monocarboxylic acid is added to function as a modulator. Benzoic acid and acetic acid has been used for such a role in this work.

Once the modulator is dissolved, the linker is added. H_2bpdc is soluble in a molar ratio of about 1:250 in hot DMF. The solution may be heated as high as 130 °C at this point to improve solubility. H_2bpydc and metal functionalized linkers are soluble in various degrees, but all are soluble to at least a 1:1000 molar ratio to DMF. Typically, the linker concentration used is 1:500, where it is rarely a problem to dissolve the linker if the temperature is high enough. The acids tend to agglomerate, thus it is recommended to crush the acid particles before addition.

In a one-pot synthesis, the metal salt is added at this point, in a molar ratio equal to H_2bpydc. Some salts, like $RhCl_3$, are scarcely soluble in DMF, but will dissolve during the MOF synthesis, as any dissolved salt will be consumed by the linker. It is recommended to crush the salt crystals in a mortar to ease this process. Sonication was sometimes used to facilitate the solution of sparingly soluble compounds.

When the linker (and salts, if required) is dissolved, the reaction will start. The magnet bar is removed, and the flask is kept at 80 – 130 °C for at least 4 days. It is not necessary to seal the flasks completely, but solvent must be prevented from evaporating by a cap or refluxing arrangement.

After the reaction is complete, the MOF product can be observed as a precipitate that covers the bottom of the reaction flask. The solvent can usually be decanted off, but it is sometimes necessary to centrifuge or filter to recover smaller particles. Different washing procedures have been tested

and evaluated and are described later. For metal modified samples, and samples made with high modulator concentrations, washing is necessary. First, the powder is suspended in anhydrous DMF and thoroughly stirred for several minutes. DMF is then removed by centrifugation and decanting. This is repeated two more times, and samples made with high modulator concentration should be stirred overnight at least once.

When the DMF wash is complete, the sample is washed three times with THF or 2-propanol in order to solvent exchange with DMF. These higher vapor pressure solvents allow for the facile activation of the MOF.

The powder is dried in air at 60 °C. It is then weighed, and the yield is calculated. This is not the real yield, since the pores are partly filled with water and solvent. TGA shows that the mass of the solvent left in the pores can be more than the mass of the MOF itself, but most often it accounts for about 40 % of the total mass. The relative yields are assumed to be comparable, since all UiO-67 undergo the same treatment.

The dry powder must be stored in a desiccator to prevent decomposition, as UiO-67 is unstable in water. The powder is hygroscopic, and absorbs significant amounts of water even when it is stored in a sealed vial in a desiccator with dry silica gel. Because of this, yields are never absolutely correct, and solvent fractions are not expected to be constant. UiO-67 is stable even when it is fully evacuated, so the powder can be stored in inert gas in an airtight container after evacuation at 300 °C.

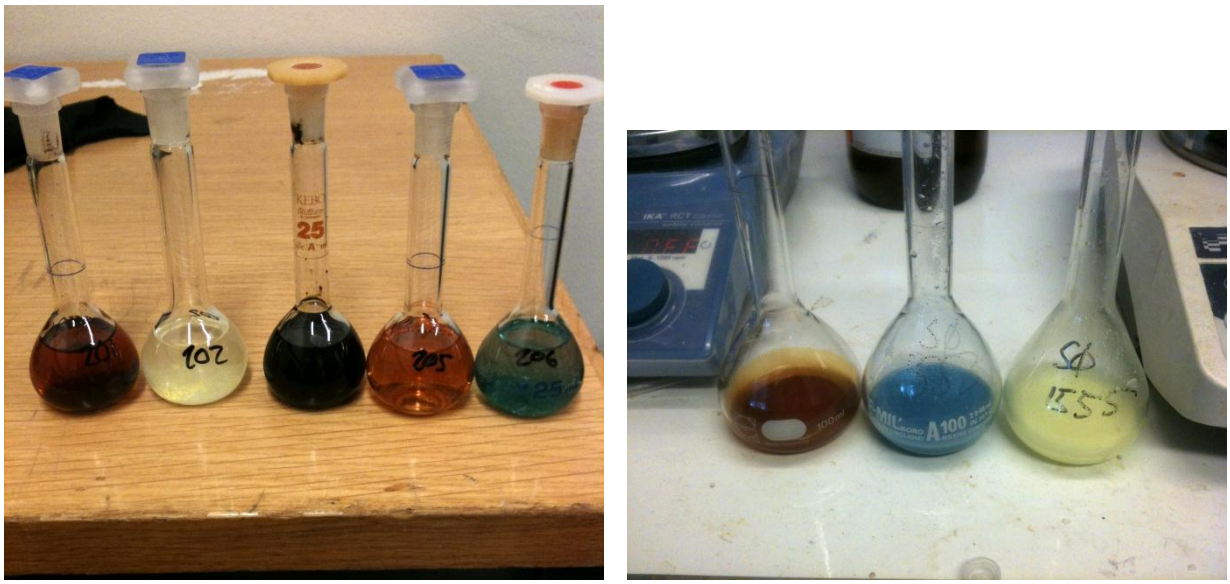

Figure 27. First photo: Prepared solutions for one pot synthesis. From left: $IrCl_3$, K_2PtCl_4, $RuCl_3$, $Pd(NO_3)_2$ and $Rh(CH_3CO_2)_2$. Second photo: MOF powders in solution as synthesized. From left: UiO-67-$Ru(bpy)_3$, UiO-67-Pt(tdt) and UiO-67-$PtCl_4$.

2.3.1 MOF synthesis using pre-functionalized linkers

Synthesis with premade linkers was carried out as previously described. The specific linkers used were $PtCl_2(H_2bpydc)$, $PtCl_4(H_2bpydc)$, $Pt(tdt)(H_2bpydc)$, $[Ru(bpy)_2(H_2bpydc)]Cl_2$ and a copper(II) based powder that was assumed to be $CuCl_2(H_2bpydc)$. The ratio of functionalized linker to H_2bpdc was in every case 1:9, with the exception of $Pt(tdt)(H_2bpydc)$, where a ratio of 1:19 was used.

The solutions with $PtCl_2(H_2bpydc)$ and $PtCl_4(H_2bpydc)$ were bright, clear yellow, and the resulting powders were also yellow. The powder of the Pt(II)-functionalized was more strongly colored than that functionalized with Pt(IV). The solution with $Pt(tdt)(H_2bpydc)$ was deep blue, and the resulting powder was blue. The solution with $[Ru(bpy)_2(H_2bpydc)]Cl_2$ was a very dark red, and the resulting powder was terracotta brown. The solution with the $Cu(H_2bpydc)$-compound was bright green, and the resulting powder was turquoise.

Example: Synthesis of Pt2-PM-1

$ZrCl_4$ (602 mg, 2.58 mmol) and H_2O (61 µL, 3.4 mmol) were dissolved in 100 mL DMF while stirring. The solution was heated, and benzoic acid (1.58 g, 12.9 mmol), H_2bpdc (563 mg, 2.33 mmol) and $PtCl_2(H_2bpydc)$ (132 mg, 0.258 mmol) were added. A clear, yellow solution was obtained after a few minutes of stirring. The solution was kept at 95 °C for 4 days.

The solution was decanted off, and a yellow crystalline powder was recovered. The powder was then washed 3 times in 15 mL portions of anhydrous DMF and 3 times in 15 mL portions of 2-propanol, before it was dried in air at 60 °C. The dry powder was weighed and stored in a desiccator. The product weight was 833 mg, and the solvent fraction was found to be 42 % by evacuation. Thus the dry product weight was estimated to 481 mg and the final yield to 52 % ($Yield_{max}$: 921 mg).

2.3.2 One-pot MOF synthesis

The ratio of H_2bpydc to H_2bpdc was in every case 1:9. This was dissolved in DMF, along with 5 equivalents of benzoic acid and acetic acid (in parallel synthesis series), and 1.3 equivalents of water (to $ZrCl_4$). The following metal salts were added in a 1:1 ratio to H_2bpydc: $Fe(NO_3)_3{\cdot}9H_2O$, $CoCl_2{\cdot}6H_2O$, $NiCl_2{\cdot}6H_2O$, $Cu(CH_3CO_2)_2{\cdot}H_2O$, $CuCl_2{\cdot}2H_2O$, $RuCl_3{\cdot}xH_2O$, $RhCl_3{\cdot}xH2O$, $Pd(NO_3)_2{\cdot}2H_2O$, $IrCl_3{\cdot}xH_2O$, K_2PtCl_4 and K_2PtCl_6 (or $Na_2PtCl_6{\cdot}6H_2O$). The clear, colored solutions were placed in an oven and heated at 95 °C for four days. The resulting colored powders were washed in DMF and 2-propanol, and then dried.

A parallel series was also made with 100 % H_2bpydc linker, with a metal salt addition of 10 %. The other synthesis parameters remained unchanged. It was not possible to form a completely clear solution of this mixture prior to the reaction due to the low solubility of H_2bpydc in DMF.

Example: Synthesis of Pt2-OP-2

$ZrCl_4$ (120 mg, 0.517 mmol) and H_2O (12 µL, 0.67 mmol) were dissolved in 20 mL DMF while stirring. The solution was heated, and H_2bpydc (13 mg, 0.052 mmol), H_2bpdc (113 mg, 0.465 mmol), acetic acid (148 µL, 2.59 mmol) and K_2PtCl_4 (21 mg, 0.052 mmol) were added. A clear, yellow solution was obtained after a few minutes of stirring. The solution was kept at 95 °C for 4 days.

The solution was decanted off, and a yellow crystalline powder was recovered. The powder was then washed 3 times in 15 mL portions of anhydrous DMF and 3 times in 15 mL portions of 2-propanol, before it was dried in air at 60 °C. The dry powder was weighed and stored in a desiccator. The product weight was 94 mg, and the solvent fraction was found to be 41 % by evacuation. Thus the dry product weight was estimated to 55 mg and the final yield to 30 % ($Yield_{max}$: 184 mg).

2.3.3 Post synthesis functionalization of UiO-67

UiO-67 with 10 % H_2bpydc or $PtCl_2(H_2bpydc)$ linker was synthesized as previously described. In a liquid-solid reaction, the MOF powder was then suspended in a DMF or 2-propanol solution with the functionalizing agent. The suspension was stirred for a period, and often heated, until the reaction was complete. The solvent was removed by centrifuge and decanting, washed with 2-propanol, and the powder is dried in air at 60 °C.

In this way, UiO-67 with 10 % H_2bpydc linker was functionalized with K_2PtCl4, K_2PtCl_6 and $Ru(bpy)_2Cl_2$ in hot DMF (100°C), and with $CuCl_2{\cdot}2H_2O$ in 2-propanol at room temperature. UiO-67 with 10 % $PtCl_2(H_2bpydc)$ linker was functionalized with H_2tdt in 2-propanol at room temperature, where the color was observed to change rapidly from yellow to blue (Figure 28).

Figure 28. PSF of Pt-PM-1 with H2tdt over 3 hours.

Gas phase functionalization was achieved by heating the powder in a cell in the presence of a gas. In an attempt to reduce Pt(II) to Pt(0), UiO-67 with 10 % $PtCl_2(H_2bpydc)$ linker was heated to 300 °C in a 10 mL/min flux of 3 % H_2 in He. The powder changed color from yellow to dirt brown. The same procedure was used before dosing in CO in the *in situ* FTIR spectroscopy studies and gaseous benzene in the *in situ* EXAFS studies.

Example: Synthesis of Pt2-PS

300 mg UiO-67-bpy-2 (approximately 0.050 mmol bpy sites with a solvent loading of 41 %) was suspended in 15 mL anhydrous DMF in a 50 mL Erlenmeyer flask. K_2PtCl_4 (22 mg, 0.053 mmol) was added and dissolved under stirring. The suspension was heated to 100 °C and left overnight. A yellow powder was recovered, washed 3 times in 15 mL portions of 2-propanol and dried in air at 60 °C.

The dry powder was weighed and stored in a desiccator. The product weight was 288 mg, and the solvent fraction was found to be 25 % by evacuation. Thus the dry product weight was estimated to 170 mg and the final yield to 96 % ($Yield_{max}$: 177 mg).

2.4 UiO-68

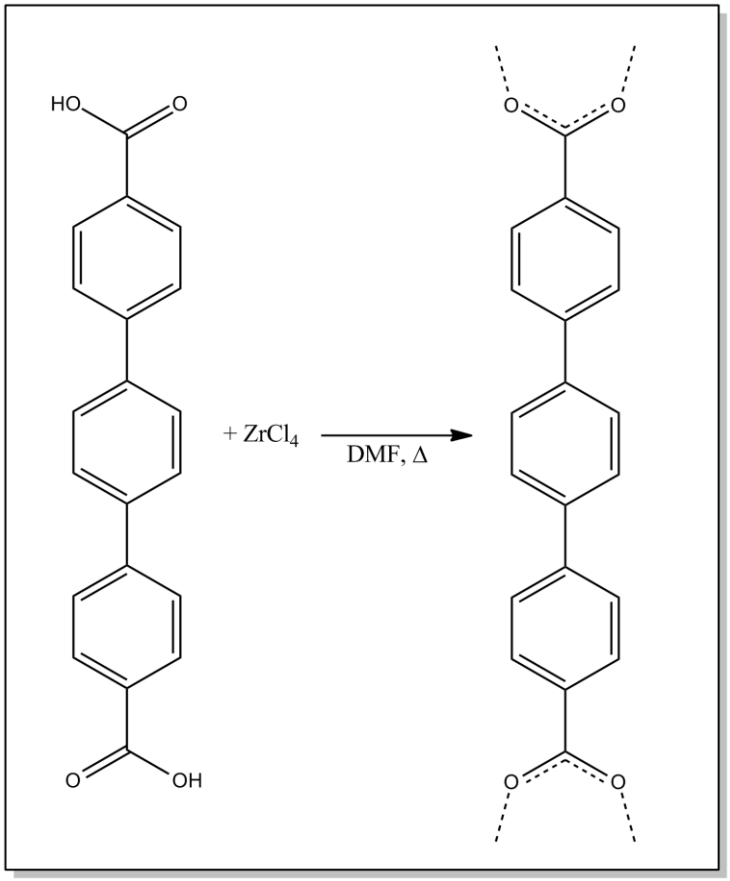

Figure 29. Synthesis of UiO-68, schematic.

All ingredients were transferred to a dry glove box.

$ZrCl_4$ (100 mg, 0.43 mmol) were dissolved in 100 mL DMF while stirring, in a 250 mL glass volumetric flask. The solution was heated and benzoic acid (16 mg, 0.13 mmol) was added, dissolving completely to obtain a colorless solution. H_2tpdc (137 mg, 0.43 mmol) was added to the solution. A clear, weakly yellow solution was obtained after about 20 minutes of stirring. The magnet was then removed and the volumetric flask was sealed, and then removed from the glove box. The seal was briefly removed only to add H_2O (10 µL, 0.56 mmol). The flask was kept at 100 °C for 4 days.

The flask was then taken out and cooled to room temperature. The now weakly yellow solution was decanted off, and a yellow powder was recovered. A PXRD pattern was acquired, showing broad peaks where the strongest reflections for UiO-68 are expected. The powder was dried in air at 60 °C. The product weight was 171 mg.

2.5 UiO-70, A new Zr-MOF

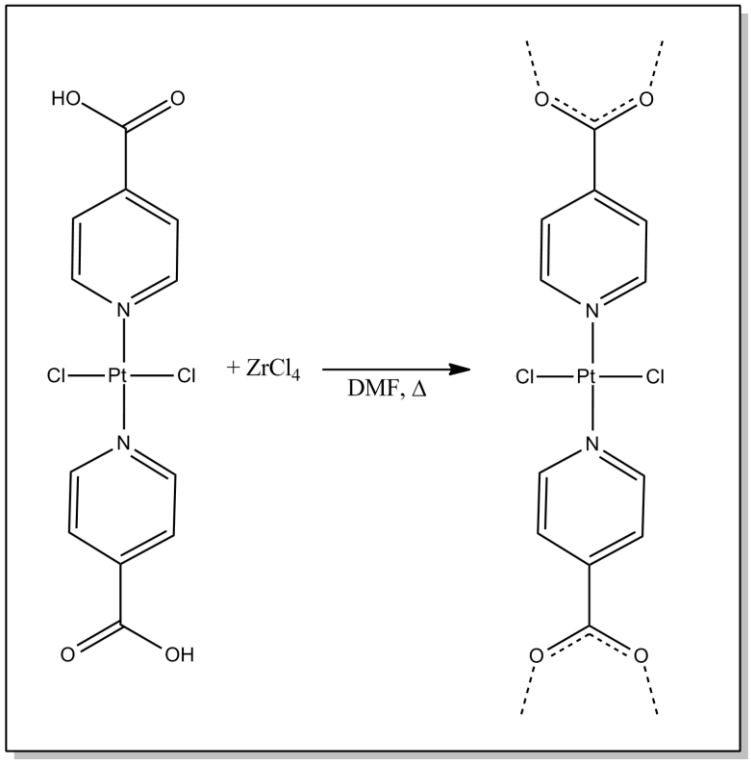

Figure 30. Synthesis of UiO-70, schematic.

The synthesis and structure of UiO-70 were reported in September 2011[68]. The general synthesis procedure for UiO-67 was followed.

$ZrCl_4$ (96 mg, 0.41 mmol) and H_2O (22 µL, 1.2 mmol) were dissolved in 8 mL DMF while stirring. The solution was heated and benzoic acid (1.54 g, 12.4 mmol) was added, dissolving completely to obtain a colorless solution. Trans-$[Pt(Hpyc)_2Cl_2]$ (211 mg, 0.41 mmol) was added to the solution. A clear, yellow solution was obtained after a few minutes of stirring. The magnet was then removed, and the solution is kept at 95 °C for 4 days.

The flask was then taken out and cooled to room temperature. The now weakly yellow solution was decanted off, and a yellow powder was recovered. A PXRD pattern was immediately acquired. A subsequent series of patterns showed the product decomposing to an amorphous state. Due to the instability of the compound, it was stored in DMF in a sealed vial. It was not possible to determine a product yield, but a qualified guess is around 50 %, based on the volume of the sample.

2.6 Characterization

2.6.1 PXRD

All PXRD patterns have been recorded on a Bruker D8 Discovery diffractometer with a Bruker LYNXEYE detector.

The powder samples (in amounts just enough to cover the Ø 2 cm glass plate) were dispersed onto a sample holder with 2-propanol. In some cases, dry powder was mounted on the sample holder, and plastic wrap was used to keep the powder on the plate. Different foils turned out to be diffracting in various degrees, and patterns of these are shown in the appendix, page 103.

2.6.2 Gas sorption measurements

All adsorption measurements were done on a BelSorp mini II adsorption instrument with nitrogen as the adsorbent at 77 K. The instrument continuously measures the dead volume in a separate cell to compensate for the inevitably sinking level of liquid nitrogen[69].

Surface area values were estimated by applying BET theory to the adsorption isotherm as described in the theory section. The theory has yet to be fully elaborated on Zr-MOFs, but they show the same type II isotherm as IRMOFs and are thus assumed to follow the same trend.

All samples were measured in 9.001 cm^3 glass cells. The activation procedure was 1 hour at 80 °C and 2 hours at 300 °C under vacuum. The cells are kept attached to the instrument between activation and measurement to prevent the sampled from adsorbing.

2.6.3 SEM and EDXS

All powders were mounted on carbon tape, just a few micrograms of each. Even though UiO MOFs are poor conductors, the powders were measured as they were, without metallic coating.

The instrument used in this work was a FEI Quanta 200 FEG-ESEM equipped with a Na EDS detector from EDAX. The internal error of an elemental peak in the EDXS spectrum is given as one standard deviation for the elemental peak intensity, and can be very high for low concentration elements.

2.6.4 TGA

Around 30 mg of powder was placed in a crucible and carefully placed in the TGA. A flow program was then initiated, keeping a constant atmosphere for the sample. The flows used were inert (pure dry N_2), synthetic air (20% O_2, 80% N_2) and 3% H_2 in He. All experiments were continuous ramping of temperature, 5° C increase per minute, unless otherwise stated.

All measurements were made on a Stanton Redcroft TGA.

2.6.5 MS

MS was used with TGA and EXAFS to identify compounds leaving the MOFs under activation. In both set-ups the flow gas was H_2/He mix, and a constant flow was kept through the cell. The purpose of the experiment was to detect hydrochloric acid after reducing MOF-incorporated $PtCl_2$ with hydrogen.

2.6.6 EXAFS

EXAFS was used to characterize the local environment around Pt and Cu atoms. Precursors and products were analyzed and compared. All samples were prepared as pellets of appropriate thickness and placed in an EXAFS cell with gas flow. The gas used was a mixture of 3 % H_2 in He. Long-acquisition spectra were made of all samples at room temperature. Then, the samples were gradually heated to 500 degrees while acquiring quick EXAFS spectra continuously. The experiments were performed at beam line I811 at MaxLab at the University of Lund, Sweden.

In an attempt to investigate the catalytic activity of UiO-67-bpy-PtCl2, the flow gas was directed through benzene before reaching the EXAFS cell. The sample was heated under these conditions while continuously measuring EXAFS.

The radial distribution data have not been phase corrected, and thus the radii in the EXAFS plots will not agree with bond lengths known from crystallography. However, the scale is still relative, and longer bond distances will be shown as signals at longer radii in the plots.

2.6.7 NMR

Solution NMR was used analyze the organic and organometallic linkers after synthesis. The products were dissolved in NMR tubes in hot DMSO-d_6. Generally, the solubility of the linkers was too poor to acquire ^{13}C-NMR spectra, but proton NMR spectra provided good enough information for structure determination. The measurements were made on a Bruker DPX 300 MHz Spectrometer. Solid state NMR experiments were performed by Sissel Jørgensen at SINTEF, using a Bruker Ultrashield 500 MHz Spectrometer with a 3.2 mm MAS probe.

2.6.8 IR and UV-vis spectroscopy

UV-vis spectroscopy was used to characterize functionalized MOFs, as the complexes often have well-known absorbance regions in the UV-visible spectral range. The samples were mounted in quartz capillaries (1 mm inner diameter) and measured using a Shimadzu UV-3600 UV-VIS-NIR spectrophotometer in reflectance mode. The reference sample for reflectance background was

$BaSO_4$. In some cases the samples were light-sensitive and changed color if subjected to light for a period of time. In this case, the capillaries were left in a glass desiccator by a window until the color changed, and then measured again.

FTIR spectroscopy was used to characterize CO adsorption on activated functionalized samples. FIR spectroscopy was used to search for metal-chlorine and metal-nitrogen bonds.

2.7 Washing, storage and water stability

To test the effect of washing, a small part of several samples were characterized as synthesized, and then again after washing. To compare stability in different atmospheres, several samples were split after synthesis, kept in dry desiccator and air (still inside a closed vial), and analyzed with PXRD after one year. Samples UiO-67-3 and UiO-67-bpy-4 were exposed to an atmosphere of 60 Pa of water in the SEM, to investigate the effect of humidity on crystal morphology. To test the stability towards liquid water, 20 different samples were mounted on PXRD plates using water. The acquired patterns were compared to those of dry as synthesized materials.

2.8 Sample and characterization overview

Table 2 gives an overview of all samples described in the Results section, and how these have been characterized. The samples functionalized with other metals have only been characterized with PXRD as of now.

Table 2. Overview of all samples and their characterization.

Sample Code	Functionalization, modulator	Characterization methods used
Linkers		
H_2bpydc		NMR
$PtCl_2(H_2bpydc)$		NMR, EXAFS
$PtCl_4(H_2bpydc)$		NMR, EXAFS
$Pt(tdt)(H_2bpydc)$		NMR
$[cis\text{-}Ru(bpy)_2]Cl_2$		NMR
$[Ru(bpy)_2(H_2bpydc)]Cl_2$		NMR
$CuCl_2(H_2bpydc)$		PXRD, EXAFS
MOFs		PXRD, SEM/EDXS (most samples)
UiO-67-1	None	GSM
UIO-67-2	None, 5 eq BA	TGA
UIO-67-3	None, 30 eq BA	TGA, GSM
UIO-67-bpy-1	10 % bpy linker, 5 eq EtA	GSM,
UIO-67-bpy-2	10 % bpy linker, 5 eq BA	GSM, NMR, UV-vis
UIO-67-bpy-3	10 % bpy linker, 30 eq EtA	
UIO-67-bpy-4	10 % bpy linker, 30 eq BA	GSM
Pt2-OP-1	10 % $PtCl_2(H_2bpydc)$ linker	
Pt2-OP-2	10 % $PtCl_2(H_2bpydc)$ linker, 5 eq EtA	
Pt2-OP-3	10 % $PtCl_2(H_2bpydc)$ linker, 5 eq BA	TGA, GSM, EXAFS, NMR, IR
Pt4-OP-1	10 % $PtCl_4(H_2bpydc)$ linker	GSM
Pt4-OP-2	10 % $PtCl_4(H_2bpydc)$ linker, 5 eq EtA	GSM
Pt4-OP-3	10 % $PtCl_4(H_2bpydc)$ linker, 5 eq BA	GSM
Pt2-PM-1	10 % $PtCl_2(H_2bpydc)$ linker, 5 eq BA	TGA, GSM, EXAFS, NMR, UV-vis
Pt2-PM-2	10 % $PtCl_2(H_2bpydc)$ linker, 30 eq BA	GSM,
Pt4-PM	10 % $PtCl_4(H_2bpydc)$ linker, 5 eq BA	TGA, GSM, EXAFS
Pt2-PS	10 % $PtCl_2(H_2bpydc)$ linker	GSM, EXAFS
Pt4-PS	10 % $PtCl_4(H_2bpydc)$ linker	EXAFS
Pt(tdt)-PM	5 % $Pt(tdt)(H_2bpydc)$ linker, 5 eq BA	GSM, UV-vis
Pt(tdt)-PS	10 % $Pt(tdt)(H_2bpydc)$ linker	GSM, EXAFS
Cu-PM	10 % $CuCl_2(H_2bpydc)$ linker, 5 eq BA	TGA, GSM, EXAFS
Cu-OP-1	10 % $CuCl_2(H_2bpydc)$ linker, 5 eq EtA	
Cu-OP-2	10 % $CuCl_2(H_2bpydc)$ linker, 5 eq BA	GSM, EXAFS
Cu-PS	10 % $CuCl_2(H_2bpydc)$ linker	GSM, EXAFS
Ru-PM	10 % $[Ru(bpy)_2(H_2bpydc)]$ Cl_2 linker, 5 eq BA	GSM, UV-vis
Ru-OP	10 % $RuCl_3$, 5 eq BA	GSM, NMR
Ru-PS	10 % $[cis\text{-}Ru(bpy)_2]Cl_2$	GSM, UV-vis
UiO-68	None	PXRD, SEM/EDX
UiO-70	None	PXRD

3 Results and discussion

The main scope of this work has been to synthesize UiO-67 with metal atoms coordinated to bipyridine linkers. Many different metal salts have been used in different synthesis strategies. In evaluating these strategies, it is sensible to have some criteria for the materials.

I. The crystal structure must be intact, with no pollutant phases.
II. The porosity must be intact, preferably with surface areas similar to unmodified UiO-67.
III. The metal must be coordinated in the intended manner.

After these criteria are met, the synthesis methods can be ranged according to their success rate, yield and specific surface areas. Yields are estimates of dry product, based on the amount on solvent in the pores, as measured by weighing the material before and after activation. If for some reason the product could not be evacuated after synthesis, estimates were made based on similar products.

Pure UiO-67 and UiO-67 with 10% H_2bpydc linker will be used as reference material throughout.

Some of the synthesis methods have been tried more than once. The methods described in the appendix are the synthesis procedure for the most thoroughly characterized material obtained from each method. Each material has a unique code, based on metal functionalization, synthesis method and a serial number.

Inorganic synthesis is not straightforward, and the mechanisms are not always fully understood. Even when the exact same synthesis procedures are used for UiO-67, significant variations in yield and product quality are observed. Uncontrollable factors will influence product quality, as in most inorganic synthesis.

In general, the syntheses always give some product if done correctly, with the following exception; one pot syntheses without modulator or with acetic acid gave amorphous product in some cases.

3.1 Metal functionalized UiO-67

There are many parameters in the synthesis of functionalized UiO-67. When taking into account ratio between linkers, type and concentration of modulator, functionalization method and metal precursor, it becomes apparent that not all can be tried. Experience, results obtained underway and scientific intuition was used during the laboratory work to determine which parameters to investigate further. These priorities will be discussed under each material.

This work focused primarily on UIO-67 with 10 % H_2bpydc linker concentration. This would ideally give a material with porosity comparable with that of UiO-67 and still a high concentration of functionalized sites in the material. Every octahedral cavity in the structure is bordered by 12 linker molecules, and a functionalization degree of 10% should thus be more than enough to functionalize most of the cavities. Syntheses with 100% H_2bpydc linker have also been tried, and yielded a crystalline product with the same PXRD pattern and crystal topology as UiO-67. The linker is however much more expensive than H_2bpdc, and it is probably not necessary with 100 % functionalization for application purposes.

The diffraction patterns of functionalized UiO-67 are indistinguishable from those of pure UiO-67. Thus all synthesis methods give the desired phase, without crystalline pollutants or byproducts. However, some patterns have peaks with lower FWHM values, more counts per second and a larger signal-to-noise ratio. While this does not give *quantitative* information about the sample, it gives a qualitative indication that one pot synthesis yields a less crystalline product.

The different synthesis methods will not produce identical MOFs. For instance, a material made with pre-functionalized linkers has presumably no open bpy seats, which may be a requirement for certain characterization techniques or PSF. Materials functionalized by the one pot method or PSF from UiO-67-bpy will have both functionalized and unfunctionalized H_2bpydc linkers, but these methods produce less waste and demands fewer working hours, and are perhaps more suitable for large scale production.

3.1.1 Reference materials

Table 3 presents a series of non-functionalized UiO-67 that was synthesized and used as reference materials, and as starting materials for PSF. The UiO-67-bpy samples are made with 10% H_2bpydc linkers. Both modulated and un-modulated synthesis was carried out, and all methods gave crystalline product (see PXRD patterns, Figure 31).

Table 3. Surface areas, yields and EDXS chlorine contents of reference MOFs.

ID number	Modulator	A_{BET}	Yield	EDXS Cl/Zr ratio
UiO-67-1	None	2324 m^2/g	56 %	11.4 % ‡
UiO-67-2	Benzoic acid (5 eq)	*	40 %	2.3 % ‡
UiO-67-3	Benzoic acid (30 eq)	1856 m^2/g	79 %	0.5 % ‡
UiO-67-bpy-1	Acetic acid (5 eq)	1952 m^2/g	84 %	*
UiO-67-bpy-2	Benzoic acid (5 eq)	2252 m^2/g	83 %	6.6 %
UiO-67-bpy-3	Acetic acid (30 eq)	*	66 %	1.5 %
UiO-67-bpy-4	Benzoic acid (30 eq)	2401m^2/g	55 %	0.0 %

***** *These materials were not tested for gas adsorption/EDXS.* ‡ *The result may be inaccurate due to high noise and background in the spectrum.*

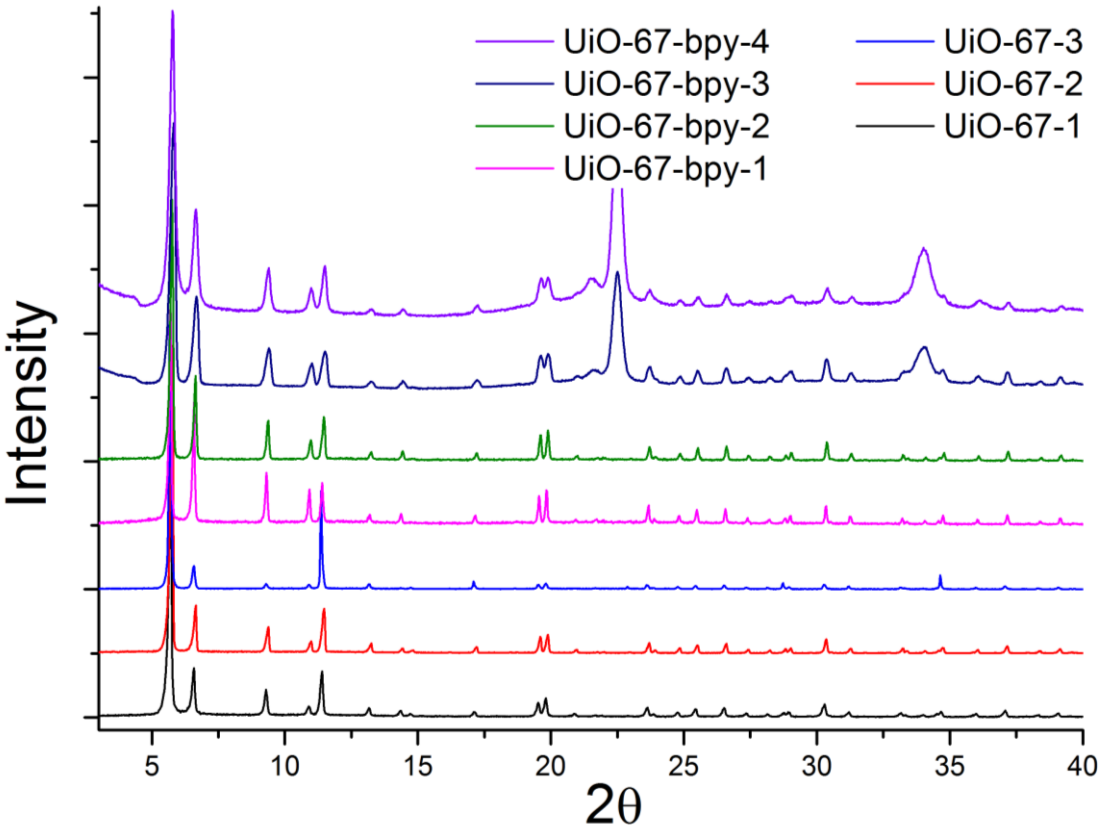

Figure 31. PXRD patterns of UiO-67. The broad peaks at 22-23° and 34° are due to diffraction from plastic film (further explained in the appendix, page 103).

The BET surface areas of benzoic acid modulated UiO-67-bpy exceeded 2000 m^2/g both for 5 and 30 equivalents. Due to the large crystallite size of material synthesized with 30 equivalents of benzoic acid, this may actually be caused by the adsorbents inability to diffuse into the core of the particles, thus not measuring the full internal surface. This consideration is also important regarding PSF and catalysis, processes that largely take place near the surface. 5 molar equivalents of benzoic acid in respect to zirconium was chosen as a standard amount of modulator because of its very high yields and more suitable crystal size.

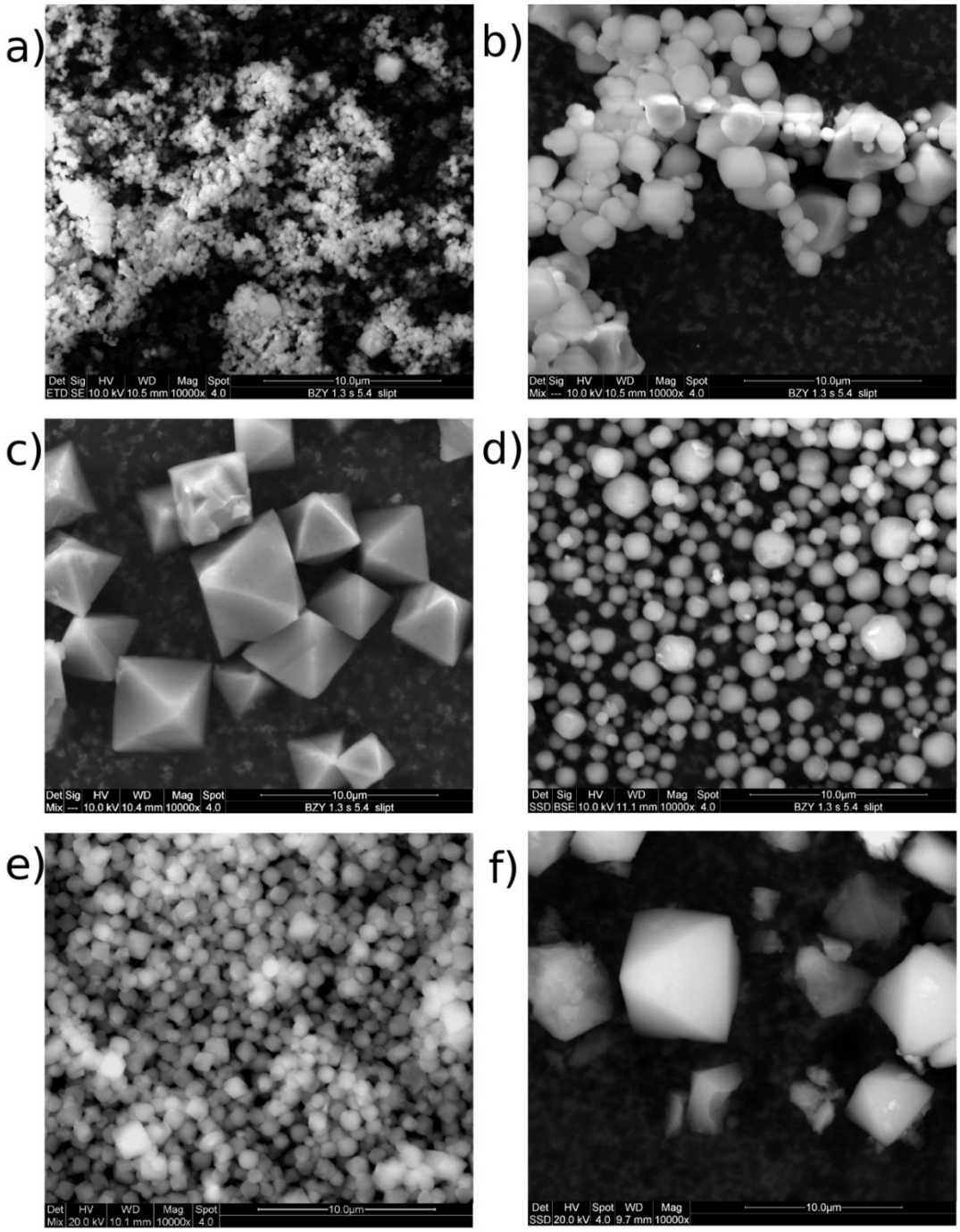

Figure 32. SEM micrographs of reference materials, to scale. (a) UiO-67-1. (b) UiO-67-2. (c) UiO-67-3. (d) UiO-67-bpy-2. (e) UiO-67-bpy-3. (f) UiO-67-bpy-4.

Residue chlorine is found in EDXS spectra of most UiO-67, except those made with high concentrations of modulator. The chlorine content in the synthesized MOF seems to follow a trend, decreasing with higher concentrations of modulator in the synthesis.

Crystal size dependency of benzoic acid concentration in the synthesis was confirmed by SEM (Figure 32). Bravais, Friedel, Donnay, Harker (BFHD) Morphology calculations predict [1 1 1] to be the dominating facet, giving octahedron-shaped crystallites (see graphical representation, Figure 33). This is not uncommon for materials with FCC lattices. SEM confirms this is the dominating topology for UiO-67 synthesized with high quantities of benzoic acid. However, syntheses without modulator or with low modulator concentration yield smaller crystals without discernible topology. This effect is especially clear in materials synthesized with functionalized linkers. These crystals appear to be almost spherical, perhaps a result of co-dominating facets, [1 1 1], [2 0 0], [2 2 0] and even more. Further investigations on the morphology on these crystals might reveal information about the growth mechanism and the effect of the modulator.

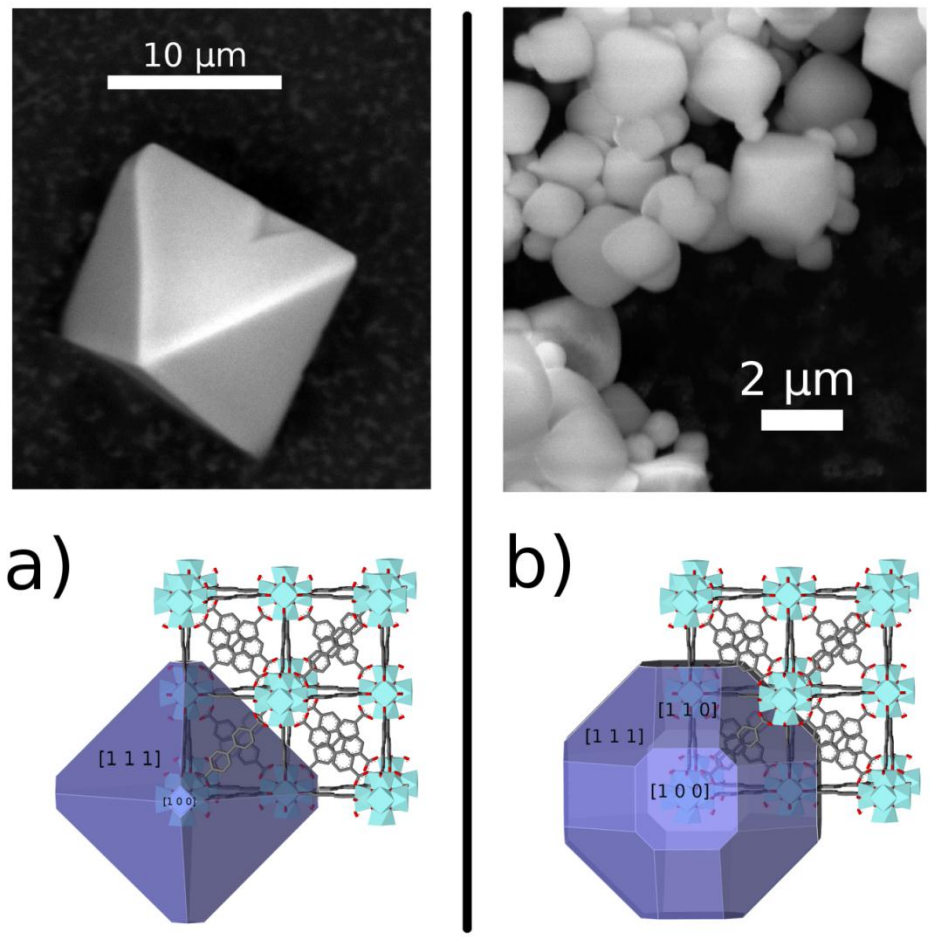

Figure 33. SEM micrographs and morphology calculations of UiO-67. (a) UiO-67 made with 30 eq benzoic acid. [1 1 1] facet dominating. (b) UiO-67 made with 5 equivalents of benzoic acid. Detailed report can be found in the appendix, page 119.

Solid state NMR

Solid state ^{1}H NMR is not quantitative enough to determine the ratio between the linkers. ^{13}C spectra for UiO-67-bpy are indistinguishable from those of pure UiO-67. ^{15}N NMR was attempted, but the concentration of active isotopes was too low to get meaningful data. It is possible to synthesize the H_2bpydc linker from ^{15}N enriched pyridine, but this is extremely expensive and a multi-step synthesis. Spectra with assignments are presented in section 3.1.5 UiO-67-Ru(bpy)$_3$ and in the appendix, page 124.

TGA

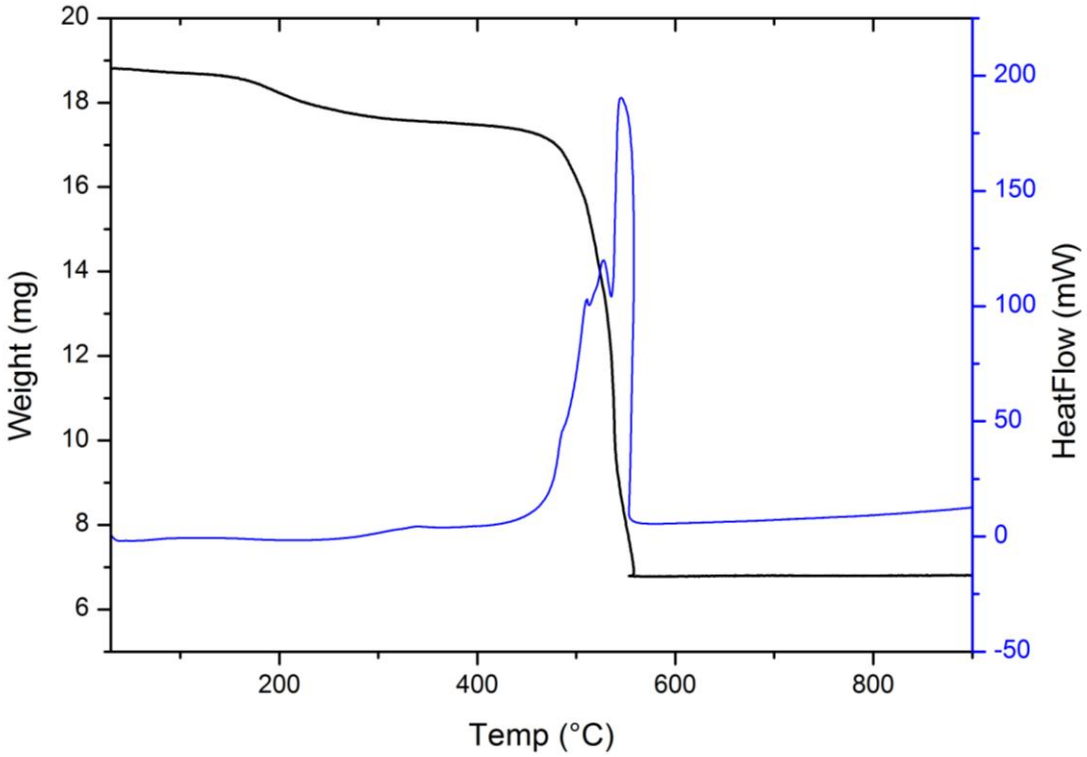

Figure 34. TGA curve of (previously evacuated) UiO-67-3 in air. Sample weight and heat flow are plotted against temperature.

Figure 34 Samples heated in air are destroyed by a combustion reaction starting at around 450° C, giving a strong exothermic heat signal. The evaporation of adsorbed water (100°C) and residue solvent (150-220°C) is slightly endothermic, but is better observed when the amount of solvent in the sample is larger. A white residue (6.8 mg) was recovered after the experiment, and found by PXRD to be ZrO_2. Assuming that the 6.8 mg is pure ZrO_2 (0.055 mmol), stoichiometry dictates that the UiO-67 sample should have weighed 19.5 mg. Since the sample weight before decomposition was significantly lower, the sample may be missing a fraction of the linkers. This phenomenon has recently been investigated in UiO-66 by Vermoortele and coworkers[70], and may be connected to the presence of chlorine in the material.

3.1.2 UiO-67-Pt

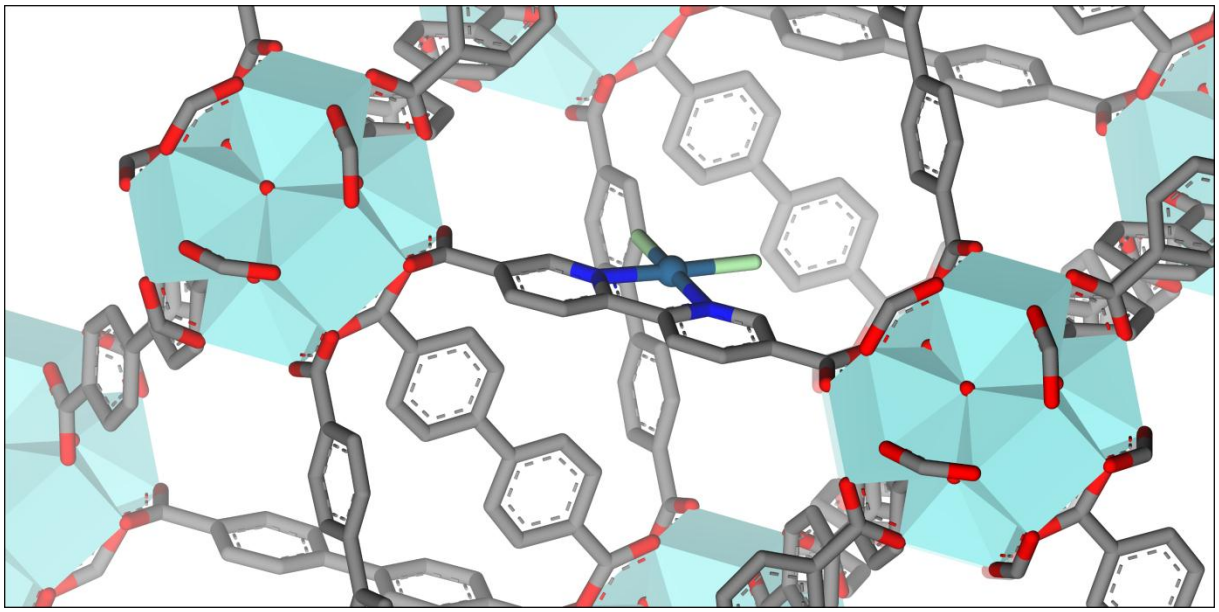

Figure 35. The $PtCl_2$ functionalization in UiO-67-bpy-$PtCl_2$.

Platinum functionalized UiO-67 appears as a yellow powder regardless of synthesis method, platinum oxidation state or synthesis parameters. All the attempted methods yielded a crystalline product, but not all methods was successful every time. The results will be organized according to which synthesis method was used.

One pot synthesis

The one-pot synthesis method is the simplest way of making UiO-67-bpy-MCl_x. However, the syntheses methods of some of the materials were frequently failing, and gave low yields (see the appendix, pages 120 to 128). For this reason, Pt2-OP-1 and Pt2-OP-2 were not characterized by gas sorption measurement. The In addition, it was assumed that they would have reasonably similar surface areas as the Pt(IV) functionalized materials. Table 4 presents the yields and BET surface areas of MOFs synthesized using this method.

Table 4. Surface areas and yields of one pot-synthesized platinum functionalized MOFs.

ID number	Precursor	Modulator	A_{BET}	Yield
Pt2-OP-1	K_2PtCl_4	None	*	44 %
Pt2-OP-2	K_2PtCl_4	Acetic acid (5 eq)	*	30 %
Pt2-OP-3	K_2PtCl_4	Benzoic acid (5 eq)	1504 m^2/g	34 %
Pt4-OP-1	K_2PtCl_6	None	121 m^2/g	36 %
Pt4-OP-2	K_2PtCl_6	Acetic acid (5 eq)	2377 m^2/g	23 %
Pt4-OP-3	K_2PtCl_6	Benzoic acid (5 eq)	2399 m^2/g	67 %

***** *These materials were not tested due to the poor success rate and low yields of the synthesis method.*

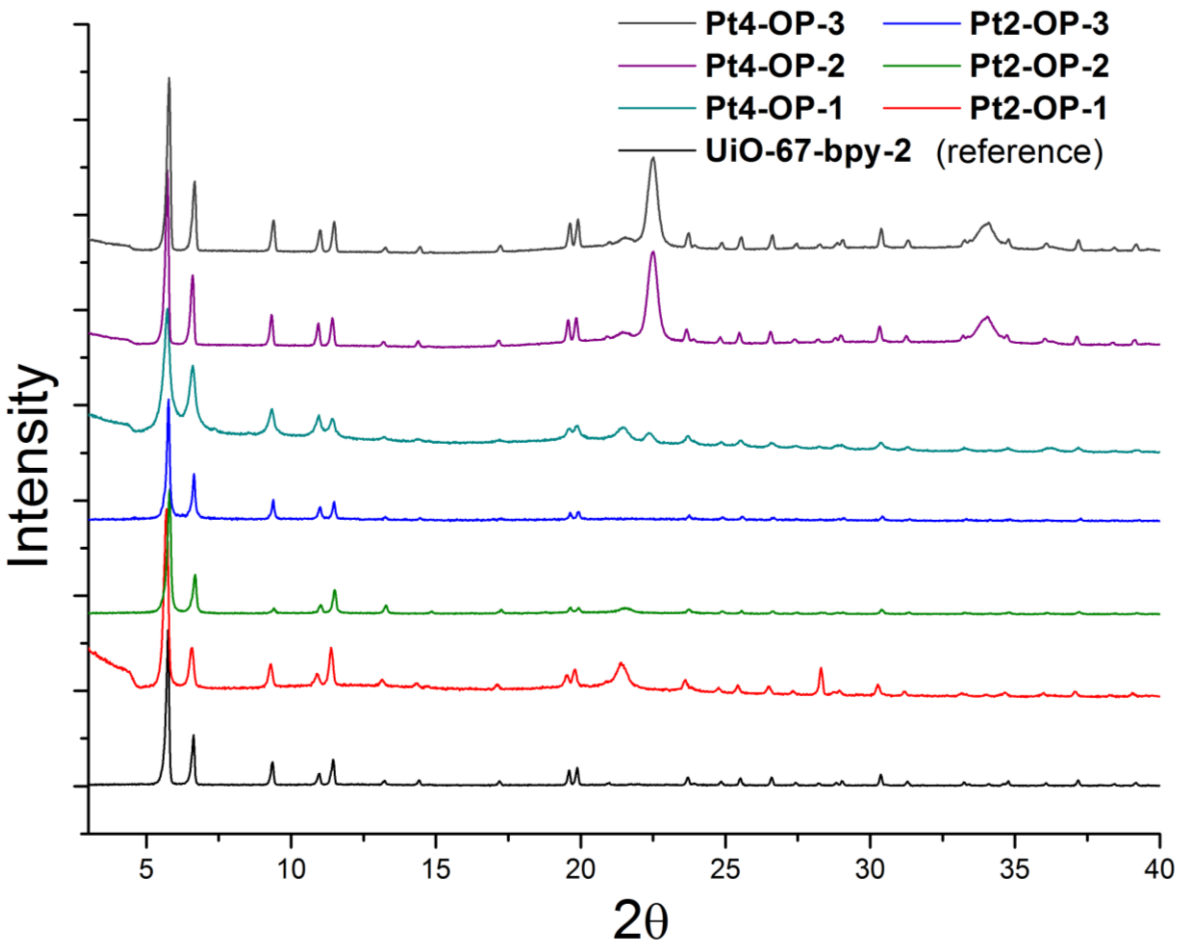

Figure 36. PXRD patterns of Pt-functionalized UiO-67 made with a one-pot method. The broad peaks at 22-23° and 34° are due to diffraction from plastic film (further explained in the appendix).

In addition to the two different platinum salts as functionalization agent, both acetic and benzoic acid were used as modulator in the synthesis. All methods produced crystalline product (Figure 36), but unmodulated synthesis failed to produce product with the desired porosity. Even though the UiO-67 phase is confirmed by PXRD, SEM micrographs of Pt4-OP-1 (Figure 37) show a crude looking product with a lot of agglomeration and what is likely to be amorphous phases.

With this method, the K_2PtCl_6 precursor seems to be favorable, producing a material with very high surface areas and good crystallinity. Unmodulated synthesis was discontinued due to lack of porosity in the product. Acetic acid modulated synthesis often failed to produce crystalline product, and by using benzoic acid as a modulator, higher yields were obtained. For these reasons, it was decided to use benzoic acid as the main modulator for the syntheses with premade linkers as well.

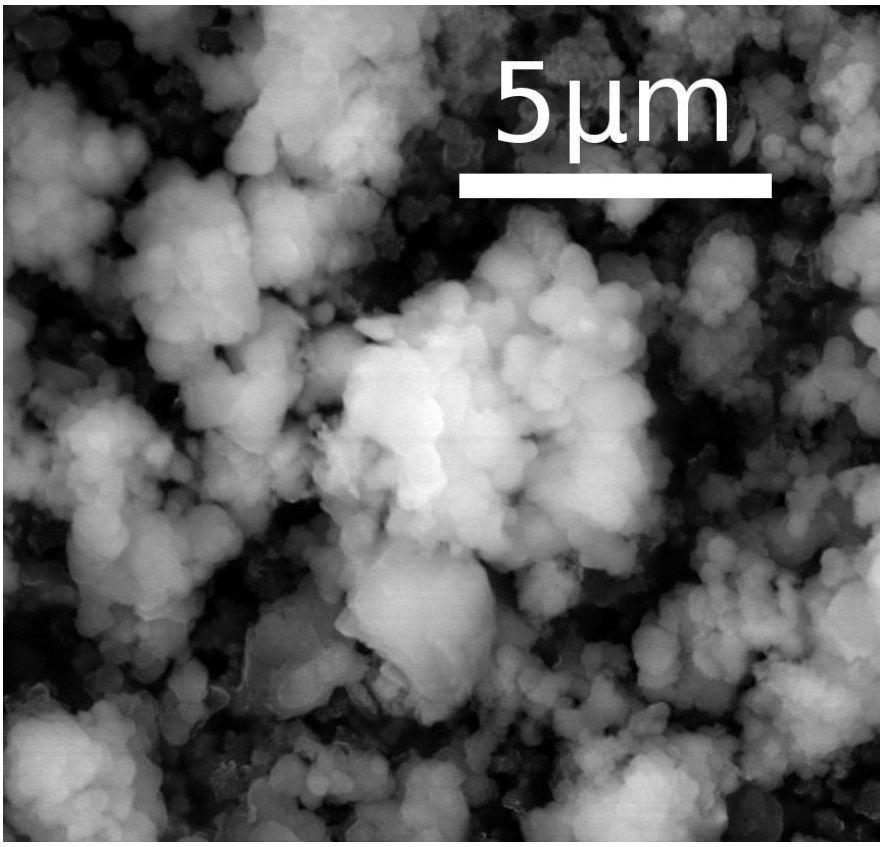

Figure 37. SEM micrograph of Pt4-OP-1.

MOF synthesis with premade linkers

Synthesis of platinum functionalized UiO-67 with premade linkers ensures a product without empty H_2bpydc linkers, assuming the platinum nitrogen coordination bond is maintained throughout the synthesis.

Table 5. Surface areas and yields of MOFs made with pre-functionalized platinum linkers.

ID number	Precursor	Modulator	A_{BET}	Yield
Pt2-PM-1	$PtCl_2(H_2bpydc)$	Benzoic acid (5 eq)	2222 m^2/g	52 %
Pt2-PM-2	$PtCl_2(H_2bpydc)$	Benzoic acid (30 eq)	2104 m^2/g	70 %
Pt4-PM	$PtCl_4(H_2bpydc)$	Benzoic acid (5 eq)	1934 m^2/g	83 %

Both UiO-67-$PtCl_2$ and UiO-67-$PtCl_4$ prepared with premade linkers gave high BET surface areas and high yields (Table 5). All syntheses produced crystalline material (Figure 38). Perhaps the most interesting feature is that Pt4-PM is a less porous product than other platinum functionalized samples. This can probably be assigned to the exceptionally high loading of platinum in this sample (see Table 7), and will be discussed in the EDXS section below.

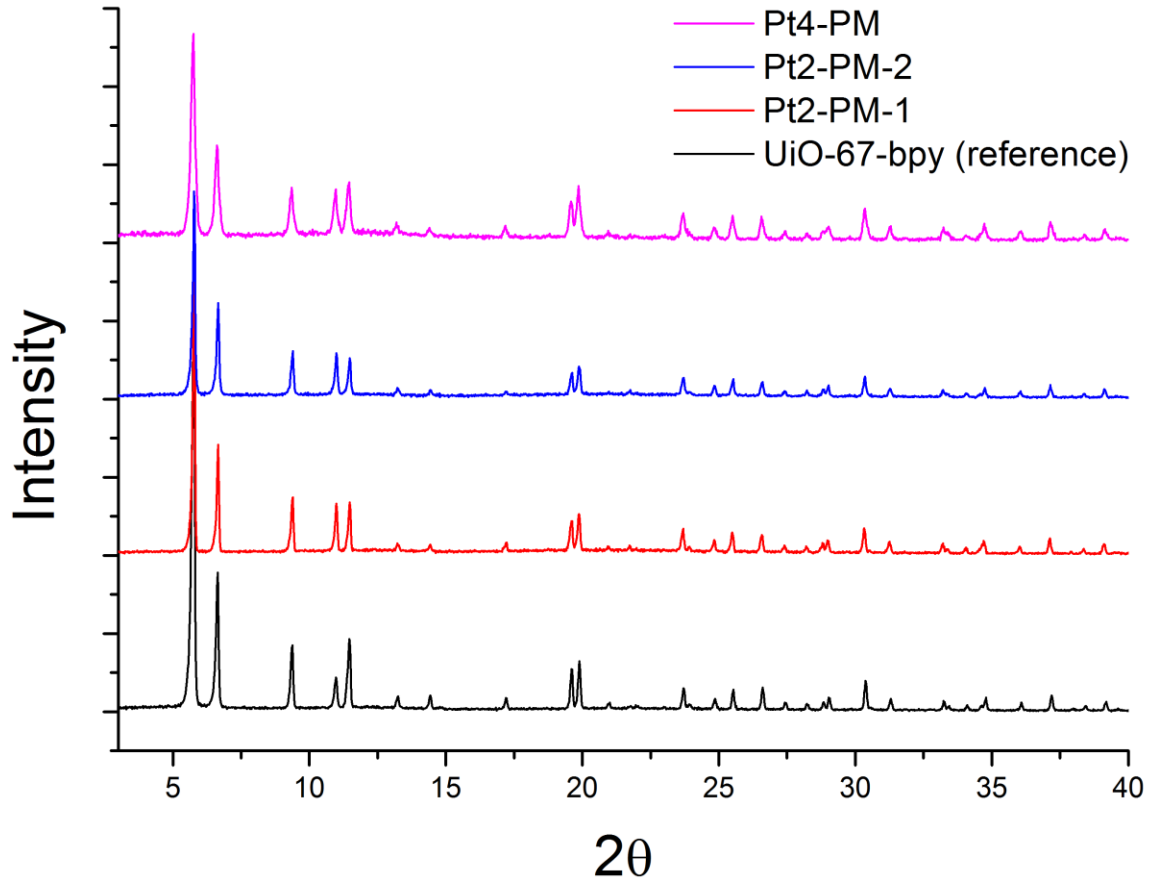

Figure 38. PXRD patterns of Pt-functionalized UiO-67 made with pre-functionalized linkers.

Post synthesis functionalization

Post synthesis functionalization of UiO-67-bpy-2 with platinum salts gave high yields, as expected (see Table 6). Small particles may be difficult to recover, and some MOF constituents may dissolve in the DMF. PXRD patterns are shown in Figure 39. The slight differences in these patterns may be due different loading of solvent in the sample, since this tends to shift the ratios of the intensities of the different peaks.

Table 6. Surface areas and yields of platinum post synthesis functionalized MOFs.

ID number	Precursor	Modulator	A_{BET}	Yield
UiO-67-bpy-2	-	Benzoic acid (5 eq)	2252 m^2/g	83 %
Pt2-PS	K_2PtCl_4	-	2126 m^2/g	96 %
Pt4-PS	$Na_2PtCl_6 \cdot 6H_2O$	-	*	~95 %

** The Pt4-PS sample was destroyed in the EXAFS cell before adsorption measurements could be made.*

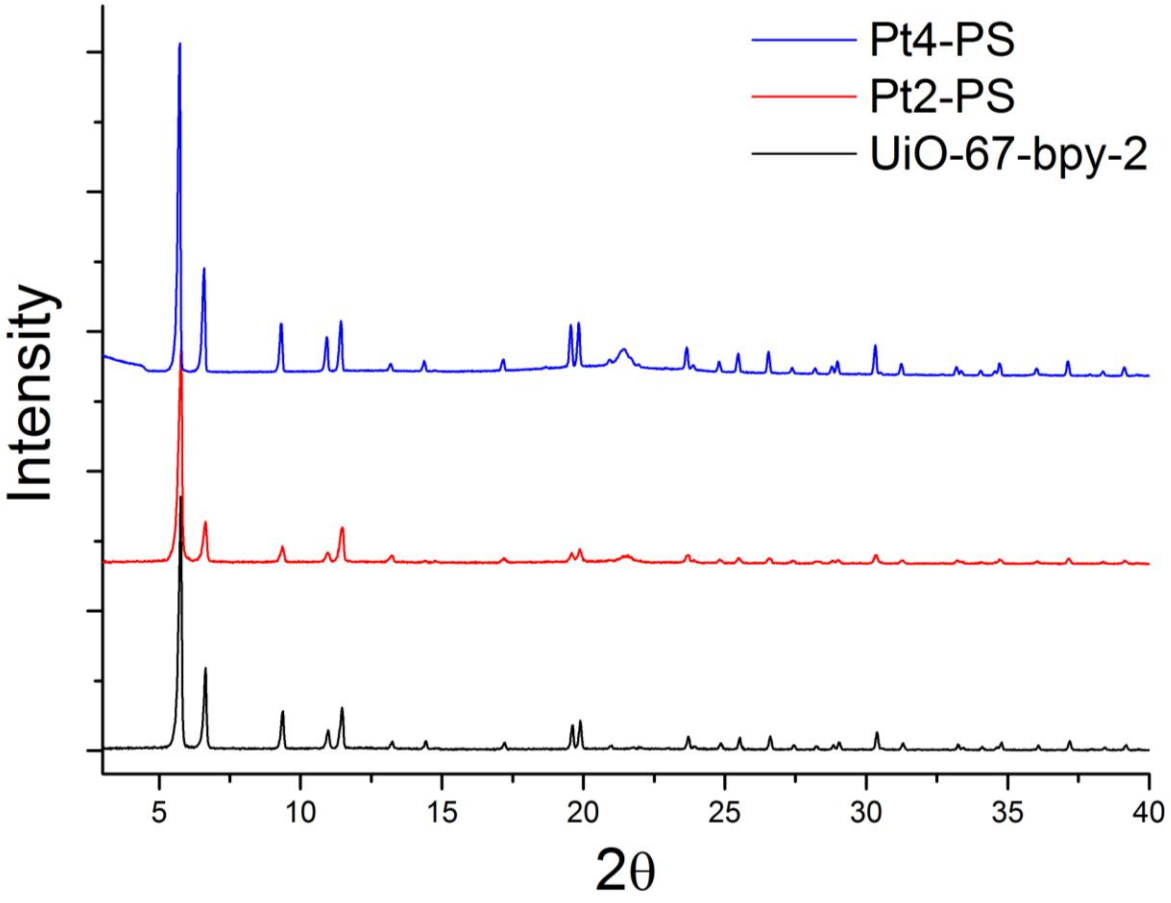

Figure 39. PXRD patterns of Pt-functionalized UiO-67 made by post synthesis functionalization. The broad peaks at 22-23° are due to diffraction from plastic film.

The Pt4-PS sample was destroyed in the EXAFS cell before adsorption measurements could be made. It was assumed that it would have a surface area in the range of 1900 to 2400 m^2/g, comparable to the other Pt(IV) functionalized samples.

Further characterization

Crystal size and morphology follows the same pattern as unfunctionalized samples. Somewhat surprisingly, the product of one pot syntheses made crystals appear cleaner and less agglomerated than samples made with premade linker (Figure 40). Of course, this will vary from sample to sample and may be coincidental or due to other parameters.

EDX spectra show a large variation in platinum content. The 1:1 ratio between platinum and chlorine in Pt4-PM-1 also shows that this technique is not sufficiently accurate for quantitative elemental

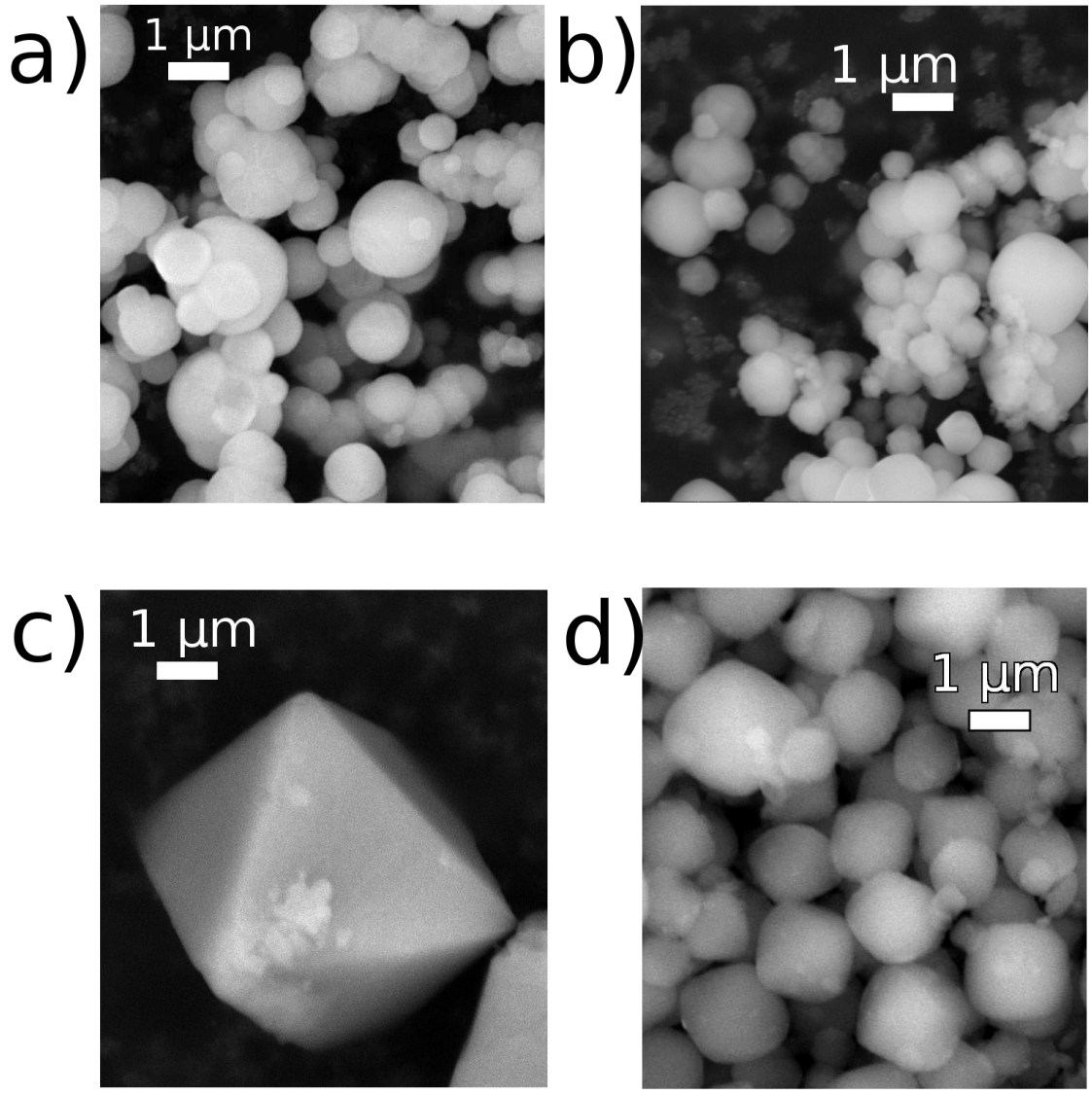

Figure 40. SEM micrographs (to scale) of platinum functionalized UiO-67. (a) Pt2-OP-3, slome agglomeration. (b) Pt2-PM-1. (c) Pt2-PM-2. 30 eq of benzoic acid gives larger crystals with well defined morphology, as in UiO-67. (d) Pt4-PS.

analysis. Comparison of X-ray adsorption in EXAFS also reveals significant errors in the EDXS measurements. Nevertheless, it determines beyond reasonable doubt whether an element is present in the sample. An EDX spectrum was acquired from a single crystal of Pt2-PM-2, and established the presence of platinum. This result is important, because it places platinum inside the crystal and not in some independent, amorphous phase. Spectra are presented in the appendix, page 132.

EDX spectra of Pt2-PM-1 before and after H_2 treatment (two hours in H_2/He gas flow at 300°C) shows a significant decrease in chlorine content (Table 7), indicating that some chlorine has been removed as HCl.

Table 7. Platinum and chlorine content in MOFs from EDXS shown as percentage in respect to zirconium.

Sample	Platinum	Chlorine
Pt2-OP-2	12.0 %	39.6 %
Pt2-OP-3	15.5 %	82.5 %
Pt4-OP-1	10.4 %	49.1 %
Pt4-OP-2	5.3 %	11.6 %
Pt4-OP-3	*	*
Pt2-PM-1	9.3 %	28.5 %
Pt2-PM-1, H_2 treated	8.3 %	7.3 %
Pt2-PM-2	6.0 %	26.6 %
Pt4-PM	29.0 %	29.6 %

** The EDXS measurement of Pt4-OP-3 was inaccurate. Pt content was confirmed by EXAFS.*

Solid state NMR of Pt2-PM-1 was done and compared to spectrum of UiO-67-bpy-2. No particular difference was observed, except the bipyridine proton peaks were weaker in the platinum sample. This may be due to ^{1}H-^{195}Pt coupling with subsequent broadening of proton peaks. The spectra were not quantitative enough to determine the ratio between the linkers, and did not provide any conclusive evidence for functionalization. ^{13}C spectra were indistinguishable from those of UiO-67-bpy-2. ^{15}N NMR was attempted, but the concentration of active isotopes was too low to get meaningful data. ^{1}H NMR spectrum of Pt2-PM-1 and Pt2-OP-3 is found in the appendix, page 124.

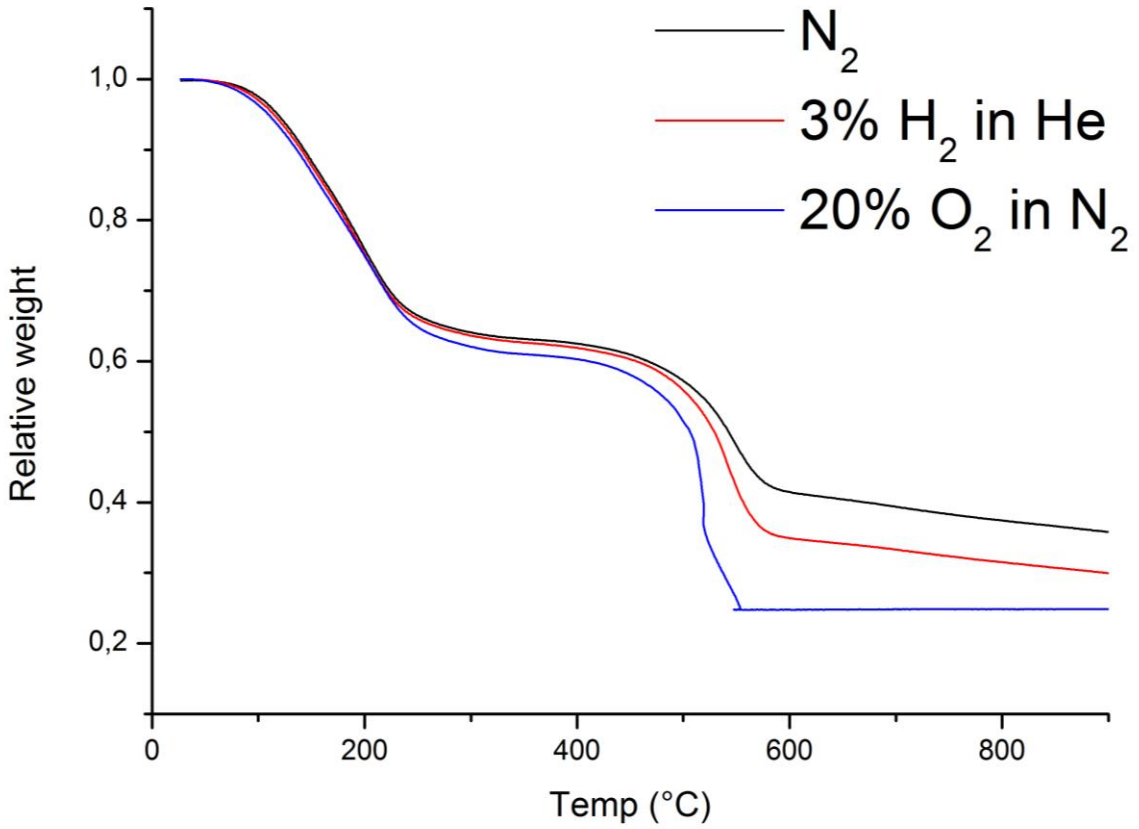

Figure 41. TGA curve of Pt2-PM-1 in different atmospheres. Other platinum functionalized samples show the same behavior.

UiO-67-Pt shows the same thermal stability as UiO-67 in different atmospheres, starting to decompose at around 450° C in the gases tested (Figure 41). The experiment is in agreement with weighing after evacuation, putting the solvent mass fraction at about 40 %. The difference between hydrogen and nitrogen atmosphere becomes apparent after the decomposition of the MOF, when a portion of the chlorine is removed as HCl. This is not detectable in MS, probably due to HCl adsorbing on surfaces in the instrument before reaching the detector.

When considering the heat signal (Figure 42), the evaporation of solvent is, not surprisingly, an endothermic process, regardless of atmosphere. Two main evaporation phases can be discerned, and are assigned to water (100 – 120 °C) and DMF (200 - 220°C), respectively. The combustion of the sample in oxygen atmosphere is of course exothermic, whereas the decomposition in other atmospheres is endothermic. The sudden exothermic signal in oxygen atmosphere at 320°C is hard to explain, as is the sudden endothermic signal in inert atmosphere at 460 °C. The latter can be a feature of the decomposition, but further experiments should be executed to investigate if these are recurring phenomena.

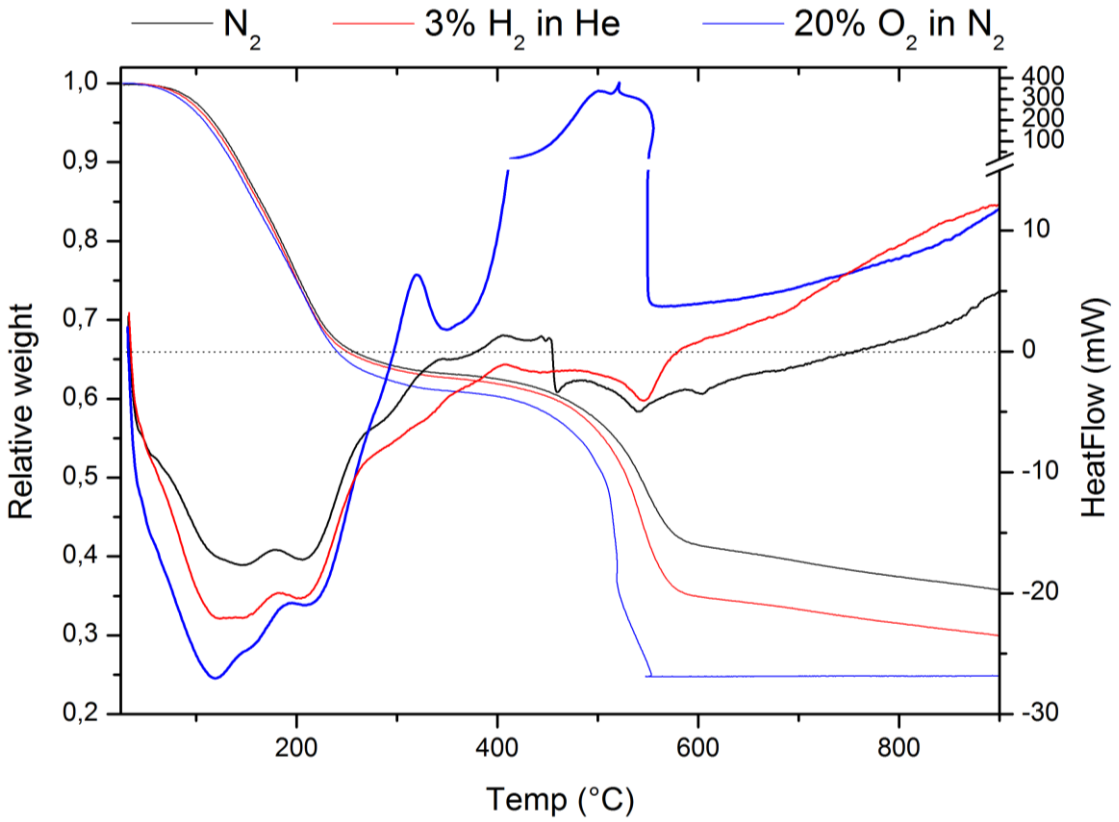

Figure 42. Heat flow diagrams of Pt2-PM-1 in different atmospheres. In non-oxidizing atmosphere, the decomposition is endotherm. Weight loss is shown with a thinner line.

PXRD analysis of residue from these experiments shows a mixture of the Baddeleyite and tetragonal phases of ZrO_2, and metallic platinum.

EXAFS spectra were acquired for precursors, linkers and MOFs, at room temperature and stepwise during activation from room temperature to 500°C (Figure 43). A mixture of 3 % H2 in He was flushed through the cell continuously, to investigate if it is possible to reduce platinum in the MOF. The spectra of platinum functionalized UiO-67 clearly show that the platinum atoms retain the same chemical environment in the MOF as in the precursor. The data is remarkably similar, regardless of synthesis method. No Pt-Pt stacking common for platinum compounds was observed in either of the materials. Pt(IV) samples give stronger signal in Pt-Cl bond region of the radial distribution functions, as expected.

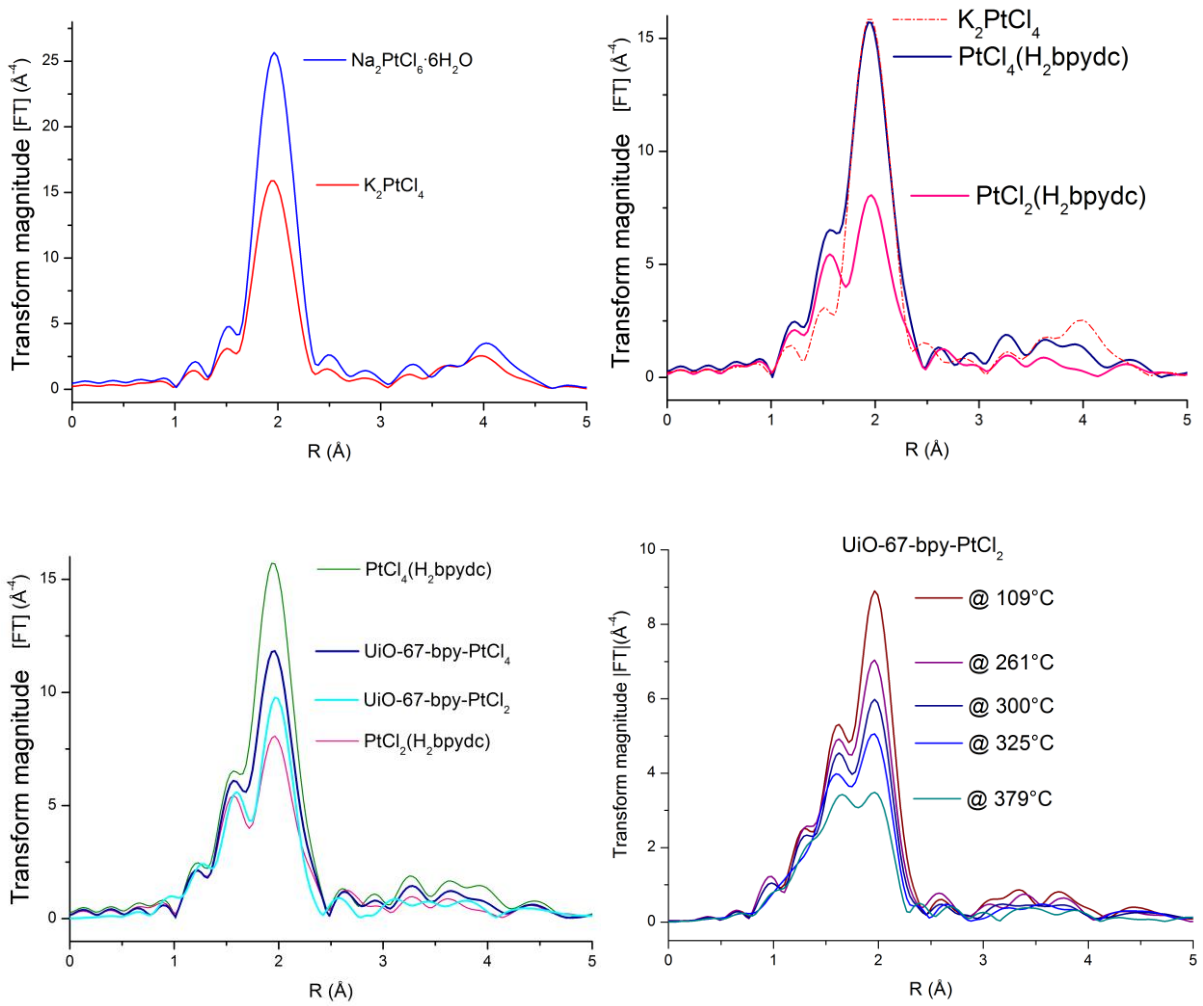

Figure 43. Fourier transformed EXAFS radial distribution functions. From top left: Precursors; Linkers; UiO-67-Pt (MOFs being Pt4-PM and Pt2-PM-1); Activation of Pt2-PM-1

The Pt – Cl and Pt – N bond lengths in these complexes are known from crystallography, and are 231-233 pm and 205-208 pm, respectively[49,71]. The EXAFS data in this thesis have not been phase corrected, and will thus display interaction distances shorter than the true bond distance. However, the data give a good indication, and longer bond distances will give signal at a higher R in the radial distribution function. The spectra were recorded on the same instrument, using the same methods and during a time interval of three days, strengthening the comparability of the data.

The continuous heating of the pellet was also done in the presence of benzene, but no Pt – benzene interaction was observed. When the material is heated in the presence of hydrogen, the Pt-Cl contribution diminishes more rapidly than the Pt-N contribution, indicating removal of chlorine (possibly as HCl), and possibly reduction of platinum. The MOF structure is still intact at these temperatures, as is evident from PXRD patterns acquired after heating the samples in air (Figure 44).

After the heating the MOF to decomposition, a green solution was recovered from the cell. Analysis by ^{1}H NMR showed that it was composed of DMF, benzene, 2-propanol and a small amount of pyridine.

Platinum functionalized UiO-67 appears as a yellow powder that turns to a dirt brown upon activation (Figure 44). This is probably an optical effect of drying, or loss of loosely coordinated solvent or water. The main absorbance peak remains un-shifted.

From these results, it is clear that each method has its advantages. While the one pot method is very simple, one cannot guarantee full functionalization, meaning there will be "empty" H_2bpydc linkers in the structure. Furthermore, the synthesis method gives variable quality of product, even when exactly the same synthesis procedure is used. The MOF synthesis with pre-functionalized linkers gives more stable results, but the variable yields of the linker synthesis makes it comparable with one pot synthesis in respect to molecular economics. Post synthesis functionalization gives higher yield and does not waste as much platinum.

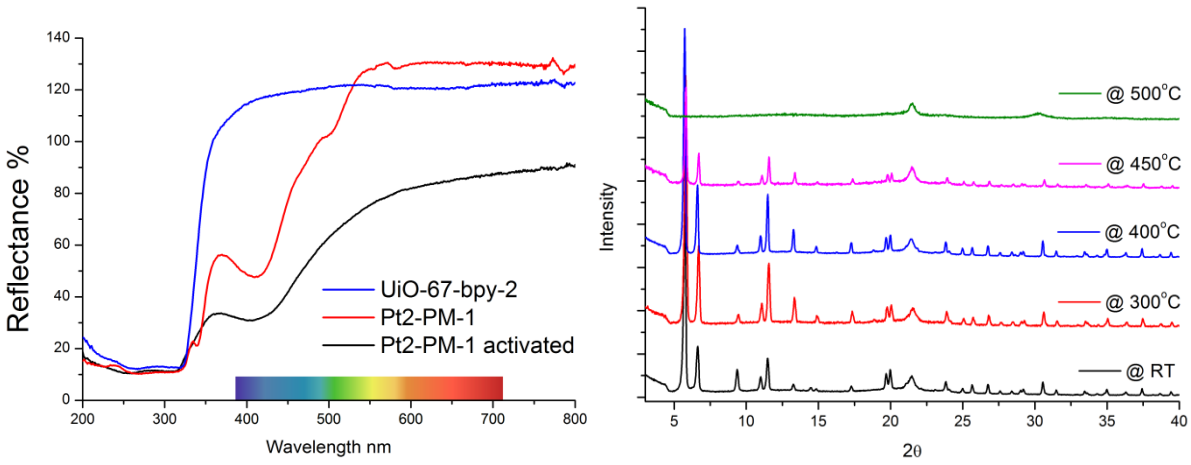

Figure 44. Left: UV-vis spectrum of Pt2-PM-1 activated at 300° C. Right: PXRD patterns of Pt2-PM-1 after being heated. The peak at 22° is due to diffraction from plastic foil.

3.1.3 UiO-67-Pt(tdt)

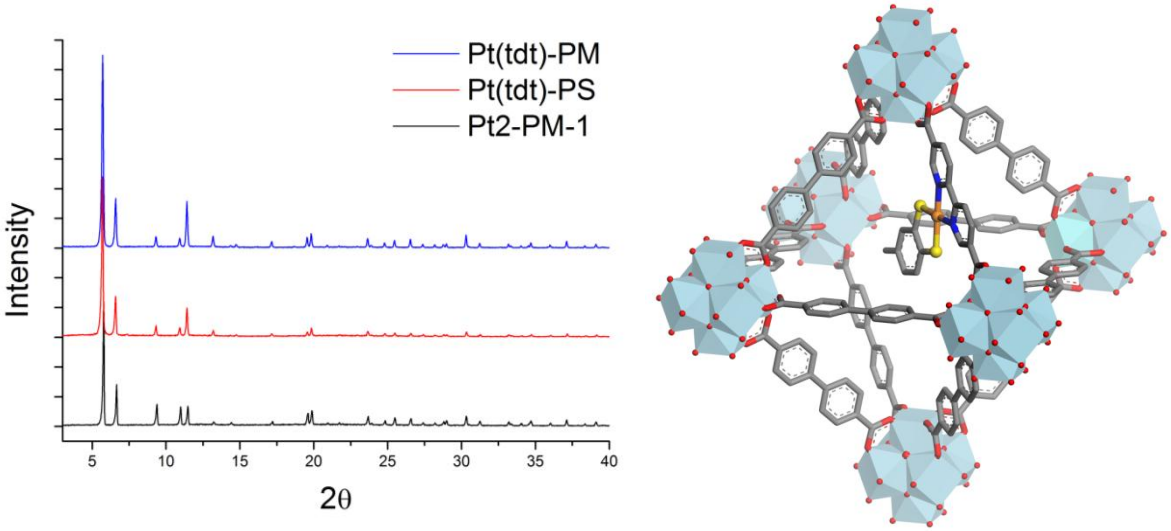

Figure 45. Left: PXRD patterns of UiO-67-Pt(tdt). Right: Octahedron cage of UiO-67 with Pt(tdt) functionalization.

UiO-67-Pt(tdt) was prepared with a premade linker, and by post synthesis functionalization. Yields and BET surface areas are reported in Table 8. PXRD patterns are displayed in Figure 45. Both appear as blue powders, although the post synthesized version with a green tint.

Table 8. Yields and BET surface areas of Pt(tdt) functionalized UiO-67.

ID number	Precursor	Modulator	A_{BET}	Yield
Pt2-PM-1	$PtCl_2(H_2bpydc)$	Benzoic acid (5 eq)	2222 m^2/g	57 %
Pt(tdt)-PM	$Pt(tdt)(H_2bpydc)$	Benzoic acid (5 eq)	2139 m^2/g	50 %
Pt(tdt)-PS	tdt		2450 m^2/g	65 % (37 %*)

**Yield in parenthesis is including all steps, not only the PSF step.*

The post synthetically modified Pt(tdt)-PS is made from the sample Pt2-PM-1, and we see a significant increase in BET surface area after the functionalization. The method cannot determine whether it is a real increase in the internal surface area, or an effect of the PSF conditions acting as an extended wash of the material. It is possible that the prolonged stirring in 2-propanol removes residue from the pores, making them more available to gas molecules.

EDXS data are reported in Table 9. The unchanged chlorine content from PSF is unexpected, but may be due to noise or bad sample preparation. If truly a ligand exchange occurs between 2 Cl^- and tdt^{2-},

chlorine content should have diminished; leaving the structure as HCl. The platinum content remains unchanged, giving some credibility to the measurement, and it is possible that chloride resides in the pores in some other way. The sulfur signal in EDXS is partly overlapped by that of zirconium, but can be made out clearly in the spectrum (presented in the appendix, page 131).

Table 9. Pt, Cl and S content in UiO-67-Pt(tdt), as found by EDXS.

Sample	Platinum	Chlorine	Sulfur
Pt2-PM-1	9.3 %	28.5 %	
Pt(tdt)-PS	9.3 %	31.0 %	28.0 %
Pt(tdt)-PM	2.2 %	4.0 %	7.9 %

The EXAFS data acquired before and after PSF clearly show that the platinum coordination changed. The sample with premade linker had too low platinum concentration to be measured. The resulting data (Figure 46) shows the MOF certainly has both $PtCl^2$ and Pt(tdt) functionalization, which was reflected in the data. The main peak was shifted to a slightly shorter distance, as expected when you change from Pt-Cl bonds (231 pm) to mainly Pt-S bonds (225 pm). Bond lengths are known from crystallography[52].

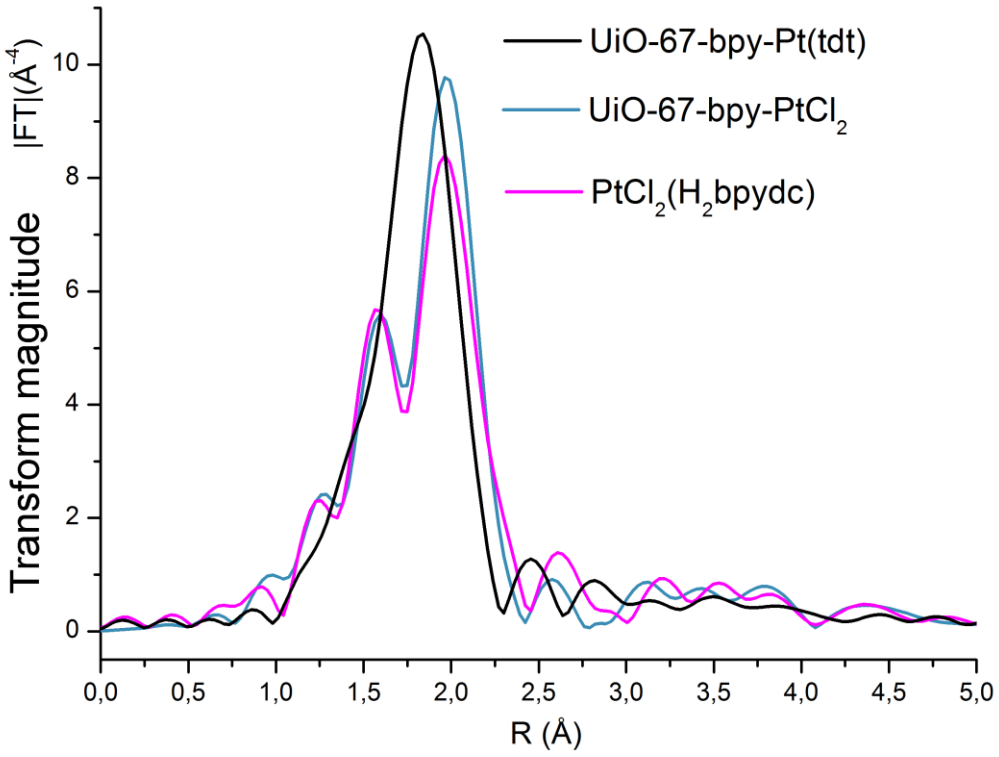

Figure 46. EXAFS radial distribution function of Pt(tdt)-PS and Pt2-PM-1.

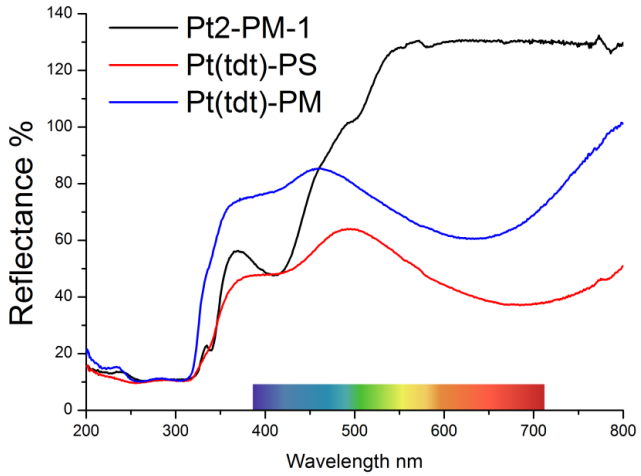

Figure 47. UV-vis spectra of Pt(tdt)-functionalized UiO-67.

Pt(tdt) functionalized UiO-67 appears as a blue powder, and absorbs in a broad range from 500 – 800 nm in the visible to near IR spectrum. Post synthetically prepared sample displays a certain red-shift in the main band, and is slightly more turquoise than blue. This is probably due to the presence of some unreacted $PtCl_2$ seats, which can be observed by comparing the UV-vis spectra (Figure 47). The intensity difference is due to concentration differences between the samples.

If exposed to light, the sample gradually change color from blue to white. The sample was exposed to sunlight in a quartz capillary in dry atmosphere. Reflectance spectra reveal that the broad absorption band in the red region is gone, meaning the complex is light sensitive (Figure 48).

Taking into account the poor yield of the linker synthesis, post synthesis functionalization is clearly the most suitable method. However, literature procedures provide 60 % yield, and it may thus be possible to make this material more efficiently. In addition, not all linkers will be functionalized by post synthesis functionalization, which may be a problem in certain cases.

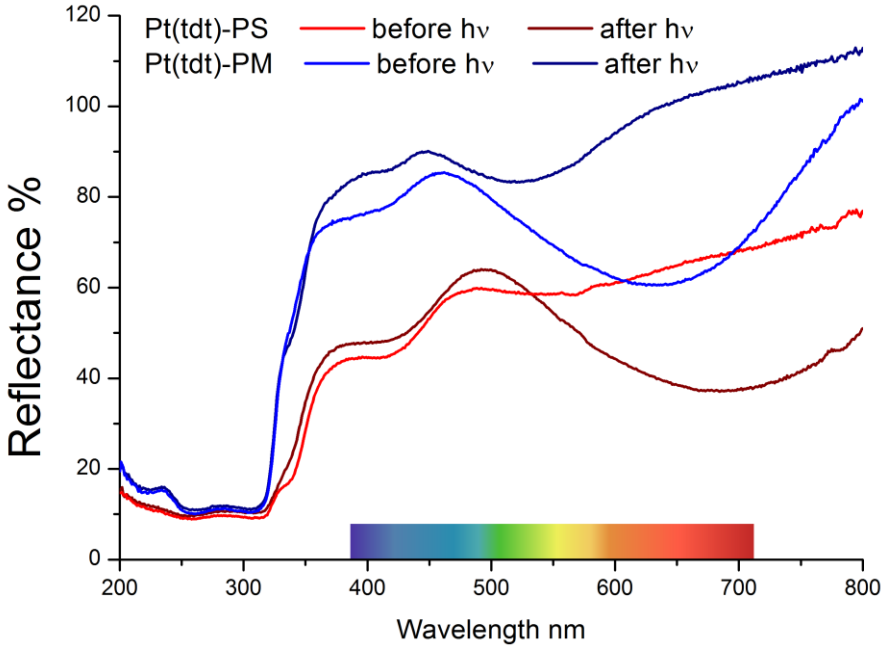

Figure 48. UV-vis spectrum of Pt(tdt)-functionalized UiO-67 before and after exposure to sunlight.

3.1.4 UiO-67-Cu

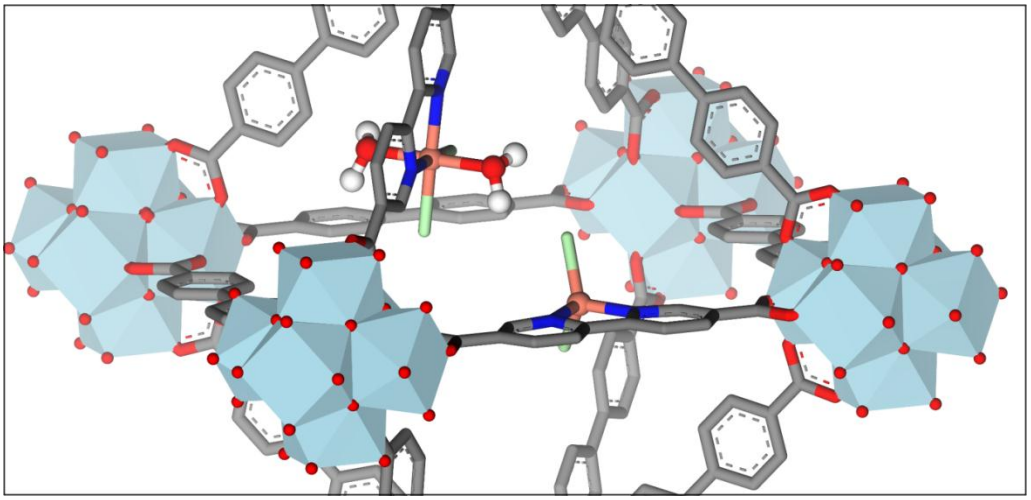

Figure 49. The possible $CuCl_2$-functionalizations in UiO-67, one tetrahedral and one hydrated octahedral.

Copper functionalized UiO-67 appears as a light green powder. Copper content is confirmed by EDX, but to determine the nature of the functionalization has proved to be difficult. Upon activation the powder changes color to grey, but it regains the green color when exposed to (humid) air. This may indicate an effect of hydration. Yields and surface areas of $CuCl_2$-functionalized UiO-67 are reported in Table 10. Synthesis with acetic acid as modulator failed to produce crystalline material, as seen on the PXRD pattern (Figure 50).

Table 10. Yields and BET surface areas of $CuCl_2$-functionalized UiO-67.

ID number	Precursor	Modulator	A_{BET}	Yield
UiO-67-bpy-2		None	2252 m^2/g	83 %
Cu-OP-1	$CuCl_2 \cdot 2H_2O$	Acetic acid (5 eq)	*	10 %
Cu-OP-2	$CuCl_2 \cdot 2H_2O$	Benzoic acid (5 eq)	2104 m^2/g	42 %
Cu-PM	$CuCl_2$.H_2bpydc	Benzoic acid (5 eq)	2212 m^2/g	16 %
Cu-PS	$CuCl_2 \cdot 2H_2O$	-	2106 m^2/g	49 % (41 %)

*Yield in parenthesis is including all steps, not only the PSF step. *Not tested for adsorption.*

EDXS indicates that the copper content of the samples are similar, and the chlorine content is very high (Table 11).

Table 11. Copper and chlorine content in respect to Zr in UiO-67-Cu.

Sample	Copper	Chlorine
Cu-OP-2	9.3 %	40.0 %
Cu-PM	8.7 %	48.1 %

EDXS has not been done on Cu-PS, but the ratio between copper concentrations in the different samples were found by EXAFS to be as follows: $[Cu]_{Cu\text{-}PS} = 2.9\ [Cu]_{Cu\text{-}OP\text{-}1} = 5.1\ [Cu]_{Cu\text{-}PM}$. This highlights the inability of EDXS to give accurate data on such dilute, non-conducting compounds.

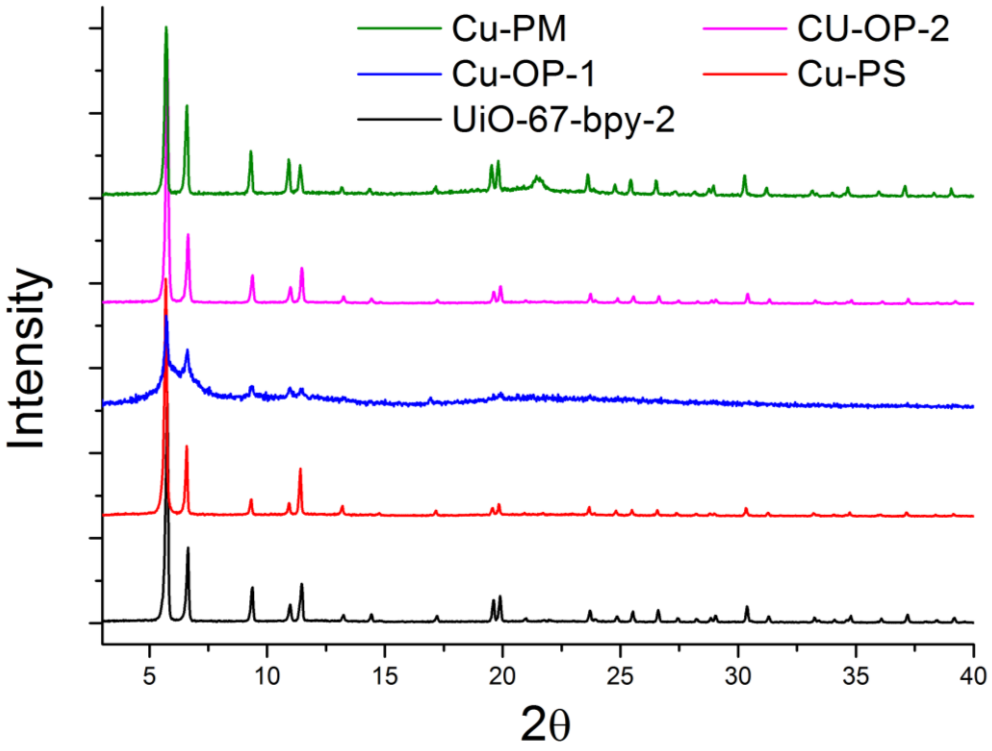

Figure 50. PXRD patterns of CuCl2-functionalized UiO-67. The peak in Cu-PM at 22° is due to diffraction from plastic foil used to cover the sample.

UiO-67-Cu has roughly the same morphology and crystal size as the other samples (Figure 51), but sample made from the $CuCl_2{\cdot}H_2$bpdc complex has smaller crystals and more well-defined octahedral topology than sample made with the one pot method.

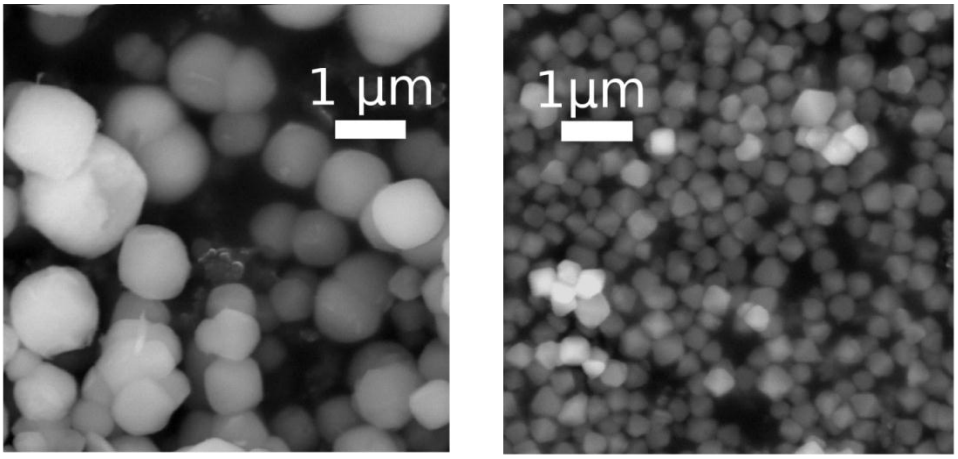

Figure 51. SEM micrographs of copper functionalized UiO-67. Left: Cu-OP-2. Right: Cu-PM.

TGA results from experiments in reducing atmosphere shows an abrupt weight loss at 375 °C, accompanied by an exothermic signal, shown in Figure 52. It is still unclear whether this is due to loss of chlorine as HCl or another decomposing phase.

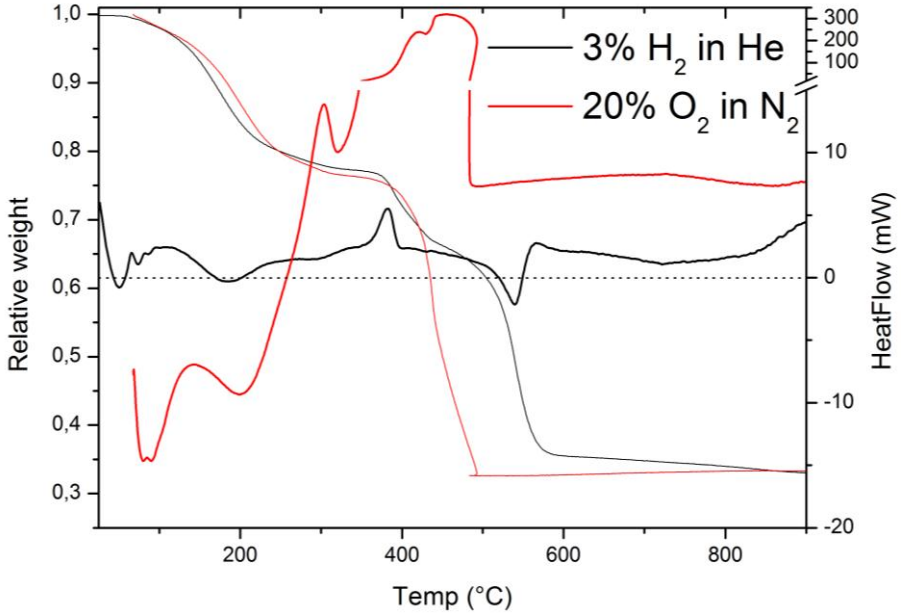

Figure 52. TGA curves of Cu-PM in different atmospheres. Weight loss is shown with a thinner line.

The EXAFS radial distribution functions show the precursor is not what it was assumed to be, as it lacks a signal corresponding to Cu-Cl bond length. Many structures are possible, as Cu(II) is known to coordinate to carboxylate groups, bipyridine and water. These ligands are difficult to distinguish between in EXAFS. A crystalline phase was discovered, but refinements of PXRD patterns have so far been inconclusive. The complex is soluble in DMF, and MOFs synthesized with this copper complex

are still only showing the UiO-67 phase in PXRD patterns. Single crystals of sufficient size for XRD have been recovered, but the characterization has not been done due to instrument malfunction.

Upon activation in EXAFS, a Cu-Cu signal starts to appear at 250 °C and 375 °C in the precursor and MOF, respectively. See appendix, page 102 for spectra of $CuCl_2 \cdot (H_2bpydc)$ and page 142 for Cu-PS. The reduction and agglomeration of copper inside the MOF corresponds with the weight loss in the TGA, and connects the weight loss with the formation of copper clusters. Further TGA and PXRD experiments will determine if the MOF phase is preserved, or if the formation of copper clusters causes the structure to collapse.

In EXAFS of the functionalized MOF, a contribution from a longer bond from Cu is observed, in comparison with the precursor. This may indicate that there are some Cu-Cl bonds in the MOF, but this is far from conclusive. Only one phase, containing copper, is observed in PXRD and SEM. This, together with the absence of Cu-Cu interaction in EXAFS before heating, suggest strongly that copper is coordinated to H_2bpydc in the MOF.

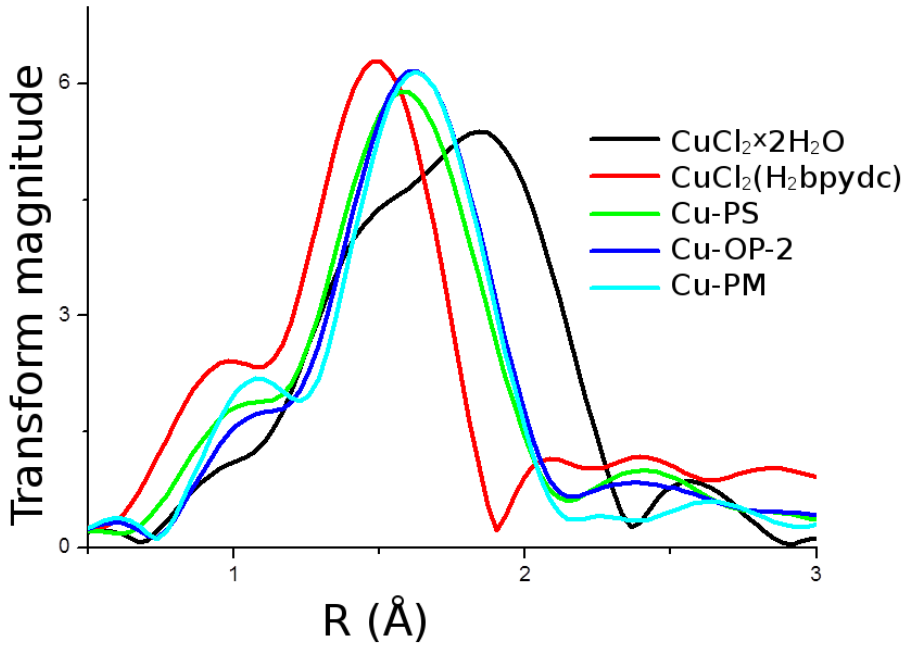

Figure 53. EXAFS radial distribution functions of copper precursors and functionalized UiO-67-bpy.

3.1.5 UiO-67-Ru(bpy)$_3$

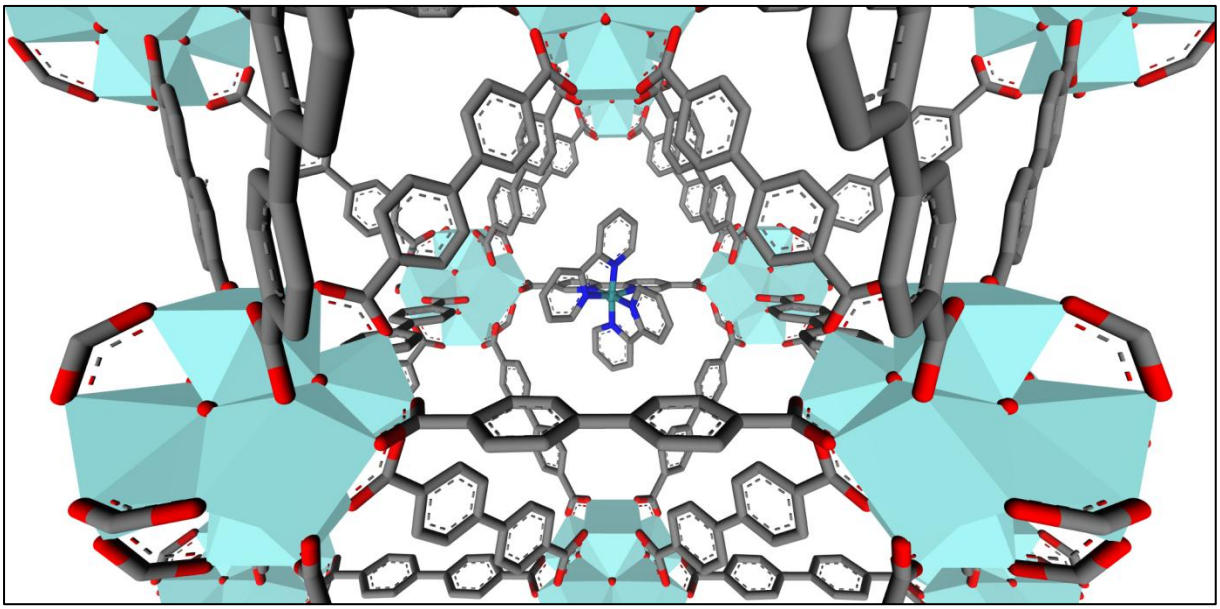

Figure 54. A representation of UiO-67-Ru(bpy)$_3$ along the [1 1 0] direction.

UiO-67-Ru(bpy)$_3$ (Figure 54) appears as pink or brown powder, depending on synthesis method, whereas Ru-OP appears as a greenish grey powder. Synthesis with pre-functionalized linker gives great yield and a very high surface area, exceeding previously reported surface areas of this compound (1277 m^2/g) by almost a factor of two[40] (Table 12). This may be due to the fact that the reported method utilizes acetic acid as modulator in the synthesis.

Table 12. Yields and BET surface areas of Ru(bpy)3-functionalized UiO-67. Yields in parenthesis include all steps.

ID number	Precursor	Modulator	A_{BET}	Yield
UiO-67-bpy-1		Acetic acid (5 eq)	1952 m^2/g	84 %
Ru-PM	[Ru(bpy)$_2$(H$_2$bpydc)]Cl$_2$	Benzoic acid (5 eq)	2272 m^2/g	68 %
Ru-OP	RuCl$_3$·xH$_2$O	Benzoic acid (5 eq)	2098 m^2/g	17 %
Ru-PS	[Ru(bpy)$_2$]Cl$_2$		2090 m^2/g	88 % (74 %)

All ruthenium modified samples are not strictly the same, since Ru-OP is only functionalized with RuCl$_3$. If this method were to work to work, it could be a step in a post synthesis functionalization method. However, the method gives low yields, and byproducts of Ru(H$_2$bpydc)$_x$Cl$_y$ (x,y=2,3) are likely to form. A more feasible method could be PSF of RuCl$_3$·xH$_2$O onto UiO-67-bpy, then a second PSF with bpy onto the resulting product.

EDXS shows a high ruthenium content in both Ru-OP and Ru-PM. However, the Cl K and Ru L_3 absorption edges differ by only 20 eV, thus the instrument has no means of distinguishing between the two species.

Solid state ^{1}H NMR (Figure 55) shows a significant difference between UiO-67-bpy and Ru-OP. Solution ^{1}H NMR of platinum functionalized linkers showed a significantly higher shift of the α-proton peak, and this would also be expected for ruthenium functionalized linkers.

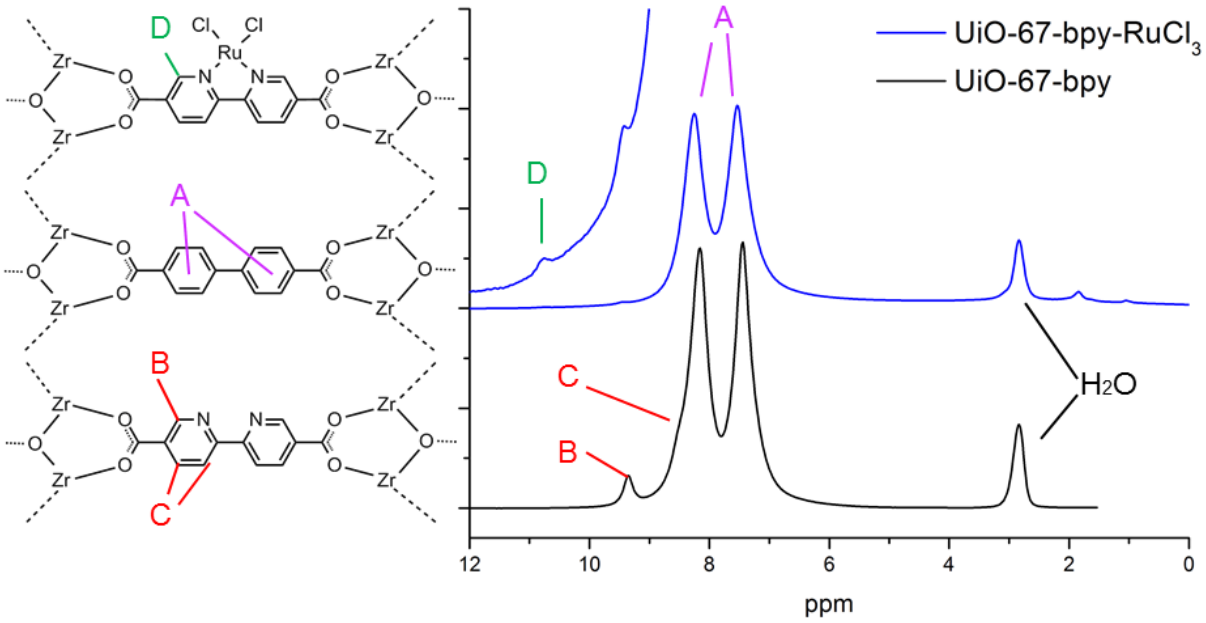

Figure 55. Solid state 1H NMR spectra of UiO-67-bpy-2 (black) and Ru-OP (blue), the latter partly magnified by a factor of 25.

The spectrum of unfunctionalized UiO-67-bpy is as expected, with the 10 % fraction of bpydc linkers being visible as a shoulder on the leftmost main peak (δ 8.5) and an independent alpha proton peak (δ 9.4). The ratios of the peak intensities roughly correspond to a 1:9 ratio between the linkers, although peak broadening makes it impossible to integrate accurately. In the spectrum of Ru-OP, no shoulder is observed, and two tiny alpha proton peaks can be distinguished. The only Ru precursor available was $RuCl_3 \cdot xH_2O$, creating a complex with Ru^{3+} as the main linker functionalization. Having a d^5 configuration, Ru^{3+} is paramagnetic and causes severe changes to the magnetic field in its immediate surroundings. The shifts of neighboring protons are broadened and shifted. Adding this to the already broadened peaks of a solid state spectrum, it is unlikely to observe signals from these linkers. The small peak at δ 10.6 may be a signal from Ru^{2+} functionalized bpy. The octahedral d^6 configuration is known to be very stable, and DMF decomposition products may act as a reducing agent in the synthesis. Still, the compound needs further characterization.

UV-vis spectroscopy was carried out on Ru-PM and Ru-PS, and shows characteristic adsorption in the visible spectrum as a broad band from 370 to 590 nm (Figure 56), in perfect agreement with reported data[72] for the isolated compound $Ru(bpy)_3^{2+}$.

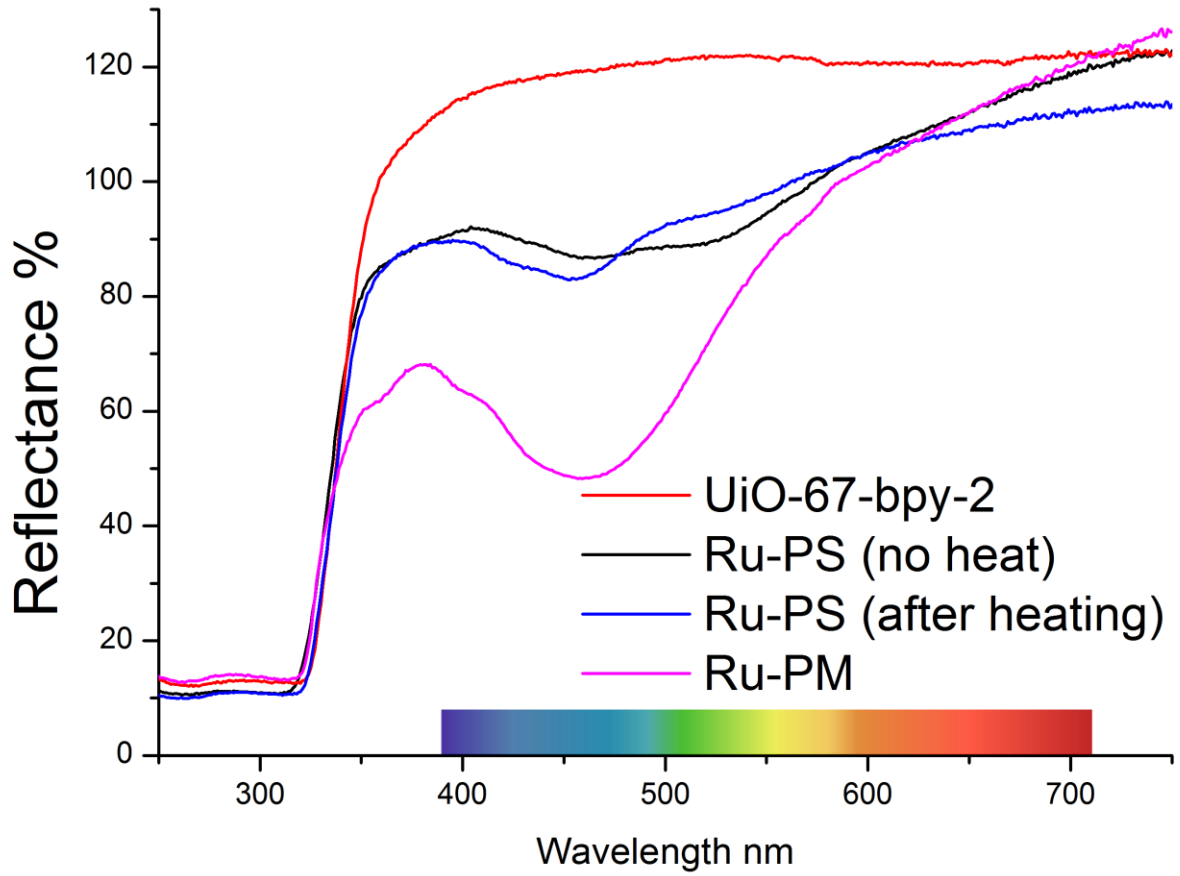

Figure 56. Uv-vis spectra of ruthenium functionalized UiO-67.

Ru-PS functionalized with heating shows absorption in the same region, but not of the same intensity as the sample made with pre-functionalized linker. The size of the functionalization compound cis-$[Ru(bpy)_2]Cl_2$ may pose steric challenges. Perhaps longer duration is required for the reaction to complete.

UiO-67-$Ru(bpy)_3$ has yet to be synthesized successfully by PSF. The two-step linker synthesis is time-consuming and could give yields up to 60 % (in respect to starting Ru) based on literature reports. A two-step PSF starting from UiO-67-bpy may be more efficient.

3.1.6 Other functionalizations

UiO-67-bpy functionalized with other metals, and UiO-67-bpy with other H_2bpydc linker concentrations than 10 % (in respect to Zr), have not been characterized to the same degree as the materials previously described. In this section follows a short account on these materials.

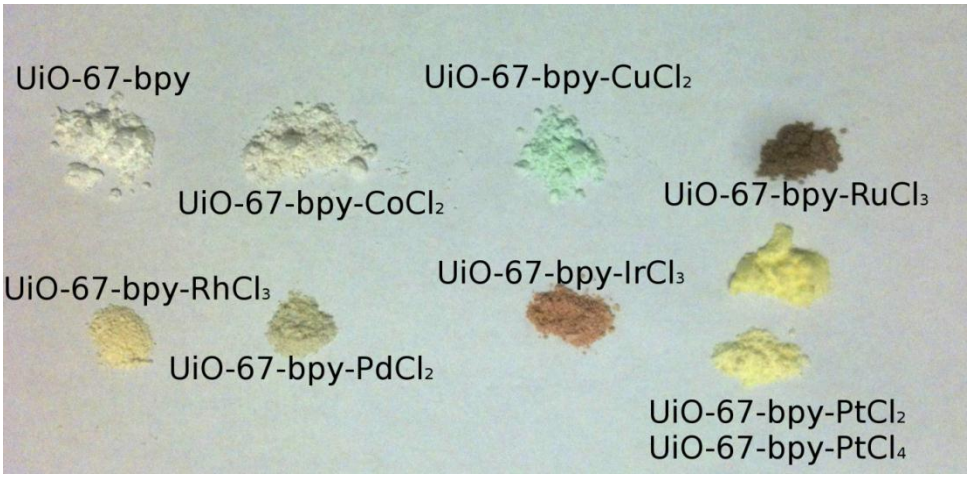

Figure 57. A picture of functionalized UiO-67 as dry powders.

The one pot method was used to synthesize UiO-67-bpy (10 %) with $Fe(NO_3)_3 \cdot 9H_2O$, $CoCl_2 \cdot 6H_2O$, $NiCl_2 \cdot 6H_2O$, $RhCl_3 \cdot xH2O$, $Pd(NO_3)_2 \cdot 2H_2O$ and $IrCl_3 \cdot xH_2O$, in addition to those previously described. A picture of most of the materials is shown in Figure 57. All of the materials are crystalline (containing only the UiO-67 crystalline phase) and are differently colored than UiO-67 (indicating metal content). $FeCl_3$, $CoCl_2$ and $NiCl_2$ functionalized UiO-67-bpy has a much weaker color than the other materials. This may indicate that these ions have lover affinity towards bpy, as would be expected of harder metals, or they could form colorless complexes. PXRD patterns are shown in Figure 58.

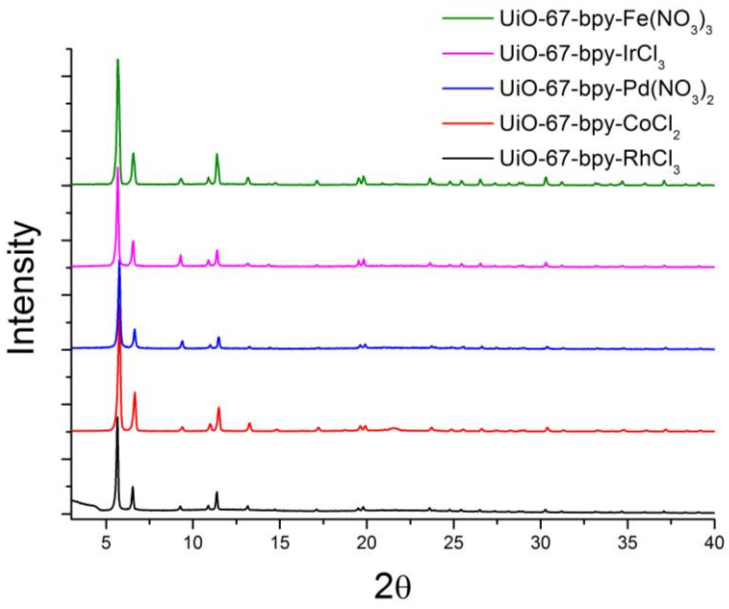

Figure 58. PXRD patterns of UiO-67-bpy functionalized with other metals than those described in previous sections.

UiO-67-bpy (with 100 % bpy linkers) was synthesized as a pure material, and functionalized with 10 % (in respect to $ZrCl_4$) $CuCl_2 \cdot 2H_2O$, $RuCl_3 \cdot xH_2O$, $IrCl_3 \cdot xH_2O$, K_2PtCl_4 and K_2PtCl_6. All of the materials are crystalline (containing only the UiO-67 crystalline phase) and the functionalized ones are differently colored than UiO-67 (indicating metal content). PXRD patterns are shown in Figure 59. The unfunctionalized material, along with $PtCl_4$ and $IrCl_3$ functionalized are porous as well, with comparable BET surface areas as their 10 % bpydc analogues. The materials also have the same thermal stability as pure UiO-67. The price and poor solubility of the linker makes it convenient to dilute it with H_2bpdc, even though their performance is similar. Synthesis description and further characterization data can be found in the appendix, page 146 to 147.

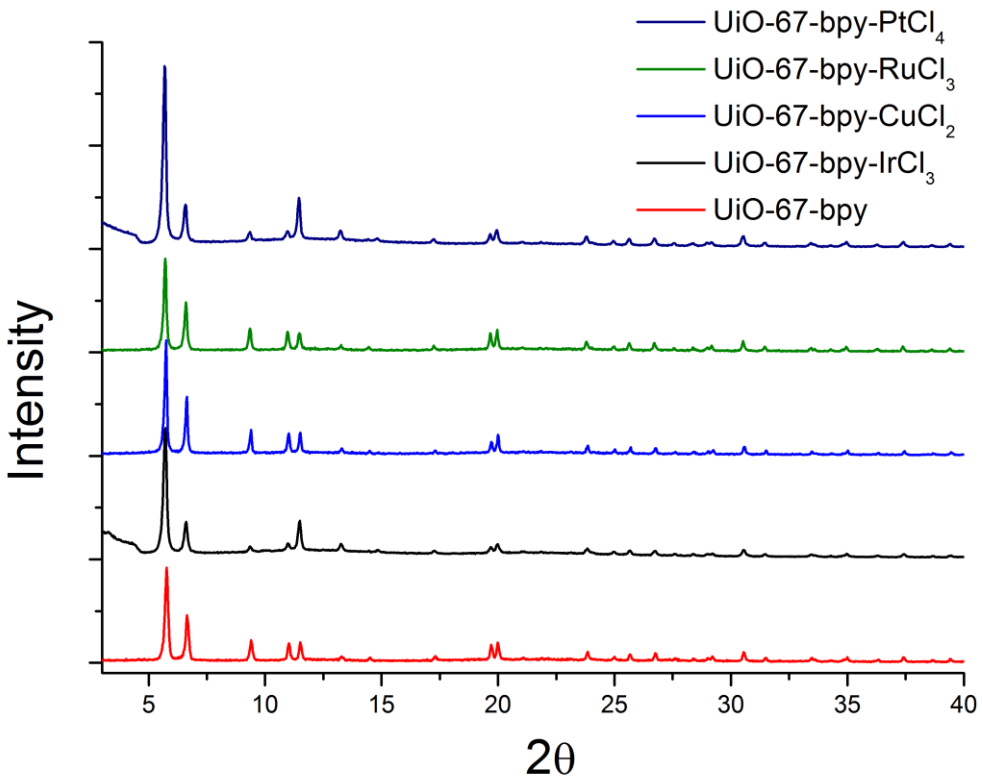

Figure 59. PXRD patterns of UiO-67-bpy made with 100 % bpy linker and 10 % metal functionalization.

3.2 Washing and storage

PXRD patterns of a number of samples were collected before and after washing. A representative collection is showed in Figure 60.

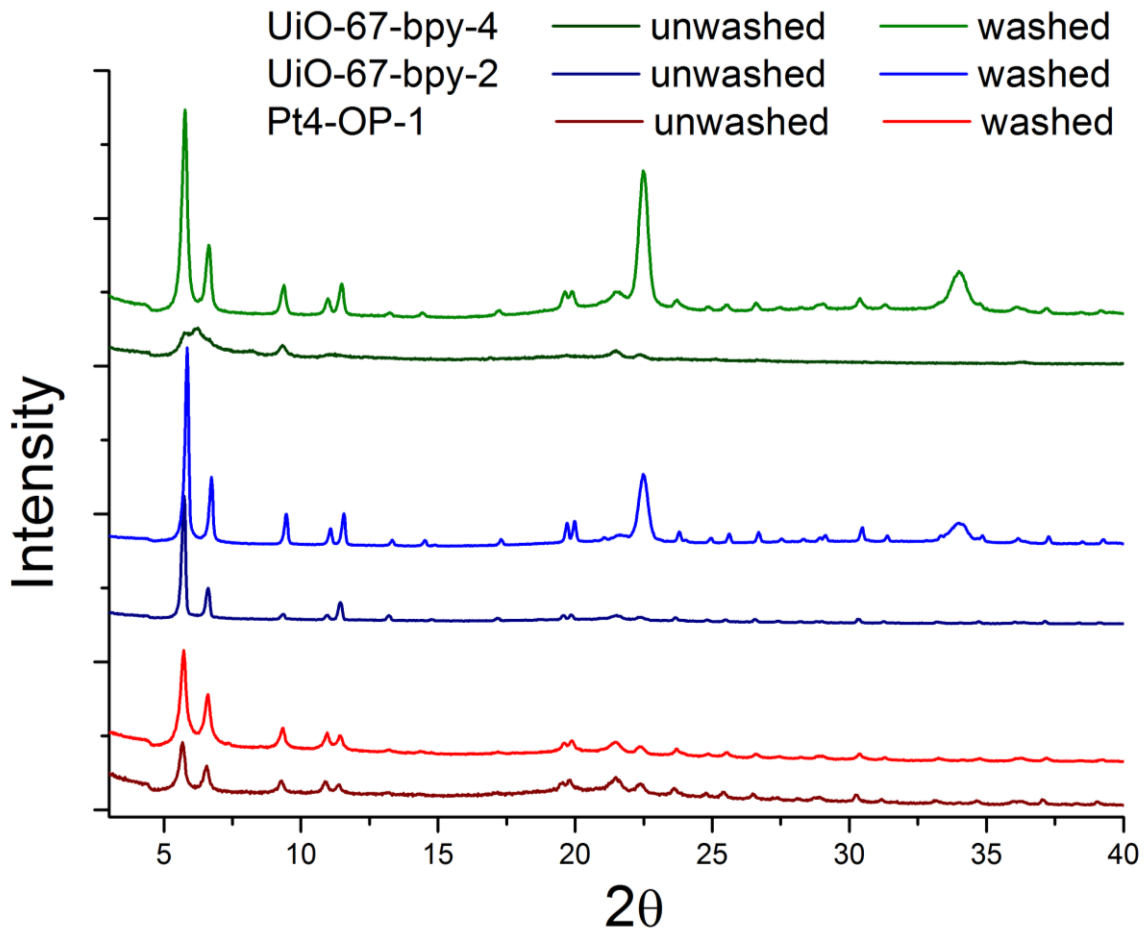

Figure 60. PXRD patterns acquired before and after washing. The broad peaks at 22° and 34° is due to diffraction from plastic foil used to cover the sample.

Washing improves the PXRD pattern for all synthesized UiO-67, but the effect is strongest on samples made with high concentrations of modulator. These results emphasize the importance of washing the product.

All UiO-67 must be kept away from water in order to preserve the crystallinity. Even slightly wet solvent can cause irreversible damage. This was discovered when mounting XRD samples with 2-propanol which had only been exposed to air for one hour, absorbing small amounts of water vapor. The result was controlled by mounting samples from the same batches with dry solvent.

PXRD patterns were acquired for three samples after splitting them in two and keeping them in a desiccator and in a vial on a laboratory shelf for one year. The results are presented in Figure 61.

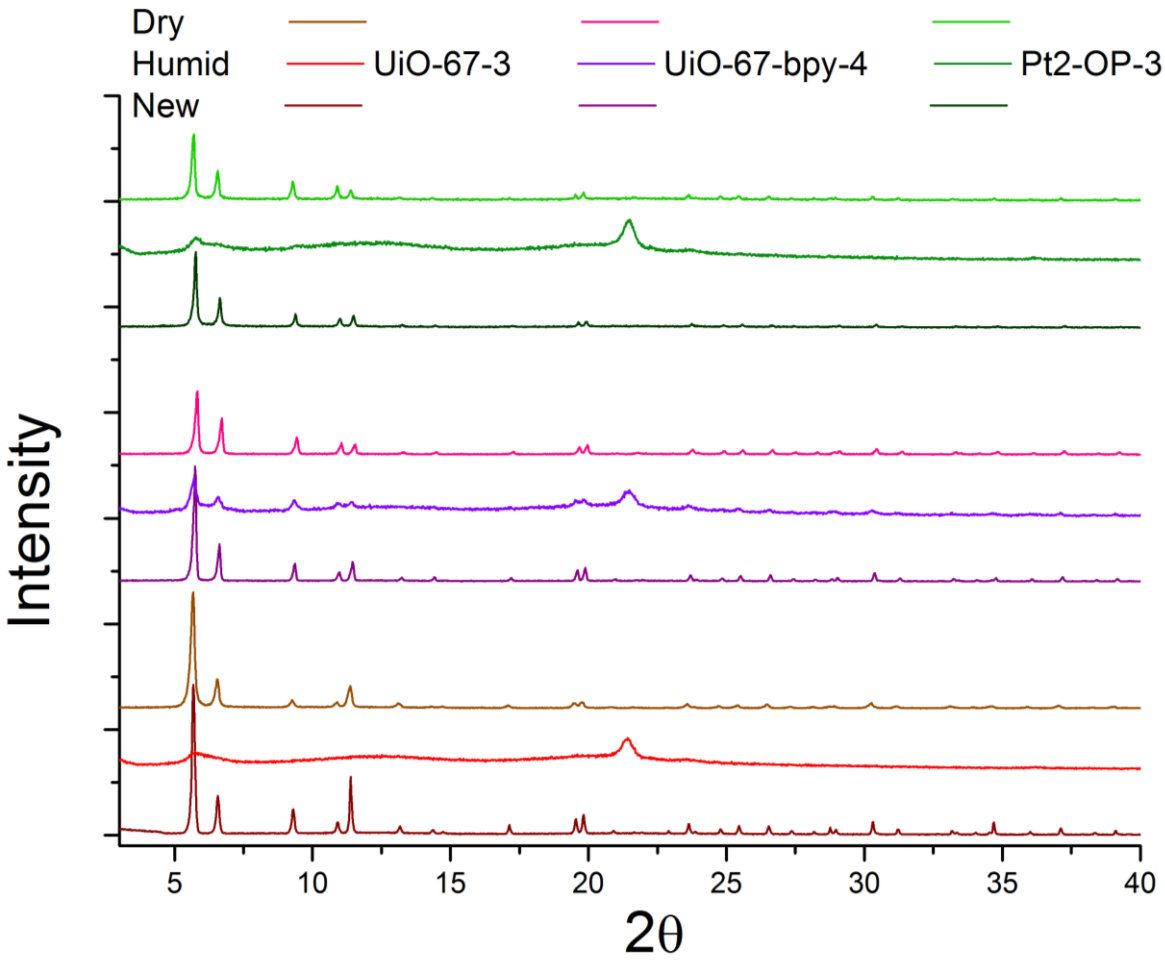

Figure 61. PXRD patterns acquired one year after synthesis for samples kept under different conditions.

Samples kept on the laboratory shelf had absorbed water and decomposed, whereas the same samples kept in dry conditions barely changed.

To investigate the stability towards liquid water, samples were prepared for PXRD with water as the mounting agent. A representative collection of the resulting PXRD patterns are presented in Figure 62.

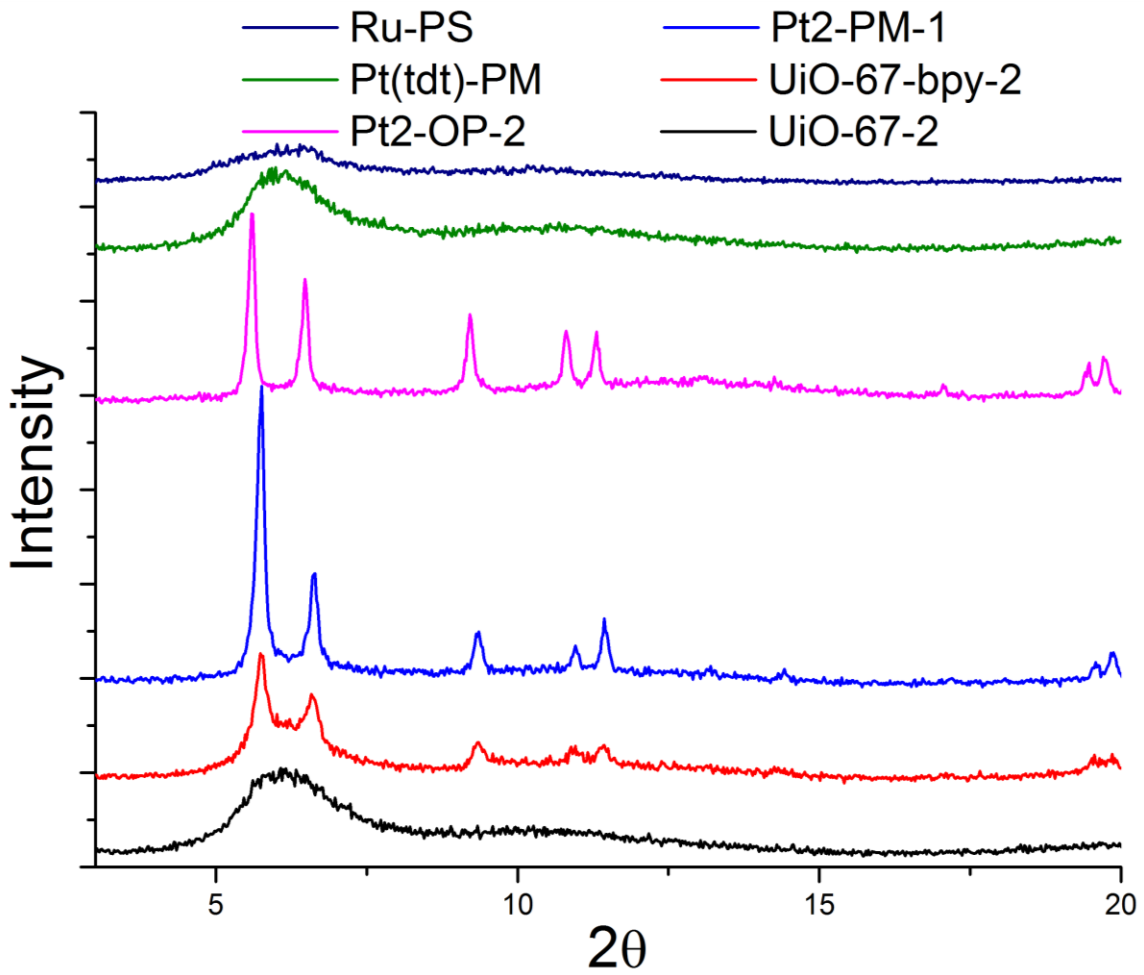

Figure 62. PXRD patterns of UiO-67 samples submerged in liquid water.

These results clearly show that platinum chloride functionalization improves the stability towards liquid water. Sample made with 10 % H_2bpydc linker retained some crystallinity, but neither pure UiO-67 nor a control sample made with 100 % H_2bpydc linkers retained any, indicating that mixed linker systems are somewhat more stable. Although most of the peaks in Pt2-PM-1 and Pt2-OP-2 can still be discerned, the reflection intensities has greatly decreased compared to those of dry sample (first peak decreased from 526 to 63 and 323 to 29 counts per second, respectively).

Figure 63 shows UiO-67-3 and UiO-67-bpy-4 after being exposed to an atmosphere of 60 Pa of water inside the SEM chamber for 30 minutes. The edges and faces seems to “sink” into the crystal body,

possibly indication a collapse of the cavities along the [1 1 1] direction. The corners seem to retain their position in relation to each other.

To summarize, UiO-67 samples must be stored under dry conditions, easily achieved with a desiccator and some drying agent such as silica gel. The results also indicate that polar, space-filling groups such as $PtCl_2$ stabilize the material towards liquid water. This will be investigated further, in order to obtain a water stable UiO-67 analogue.

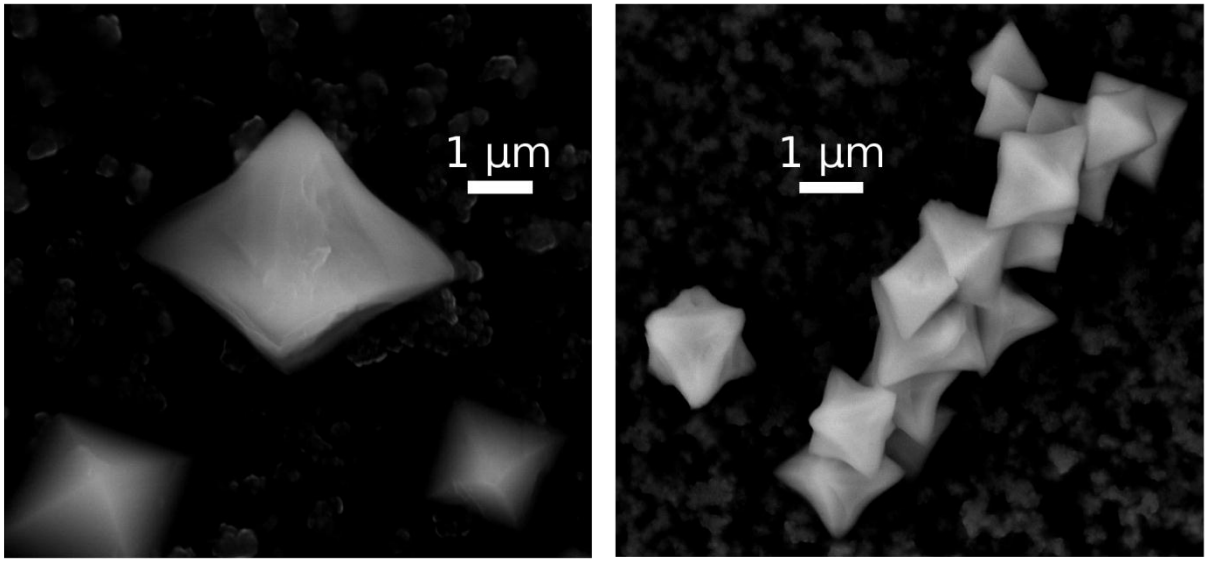

Figure 63. SEM micrographs of UiO-67-bpy-4 (left) and UiO-67-3 (right).

3.3 The elusive UiO-68

A lot of effort has been made to synthesize pure UiO-68. Schaate and coworkers successfully synthesized UiO-68-NH2 (the linker being 2'-amino-4,4''-*para*-terphenyl dicarboxylic acid) using the modulator approach, but failed to produce amine free material[28].

In this work, the regular UiO-67 synthesis previously described was used as a starting point, but yielded poor results. Different modulators, precursor concentrations and synthesis conditions were tried. The most successful attempt was a series of UiO-68 prepared in a glove box; with excess water added after all other reagents were completely dissolved. The PXRD pattern of this product, along with a calculated one is shown in Figure 64. The two peaks visible, at 4.7° and 8.9°, roughly corresponds to the calculated reflections from the planes [1 1 1] and [2 2 2].

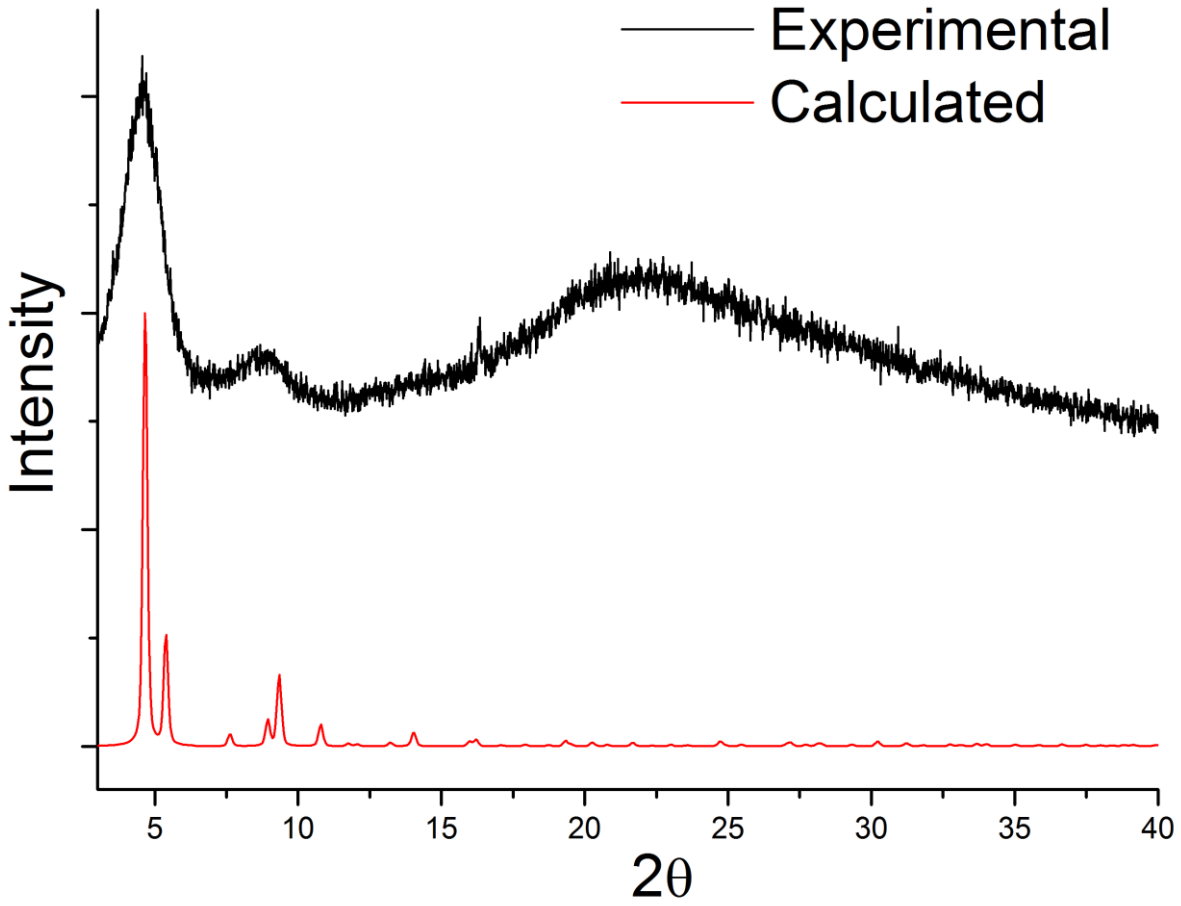

Figure 64. PXRD patterns of UiO-68, experimental and calculated.

There may be multiple reasons why this material is difficult to synthesize. One factor may be the insolubility of the linker, but there is also logical to assume that UiO-68 has poor stability towards water, and thus sensitive towards water in the synthesis. The long linkers may also provide steric difficulties in lattice formation. If the SBUs does not have the ability to attach and detach, formation

of a periodic crystalline phase is very unlikely, with the formation of an amorphous network as a consequence.

There is a physical resemblance between samples of this partly crystalline UiO-68 and products of unsuccessful UiO-67 syntheses, e.g. syntheses with too high water content. Both are recovered from synthesis as a porridge-like gel, and when dry they make agglomerating small-particle powders.

Possible synthesis strategies for UiO-68 synthesis include tuning the synthesis temperature, modulator type and concentration, and possibly addition of other oxide donors than water.

3.4 UiO-70

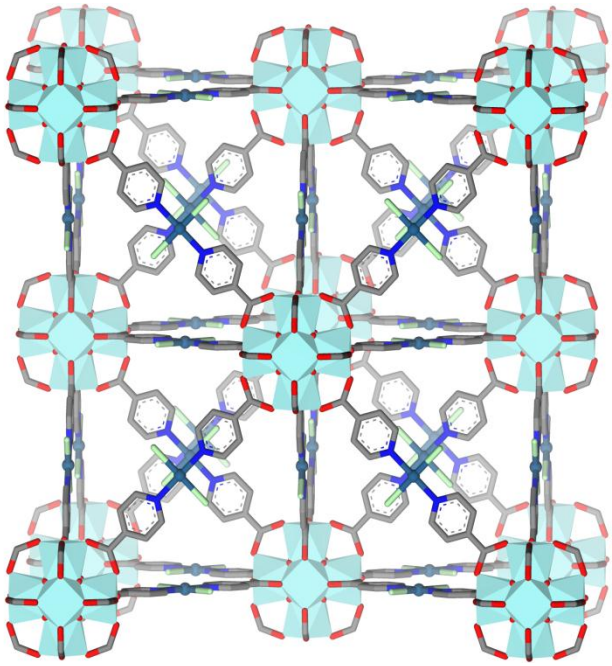

Figure 65. The structure of UiO-70.

A new Zr-MOF with space group $Fm\bar{3}m$ (a = 30.19 Å) was synthesized, using trans-$[Pt(Hpyc)_2Cl_2]$ as linker. The resulting compound, named UiO-70, was characterized by PXRD immediately after being recovered from the synthesis flask (Figure 66). Subsequent PXRD scans showed that the material was rapidly decomposing in air. A refinement was made in Materials Studio, using a geometrically optimized structure (Figure 65). Full details of the refinement can be found in the appendix, page 148. Additional crystalline phases are present in the pattern, but these are also present after the MOF has fully decomposed. Because of stability issues, it is unlikely to see any application for this material.

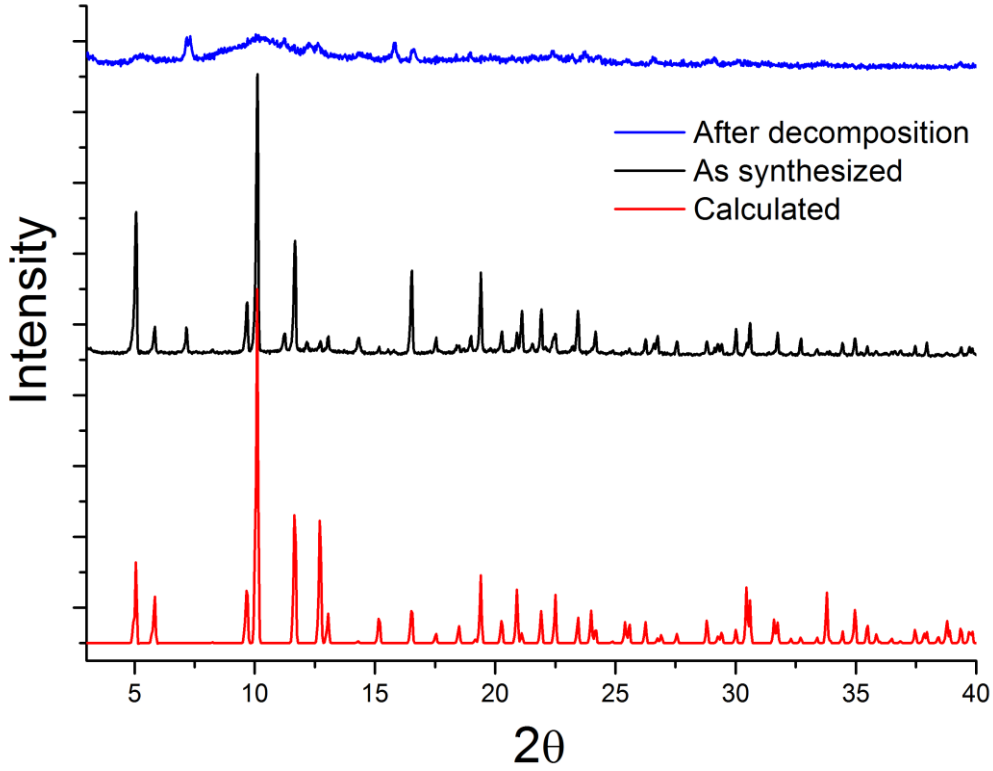

Figure 66. PXRD scans of UiO-70, experimental and calculated.

4 Conclusions

It has been demonstrated that UiO-67 can be made with a large variety of metal complexes based on H_2bpydc, using three different synthesis strategies. These complexes function as linkers in the UiO-67 crystal structure and are stable throughout the MOF synthesis. The bulk material itself retains the porosity as well as the chemical and thermal stability of pure UiO-67. In some cases the stability towards water is improved. From the previously established criteria, all synthesis methods are able to produce high-quality functionalized UiO-67. Platinum functionalized UiO-67 has furthermore been shown to undergo ligand exchange and possible reduction in the gas phase, demonstrating some of the possibilities of these materials.

To choose a common standard method for all the compounds is not possible, since the different methods produce slightly different products. Thus, the method must be chosen according to the given requirements for the synthesized material. As a general conclusion, the one pot method impairs the porosity and yield of the synthesized material more than the other methods.

In all syntheses of functionalized UiO-67, the presence of a modulator improves the porosity of the product, controls the crystal size and reduces particle agglomeration.

To determine the local structure of the (H_2bpydc)MCl_x functionalizations as they are inside MOF has only been possible by EXAFS. Comparing the EXAFS data of the precursor and the final material is a generalizable technique, and could be used on all elements eligible for EXAFS. With this technique, the local structure of platinum functionalized UiO-67 is established, and copper functionalized UiO-67 is established beyond reasonable doubt. At the time of writing, it has not been proven to this degree of certainty that functionalized linkers can retain their structure throughout the MOF synthesis, although many reports of such syntheses exist.

The results from stability tests emphasize the need for UiO-67 materials to be stored under dry conditions to prevent decomposition. It also suggests that the inclusion of hydrophilic groups ($PtCl_2$) somewhat improves the stability of the material towards water.

EXAFS data from heated UiO-67-bpy-$PtCl_2$ in the presence of H_2 and benzene shows no indication of interaction between platinum and benzene. Further testing must be carried out to determine whether these materials are catalytically active. In any case, it has been demonstrated that the materials are susceptible to reactions and ligand exchange in heterogeneous systems.

UiO-70, a new Zr based MOF isoreticular to UiO-66 has been reported. Unfortunately, the MOF is not air stable. It may be worth looking into other metals which may be incorporated into the linker of UiO-70, e.g. palladium or cobalt, as this may result in a stable MOF.

To summarize, an investigation and evaluation of different synthesis strategies to obtain UiO-67 functionalized with various metal complexes on H_2bpydc linkers has been carried out. The materials obtained are promising as starting materials on which PSF may be carried out to incorporate catalytic sites into UiO-67.

The work on functionalizing UiO-67 will continue with the thorough characterization of samples functionalized with other metals, catalytic testing and further PSF, the long term goal being the development of a class of versatile porous materials for selective adsorption and catalysis. Water stability issues will be addressed through linker functionalization, namely by the introduction of hydrophobic and hydrophilic functional groups.

References

(1) Hafizovic, J. C.; Jakobsen, S.; Olsbye, U.; Guillou, N.; Lamberti, C.; Bordiga, S.; Lillerud, K. P. *J. Am. Chem. Soc.* **2008**, *130*, 13850.
(2) Zhou, H. C.; Long, J. R.; Yaghi, O. M. *Chem. Rev. (Washington, DC, U. S.)* **2012**, *112*, 673.
(3) Li, H.; Eddaoudi, M.; O'Keeffe, M.; Yaghi, M. *Nature (London, U.K.)* **1999**, *402*, 276.
(4) Xuan, W.; Zhu, C.; Liu, Y.; Cui, Y. *Chem. Soc. Rev.* **2012**, *41*, 1677.
(5) Lee, J. Y.; Farha, O. K.; Roberts, J.; Scheidt, K. A.; Nguyen, S. B. T.; Hupp, J. T. *Chem. Soc. Rev.* **2009**, *38*, 1450.
(6) Horike, S.; Kitagawa, S. In *Metal-Organic Frameworks: Applications from Catalysis to Gas Storage*; Farrusseng, D., Ed.; Wiley-VCH: Weinheim, Germany, 2011, pp 1-19.
(7) Wee, L. H.; Wiktor, C.; Turner, S.; Vanderlinden, W.; Janssens, N.; Bajpe, S. R.; Houthoofd, K.; Van, T. G.; De, F. S.; Kirschhock, C. E. A.; Martens, J. A. *J. Am. Chem. Soc.* **2012**, *134*, 10911.
(8) Furukawa, H.; Ko, N.; Go, Y. B.; Aratani, N.; Choi, S. B.; Choi, E.; Yazaydin, A. O.; Snurr, R. Q.; O'Keeffe, M.; Kim, J.; Yaghi, O. M. *Science (Washington, DC, U.S.)* **2010**, *329*, 424.
(9) Park, K. S.; Ni, Z.; Cote, A. P.; Choi, J. Y.; Huang, R.; Uribe-Romo, F. J.; Chae, H. K.; O'Keeffe, M.; Yaghi, O. M. *Proc. Natl. Acad. Sci. U. S. A.* **2006**, *103*, 10186.
(10) Tsuruoka, T.; Furukawa, S.; Takashima, Y.; Yoshida, K.; Isoda, S.; Kitagawa, S. *Angew. Chem. Int. Ed.* **2009**, *48*, 4739.
(11) Tranchemontagne, D. J.; Mendoza-Cortes, J. L.; O'Keeffe, M.; Yaghi, O. M. *Chem. Soc. Rev.* **2009**, *38*, 1257.
(12) Eddaoudi, M.; Kim, J.; Rosi, N.; Vodak, D.; Wachter, J.; O'Keeffe, M.; Yaghi, O. M. *Science (Washington, DC, U.S.)* **2002**, *295*, 469.
(13) Chui, S. S. Y.; Lo, S. M. F.; Charmant, J. P. H.; Orpen, A. G.; Williams, I. D. *Science (Washington, DC, U.S.)* **1999**, *283*, 1148.
(14) Férey, G.; Mellot-Draznieks, C.; Serre, C.; Millange, F.; Dutour, J.; Surble, S.; Margiolaki, I. *Science (Washington, DC, U.S.)* **2005**, *309*, 2040.
(15) Batten, S. R.; Champness, N. R.; Chen, X.-M.; Garcia-Martinez, J.; Kitagawa, S.; Oehrstroem, L.; O'Keeffe, M.; Suh, M. P.; Reedijk, J. *CrystEngComm* **2012**, *14*, 3001.
(16) Seyferth, D. *Organometallics* **2001**, *20*, 2.
(17) Ritter, S. K. *Chem. Eng. News* **2005**, *83*, 32.
(18) Koyama, H.; Saito, Y. *Bull. Chem. Soc. Jpn.* **1954**, *27*, 112.
(19) Kickelbick, G.; Schubert, U. *Chem. Ber./Recl.* **1997**, *130*, 473.
(20) Stock, N.; Biswas, S. *Chem. Rev. (Washington, DC, U. S.)* **2011**, *112*, 933.
(21) Yaghi, O. M.; Li, H. *J. Am. Chem. Soc.* **1995**, *117*, 10401.
(22) O'Keeffe, M. *Chem. Soc. Rev.* **2009**, *38*, 1215.
(23) Yaghi, O. M.; O'Keeffe, M.; Ockwig, N. W.; Chae, H. K.; Eddaoudi, M.; Kim, J. *Nature (London, U.K.)* **2003**, *423*, 705.
(24) Yaghi, O. M.; Eddaoudi, M.; Li, H.; Kim, J.; Rosi, N.; Preparation of isoreticular metal-organic frameworks and systematic design of pore size and functionality, with application for gas storage. International patent number WO2002088148A1, November 7, 2002.
(25) *SciFinder*, 2012, Chemical Abstracts Service: Columbus, OH.
(26) *Statistical Summary 1907-2007*, 2007, Chemical Abstracts Service: Columbus, OH.

(27) Valenzano, L.; Civalleri, B.; Chavan, S.; Bordiga, S.; Nilsen, M. H.; Jakobsen, S.; Lillerud, K. P.; Lamberti, C. *Chem. Mat.* **2011**, *23*, 1700.
(28) Schaate, A.; Roy, P.; Godt, A.; Lippke, J.; Waltz, F.; Wiebcke, M.; Behrens, P. *Chemistry* **2011**, *17*, 6643.
(29) Kim, M.; Cohen, S. M. *CrystEngComm* **2012**, *14*, 4096.
(30) Housecroft, C. E.; Sharpe, A. G. In *Inorganic Chemistry*; 3rd ed.; Pearson Prentice Hall: Essex, England, 2008, pp 207-208 and 752-753.
(31) Nilsen, M. H.; Jakobsen, S.; Lamberti, C.; Bonino, F.; Gianolio, D.; Bordiga, S.; Olsbye, U.; Lillerud, K. P. Crystallization kinetics of Zr-MOF: An in situ study. Presented at The 34th Annual BZA conference, Edinburgh, 2011.
(32) Schubert, U.; Hüsing, N. In *Synthesis of inorganic materials*; 2nd ed.; Wiley-VCH: Weinheim, Germany, 2004, pp 335-340.
(33) Ganesan, S. V.; Lightfoot, P.; Natarajan, S. *Solid State Sci.* **2004**, *6*, 757.
(34) Maniam, P.; Stock, N. *Inorg. Chem.* **2011**, *50*, 5085.
(35) Hausdorf, S.; Baitalow, F.; Seidel, J.; Mertens, F. O. R. L. *J. Phys. Chem. A* **2007**, *111*, 4259.
(36) Yaghi, O. M.; Li, G.; Li, H. *Nature (London, U.K.)* **1995**, *378*, 703.
(37) Mueller, M.; Hermes, S.; Kaehler, K.; van, d. B. M. W. E.; Muhler, M.; Fischer, R. A. *Chem. Mat.* **2008**, *20*, 4576.
(38) Lillerud, K. P.; Olsbye, U.; Tilset, M. *Top. Catal.* **2010**, *53*, 859.
(39) Kitagawa, S.; Noro, S.; Nakamura, T. *Chem. Commun. (Cambridge, U. K.)* **2006**, *42*, 701.
(40) Wang, C.; Xie, Z.; deKrafft, K. E.; Lin, W. *J. Am. Chem. Soc.* **2011**, *133*, 13445.
(41) Lersch, M. 1,4-diaza-1,3-butadiene platinum complexes for C-H activation - syntheses, mechanisms and trends. Doctor Scientiarum Thesis, University of Oslo, 2006.
(42) Lersch, M.; Tilset, M. *Chem. Rev. (Washington, DC, U. S.)* **2005**, *105*, 2471.
(43) Szeto, K. C.; Prestipino, C.; Lamberti, C.; Zecchina, A.; Bordiga, S.; Bjorgen, M.; Tilset, M.; Lillerud, K. P. *Chem. Mat.* **2007**, *19*, 211.
(44) Cummings, S. D.; Eisenberg, R. *J. Am. Chem. Soc.* **1996**, *118*, 1949.
(45) Selmeczi, K.; Reglier, M.; Giorgi, M.; Speier, G. *Coord. Chem. Rev.* **2003**, *245*, 191.
(46) Balzani, V.; Bergamini, G.; Marchioni, F.; Ceroni, P. *Coord. Chem. Rev.* **2006**, *250*, 1254.
(47) Schoenecker, P. M.; Belancik, G. A.; Grabicka, B. E.; Walton, K. S. *AIChE Journal* [online early access]. DOI: 10.1002/aic.13901. Published online: Aug 30, 2012.
(48) Constable, E. C. *Adv. Inorg. Chem.* **1989**, *34*, 1.
(49) Jakobsen, S. Nye ligander for Pt-MOF strukturer. M.Sc. Thesis, University of Oslo, 2006.
(50) Lundvall, F. Nye koordinasjonspolymerer basert på Pt(IV). M.Sc. Thesis, University of Oslo, 2009.
(51) Jakobsen, S.; Regno, A. D.; Jung, A.; Wragg, D.; Tilset, M.; Unpublished work: 2012.
(52) Geary, E. A. M.; Hirata, N.; Clifford, J.; Durrant, J. R.; Parsons, S.; Dawson, A.; Yellowlees, L. J.; Robertson, N. *Dalton Trans.* **2003**, *32*, 3757.
(53) Sullivan, B. P.; Salmon, D. J.; Meyer, T. J. *Inorg. Chem.* **1978**, *17*, 3334.
(54) Muzart, J. *Tetrahedron* **2009**, *65*, 8313.
(55) Xie, P.-H.; Hou, Y.-J.; Zhang, B.-W.; Cao, Y.; Wu, F.; Tian, W.-J.; Shen, J.-C. *Dalton Trans.* **1999**, *28*, 4217.
(56) Goddard, R.; Hemalatha, B.; Rajasekharan, M. V. *Acta Crystallogr., Sect. C: Cryst. Struct. Commun.* **1990**, *46*, 33.

(57) Bloch, E. D.; Britt, D.; Lee, C.; Doonan, C. J.; Uribe-Romo, F. J.; Furukawa, H.; Long, J. R.; Yaghi, O. M. *J. Am. Chem. Soc.* **2010**, *132*, 14382.
(58) Brandon, D. K., Wayne D. In *Microstructural Characterization of Materials*; John Wiley and Sons, Ltd: West Sussex, UK, 2008, pp 55-76 and 271-277.
(59) Atkins, P.; De Paula, J. In *Physical Chemistry*; 8th ed.; Oxford University Press: Oxford, UK, 2006, pp 916-922.
(60) Langmuir, I. *J. Am. Chem. Soc.* **1918**, *40*, 1361.
(61) Brunauer, S.; Emmett, P. H.; Teller, E. *J. Am. Chem. Soc.* **1938**, *60*, 309.
(62) Walton, K. S.; Snurr, R. Q. *J. Am. Chem. Soc.* **2007**, *129*, 8552.
(63) Düren, T.; Millange, F.; Férey, G.; Walton, K. S.; Snurr, R. Q. *J. Phys. Chem. C* **2007**, *111*, 15350.
(64) Connolly, M. L. *J. Appl. Crystallogr.* **1983**, *16*, 548.
(65) Williams, D. H.; Fleming, I. In *Spectroscopic methods in organic chemistry*; 5 ed.; McGraw-Hill: Berkshire, U.K., 1995, pp 1-3, 63-70 and 170-171.
(66) Campbell, T. W. *J. Am. Chem. Soc.* **1960**, *82*, 3126.
(67) Xu-jie, Y.; Xin, W.; Song, J.; Dao-yong, C.; Jiang-run, Z.; Lu-de, L. *Spectrosc. Lett.* **2000**, *33*, 415.
(68) Øien, S.; Nilsen, M. H.; Lundvall, F.; Bordiga, S.; Tilset, M.; Olsbye, U.; Lillerud, K. P. Synthesis and characterization of new platinum-containing Zr-based metal organic frameworks. Presented at Norwegian catalysis symposium, Lillestrøm, Norway, 2011.
(69) Nakai, K.; Sonoda, J.; Iegami, H.; Naono, H. *Adsorption* **2005**, *11*, 227.
(70) Vermoortele, F.; Vandichel, M.; Van de Voorde, B.; Ameloot, R.; Waroquier, M.; Van Speybroeck, V.; De Vos, D. E. *Angewandte Chemie International Edition* **2012**, *51*, 4887.
(71) Hafizovic, J.; Olsbye, U.; Lillerud, K. P. *Acta Crystallogr., Sect. E: Struct. Rep. Online* **2006**, *62*, 414.
(72) Paris, J. P.; Brandt, W. W. *J. Am. Chem. Soc.* **1959**, *81*, 5001.

Appendix

Table of Contents

Synthesis and characterization of new platinum-containing Zr-based metal organic frameworks

Sigurd Øien[a], Merete H Nilsen[a], Fredrik Lundvall[a], Silvia Bordiga[b],Mats Tilset[a], Unni Olsbye[a], Karl Petter Lillerud[a]

[a]Department of Chemistry, University of Oslo, P.O. Box 1033, N-0315 Oslo, Norway
[b]Dipartimento di Chimica IFM and NIS Centre of Excellence, Via P. Giuria 7, Università di Torino, Italy

In this work, two new Zr-based MOFs with the UiO-67 topology have been synthesized and characterized. These new MOFs have a very high internal surface area, and open Pt-sites suitable for catalysis.

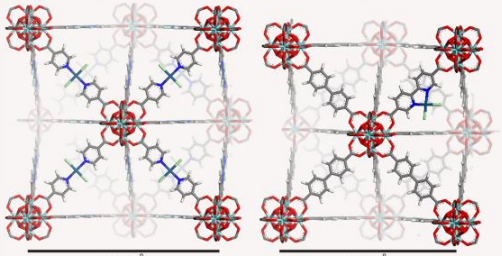

New MOF (UiO-70) UiO-67-($PtCl_2$)BiPy

Metal organic frameworks (MOFs) are steadily becoming more attractive and promising materials for heterogeneous catalysis, due to their high internal surface area, stability and diversity[1]. The isoreticular Zr-based MOFs (the UiO-series) are among the most stable of these compounds, and has been shown to exhibit catalytic activity on modified linkers[2].

The synthesis

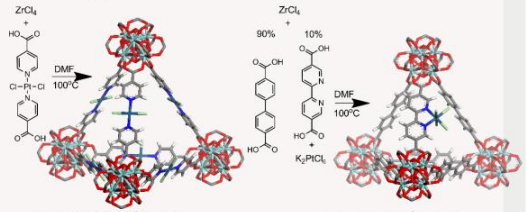

New MOF (UiO-70) UiO-67-($PtCl_4$)BiPy

The synthesis is carried out in a glass container, where the reagents are dissolved in dimethyl formamide. Competing ligands are added to inhibit fast crystal growth, hence slowing crystal growth and improving product quality[3]. UiO-67-BiPy is made with 10% bipyridine linkers. Then we add either K2PtCl4 or K2PtCl6 which is later reduced. Reference samples are made the same way, but without platinum chloride.

Characterization

-X-ray powder diffraction

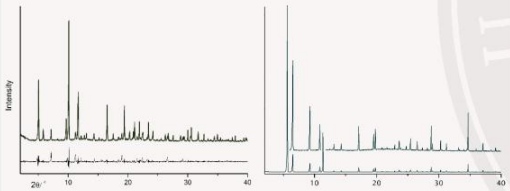

PXRD pattern of UiO-70 with deviation from estimated values

PXRD pattern of UiO-67 with BiPy-linkers (partly magnified 5x)

The UiO-67 topology is identified by PXRD. No major differences can be seen between UiO-67-BiPy with and without platinum considering the diffraction patterns. The measured diffractogram of UiO-70 fits well with calculations (Rpw = 15,9%). Some extra peaks is probably due to solvent molecules, as the MOF is not air stable.

-Scanning electron microscope

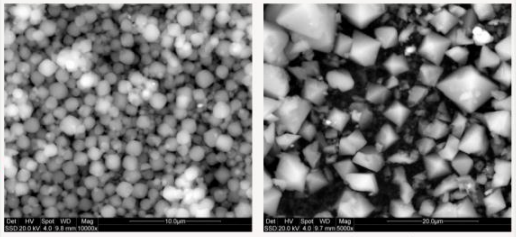

UiO-67-($PtCl_4$)BiPy UiO-67-BiPy

SEM is used to identify the morphology of the crystallites. UiO-67 made with a 0.1 fraction of bipyridine linkers shows a clear octahedral shape. The edges tend to be rounded when platinum chlorides are added to the synthesis. EDS, along with visible color change, confirms the presence of platinum in the structure.

-Adsorption measurements

By introducing competing ligands to the synthesis, and keeping the BiPy linker concentration low, the Langmuir surface of UiO-67-BiPy is almost as large as the empty framework.

MOF	UiO-67-BiPy	UiO-67-($PtCl_4$)BiPy
Measured	2854 m^2/g	2732 m^2/g
Theoretical	3000 m^2/g[1]	---

-Infrared spectroscopy

FTIR of UiO-67-($PtCl_4$)BiPy shows what is probably CO stretching mode of Pt-carbonyl at 2044 cm^{-1}. The MOF topology is intact throughout the experiment, as the framework vibrational modes remain unchanged. Another unidentified peak appears at 2108 cm^{-1}.which will be subject to further investigations

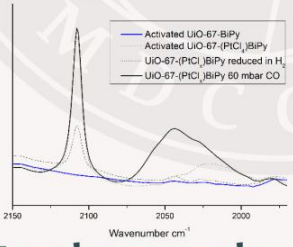

Further work

The MOFs will be characterized further, with solid state NMR and possibly EXAFS. More FTIR and adsorption measurements will also be carried out. The synthesis is currently applied to other metals, and the materials will be tested for catalytic activity.

Cited literature

[1] A New Zirconium Inorganic Building Brick Forming Metal Organic Frameworks with Exceptional Stability
Jasmina Hafizovic Cavka, Søren Jakobsen, Unni Olsbye, Nathalie Guillou, Carlo Lamberti, Silvia Bordiga, Karl Petter Lillerud
Journal of the American Chemical Society, 2008, 130 (42), 13850-13851

[2] Doping Metal–Organic Frameworks for Water Oxidation, Carbon Dioxide Reduction, and Organic Photocatalysis
Cheng Wang, Zhigang Xie, Kathryn E. deKrafft, Wenbin Lin
Journal of the American Chemical Society, 2011, 133 (34), 13445-13454

[3] Modulated Synthesis of Zr-Based Metal–Organic Frameworks: From Nano to Single Crystals
Andreas Schaate,Pascal Roy, Adelheid Godt, Jann Lippke, Florian Waltz, Michael Wiebcke, Peter Behrens
Chemistry - A European Journal, 2011, 17 (24), 6643-6650

UiO : Department of Chemistry
University of Oslo

Abstract, MOF12

This abstract was submitted to the MOF12 conference, and I was invited to give a 15 minute talk on the work.

From framework to catalyst: Isolated noble metal sites in UiO-67

S. Øien, G.C. Shearer, S. Svelle, M. Tilset, K.P. Lillerud, Department of Chemistry, University of Oslo, Oslo, Norway;

S. Bordiga, C. Lamberti, Dipartimento Chimica IFM, Turin, Italy

The Zr(bpdc)-based MOF, UiO-67, can be functionalized with a wide range of catalytically important metals (Rh, Ru, Pt, Ir, Pd, Co, Cu). When prepared with a mixture of biphenyl and 2,2'-bipyridine dicarboxylate linkers, these MOFs retain the high stability known for this topology, even with metal loadings as high as M/Zr =1/10. Previously observed problems with metal-metal stacking preventing access to the metal sites is not observed for these materials.

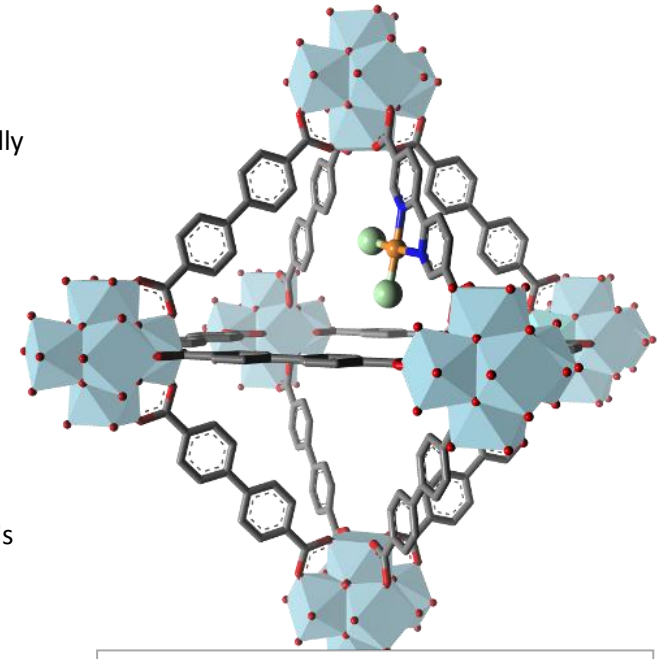

Figure 67. The large octahedral cage of the UiO-67 with one metal chloride

Simple synthesis

A key issue is how the synthesis procedure influences the final material. We seek to develop a simple, few-step process that gives reproducible results and allows inclusion of a large number of d or f-metals.

Towards a robust heterogeneous catalyst

The presence of metal within the MOFs is confirmed by EDX and UV/vis spectroscopies. Additional techniques are now being used to characterize the local environment around the metal centers after various pretreatments. Solid state NMR shows the presence of N-M interactions. With in situ IR spectroscopy it has been further demonstrated that CO interacts with Pt after reduction with H_2. In situ EXAFS utilizing the Pt adsorption edge is in progress and will hopefully confirm that metal sites are open for interaction with probe molecules.

[1] J.H. Cavka, S. Jakobsen et al. J. Am. Chem. Soc. 130 (2008) 13850-13851.

Characterization of linkers

This section contains relevant characterization data not presented in the main text.

Linkers

NMR spectra show two sets of integral values. The top one is the experimental integral, while the bottom one is the estimated value calculated from the peak type. The two are used complementary.

H_2bpdc

^1H NMR

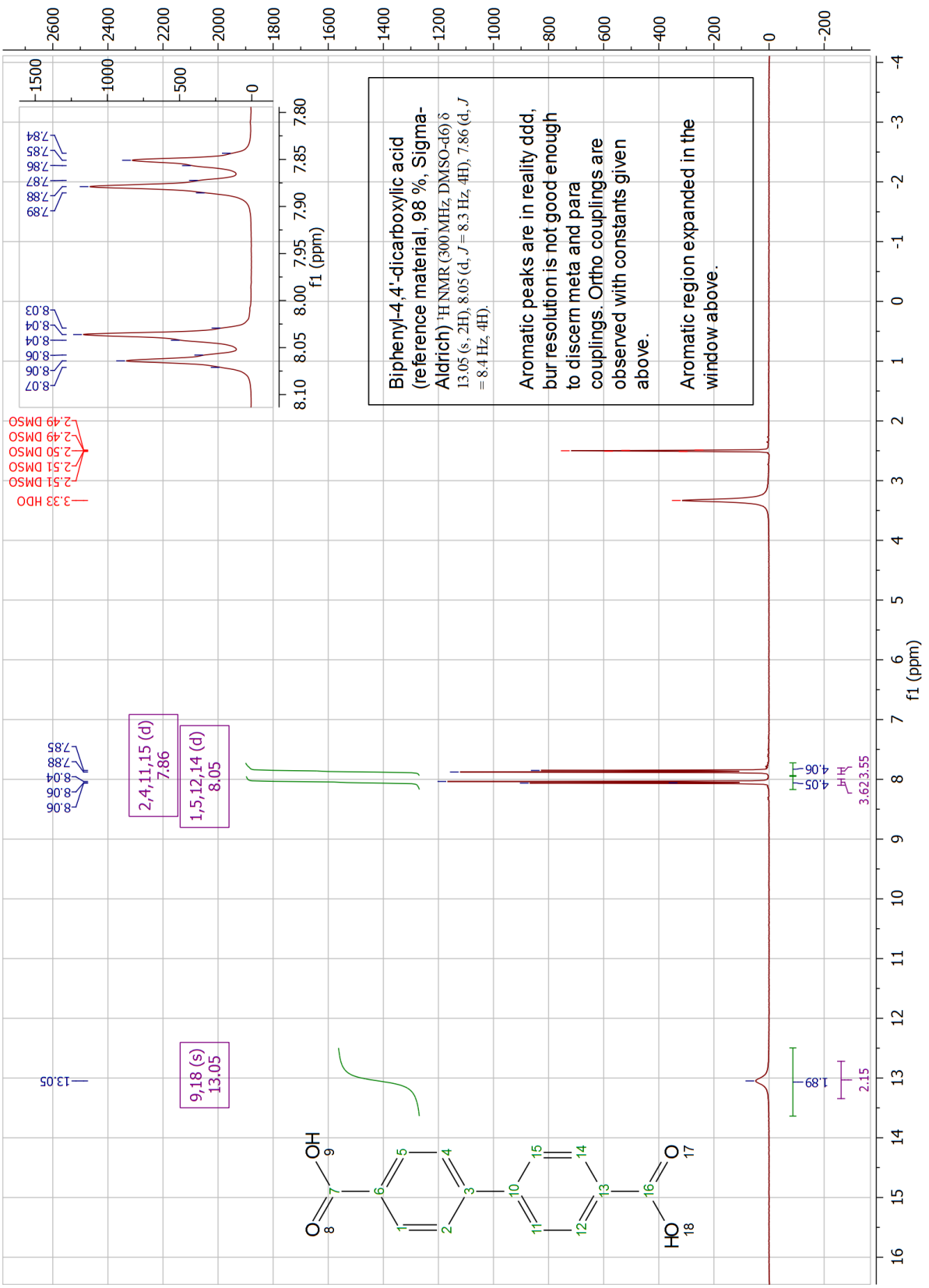

H_2bpdc. ^{13}C NMR (75 MHz, DMSO) δ 167.87, 143.96, 131.21, 130.87, 128.01. The signal at 79.0 ppm is an instrument artifact.

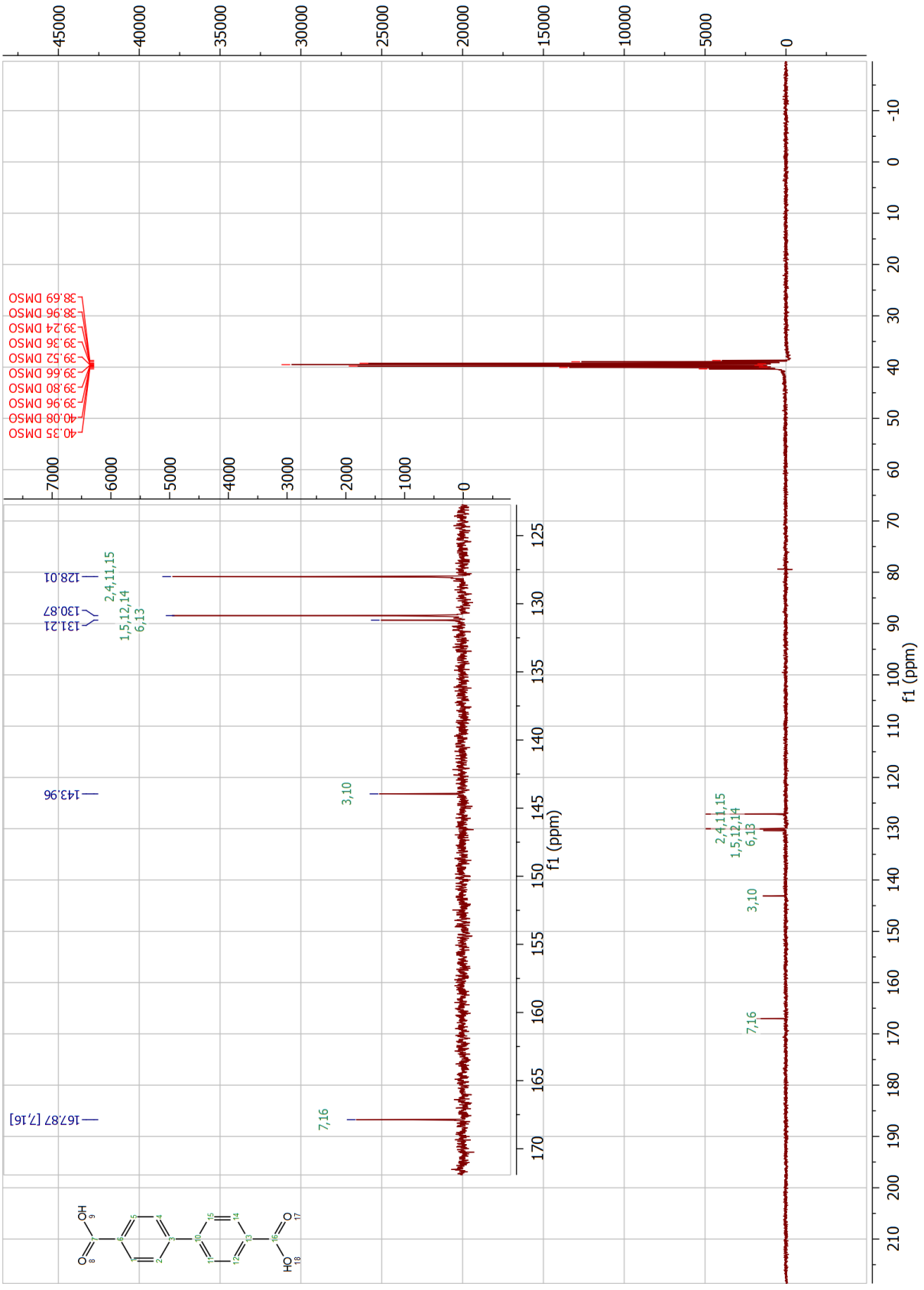

H_2bpydc

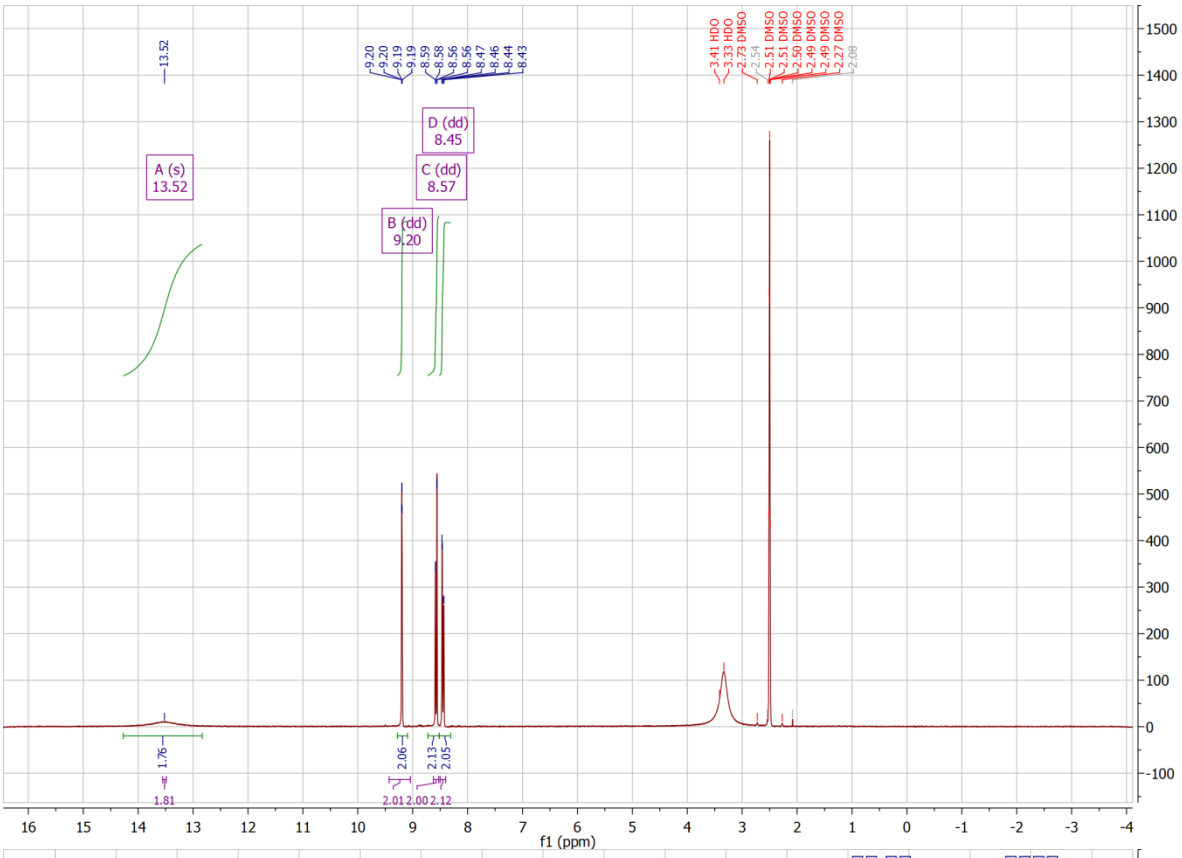

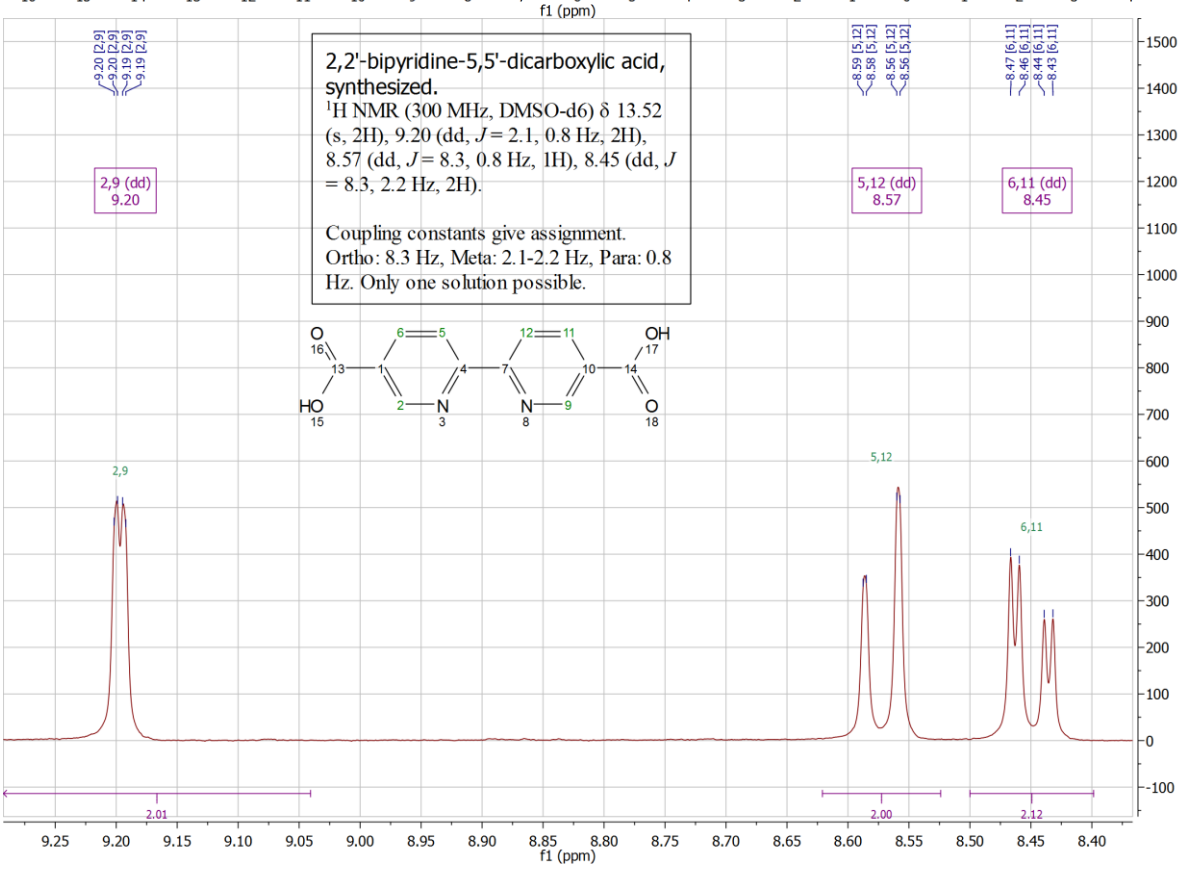

2,2'-bipyridine-5,5'-dicarboxylic acid, synthesized.
^{1}H NMR (300 MHz, DMSO-d6) δ 13.52 (s, 2H), 9.20 (dd, J = 2.1, 0.8 Hz, 2H), 8.57 (dd, J = 8.3, 0.8 Hz, 1H), 8.45 (dd, J = 8.3, 2.2 Hz, 2H).

Coupling constants give assignment. Ortho: 8.3 Hz, Meta: 2.1-2.2 Hz, Para: 0.8 Hz. Only one solution possible.

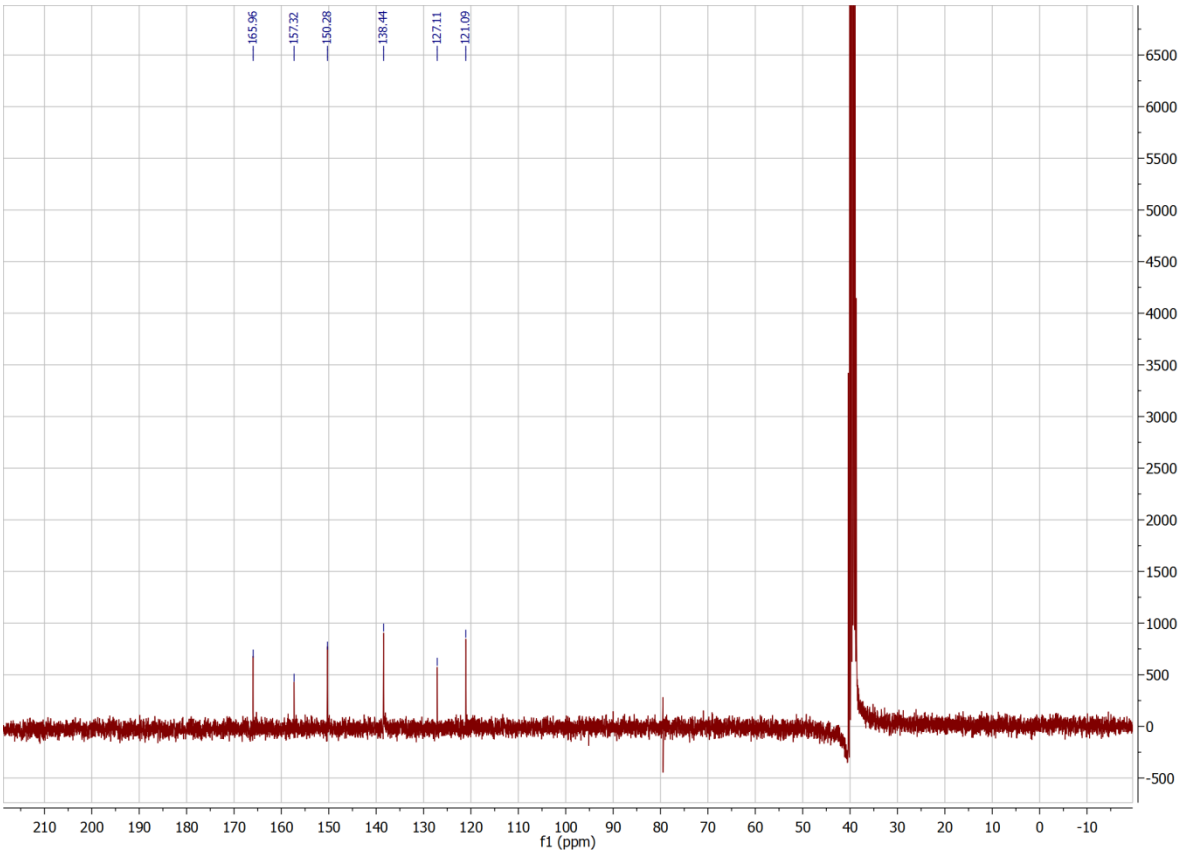

13C-spectrum showing 5 unique carbons in the molecule. The signal at 79.0 ppm is an instrument artifact.

$PtCl_2(H_2bpydc)$

Peaks at 1.01 and 3.77 ppm is due to leftover 2-propanol from washing. In the multiplet at 8.8, the two higher-shift peaks display para-coupling, so they can be assigned to 5 and 12. Thus 6 and 11 are the low shift peaks.

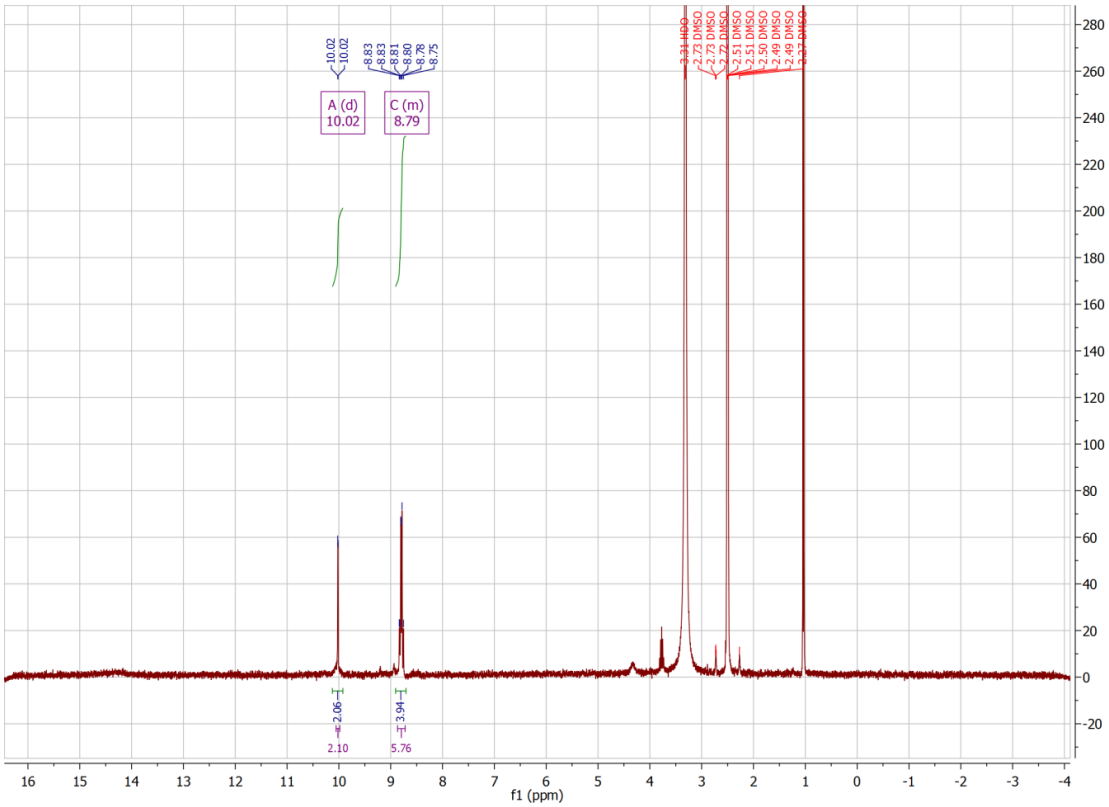

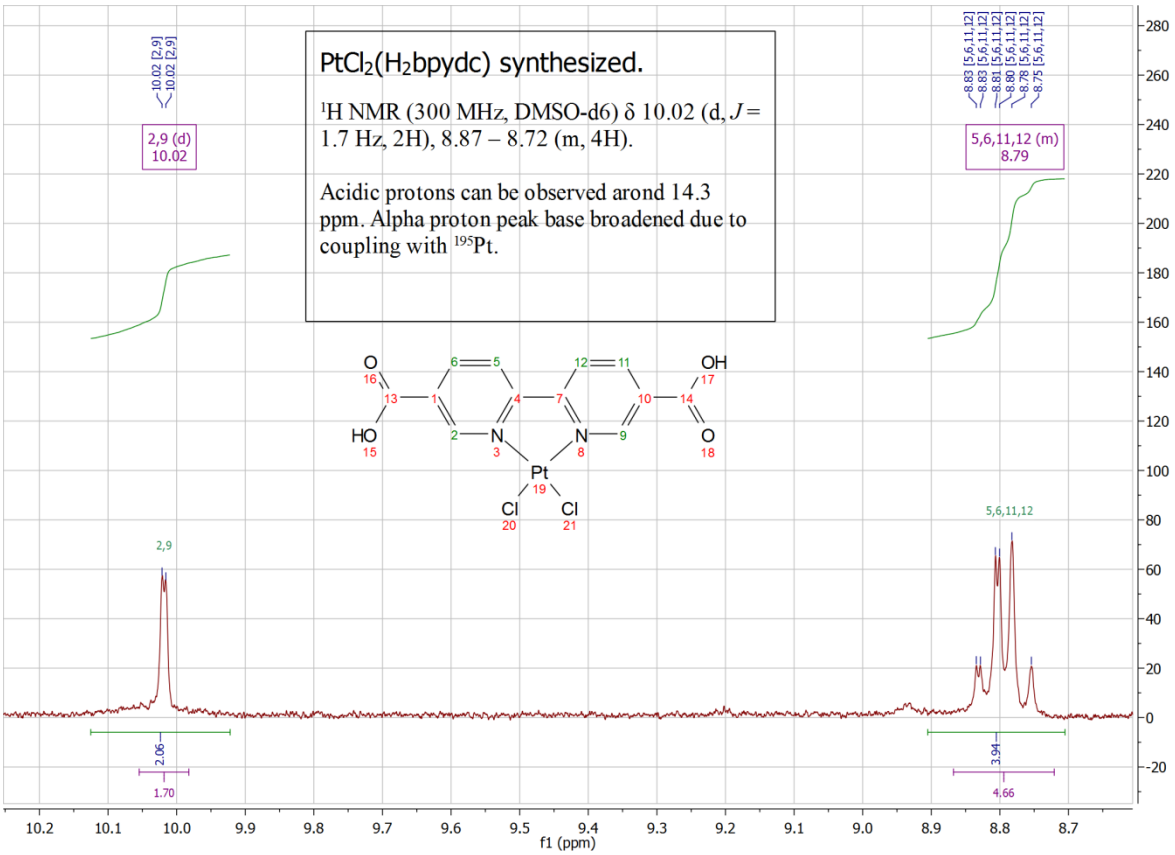

$PtCl_4(H_2bpydc)$

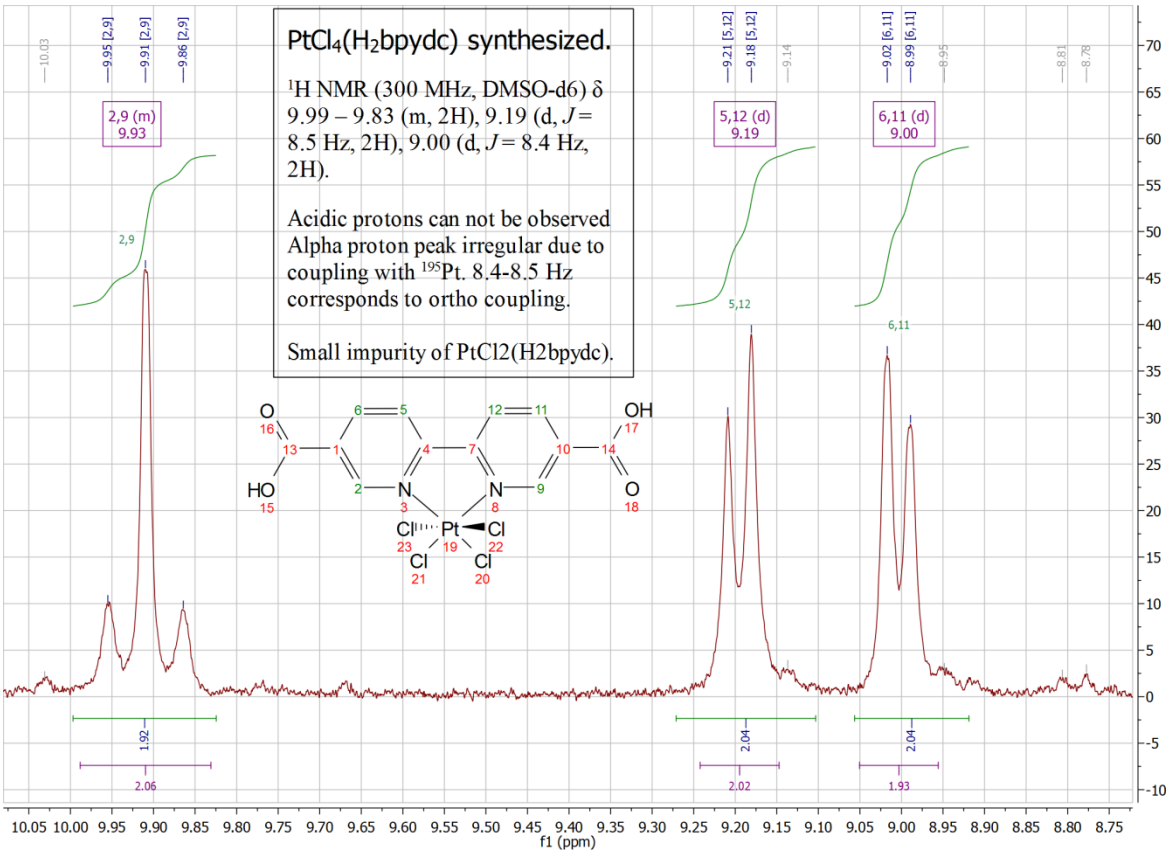

Pt(tdt)(H_2bpydc)

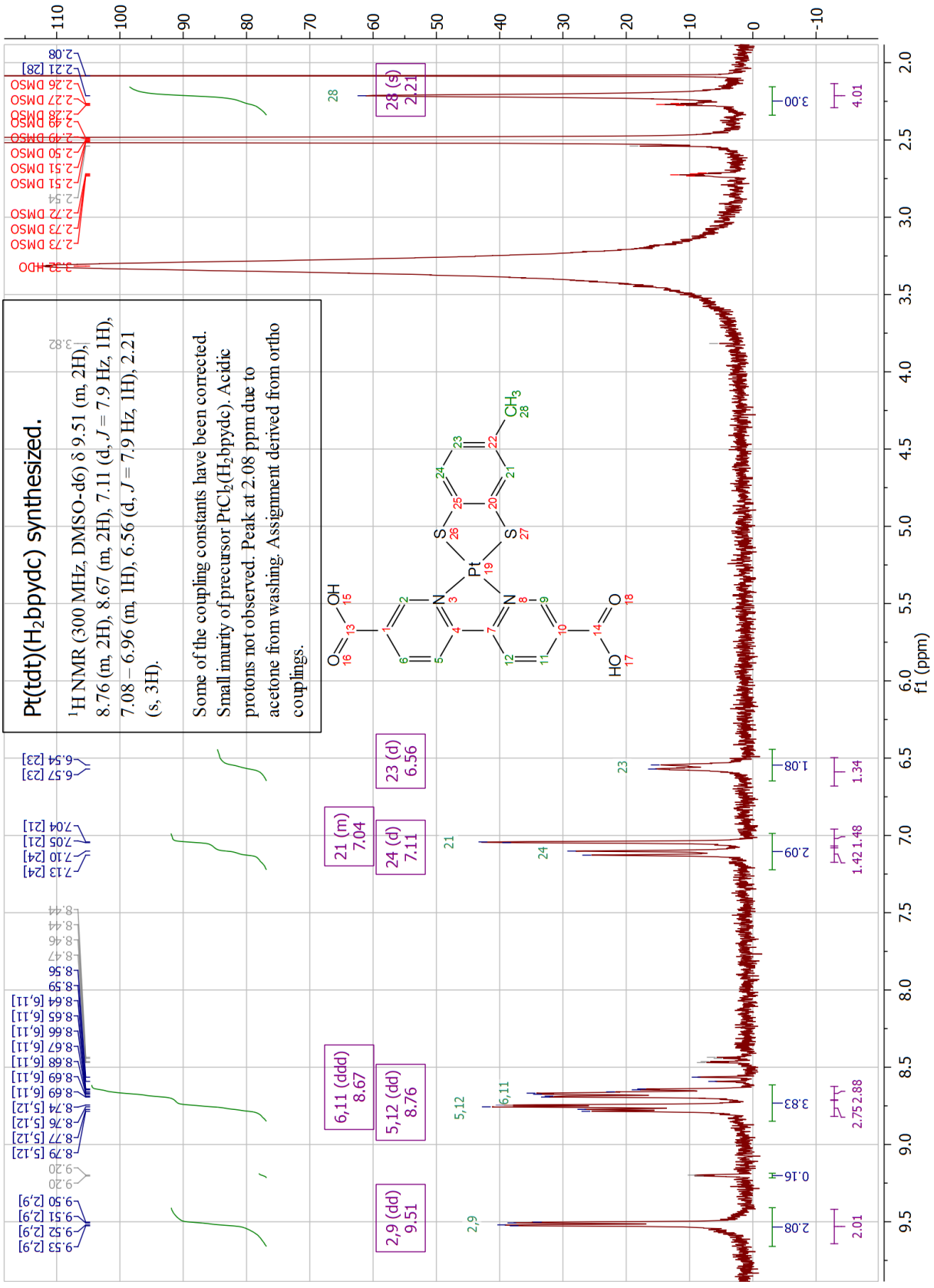

EXAFS of platinum precursors and linkers

EXAFS was measured on precursors, linkers and MOFs containing Pt and Cu. Bond lengths for Pt compounds are known from crystallography. EXAFS data are not phase corrected, but the scale is relative. Data on MOFs are presented in the MOF section.

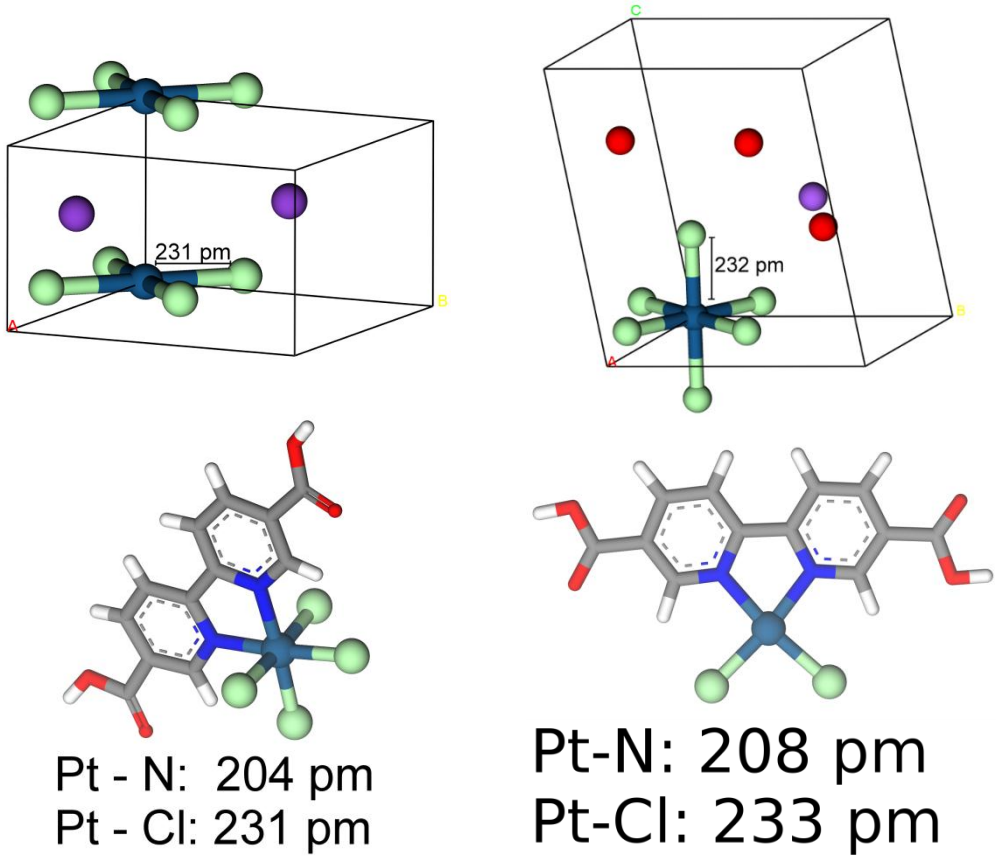

Structures with relevant bond lengths for K_2PtCl_4, $Na_2PtCl_6 \cdot 6H_2O$, $PtCl_4(H_2bpydc)$, $Pt\ Cl_2(H_2bpydc)$.

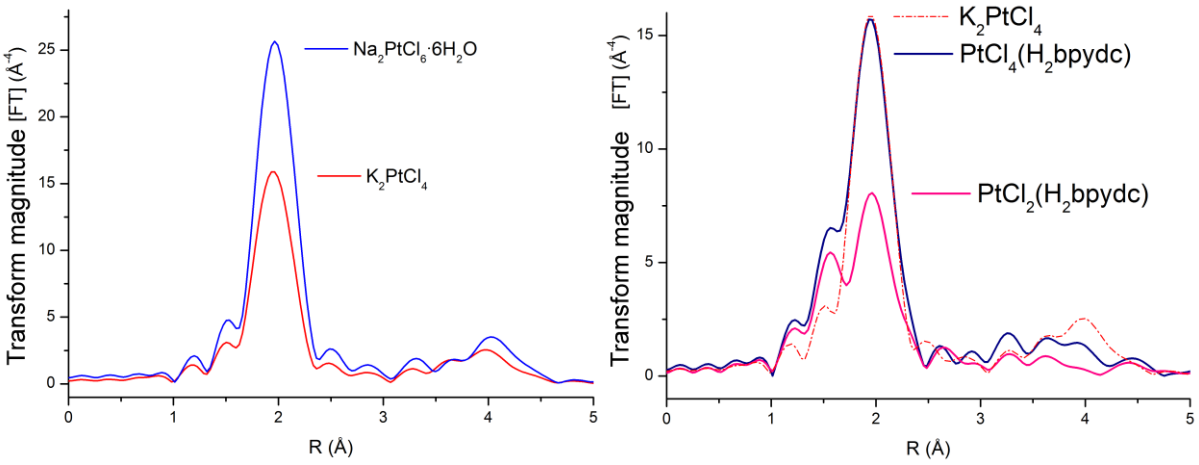

EXAFS radial distribution functions of precursor salts (left) and linkers (right). The main contribution is from Pt-Cl interaction (1.9 – 2.0 Å), while the minor contribution is from Pt-N interaction (1.6 Å).

$[cis\text{-}Ru(bpy)_2]Cl_2$

^{1}H NMR ≈90 % pure. The NMR spectrum also confirms that Ruthenium is diamagnetic in oxidation state 2+.

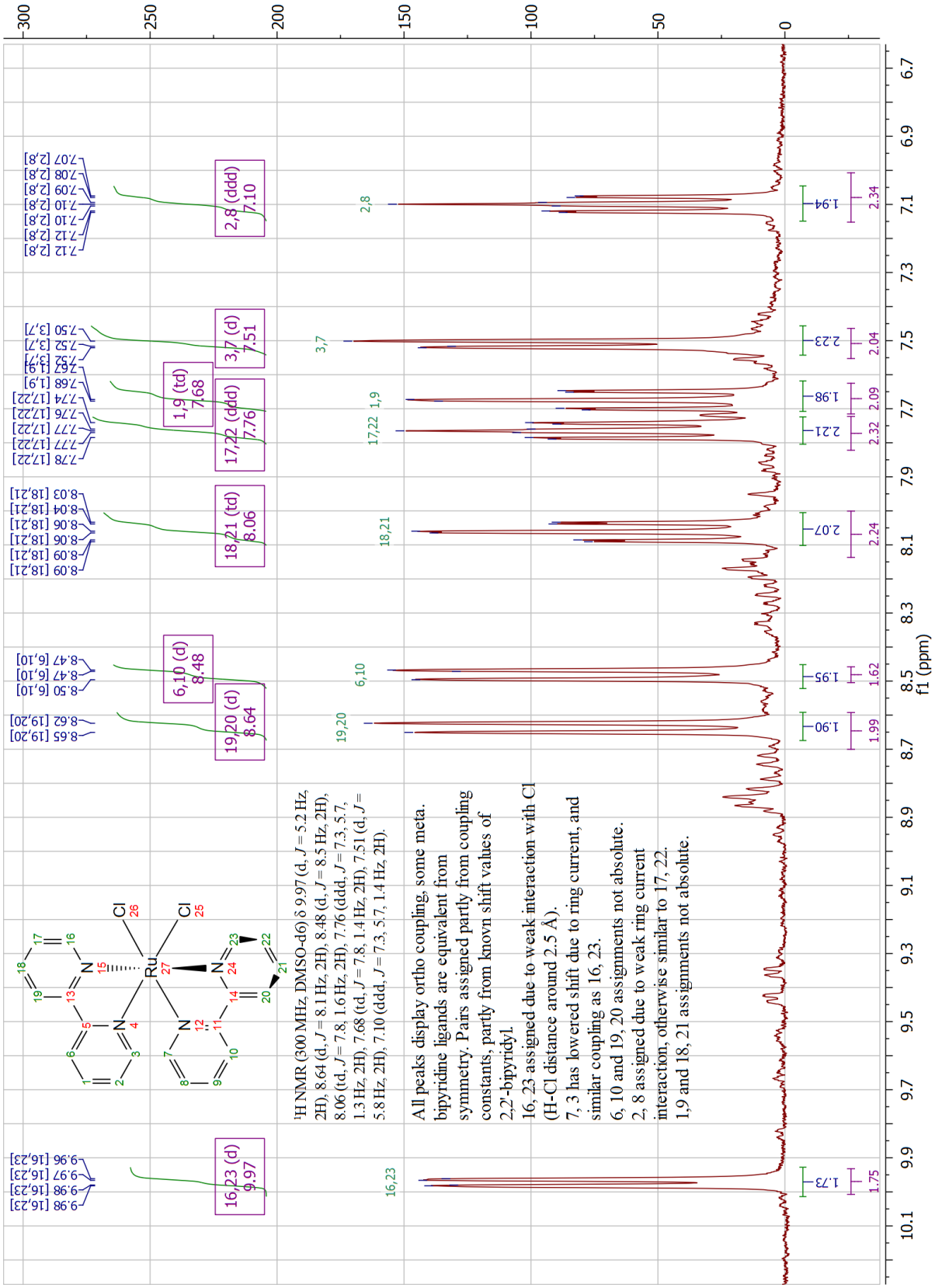

$[Ru(bpy)_2(H_2bpydc)]Cl_2$

^{1}H NMR

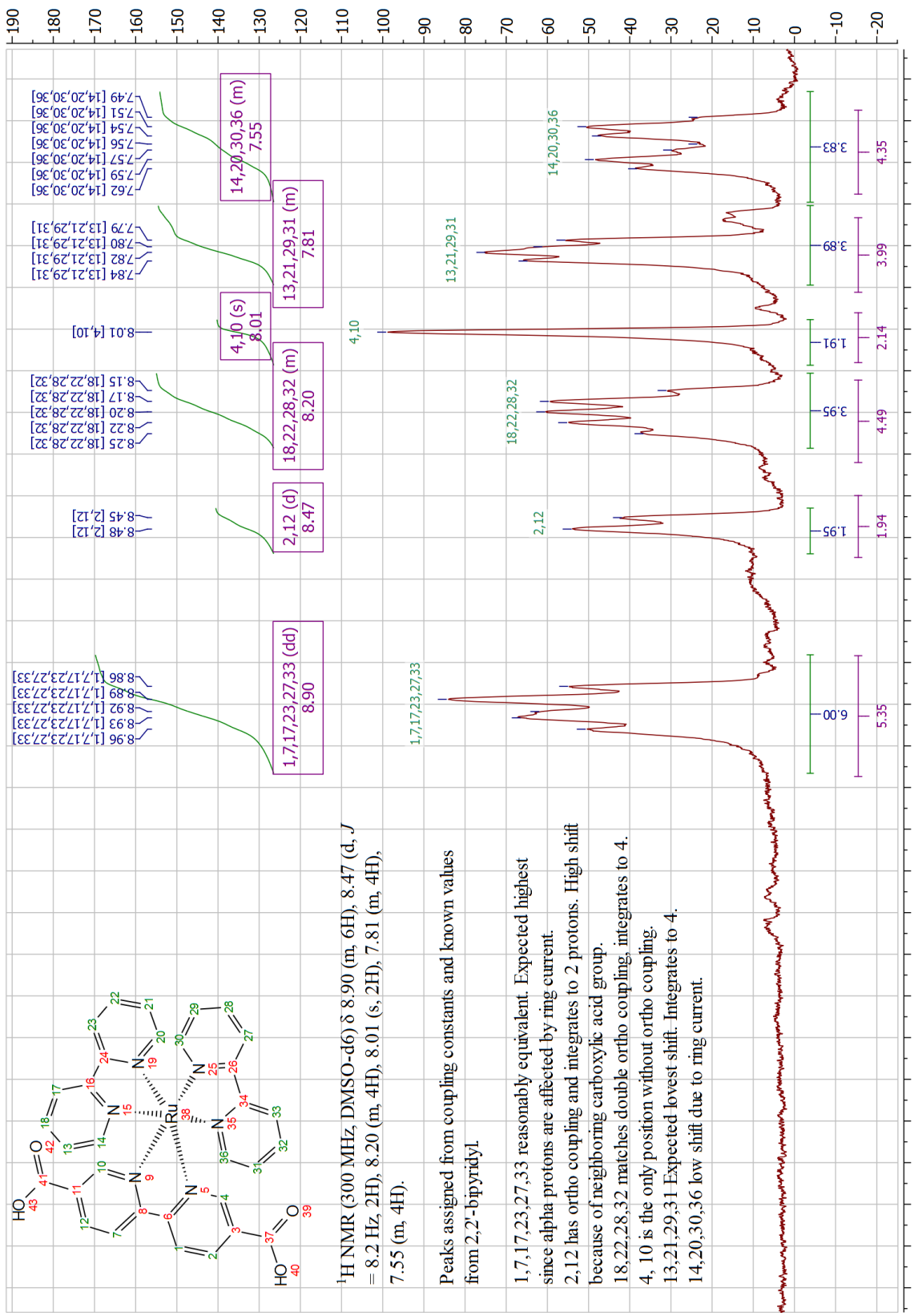

^{1}H NMR (300 MHz, DMSO-d6) δ 8.90 (m, 6H), 8.47 (d, J = 8.2 Hz, 2H), 8.20 (m, 4H), 8.01 (s, 2H), 7.81 (m, 4H), 7.55 (m, 4H).

Peaks assigned from coupling constants and known values from 2,2'-bipyridyl.

1,7,17,23,27,33 reasonably equivalent. Expected highest since alpha protons are affected by ring current.

2,12 has ortho coupling and integrates to 2 protons. High shift because of neighboring carboxylic acid group.

18,22,28,32 matches double ortho coupling, integrates to 4.

4, 10 is the only position without ortho coupling.

13,21,29,31 Expected lowest shift. Integrates to 4.

14,20,30,36 low shift due to ring current.

CuCl2· H_2bpydc complex

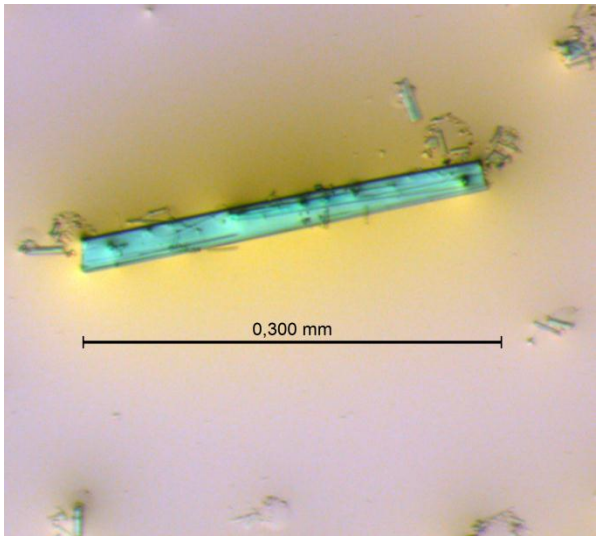

Needle shaped single crystal

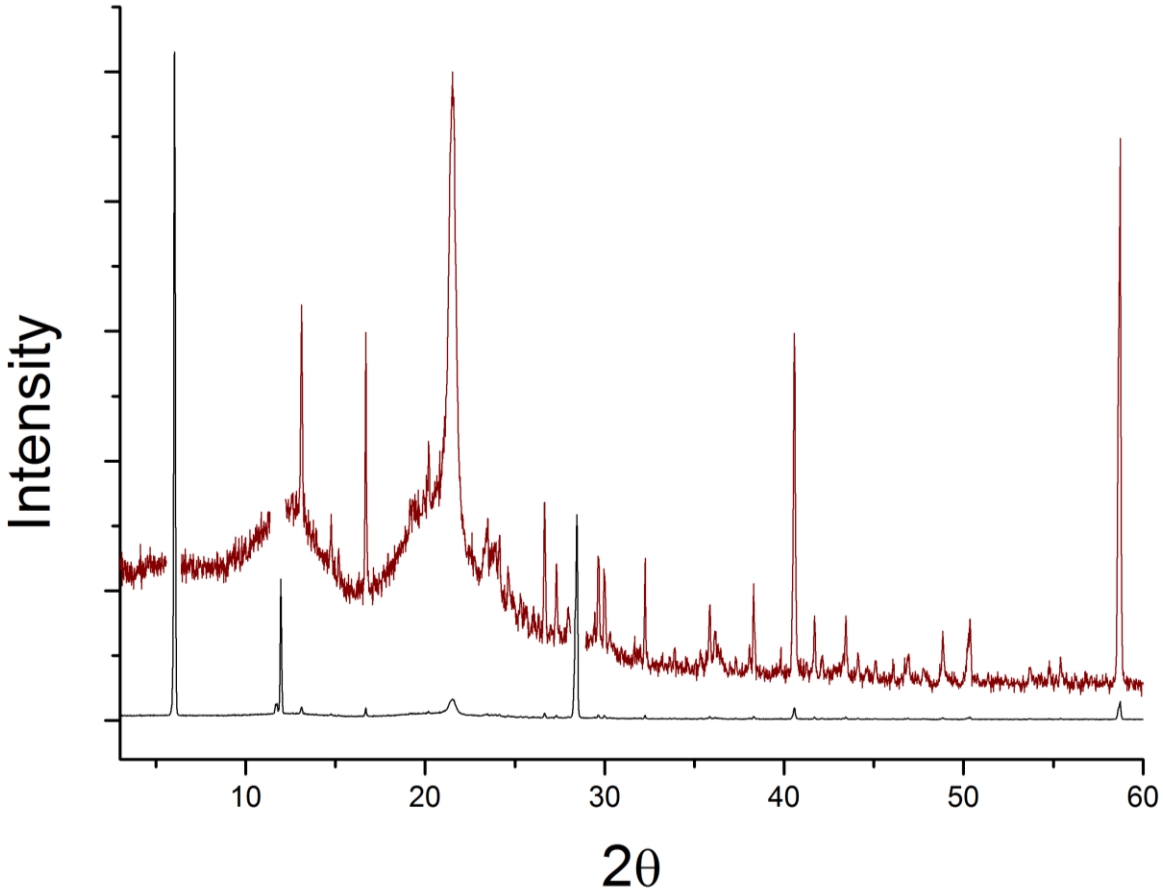

Powder diffraction pattern of Cu(H_2bpydc) complex and KCl. Intensities are likely due to preferred orientation of crystals. Red scaled 30 times.

EXAFS

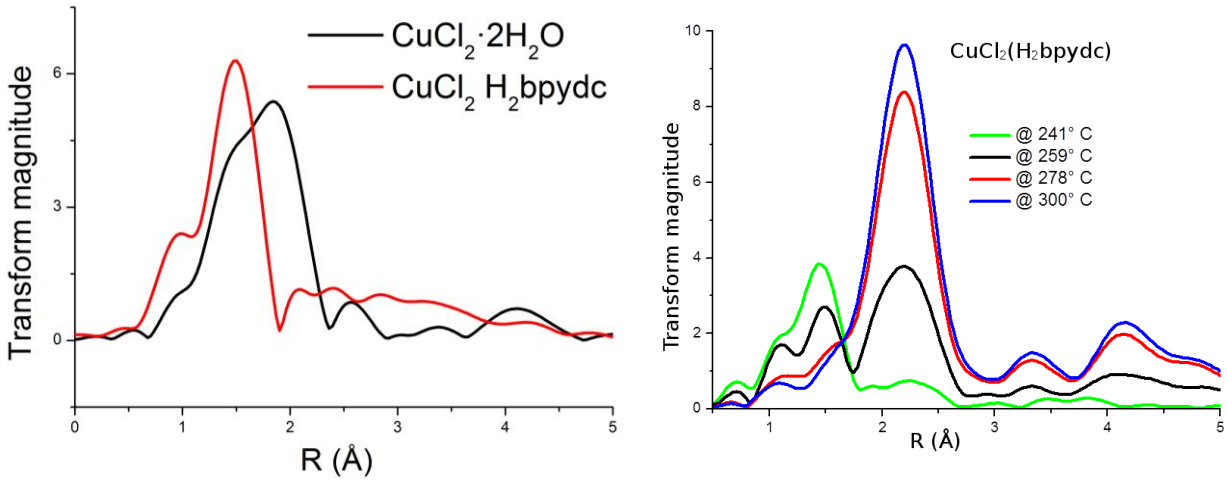

The above figures show the EXAFS radial distribution functions of $CuCl_2$ and its complex with H_2bpydc. It is evident that there are no Cu-Cl bonds in the complex, but the Cu-O. Cu-O and Cu-N bonds are usually not discernible from each other in EXAFS, although Cu-O bond lengths vary greatly depending on the nature of the oxygen. This gives several opportunities: The Cu can be coordinated to carboxylate groups, bipyridine, hydroxide and/or water. The left figure shows metallic Cu being formed at 250°C.

The diffraction pattern does not match reported structures of similar compositions. The

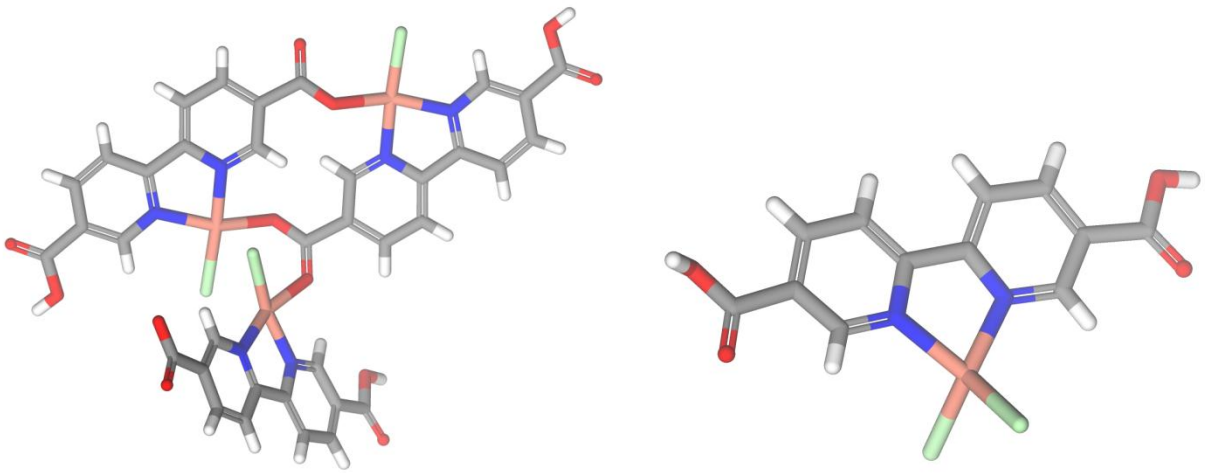

characterization data obtained in this work is not sufficient for structure determination.

Reported structures of $CuCl_x$-H_2bpydc complexes[73]. Given the lack of Cu-Cl bonds and non-matching PXRD patterns, it is evident that the compound we obtained is something different.

Diffraction from plastic foils

Some of the samples have been run in the diffractometer covered by plastic foil, some of which are strongly diffracting. Diffraction patterns in the thesis are marked.

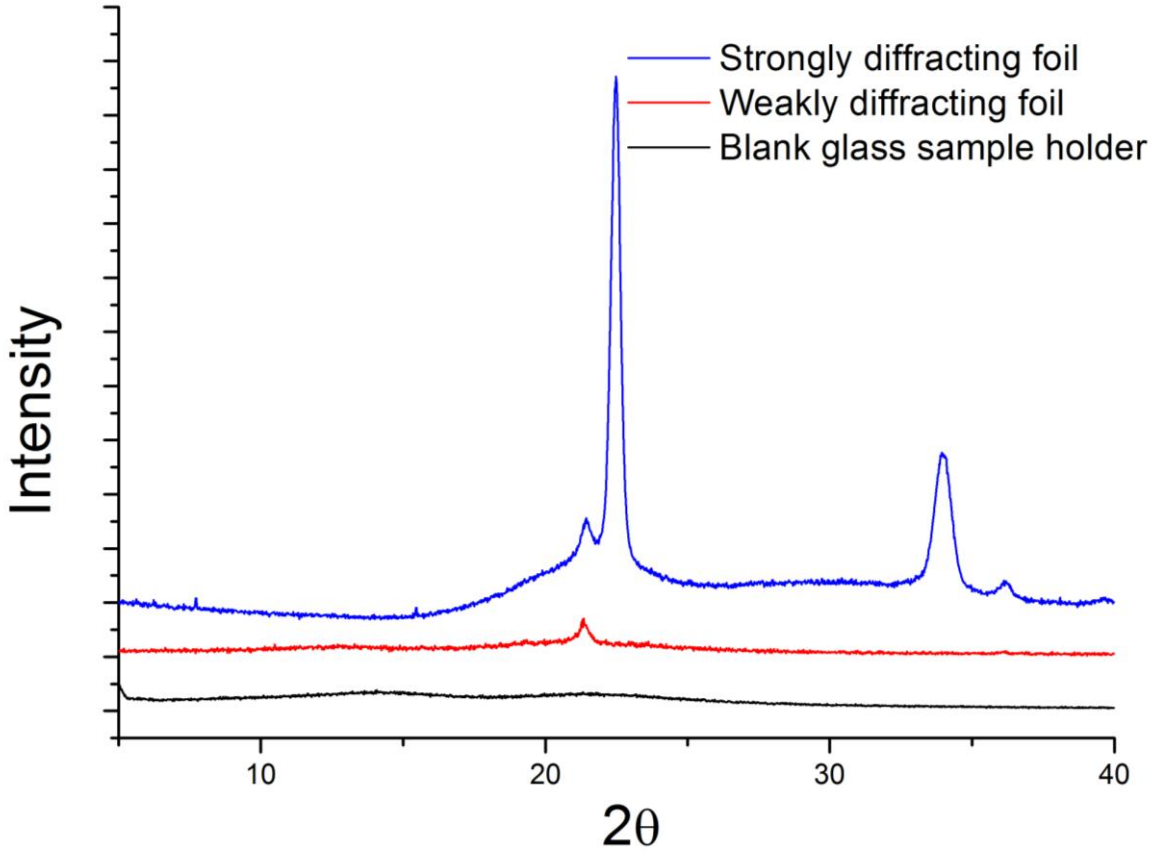

Reference materials synthesis and characterization

UiO-67-synthesis

UiO-67 was prepared by three different methods, differing in the concentration of the modulator.

$ZrCl_4$ (≥99.5 % anhydrous, Sigma-Aldrich), H_2bpdc (98%, Sigma-Aldrich), benzoic acid (≥99.5 %, SMPC) and 2-propanol (≥99.8 %, Sigma-Aldrich) were used as received. H_2bpydc was synthesized as previously described. DMF (≥99.5 %, Merck) was purified using a MBraun MB-SPS-800 encapsulated solvent purification system. Water was distilled in a GFL 2002 distillator.

Powder diffraction patterns are excluded from the appendix as they are presented in the main text. Yields of the main product is accurate, and based on TGA experiments, and evacuation before weighing. Yields given in for the other syntheses are most often rough estimates, based on the solvent loading of the more thoroughly characterized, similar samples.

UiO-67-1

$ZrCl_4$ (1.08 g, 4.65 mmol) and H_2O (109 µL, 6.04 mmol) were dissolved in 180 mL DMF while stirring. The solution was heated and H_2bpdc (1.13 g, 4.65 mmol) was added. A clear, colorless solution was obtained after a few minutes of stirring. The solution was kept at 95 °C for 4 days.

The solution was decanted off, and a white crystalline powder was recovered. The powder was then washed 3 times in 15 mL portions of anhydrous DMF and 3 times in 15 mL portions of 2-propanol, before it was dried in air at 60 °C. The dry powder was weighed and stored in a desiccator. The product weight was 1.55 g, and the solvent fraction was found to be 40 % by evacuation. Thus the dry product weight was estimated to 930 mg and the final yield to 56 % ($Yield_{max}$: 1.66 g).

This synthesis was repeated with the same ratio of reagents, although not always the same amounts, a total of 4 times, out of which all gave a crystalline product.

SEM micrograph shows a mean size of about 300 – 400 nm, with a few as large as 2 µm. Some agglomeration is observed.

Adsorption data

Starting point	5	
End point	17	
Slore	0,0018719	
Intercept	8,2961E-07	
Correlation coefficient	1	
Vm	533,97	[cm^3(STP) g^{-1}]
$a_{s,BET}$	2324,1	[m^2 g^{-1}]
C	2257,4	
Total pore volume (p/p_0=0.953)	0,9262	[cm^3 g^{-1}]
Average pore diameter	1,5941	[nm]

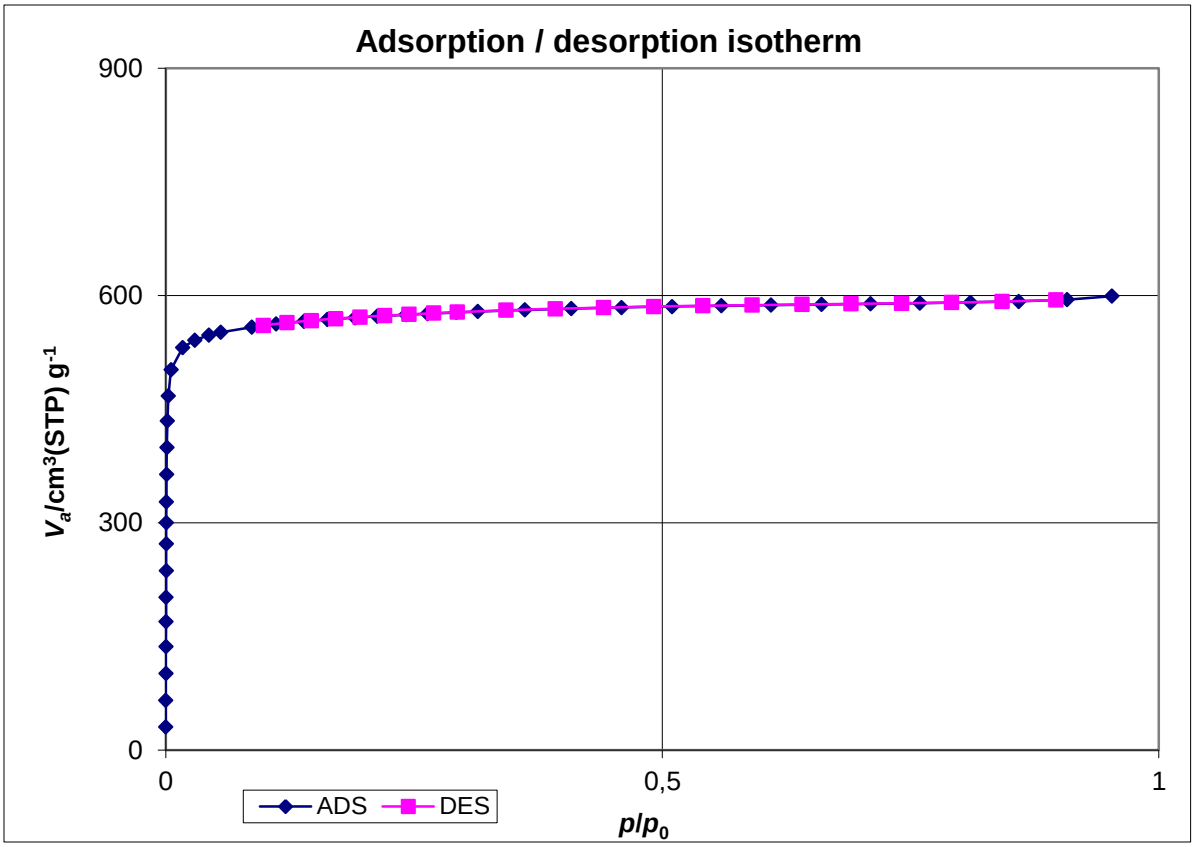

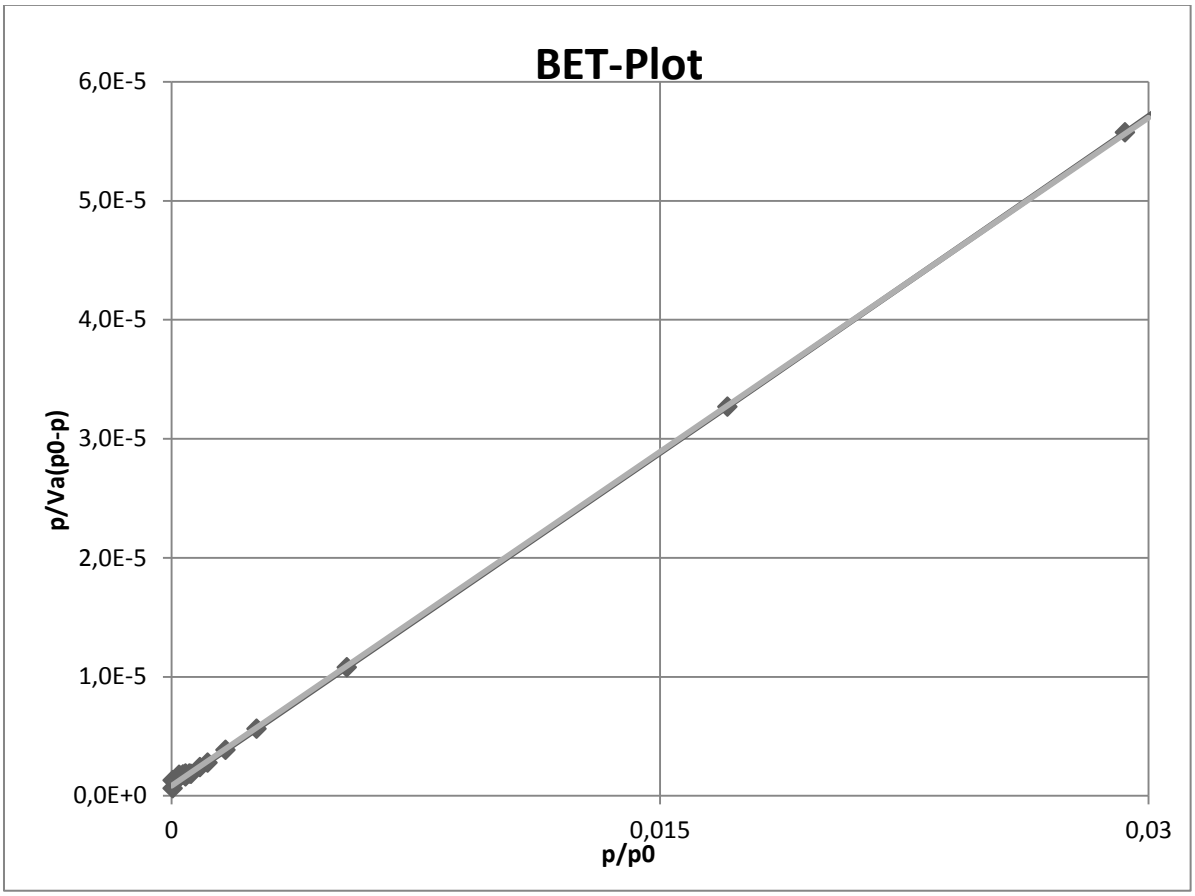

Adsorption/desorption isotherm and BET plot for UiO-67-1. For the other samples, only the data output will be shown.

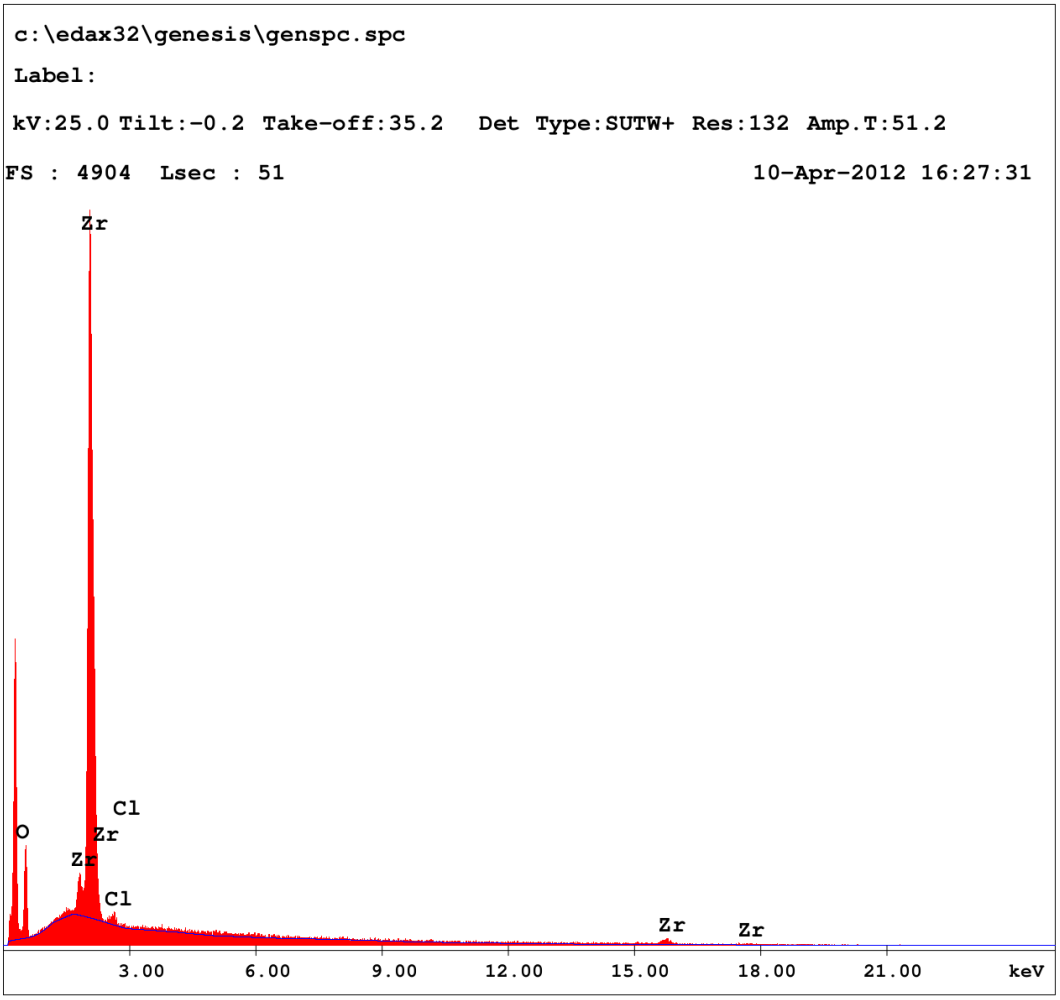

Element	Wt %	At %	K-Ratio	Z	A	F
O K	48.68	83.52	0.0907	1.0964	0.1699	1.0003
ClK	2.19	1.69	0.0106	1.0079	0.4788	1.0000
ZrK	49.13	14.78	0.4146	0.8406	1.0039	1.0000
Total	100.00	100.00				

Element	Net Inte.	Bkgd Inte.	Inte. Error	P/B
O K	75.24	7.44	1.77	10.11
ClK	12.65	29.10	9.31	0.43
ZrK	11.18	1.88	4.84	5.95

EDXS showing somewhat high chlorine content, but the internal error is significant, comparable to the intensity of the peak itself.

UiO-67-2

$ZrCl_4$ (1.08 g, 4.65 mmol) and H_2O (109 µL, 6.04 mmol) were dissolved in 180 mL DMF while stirring. The solution was heated, and benzoic acid (2.84 g, 23.3 mmol) and H_2bpdc (1.13 g, 4.65 mmol) were added. A clear, colorless solution was obtained after a few minutes of stirring. The solution was kept at 95 °C for 4 days.

The solution was decanted off, and a white crystalline powder was recovered. The powder was then washed 3 times in 15 mL portions of anhydrous DMF and 3 times in 15 mL portions of 2-propanol, before it was dried in air at 60 °C. The dry powder was weighed and stored in a desiccator. The product weight was 1.10 g, and the solvent fraction was found to be 40 % by evacuation. Thus the dry product weight was estimated to 660 mg and the final yield to 40 % ($Yield_{max}$: 1.66 g).

This synthesis was repeated with the same ratio of reagents, although not always the same amounts, a total of 4 times, out of which all gave a crystalline product. Yields ranged from 20 to 40 %.

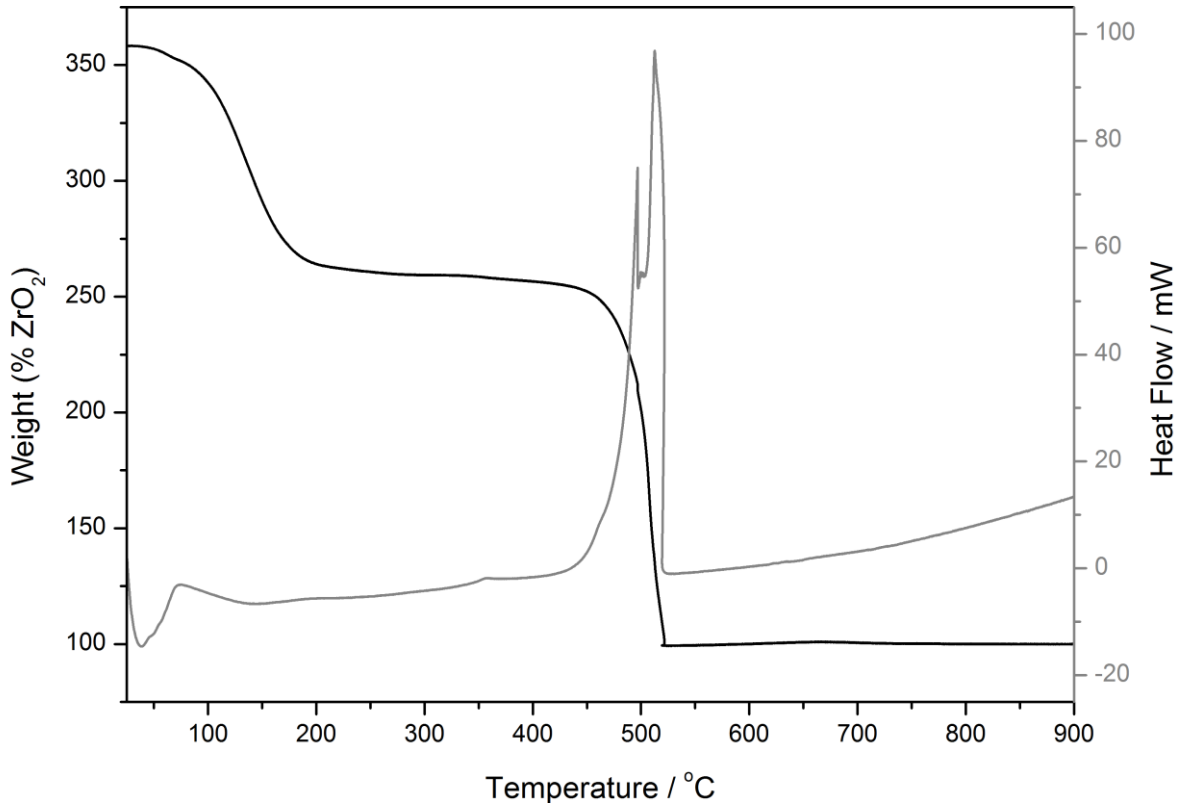

TGA curves of UiO-67-2 in air, confirming the thermal stability of the material.

\\Supportqfe21\shareddata2\MasterStudents\Sigurd\120410\0595t\edax.spc

Label:

kV:25.0 Tilt:-0.3 Take-off:35.1 Det Type:SUTW+ Res:132 Amp.T:51.2

FS : 5196 Lsec : 50 10-Apr-2012 16:11:50

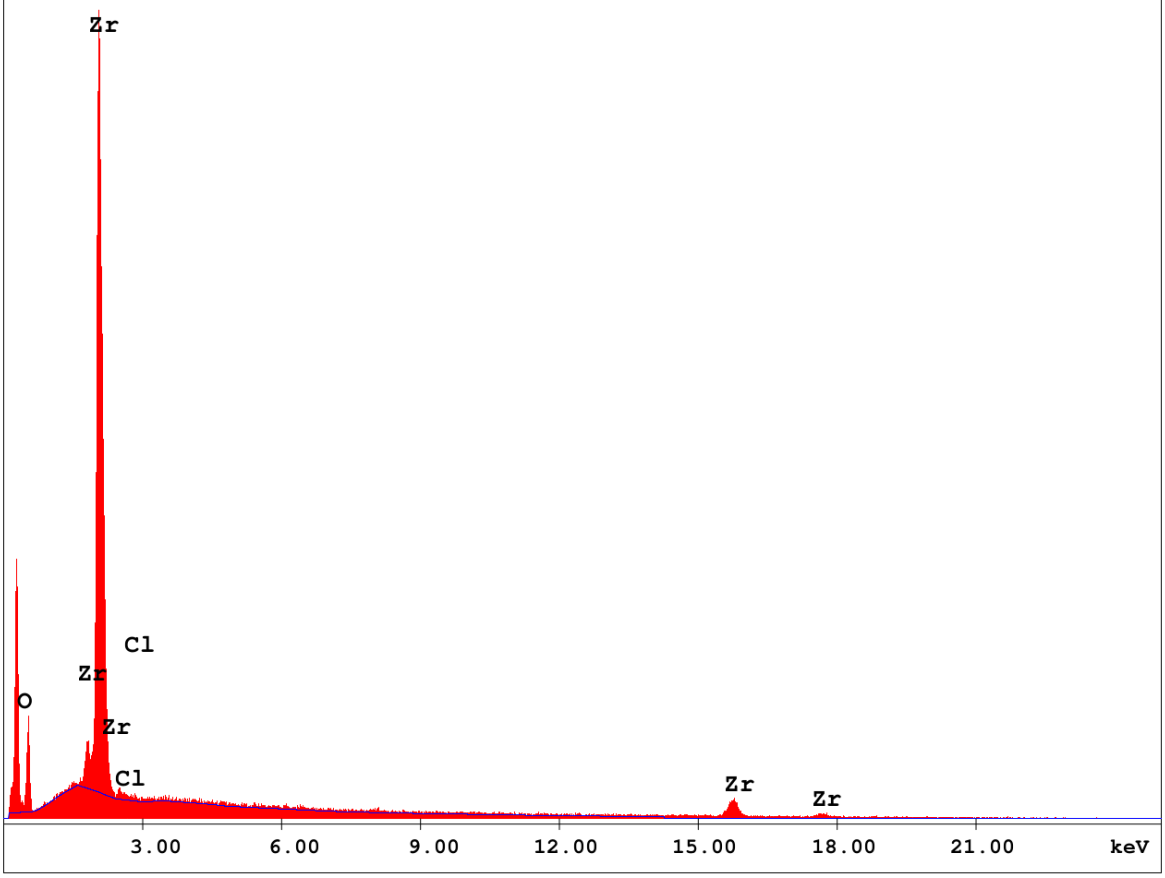

Element	Wt %	At %	K-Ratio	Z	A	F
O K	25.43	65.73	0.0369	1.1590	0.1252	1.0004
ClK	0.65	0.76	0.0026	1.0752	0.3752	1.0000
ZrK	73.92	33.52	0.6733	0.9089	1.0021	1.0000
Total	100.00	100.00				

Element	Net Inte.	Bkgd Inte.	Inte. Error	P/B
O K	68.81	6.52	1.86	10.55
ClK	7.06	26.03	15.38	0.27
ZrK	40.89	0.00	2.21	40.89

EDXS shows low, but detectable chlorine content. The internal error is large compared to the peak intensity, making the result unreliable.

UiO-67-3

$ZrCl_4$ (1.08 g, 4.65 mmol) and H_2O (109 µL, 6.04 mmol) were dissolved in 180 mL DMF while stirring. The solution was heated, and benzoic acid (17.0 g, 139 mmol) and H_2bpdc (1.13 g, 4.65 mmol) were added. A clear, colorless solution was obtained after a few minutes of stirring. The solution was kept at 95 °C for 4 days.

The solution was decanted off, and a white crystalline powder was recovered. The powder was then washed 3 times in 15 mL portions of anhydrous DMF and 3 times in 15 mL portions of 2-propanol, before it was dried in air at 60 °C. The dry powder was weighed and stored in a desiccator. The product weight was 1.46 g, and the solvent fraction was found to be 36 % by evacuation. Thus the dry product weight was estimated to 937 mg and the final yield to 57 % ($Yield_{max}$: 1.66g).

This synthesis was repeated with the same ratio of reagents, although not always the same amounts, a total of 4 times, out of which all gave a crystalline product. Yields ranged from 15 to 80 %.

Adsorption data

Starting point	6	
End point	23	
Slore	0,0023443	
Intercept	7,6221E-07	
Correlation coefficient	0,9998	
Vm	426,43	[cm^3(STP) g^{-1}]
$a_{s,BET}$	1856	[m^2 g^{-1}]
C	3076,7	
Total pore volume (p/p_0=0.990)	0,8621	[cm^3 g^{-1}]
Average pore diameter	1,8579	[nm]

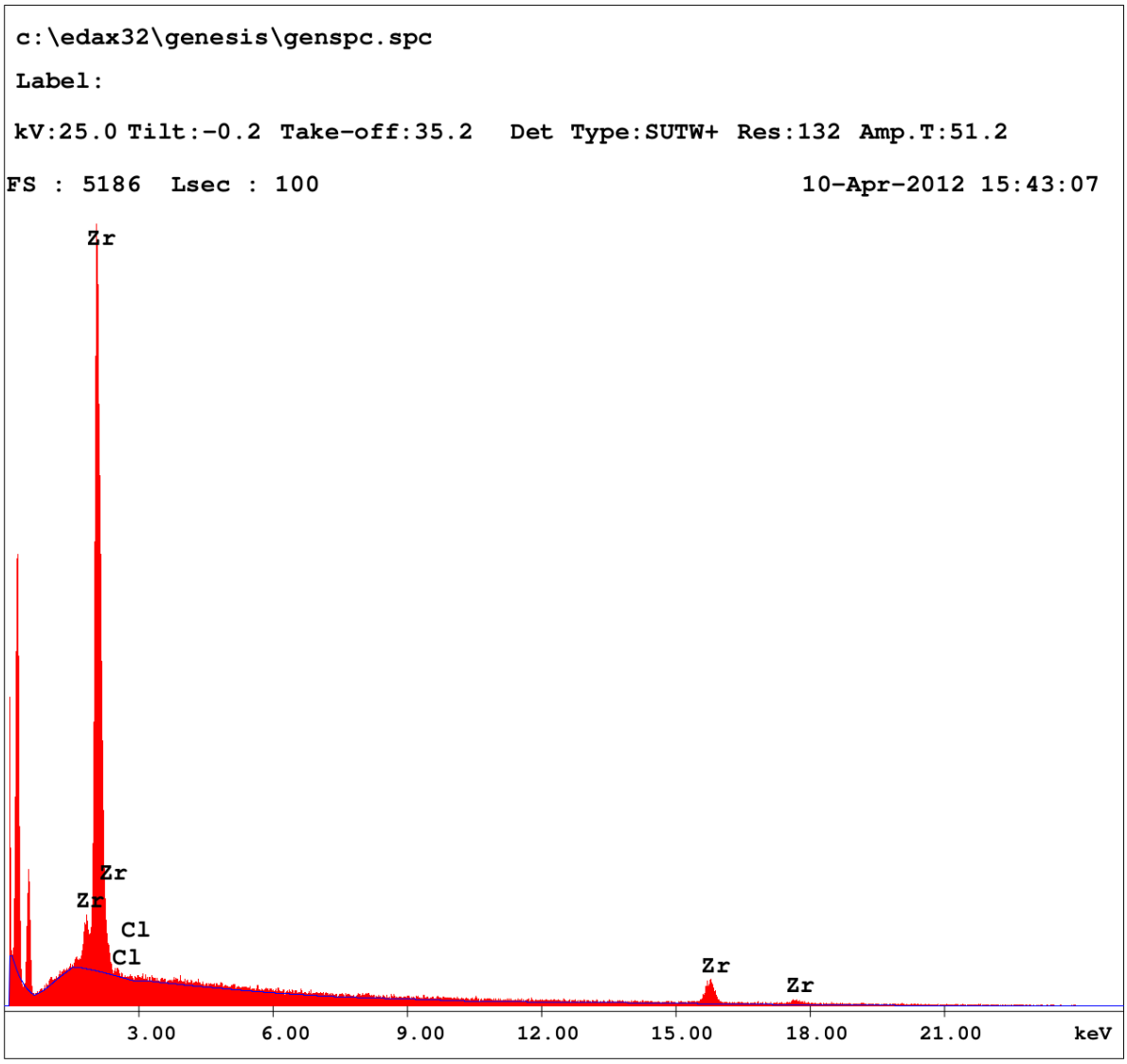

Element	Wt %	At %	K-Ratio	Z	A	F
ClK	0.20	0.51	0.0007	1.1662	0.3013	1.0000
ZrK	99.80	99.49	0.9976	0.9995	1.0000	1.0000
Total	100.00	100.00				

Element	Net Inte.	Bkgd Inte.	Inte. Error	P/B
ClK	0.77	20.45	83.83	0.04
ZrK	24.90	2.91	2.23	8.56

EDXS shows very low chlorine content, which may be only noise. The internal error is much higher than the peak intensity, making the result unreliable.

UiO-67-bpy synthesis

UiO-67-bpy is the term used in this work for UiO-67 made with 10% H_2bpydc linker. It has been prepared by four different methods, differing in the type and concentration of the modulator.

UiO-67-bpy-1

$ZrCl_4$ (602 mg, 2.58 mmol) and H_2O (61 µL, 3.4 mmol) were dissolved in 100 mL DMF while stirring. The solution was heated, and acetic acid (739 µL, 12.9 mmol), H_2bpydc (63 mg, 0.26 mmol) and H_2bpdc (563 mg, 2.33 mmol) were added. A clear, colorless solution was obtained after a few minutes of stirring. The solution was kept at 95 °C for 4 days.

The solution was decanted off, and a white crystalline powder was recovered. The powder was then washed 3 times in 15 mL portions of anhydrous DMF and 3 times in 15 mL portions of 2-propanol, before it was dried in air at 60 °C. The dry powder was weighed and stored in a desiccator. The product weight was 1.35 g, and the solvent fraction was found to be 42.5 % by evacuation. Thus the dry product weight was estimated to 778 mg and the final yield to 84 % ($Yield_{max}$: 921 mg).

This synthesis was repeated with the same ratio of reagents, although not always the same amounts, a total of 6 times, out of which all gave a crystalline product. Yields ranged from 32 to 84 %.

Adsorption data:

Starting point	9	
End point	17	
Slore	0,0022283	
Intercept	1,4355E-06	
Correlation coefficient	1	
Vm	448,49	[cm^3(STP) g^{-1}]
$a_{s,BET}$	1952	[m^2 g^{-1}]
C	1553,3	
Total pore volume (p/p_0=0.990)	0,7946	[cm^3 g^{-1}]
Average pore diameter	1,6282	[nm]

UiO-67-bpy-2

$ZrCl_4$ (602 mg, 2.58 mmol) and H_2O (61 µL, 3.4 mmol) were dissolved in 100 mL DMF while stirring. The solution was heated, and benzoic acid (1.58 g, 12.9 mmol), H_2bpydc (63 mg, 0.26 mmol) and H_2bpdc (563 mg, 2.33 mmol) were added. A clear, colorless solution was obtained after a few minutes of stirring. The solution was kept at 95 °C for 4 days.

The solution was decanted off, and a white crystalline powder was recovered. The powder was then washed 3 times in 15 mL portions of anhydrous DMF and 3 times in 15 mL portions of 2-propanol, before it was dried in air at 60 °C. The dry powder was weighed and stored in a desiccator. The product weight was 1.30 g, and the solvent fraction was found to be 41 % by evacuation. Thus the dry product weight was estimated to 764 mg and the final yield to 83 % ($Yield_{max}$: 921 mg).

This synthesis was repeated with the same ratio of reagents, although not always the same amounts, a total of 5 times, out of which all gave a crystalline product. Yields ranged from 23 to 83 %.

Adsorption data:

Starting point	3	
End point	19	
Slore	0,001932	
Intercept	9,2408E-07	
Correlation coefficient	1	
Vm	517,34	[cm^3(STP) g^{-1}]
$a_{s,BET}$	2251,7	[m^2 g^{-1}]
C	2091,8	
Total pore volume (p/p_0=0.990)	0,916	[cm^3 g^{-1}]
Average pore diameter	1,6273	[nm]

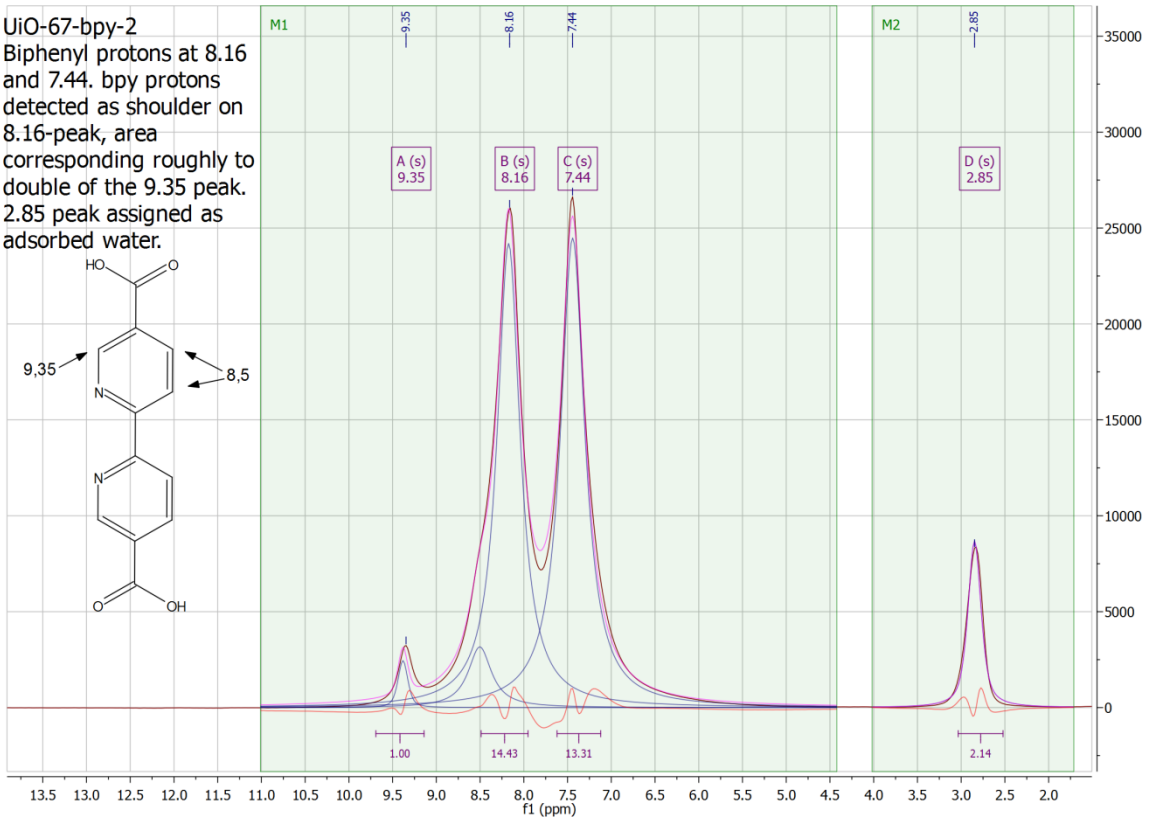

Solid state NMR spectrum of UiO-67-bpy-2. Below: Estimated integral values showing a bpy content of approximately 10 %. This estimate is of course very rough.

Peak #	ppm	Height	Width(Hz)	L/G	Area	Normalized to #1
1	9,375	2456,91	66	0,53	25540,12	1
2	8,504	3166,43	161	1	87377,466	3,42
3	8,171	24200,85	158	1	656990,433	25,72
4	7,441	24489,56	167	1	701410,393	27,46
5	2,854	8686,28	89	0,65	124126,495	4,86

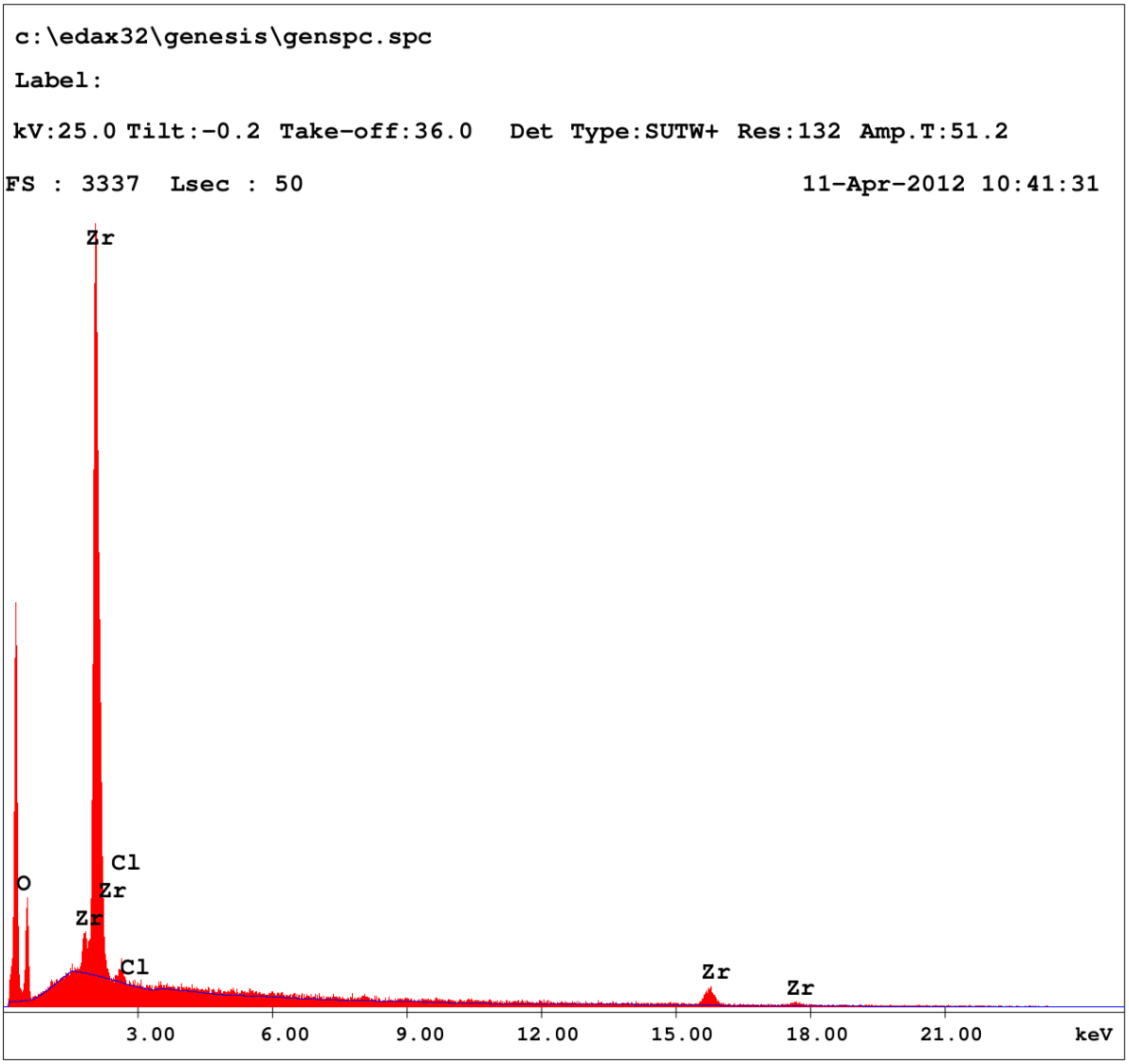

Element	Wt %	At %	K-Ratio	Z	A	F
O K	29.59	69.75	0.0448	1.1456	0.1322	1.0004
ClK	1.75	1.86	0.0074	1.0608	0.3994	1.0000
ZrK	68.66	28.38	0.6154	0.8942	1.0024	1.0000
Total	100.00	100.00				

Element	Net Inte.	Bkgd Inte.	Inte. Error	P/B
O K	52.48	4.28	2.11	12.26
ClK	12.42	22.70	8.66	0.55
ZrK	23.10	2.64	3.26	8.75

EDXS show detectable chlorine content, with significant insecurity.

UiO-67-bpy-3

$ZrCl_4$ (120 mg, 0.517 mmol) and H_2O (12 µL, 0.67 mmol) were dissolved in 20 mL DMF while stirring. The solution was heated, and acetic acid (887 µL, 15.5 mmol), H_2bpydc (13 mg, 0.052 mmol) and H_2bpdc (113 mg, 0.465 mmol) were added. A clear, colorless solution was obtained after a few minutes of stirring. The solution was kept at 95 °C for 4 days.

The solution was decanted off, and a white crystalline powder was recovered. The powder was then washed 3 times in 15 mL portions of anhydrous DMF and 3 times in 15 mL portions of 2-propanol, before it was dried in air at 60 °C. The dry powder was weighed and stored in a desiccator. The product weight was 213 mg, and the solvent fraction was found to be 36 % by evacuation. Thus the dry product weight was estimated to 136 mg and the final yield to 74 % ($Yield_{max}$: 184 mg).

This synthesis was only performed once.

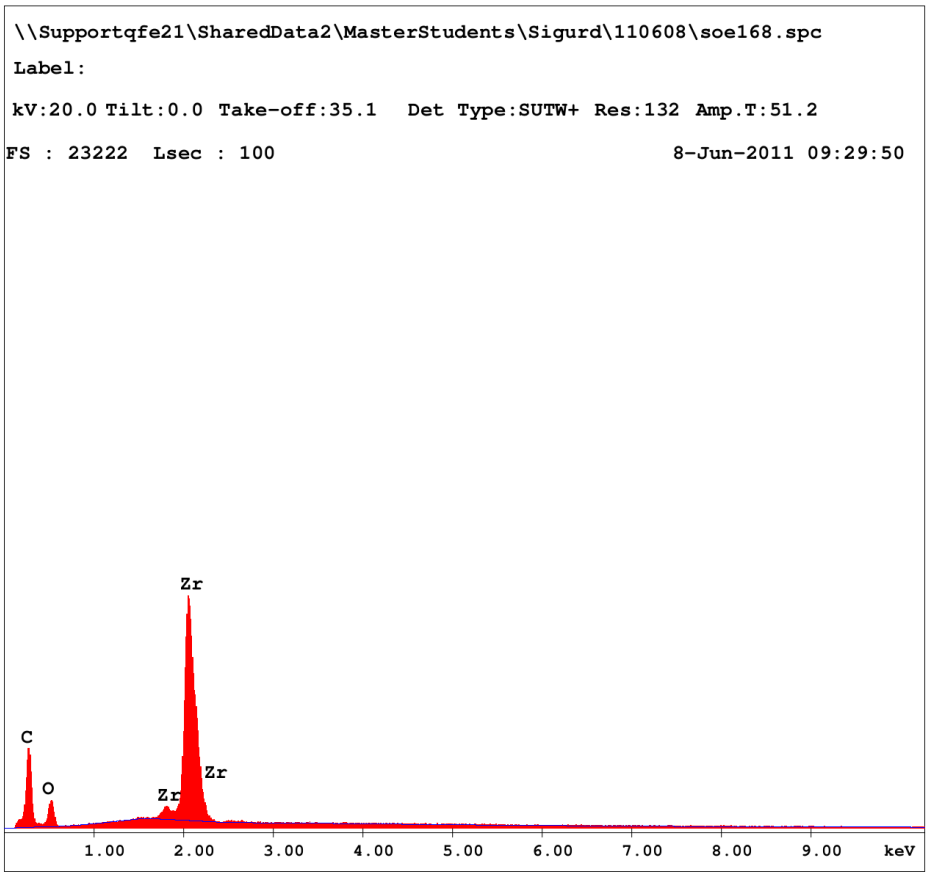

Element	Wt %	At %	K-Ratio	Z	A	F
C K	52.92	79.85	0.1103	1.0755	0.1937	1.0001
O K	11.55	13.09	0.0170	1.0573	0.1393	1.0002
ZrL	35.53	7.06	0.3253	0.8148	1.1235	1.0000
Total	100.00	100.00				

Element	Net Inte.	Bkgd Inte.	Inte. Error	P/B
C K	144.77	2.04	0.84	70.97
O K	59.02	4.52	1.40	13.06
ZrL	616.76	25.28	0.42	24.40

EDXS shows no significant chlorine content. A slight deviation from the background is observed around 2.5 keV, indicating a minimal presence of chloride.

UiO-67-bpy-4

$ZrCl_4$ (602 mg, 2.58 mmol) and H_2O (61 µL, 3.4 mmol) were dissolved in 100 mL DMF while stirring. The solution was heated, and benzoic acid (9.46 g, 77.5 mmol), H_2bpydc (63 mg, 0.26 mmol) and H_2bpdc (563 mg, 2.33 mmol) were added. A clear, colorless solution was obtained after a few minutes of stirring. The solution was kept at 95 °C for 4 days.

The solution was decanted off, and a white crystalline powder was recovered. The powder was then washed 3 times in 15 mL portions of anhydrous DMF and 3 times in 15 mL portions of 2-propanol, before it was dried in air at 60 °C. The dry powder was weighed and stored in a desiccator. The product weight was 847 mg, and the solvent fraction was found to be 36 % by evacuation. Thus the dry product weight was estimated to 538 mg and the final yield to 58 % ($Yield_{max}$: 921 mg).

This synthesis was done with the same ratio of reagents, although not always the same amounts, a total of 7 times, out of which all gave a crystalline product. Yields ranged from 15 to 75 %.

Adsorption data:

Starting point	4	
End point	24	
Slore	0,001808	
Intercept	9,7923E-07	
Correlation coefficient	1	
Vm	552,78	[cm^3(STP) g^{-1}]
$a_{s,BET}$	2406	[m^2 g^{-1}]
C	1847,4	
Total pore volume (p/p_0=0.990)	0,9663	[cm^3 g^{-1}]
Average pore diameter	1,6065	[nm]

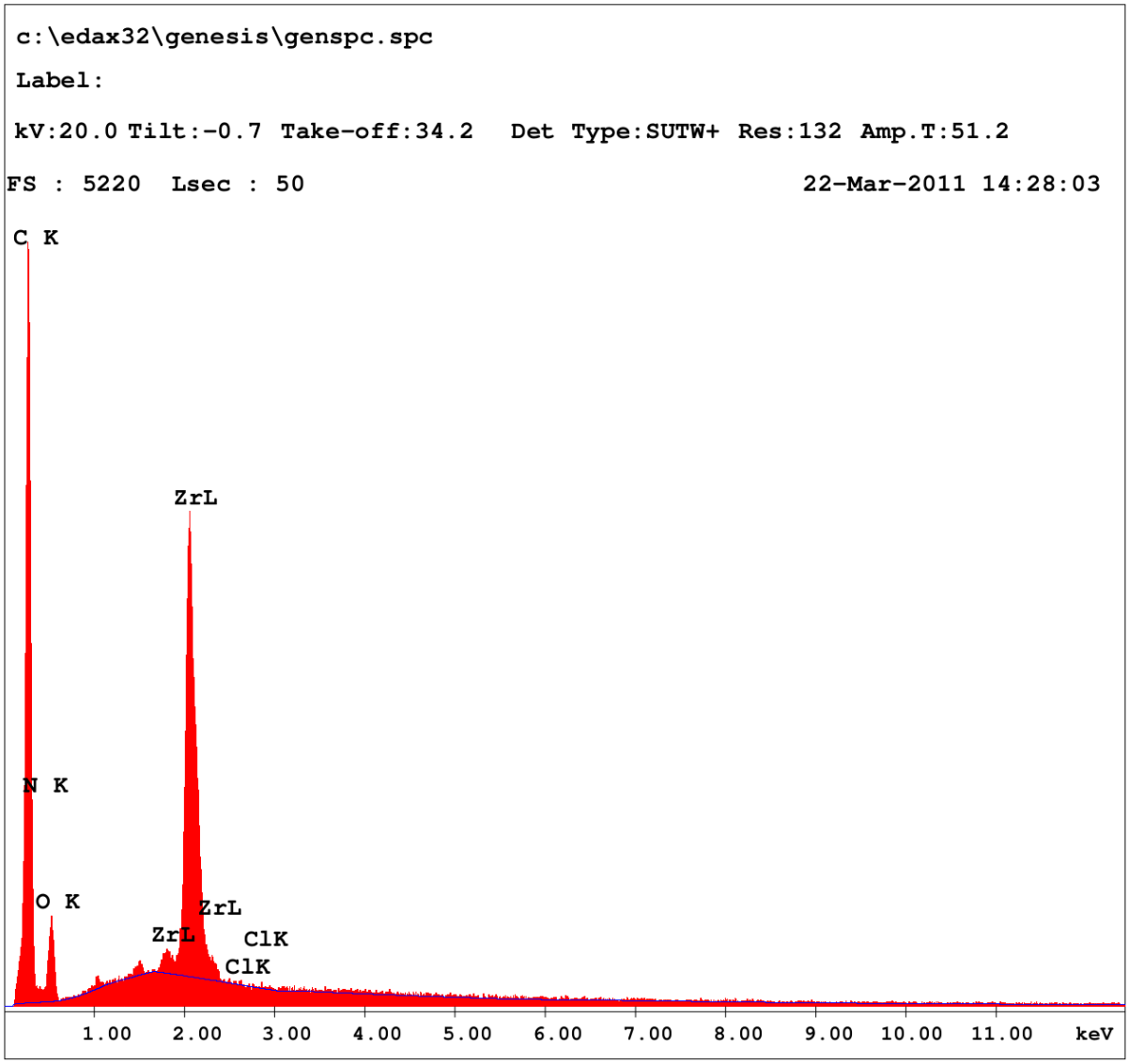

Element	Wt %	At %	K-Ratio	Z	A	F
C K	70.34	84.69	0.2403	1.0329	0.3307	1.0001
N K	5.07	5.23	0.0047	1.0238	0.0913	1.0001
O K	8.28	7.49	0.0115	1.0156	0.1362	1.0001
ZrL	16.31	2.59	0.1491	0.7775	1.1757	1.0000
ClK	0.00	0.00	0.0000	0.9157	0.8477	1.0000
Total	100.00	100.00				

Element	Net Inte.	Bkgd Inte.	Inte. Error	P/B
C K	516.88	2.66	0.63	194.32
N K	13.02	3.64	4.89	3.58
O K	65.50	4.96	1.88	13.21
ZrL	468.50	35.54	0.70	13.18
ClK	0.00	31.08	0.00	0.00

EDXS shows no chlorine content, even when forced to integrate the noise.

Morphology calculations

Morphology calculations were made in Materials Studio v5.5.3, using The BFHD method. The method uses Donnay-Harker rules to isolate the likely growth planes, then the Bravais-Friedel rules to deduce their relative growth rates. The method is an approximation and does not account for the energetics of the system. Nevertheless, one often gets useful approximations.

Raw output of calculation, made on a crystallographic information file of pure UiO 67:

```
Module                          : Morphology
Version                         : 5.5
Build date                      : Mar 22 2011
Host                            : PH-3146
Operating system                : MSWin32
Task started                    : Mon May 07 15:50:21 2012


---- Morphology parameters ----

Job mode                        : New calculation
Morphology method               : BFDH
Face list generation            : Create new face list

---- Face list generator parameters ----

Minimum dhkl                    :  1.300
Maximum h, k, l                 : 3, 3, 3
Maximum number of faces         :  200


---- Face list generation ----
Number of unique faces          :  13

---- BFDH calculation ----

---- Habit generation ----
Aspect ratio                    :  1.291
Unique number of facets         :  2


Task terminated                 : Mon May 07 15:50:22 2012
Total CPU time used             : 0 seconds
Termination status              : Normal
```

hkl	Multiplicity	dhkl	Distance	Total facet area	% Total facet area
1 1 1	8	15,49826	6,452338	576,8792	95
2 0 0	6	13,42189	7,450518	166,5307	5
2 2 0	12	9,490706	10,53662		
3 1 1	24	8,093701	12,35529		
3 3 1	24	6,158383	16,23803		
4 2 0	24	6,002449	16,65987		
4 2 2	24	5,479462	18,24997		
4 4 2	24	4,473962	22,35155		
6 2 0	24	4,244373	23,56061		
6 4 0	24	3,722561	26,86323		
6 4 2	48	3,58715	27,87729		
6 4 4	24	3,255285	30,71927		
6 6 4	24	2,861556	34,94603		

Functionalized MOF synthesis procedures and characterization data

Data directly presented in the main text, such as PXRD patterns, will not be repeated in this section. As the EXAFs data are not yet properly refined, they are excluded from the appendix to avoid large amounts of unexplained raw data.

UiO-67-Pt synthesis

The term used in this work for platinum modified UiO-67-bpy is PtX-YY-Z, where X is the oxidation state of platinum (2 or 4), YY is the preparation method (PM: Premade precursor; OP: One-Pot synthesis; and PS: Post synthesis functionalization) and Z is a serial number that distinguishes materials made with different modulator types and concentrations.

K_2PtCl_4 (≥99,5 %, Sigma), K_2PtCl_6 (≥99,5 %, Sigma) and $Na_2PtCl_6{\cdot}6H_2O$ (>98%, Strem chemicals) were used as received. $PtCl_2(H_2bpydc)$ and $PtCl_4(H_2bpydc)$ were synthesized as previously described.

Pt2-OP-1

$ZrCl_4$ (90 mg, 0.39 mmol) and H_2O (9 µL, 0.5 mmol) were dissolved in 15 mL DMF while stirring. The solution was heated, and H_2bpydc (9 mg, 0.04 mmol), H_2bpdc (84 mg, 0.35 mmol) and K_2PtCl_4 (16 mg, 0.039 mmol) were added. A clear, yellow solution was obtained after a few minutes of stirring. The solution was kept at 95 °C for 4 days.

The solution was decanted off, and a yellow crystalline powder was recovered. The powder was then washed 3 times in 15 mL portions of anhydrous DMF and 3 times in 15 mL portions of 2-propanol, before it was dried in air at 60 °C. The dry powder was weighed and stored in a desiccator. The product weight was 102 mg, and the solvent fraction was found to be 40 % by evacuation. Thus the dry product weight was estimated to 61 mg and the final yield to 44 % ($Yield_{max}$: 140 mg).

This synthesis was done with the same ratio of reagents, although not always the same amounts, a total of 3 times, out of which one gave a crystalline product.

Pt2-OP-2

$ZrCl_4$ (120 mg, 0.517 mmol) and H_2O (12 µL, 0.67 mmol) were dissolved in 20 mL DMF while stirring. The solution was heated, and H_2bpydc (13 mg, 0.052 mmol), H_2bpdc (113 mg, 0.465 mmol), acetic acid (148 µL, 2.59 mmol) and K_2PtCl_4 (21 mg, 0.052 mmol) were added. A clear, yellow solution was obtained after a few minutes of stirring. The solution was kept at 95 °C for 4 days.

The solution was decanted off, and a yellow crystalline powder was recovered. The powder was then washed 3 times in 15 mL portions of anhydrous DMF and 3 times in 15 mL portions of 2-propanol, before it was dried in air at 60 °C. The dry powder was weighed and stored in a desiccator. The product weight was 94 mg, and the solvent fraction was found to be 41 % by evacuation. Thus the dry product weight was estimated to 55 mg and the final yield to 30 % ($Yield_{max}$: 184 mg).

This synthesis was done with the same ratio of reagents, although not always the same amounts, a total of 5 times, out of which 3 gave a crystalline product. Yields ranged from 17 to 30 %.

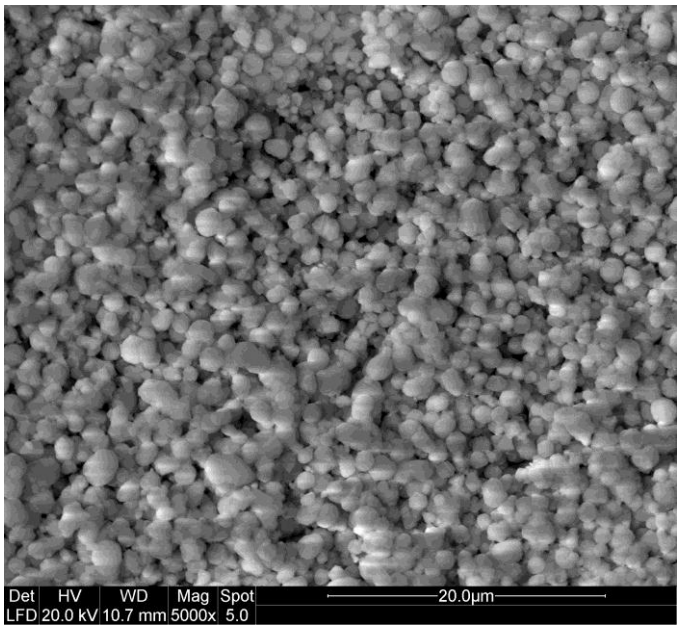

SEM micrograph and EDX spectrum of Pt2-OP-2.

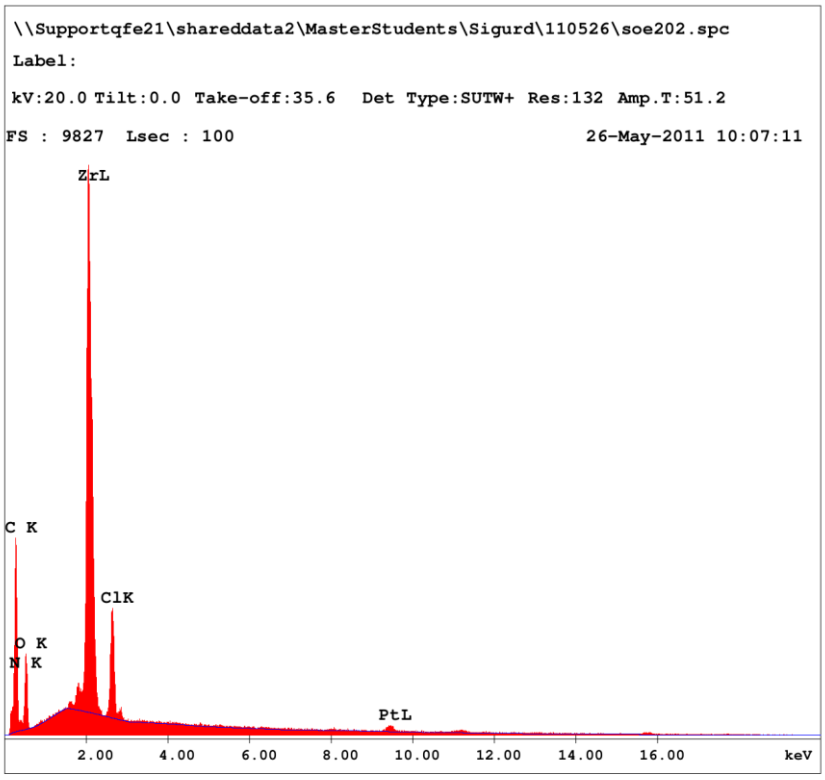

Element	Wt %	At %	K-Ratio	Z	A	F
C K	45.67	73.02	0.0870	1.0839	0.1758	1.0001
N K	4.07	5.59	0.0044	1.0743	0.1003	1.0002
O K	10.28	12.34	0.0153	1.0655	0.1399	1.0002
ZrL	28.44	5.99	0.2594	0.8232	1.1059	1.0016
ClK	4.37	2.37	0.0297	0.9697	0.7014	1.0000
PtL	7.16	0.71	0.0502	0.6783	1.0336	1.0000
Total	100.00	100.00				

Element	Net Inte.	Bkgd Inte.	Inte. Error	P/B
C K	166.81	3.53	0.79	47.25
N K	10.69	5.47	4.35	1.95
O K	77.23	8.01	1.25	9.64
ZrL	712.65	35.29	0.39	20.19
ClK	161.70	32.52	0.93	4.97
PtL	14.69	10.35	4.05	1.42

Pt2-OP-3

$ZrCl_4$ (602 mg, 2.58 mmol) and H_2O (61 µL, 3.4 mmol) were dissolved in 100 mL DMF while stirring. The solution was heated, and benzoic acid (1.58 g, 12.9 mmol), H_2bpydc (63 mg, 0.26 mmol), H_2bpdc (563 mg, 2.33 mmol) and K_2PtCl_4 (107 mg, 0.258 mmol) were added. A clear, yellow solution was obtained after a few minutes of stirring. The solution was kept at 95 °C for 4 days.

The solution was decanted off, and a yellow crystalline powder was recovered. The powder was then washed 3 times in 15 mL portions of anhydrous DMF and 3 times in 15 mL portions of 2-propanol, before it was dried in air at 60 °C. The dry powder was weighed and stored in a desiccator. The product weight was 553 mg, and the solvent fraction was found to be 44 % by evacuation. Thus the dry product weight was estimated to 310 mg and the final yield to 34 % ($Yield_{max}$: 921 mg).

This synthesis was done with the same ratio of reagents, although not always the same amounts, a total of 3 times, out of which all gave a crystalline product. Yields ranged from 23 to 48 %.

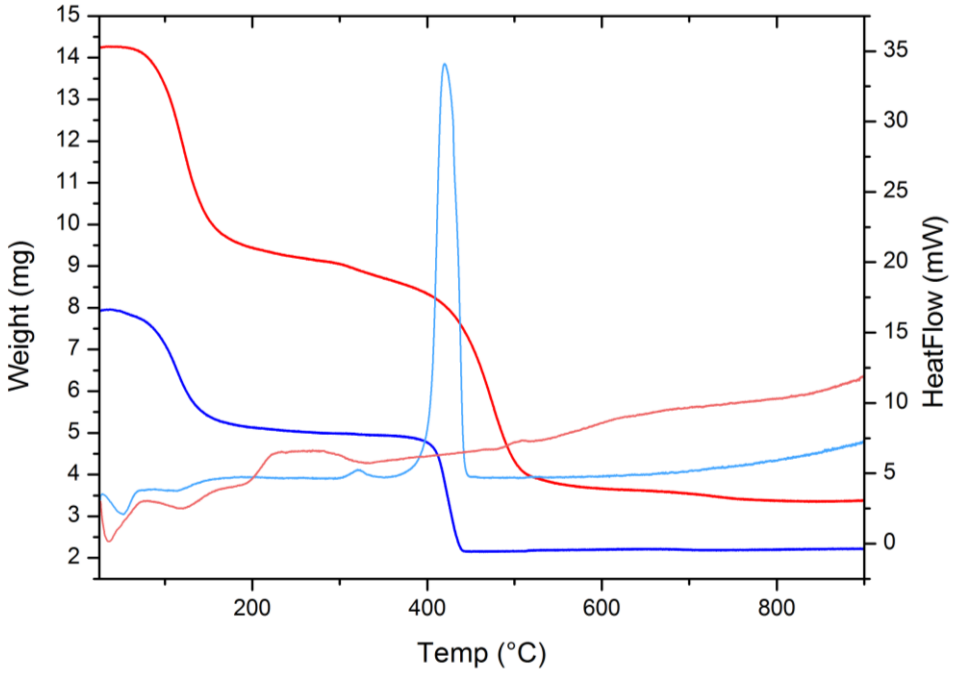

TGA curves of Pt2-OP-3 in synthetic air (blue) and 3 % H_2 in He (red).

Adsorption data of Pt2-OP-3:

Starting point	8	
End point	18	
Slore	0,0028916	
Intercept	2,0903E-06	
Correlation coefficient	1	
Vm	345,58	[cm^3(STP) g^{-1}]
$a_{s,BET}$	1504,1	[m^2 g^{-1}]
C	1384,3	
Total pore volume (p/p_0=0.990)	0,625	[cm^3 g^{-1}]
Average pore diameter	1,6621	[nm]

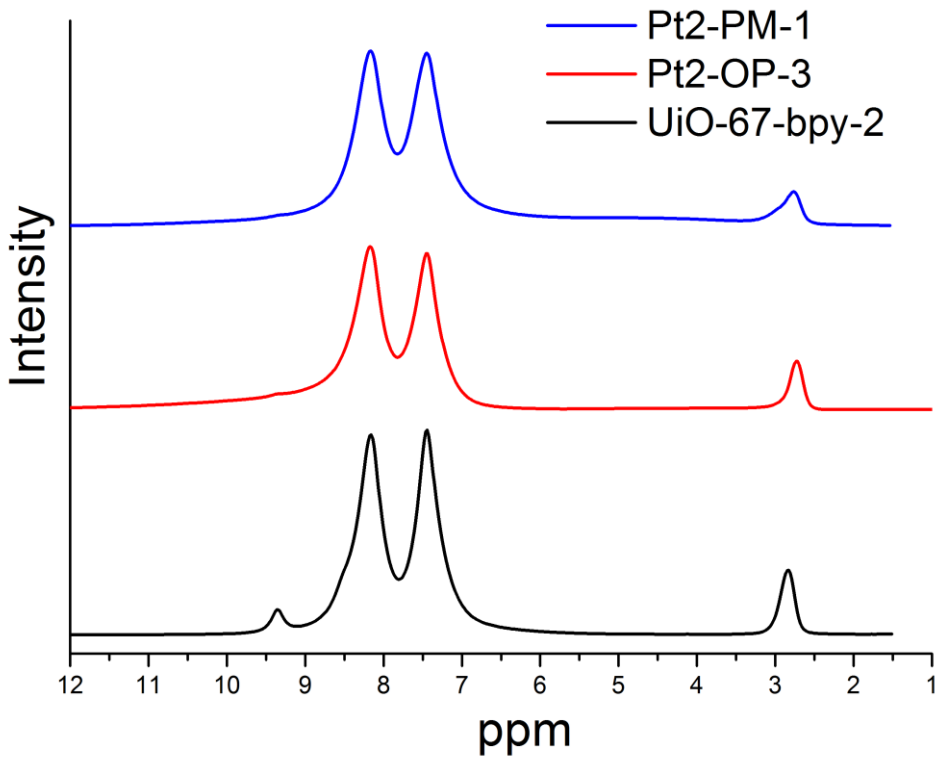

The figure above shows solid state ^{1}H NMR spectra of three MOFs. Platinum functionalization causes the bpy linker to become “invisible” in NMR, perhaps due to significant peak broadening.

Pt4-OP-1

$ZrCl_4$ (120 mg, 0.517 mmol) and H_2O (12 µL, 0.67 mmol) were dissolved in 20 mL DMF while stirring. The solution was heated, and H_2bpydc (13 mg, 0.052 mmol), H_2bpdc (113 mg, 0.465 mmol) and K_2PtCl_6 (25 mg, 0.052 mmol) were added. A clear, yellow solution was obtained after a few minutes of stirring. The solution was kept at 95 °C for 4 days.

The solution was decanted off, and a yellow crystalline powder was recovered. The powder was then washed 3 times in 15 mL portions of anhydrous DMF and 3 times in 15 mL portions of 2-propanol, before it was dried in air at 60 °C. The dry powder was weighed and stored in a desiccator. The product weight was 109 mg, and the solvent fraction was found to be 39 % by evacuation. Thus the dry product weight was estimated to 66 mg and the final yield to 36 % ($Yield_{max}$: 184 mg).

This synthesis was only performed once.

```
\\Supportqfe21\shareddata2\MasterStudents\Sigurd\SOE-161-v_1.spc
Label :
Acquisition Time  : 17:42:55      Date:11-Mar-2011

kV : 20.00   Tilt:-1.50   Take-off:34.22   AmpT : 51.2
Detector Type:SUTW, Sapphire   Resolution:132.36   Lsec:50

Element   Wt %    At %   K-Ratio    Z        A        F
   C K    51.62   78.37    0.1004   1.0745   0.1811   1.0001
   O K    11.71   13.35    0.0176   1.0564   0.1419   1.0001
   ZrL    25.96    5.19    0.2376   0.8147   1.1211   1.0019
   ClK     4.96    2.55    0.0343   0.9597   0.7204   1.0000
   PtL     5.75    0.54    0.0399   0.6702   1.0361   1.0000
 Total   100.00  100.00

Element  Net Inte.    Bkgd Inte.   Inte. Error      P/B
  C K      190.94          2.72          1.04        70.20
  O K       88.74          6.02          1.60        14.74
  ZrL      659.76         34.56          0.58        19.09
  ClK      189.98         29.26          1.17         6.49
  PtL       11.92          7.64          6.19         1.56
```

EDXS data for Pt4-OP-1.

Adsorption data:

Starting point	1	
End point	19	
Slore	0,035815	
Intercept	0,000029007	
Correlation coefficient	1	
Vm	27,898	[cm^3(STP) g^{-1}]
$a_{s,BET}$	121,43	[m^2 g^{-1}]
C	1235,7	
Total pore volume (p/p_0=0.990)	0,055264	[cm^3 g^{-1}]
Average pore diameter	1,8205	[nm]

Pt4-OP-2

$ZrCl_4$ (120 mg, 0.517 mmol) and H_2O (12 µL, 0.67 mmol) were dissolved in 20 mL DMF while stirring. The solution was heated, and H_2bpydc (13 mg, 0.052 mmol), H_2bpdc (113 mg, 0.465 mmol), acetic acid (148 µL, 2.59 mmol) and K_2PtCl_6 (25 mg, 0.052 mmol) were added. A clear, yellow solution was obtained after a few minutes of stirring. The solution was kept at 95 °C for 4 days.

The solution was decanted off, and a yellow crystalline powder was recovered. The powder was then washed 3 times in 15 mL portions of anhydrous DMF and 3 times in 15 mL portions of 2-propanol, before it was dried in air at 60 °C. The dry powder was weighed and stored in a desiccator. The product weight was 69 mg, and the solvent fraction was found to be 39 % by evacuation. Thus the dry product weight was estimated to 42 mg and the final yield to 23 % ($Yield_{max}$: 184 mg).

This synthesis was done with the same ratio of reagents, although not always the same amounts, a total of 4 times, out of which 3 gave a crystalline product. Yields ranged from 13 to 30 %.

Adsorption data for Pt4-OP-2:

Starting point	1	
End point	21	
Slore	0,0018303	
Intercept	1,0003E-06	
Correlation coefficient	1	
Vm	546,06	[cm^3(STP) g^{-1}]
$a_{s,BET}$	2376,7	[m^2 g^{-1}]
C	1830,8	
Total pore volume (p/p_0=0.990)	0,9909	[cm^3 g^{-1}]
Average pore diameter	1,6677	[nm]

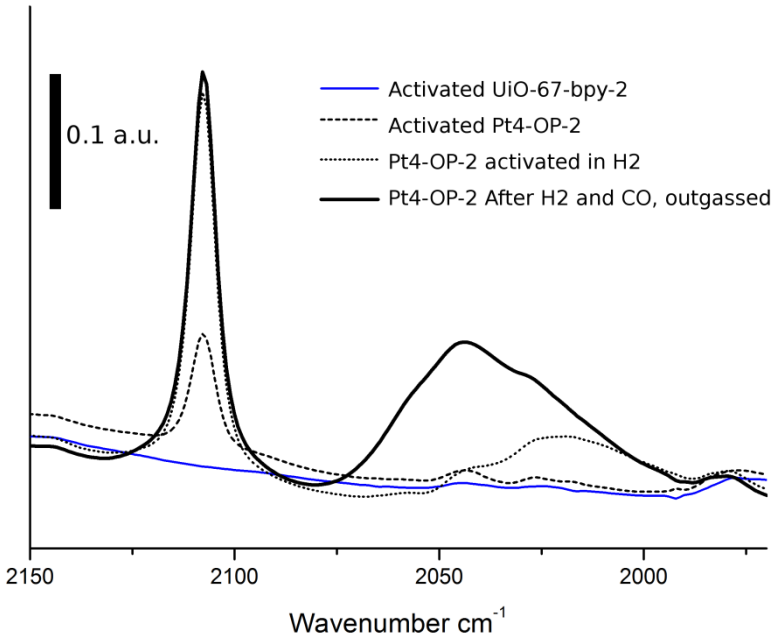

Section of IR spectrum of Pt4-OP-2. Activation procedure was two hours in vacuum at 300°C. Hydrogen activation was done by submitting MOF to 60 mbar H_2 atmosphere at 250°C. CO was dosed and outgassed at room temperature.

Hydrogen activation gives a sharp peak at 2108 cm^{-1}. CO gives a broad peak at 2045 cm^{-1}. Both of these peaks remain when the gases are removed, and may be due to formation of platinum carbonyls.

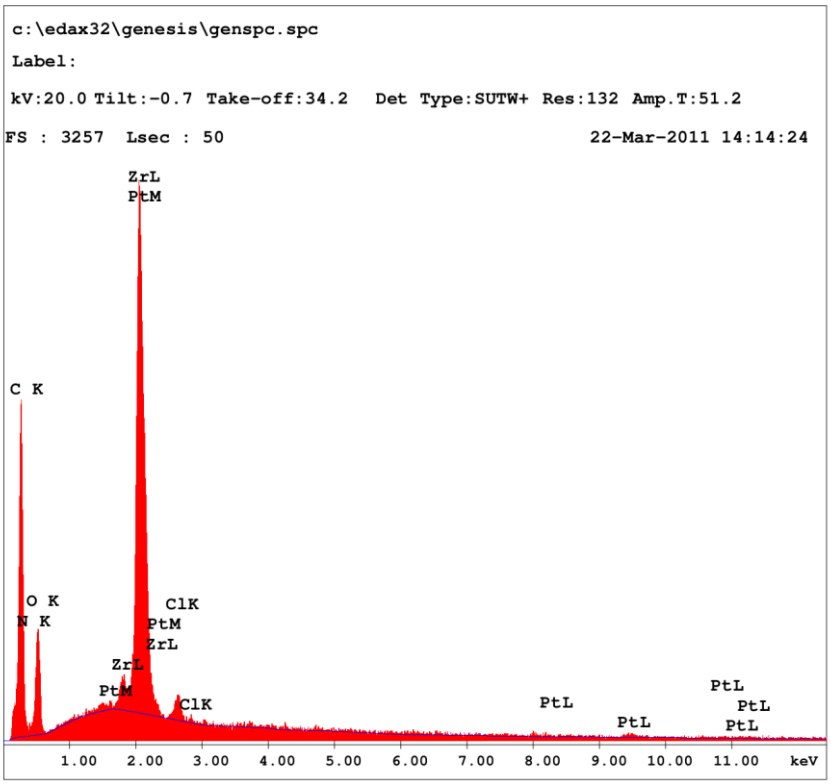

Element	Wt %	At %	K-Ratio	Z	A	F
C K	58.58	74.87	0.1824	1.0406	0.2992	1.0002
N K	5.30	5.81	0.0056	1.0314	0.1031	1.0003
O K	16.89	16.21	0.0259	1.0231	0.1498	1.0001
ZrL	13.95	2.35	0.1252	0.7848	1.1427	1.0005
ClK	0.98	0.42	0.0075	0.9244	0.8276	1.0000
PtL	4.30	0.34	0.0287	0.6422	1.0410	1.0000
Total	100.00	100.00				

Element	Net Inte.	Bkgd Inte.	Inte. Error	P/B
C K	196.44	2.64	1.02	74.41
N K	7.76	3.76	7.12	2.06
O K	74.14	5.28	1.76	14.04
ZrL	196.88	28.26	1.14	6.97
ClK	23.48	25.46	5.20	0.92
PtL	4.86	6.46	12.27	0.75

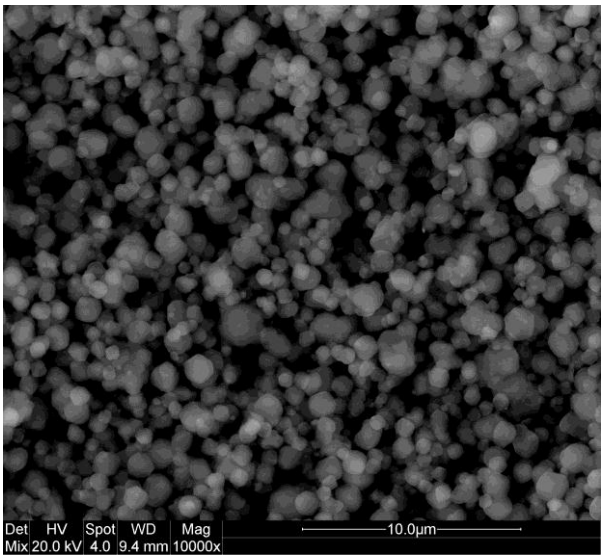

EDX spectrum and SEM micrograph of Pt4-OP-2.

Pt4-OP-3

$ZrCl_4$ (120 mg, 0.517 mmol) and H_2O (12 µL, 0.67 mmol) were dissolved in 20 mL DMF while stirring. The solution was heated, and benzoic acid (315 mg, 2.59 mmol), H_2bpydc (13 mg, 0.052 mmol), H_2bpdc (113 mg, 0.465 mmol) and K_2PtCl_6 (25 mg, 0.052 mmol) were added. A clear, yellow solution was obtained after a few minutes of stirring. The solution was kept at 95 °C for 4 days.

The solution was decanted off, and a yellow crystalline powder was recovered. The powder was then washed 3 times in 15 mL portions of anhydrous DMF and 3 times in 15 mL portions of 2-propanol, before it was dried in air at 60 °C. The dry powder was weighed and stored in a desiccator. The product weight was 203 mg, and the solvent fraction was found to be 39 % by evacuation. Thus the dry product weight was estimated to 124 mg and the final yield to 67 % ($Yield_{max}$: 184 mg).

This synthesis was done with the same ratio of reagents, although not always the same amounts, a total of 3 times, out of which all gave a crystalline product. Yields ranged from 14 to 67 %.

Adsorption data:

Starting point	12	
End point	28	
Slore	0,0018131	
Intercept	1,4314E-06	
Correlation coefficient	1	
Vm	551,11	[cm^3(STP) g^{-1}]
$a_{s,BET}$	2398,7	[m^2 g^{-1}]
C	1267,6	
Total pore volume (p/p_0=0.990)	0,9762	[cm^3 g^{-1}]
Average pore diameter	1,6278	[nm]

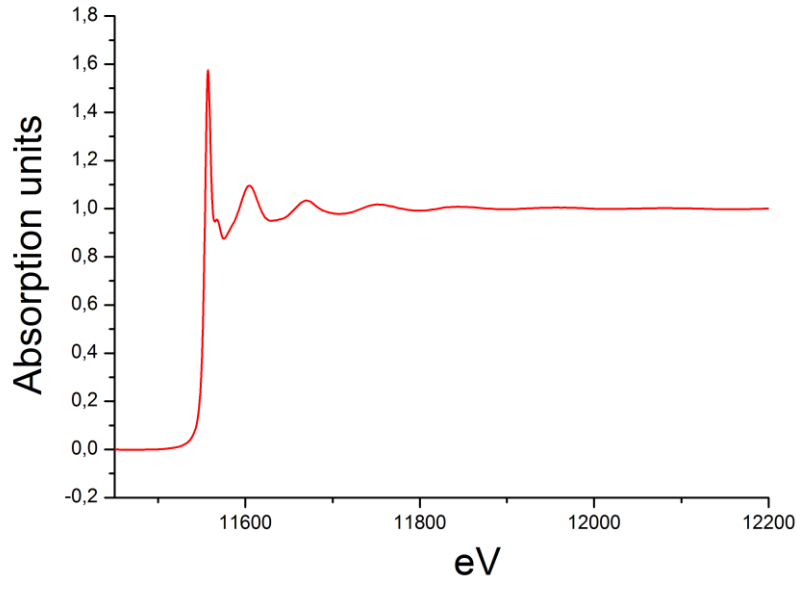

XAS spectrum of Pt-OP-4.

Pt2-PM-1

$ZrCl_4$ (602 mg, 2.58 mmol) and H_2O (61 µL, 3.4 mmol) were dissolved in 100 mL DMF while stirring. The solution was heated, and benzoic acid (1.58 g, 12.9 mmol), H_2bpdc (563 mg, 2.33 mmol) and $PtCl_2(H_2bpydc)$ (132 mg, 0.258 mmol) were added. A clear, yellow solution was obtained after a few minutes of stirring. The solution was kept at 95 °C for 4 days.

The solution was decanted off, and a yellow crystalline powder was recovered. The powder was then washed 3 times in 15 mL portions of anhydrous DMF and 3 times in 15 mL portions of 2-propanol, before it was dried in air at 60 °C. The dry powder was weighed and stored in a desiccator. The product weight was 833 mg, and the solvent fraction was found to be 42 % by evacuation. Thus the dry product weight was estimated to 481 mg and the final yield to 52 % ($Yield_{max}$: 921 mg).

This synthesis was done with the same ratio of reagents, although not always the same amounts, a total of 3 times, out of which all gave a crystalline product. Yields ranged from 44 to 52 %.

Adsorption data:

Starting point	1	
End point	14	
Slore	0,0019559	
Intercept	2,6652E-06	
Correlation coefficient	1	
Vm	510,58	[cm^3(STP) g^{-1}]
$a_{s,BET}$	2222,3	[m^2 g^{-1}]
C	734,87	
Total pore volume (p/p_0=0.990)	1,1022	[cm^3 g^{-1}]
Average pore diameter	1,9839	[nm]

Solid state NMR spectrum is presented in the Pt2-OP-3 section.

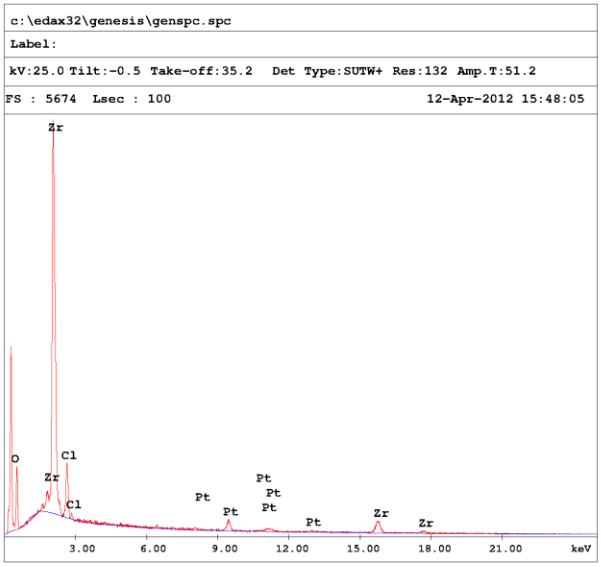

Element	Wt %	At %	K-Ratio	Z	A	F
O K	22.66	61.36	0.0339	1.1645	0.1286	1.0003
ClK	6.53	7.99	0.0280	1.0838	0.3950	1.0000
PtL	11.79	2.62	0.0982	0.8046	1.0355	1.0000
ZrK	59.02	28.04	0.5423	0.9219	0.9967	1.0000
Total	100.00	100.00				

Element	Net Inte.	Bkgd Inte.	Inte. Error	P/B
O K	52.44	5.24	1.51	10.01
ClK	62.47	24.75	1.69	2.52
PtL	18.50	7.69	3.15	2.41
ZrK	27.24	3.31	2.14	8.23

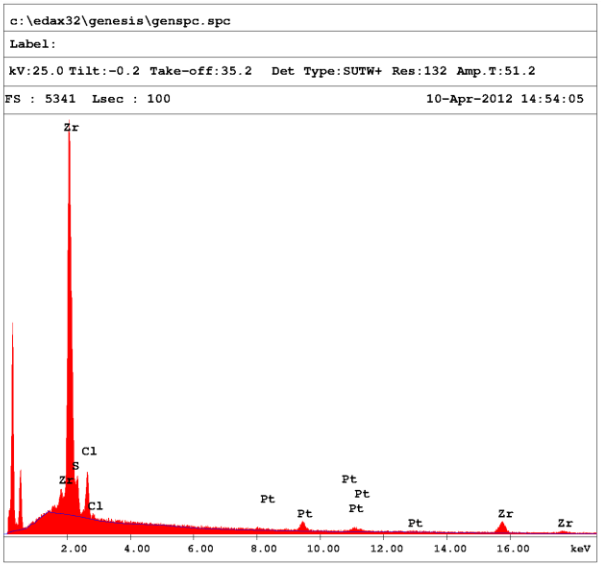

Element	Wt %	At %	K-Ratio	Z	A	F
S K	6.95	16.65	0.0244	1.1608	0.3024	1.0023
ClK	8.50	18.41	0.0325	1.1443	0.3344	1.0000
PtL	13.98	5.51	0.1221	0.8511	1.0256	1.0000
ZrK	70.57	59.43	0.6896	0.9831	0.9941	1.0000
Total	100.00	100.00				

Element	Net Inte.	Bkgd Inte.	Inte. Error	P/B
S K	39.61	22.89	2.33	1.73
ClK	50.29	22.34	1.94	2.25
PtL	15.92	6.57	3.39	2.42
ZrK	23.99	2.64	2.26	9.09

EDX spectrums of Pt2-PM-1.

Top left: As synthesized.

Top right: After Hydrogen activation under flow at 300°C.

Bottom right: EDX spectrum of Pt(tdt)-PS, which is Pt2-PM-2 reacted with H_2tdt.

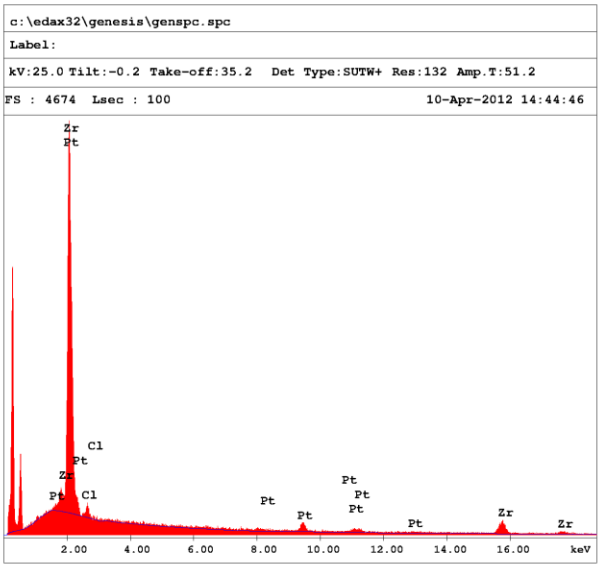

Element	Wt %	At %	K-Ratio	Z	A	F
ClK	2.47	6.62	0.0091	1.1784	0.3128	1.0000
PtL	14.63	7.12	0.1314	0.8776	1.0236	1.0000
ZrK	82.90	86.27	0.8385	1.0182	0.9934	1.0000
Total	100.00	100.00				

Element	Net Inte.	Bkgd Inte.	Inte. Error	P/B
ClK	10.98	21.53	6.70	0.51
PtL	13.36	6.13	3.79	2.18
ZrK	22.74	2.86	2.35	7.95

Pt2-PM-2

$ZrCl_4$ (602 mg, 2.58 mmol) and H_2O (61 µL, 3.4 mmol) were dissolved in 100 mL DMF while stirring. The solution was heated, and benzoic acid (9.46 g, 77.5 mmol), H_2bpdc (563 mg, 2.33 mmol) and $PtCl_2(H_2bpydc)$ (132 mg, 0.258 mmol) were added. A clear, yellow solution was obtained after a few minutes of stirring. The solution was kept at 95 °C for 4 days.

The solution was decanted off, and a yellow crystalline powder was recovered. The powder was then washed 3 times in 15 mL portions of anhydrous DMF and 3 times in 15 mL portions of 2-propanol, before it was dried in air at 60 °C. The dry powder was weighed and stored in a desiccator. The product weight was 1.17 g, and the solvent fraction was found to be 45 % by evacuation. Thus the dry product weight was estimated to 640 mg and the final yield to 70 % ($Yield_{max}$: 921 mg).

This synthesis was done with the same ratio of reagents, although not always the same amounts, a total of two times, out of which both gave a crystalline product. The yields were 53 % and 70 %.

Adsorption data:

Starting point	1	
End point	16	
Slore	0,0020675	
Intercept	9,3016E-07	
Correlation coefficient	1	
Vm	483,46	[cm^3(STP) g^{-1}]
$a_{s,BET}$	2104,3	[m^2 g^{-1}]
C	2223,7	
Total pore volume (p/p_0=0.990)	0,8762	[cm^3 g^{-1}]
Average pore diameter	1,6655	[nm]

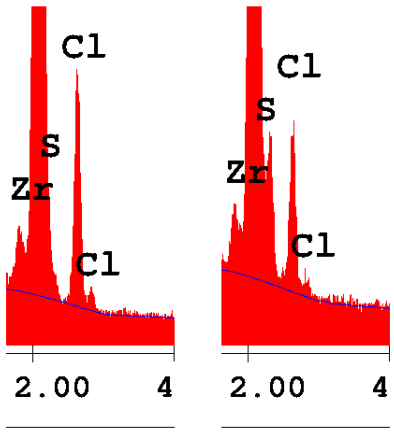

This MOF was functionalized with H2tdt in order to perform single crystal EDXS. This PSF sample is not mentioned in the main text and does not have a serial number.

The figure above shows that sulfur content in H_2tdt functionalized MOF is evident by the appearance of a discernible S peak in the EDX spectra of single crystals. Full spectra are shown on the next page. Left: Pt2-PM-2. Right: Pt2-PM-2 functionalized with H_2tdt.

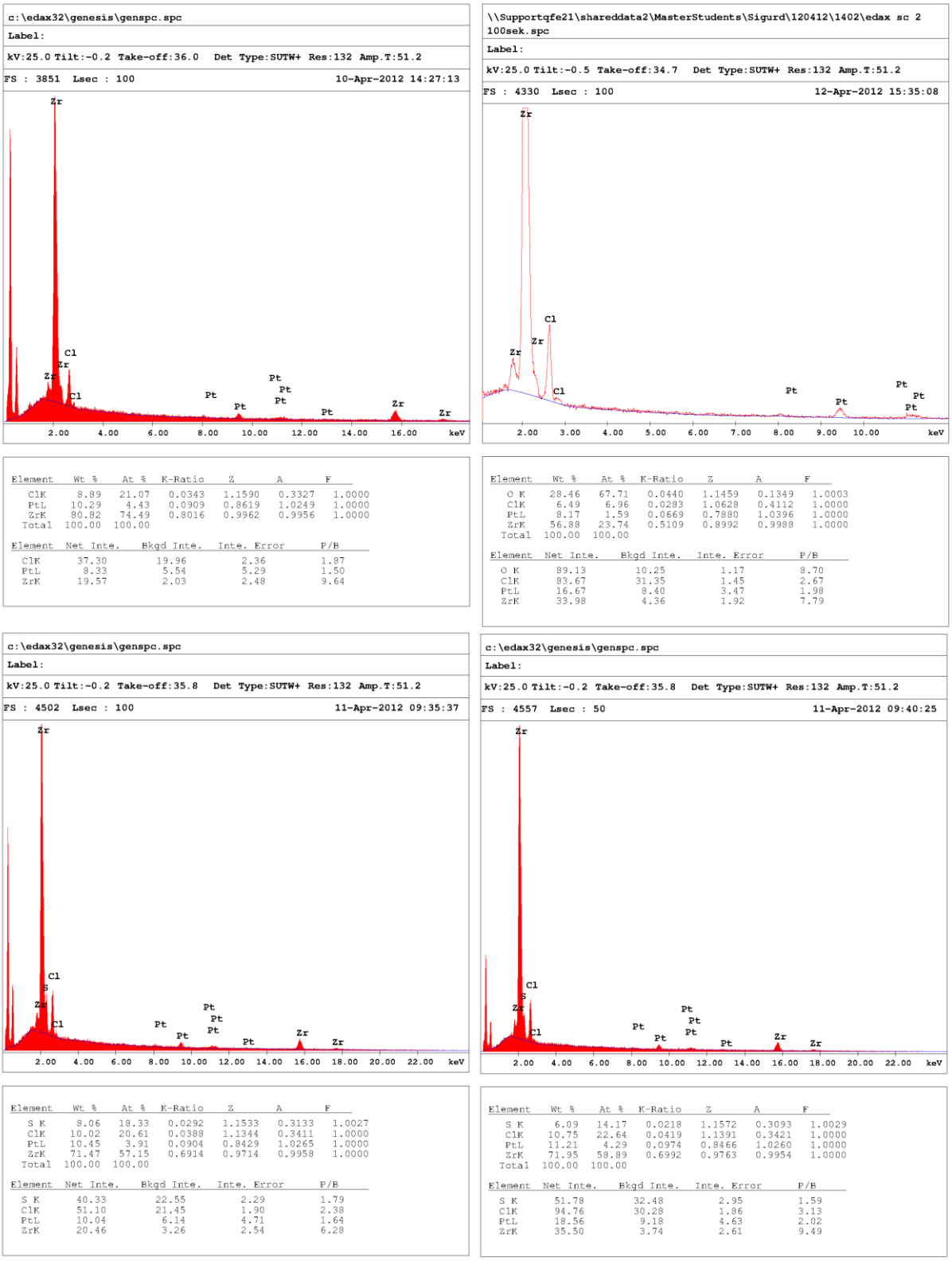

EDX spectra of Pt2-PM-2. Top left: Pt2-PM-2, 50 x 50 µm area. Top right: Pt2-PM-2 single crystal spot scan. Bottom left: Pt2-PM-2 reacted with H_2tdt, 50 x 50 µm area. Bottom right: Pt2-PM-2 reacted with H_2tdt, single crystal spot scan.

Pt4-PM

$ZrCl_4$ (602 mg, 2.58 mmol) and H_2O (61 µL, 3.4 mmol) were dissolved in 100 mL DMF while stirring. The solution was heated, and benzoic acid (1.58 g, 12.9 mmol), H_2bpdc (563 mg, 2.33 mmol) and $PtCl_4(H_2bpydc)$ (150 mg, 0.258 mmol) were added. A clear, yellow solution was obtained after a few minutes of stirring. The solution was kept at 95 °C for 4 days.

The solution was decanted off, and a yellow crystalline powder was recovered. The powder was then washed 3 times in 15 mL portions of anhydrous DMF and 3 times in 15 mL portions of 2-propanol, before it was dried in air at 60 °C. The dry powder was weighed and stored in a desiccator. The product weight was 1.22 g, and the solvent fraction was found to be 37 % by evacuation. Thus the dry product weight was estimated to 763 mg and the final yield to 83 % ($Yield_{max}$: 921 mg).

This synthesis was only performed once.

Adsorption data:

Starting point	5	
End point	31	
Slore	0,002248	
Intercept	2,8812E-06	
Correlation coefficient	0,9999	
Vm	444,28	[cm^3(STP) g^{-1}]
$a_{s,BET}$	1933,7	[m^2 g^{-1}]
C	781,21	
Total pore volume (p/p_0=0.990)	0,8682	[cm^3 g^{-1}]
Average pore diameter	1,7959	[nm]

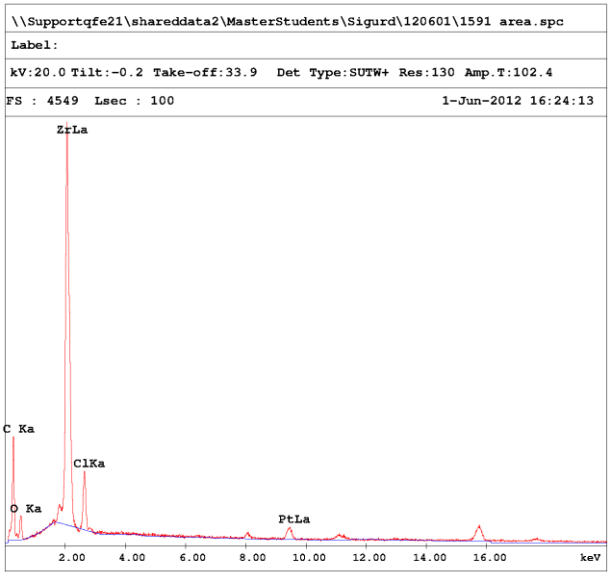

Element	Wt %	At %	K-Ratio	Z	A	F
C K	40.89	80.41	0.0727	1.1273	0.1578	1.0000
O K	4.53	6.68	0.0068	1.1080	0.1363	1.0002
ZrL	31.46	8.15	0.2916	0.8637	1.0722	1.0011
ClK	3.61	2.41	0.0224	1.0175	0.6094	1.0000
PtL	19.52	2.36	0.1444	0.7187	1.0291	1.0000
Total	100.00	100.00				

Element	Net Inte.	Bkgd Inte.	Inte. Error	P/B
C K	56.01	1.74	1.38	32.19
O K	14.03	1.94	3.02	7.23
ZrL	329.72	17.34	0.58	19.01
ClK	50.66	13.94	1.75	3.63
PtL	17.60	5.95	3.09	2.96

Left: EDX spectrum of Pt4-PM.

Pt2-PS

300 mg UiO-67-bpy-2 (approximately 0.050 mmol bpy sites with a solvent loading of 41 %) was suspended in 15 mL anhydrous DMF in a 50 mL Erlenmeyer flask. K_2PtCl_4 (22 mg, 0.053 mmol) was added and dissolved under stirring. The suspension was heated to 100 °C and left overnight. A yellow powder was recovered, washed 3 times in 15 mL portions of 2-propanol and dried in air at 60 °C.

The dry powder was weighed and stored in a desiccator. The product weight was 288 mg, and the solvent fraction was found to be 25 % by evacuation. Thus the dry product weight was estimated to 170 mg and the final yield to 96 % ($Yield_{max}$: 177 mg).

This post synthetic modification was repeated three times. EDXS has not been performed on this sample, but platinum content similar to the other Pt(II) samples has been confirmed by EXAFS.

Adsorption data:

Starting point	17	
End point	32	
Slore	0,0020531	
Intercept	1,4938E-06	
Correlation coefficient	1	
Vm	486,72	[cm^3(STP) g^{-1}]
$a_{s,BET}$	2118,4	[m^2 g^{-1}]
C	1375,4	
Total pore volume (p/p_0=0.990)	0,8645	[cm^3 g^{-1}]
Average pore diameter	1,6323	[nm]

Pt4-PS

300 mg UiO-67-bpy-2 (approximately 0.050 mmol bpy sites with a solvent loading of 41 %) was suspended in 15 mL anhydrous DMF in a 50 mL Erlenmeyer flask. $Na_2PtCl_6{\cdot}6H_2O$ (29 mg, 0.052 mmol) was added and dissolved under stirring. The suspension was heated to 100 °C and left overnight. A yellow powder was recovered, washed 3 times in 15 mL portions of 2-propanol and dried in air at 60 °C.

The dry powder was weighed and stored in a desiccator. The product weight was 310 mg. The yield was estimated to be close to 100 % since this was the case for Pt2-PS. There was no possibility of evacuating the sample at the time to determine solvent loading, and the sample was destroyed in an EXAFS experiment.

This post synthetic modification was repeated three times. EDXS has not been performed on this sample, but platinum content similar to the other Pt(IV) samples has been confirmed by EXAFS.

UiO-67-Pt(tdt) synthesis

Toluene-3,4-dithiol (H_2tdt) (>90%, Sigma-Aldrich) was used as received. Pt(tdt)(H_2bpydc) was synthesized as previously described.

Pt(tdt)-PM

$ZrCl_4$ (181 mg, 0.775 mmol) and H_2O (18 µL, 1.0 mmol) were dissolved in 30 mL DMF while stirring. The solution was heated, and benzoic acid (473 mg, 3.87 mmol), H_2bpdc (178 mg, 0.736 mmol) and Pt(tdt)(H_2bpydc) (23 mg, 0.039 mmol) were added. A clear, dark blue solution was obtained after a few minutes of stirring. The solution was kept at 95 °C for 4 days.

The solution was decanted off, and a blue crystalline powder was recovered. The powder was then washed 3 times in 15 mL portions of anhydrous DMF and 3 times in 15 mL portions of 2-propanol, before it was dried in air at 60 °C. The dry powder was weighed and stored in a desiccator. The product weight was 205 mg, and the solvent fraction was found to be 34 % by evacuation. Thus the dry product weight was estimated to 136 mg and the final yield to 50 % ($Yield_{max}$: 276 mg).

Adsorption data:

Starting point	5	
End point	42	
Slore	0,0020342	
Intercept	8,9402E-07	
Correlation coefficient	0,9999	
Vm	491,38	[cm^3(STP) g^{-1}]
$a_{s,BET}$	2138,7	[m^2 g^{-1}]
C	2276,3	
Total pore volume (p/p_0=0.990)	1,0391	[cm^3 g^{-1}]
Average pore diameter	1,9434	[nm]

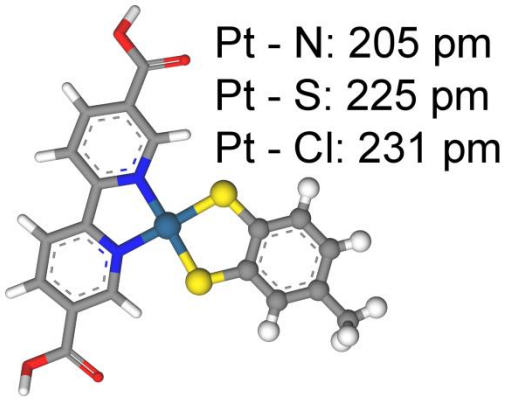

Left: Structure of the linker Pt(tdt)(H_2bpydc) with bond lengths known from crystallography.

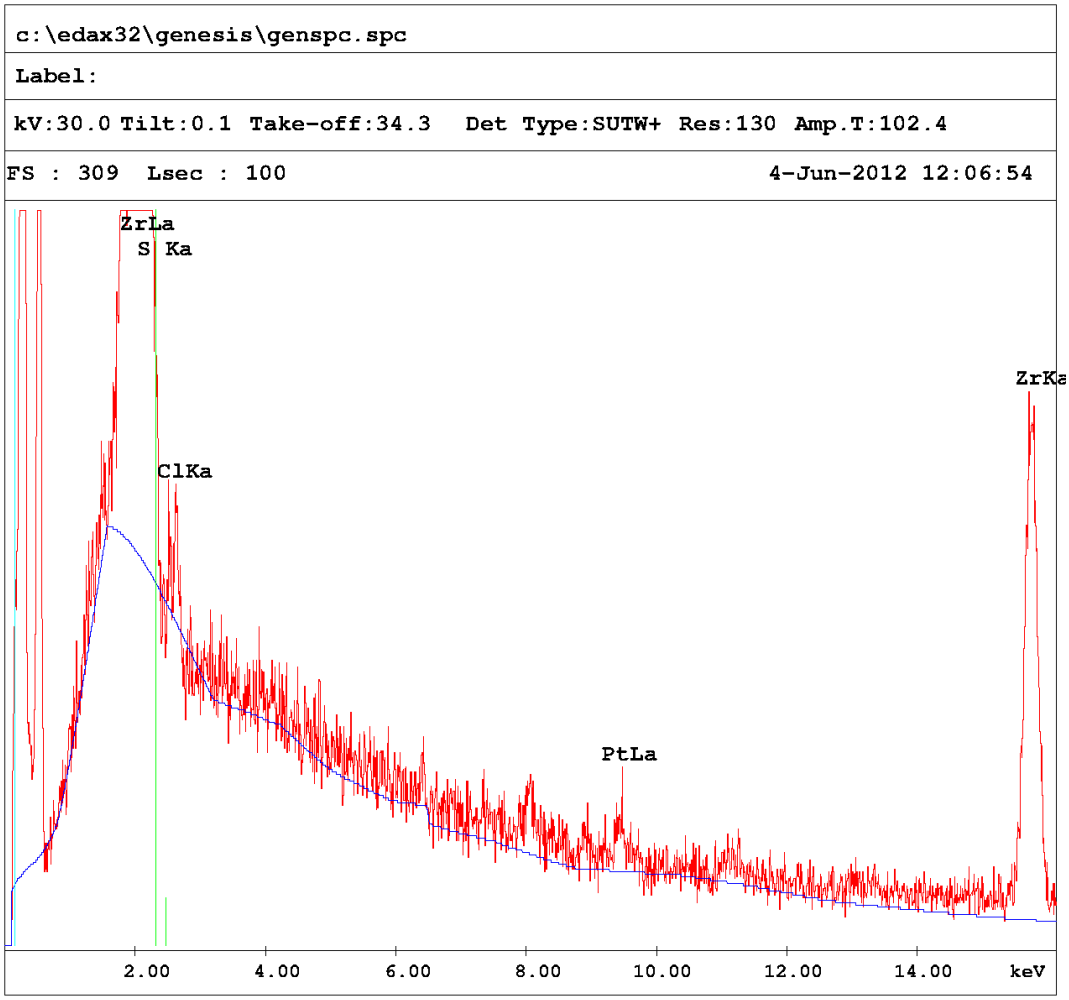

Element	Wt %	At %	K-Ratio	Z	A	F
S K	2.57	6.95	0.0064	1.1679	0.2128	1.0004
ClK	1.45	3.55	0.0038	1.1181	0.2375	1.0000
PtL	3.57	1.59	0.0327	0.8835	1.0380	1.0000
ZrK	92.41	87.92	0.9171	0.9951	0.9974	1.0000
Total	100.00	100.00				

Element	Net Inte.	Bkgd Inte.	Inte. Error	P/B
S K	5.55	15.25	10.82	0.36
ClK	3.25	13.53	16.94	0.24
PtL	3.02	5.27	12.19	0.57
ZrK	36.13	2.35	1.77	15.37

EDX spectrum of Pt(tdt)-PM. The sample was made with only 5 % functionalized linker, and the Pt content is barely detectable by EDXS. Still, the sample's bright blue color and UV-vis spectrum establishes the presence of platinum.

Pt(tdt)-PS

300 mg Pt2-PM-1 (approximately 0.050 mmol $PtCl_2$ sites with a solvent loading of 42 %) was suspended in 15 mL 2-propanol in a 25 mL Erlenmeyer flask. H_2tdt (11 mg, 0.071 mmol) was added and dissolved under stirring. The powder in suspension was kept stirring at 25 °C and, changed color from yellow to blue in two hours, but left overnight to let the reaction go to completion. A blue powder was recovered, washed 3 times in 15 mL portions of 2-propanol and dried in air at 60 °C.

The dry powder was weighed and stored in a desiccator. The product weight was 160 mg, and the solvent fraction was found to be 19 % by evacuation. Thus the dry product weight was estimated to 129 mg and the final yield to 65 % ($Yield_{max}$: 177 mg). This unexpected loss of sample can be due to incomplete recovery of product, e.g. if some crystals are very small.

EDX data presented previously, under Pt2-PM-1.

UiO-67-Cu synthesis

$CuCl_2 \cdot 2H_2O$ (>99%, Sigma-Aldrich) was used as received. CuCl2· H_2bpydc complex was synthesized as previously described.

EXAFS pellet weight and absorption jump ($\Delta\mu_0$). Since the jump is proportional to the amount of copper in the pellet, it can determine which sample has higher concentration. All pellets have the same area.

Sample	$\Delta\mu_0$	Pellet weight
Cu-PM	0,20	180 mg
Cu-OP-2	0,38	193 mg
Cu-PS	0,43	76 mg

$[Cu]_{Cu\text{-}PS} = 2.9\ [Cu]_{Cu\text{-}OP\text{-}1} = 5.1\ [Cu]_{Cu\text{-}PM}$.

Cu-PM

When the synthesis was performed, it was assumed that the CuCl2· H_2bpydc complex was $CuCl_2(H_2bpydc)$.

$ZrCl_4$ (602 mg, 2.58 mmol) and H_2O (61 µL, 3.4 mmol) were dissolved in 100 mL DMF while stirring. The solution was heated, and benzoic acid (1.58 g, 12.9 mmol), H_2bpdc (563 mg, 2.33 mmol) and $CuCl_2(H_2bpydc)$ (98 mg, 0.258 mmol) were added. A clear, green solution was obtained after a few minutes of stirring. The solution was kept at 95 °C for 4 days.

The solution was decanted off, and a green crystalline powder was recovered. The powder was then washed 3 times in 15 mL portions of anhydrous DMF and 3 times in 15 mL portions of 2-propanol, before it was dried in air at 60 °C. The dry powder was weighed and stored in a desiccator. The product weight was 311 mg, and the solvent fraction was found to be 54 % by evacuation. Thus the dry product weight was estimated to 144 mg and the final yield to 16 % ($Yield_{max}$: 921 mg). The low yield is partly due to problems with powder recovery. Some of the particles were extremely small, and were discarded.

This synthesis was done with the same ratio of reagents, although not always the same amounts, a total of 5 times, out of which 3 gave a crystalline product. Yields ranged from 4 to 35 %.

The powder turned grey upon activation, but regained a bright green color when reintroduced to humid air. This may indicate that water reversibly adsorbs on copper.

Adsorption data:

Starting point	2	
End point	32	
Slore	0,001965	
Intercept	2,9813E-06	
Correlation coefficient	0,9998	
Vm	508,12	[cm^3(STP) g^{-1}]
$a_{s,BET}$	2211,6	[m^2 g^{-1}]
C	660,13	
Total pore volume (p/p_0=0.989)	1,2077	[cm^3 g^{-1}]
Average pore diameter	2,1842	[nm]

c:\edax32\genesis\genspc.spc

Label:

kV:25.0 Tilt:-0.2 Take-off:36.0 Det Type:SUTW+ Res:132 Amp.T:51.2

FS : 8150 Lsec : 100 11-Apr-2012 10:10:43

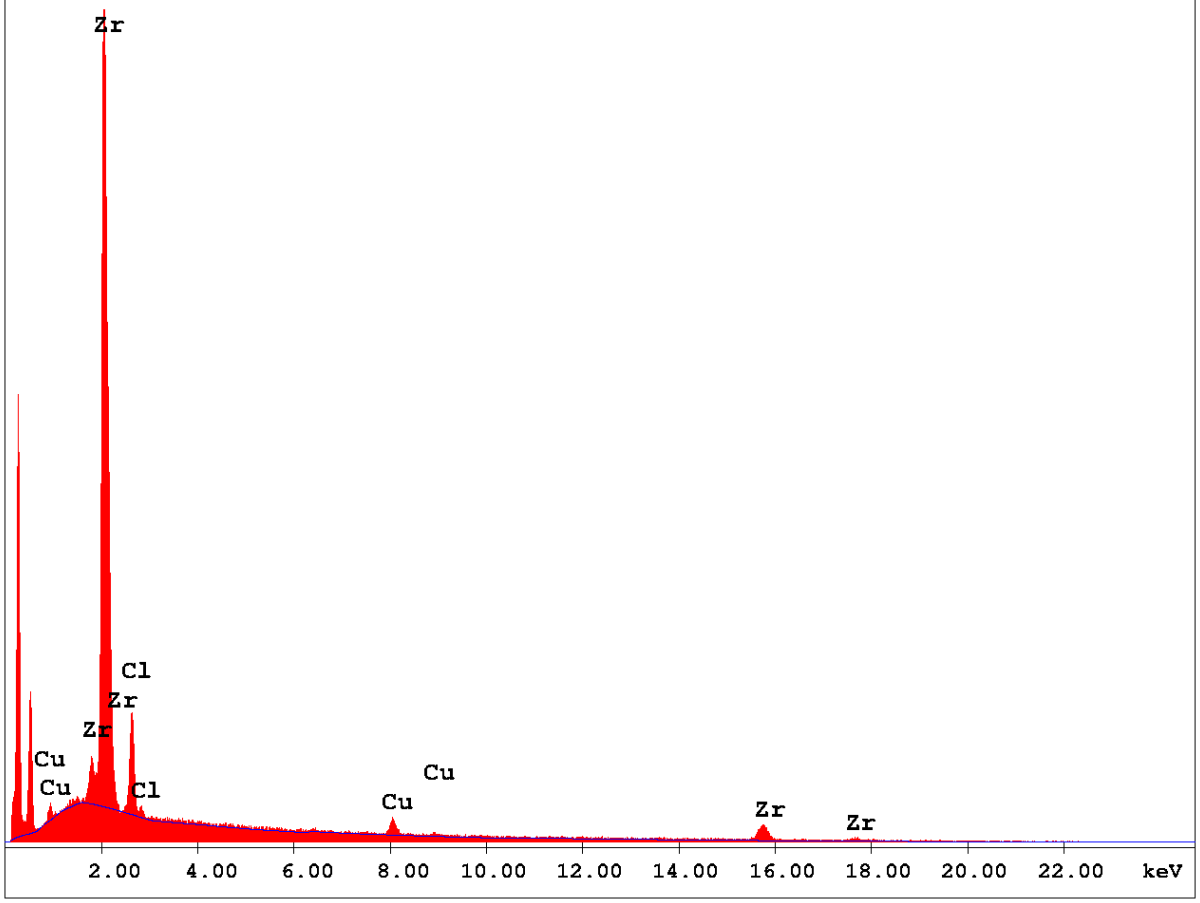

Element	Wt %	At %	K-Ratio	Z	A	F
ClK	14.98	30.67	0.0602	1.1318	0.3549	1.0000
CuK	4.87	5.56	0.0480	1.0320	0.9557	1.0000
ZrK	80.15	63.77	0.7717	0.9633	0.9995	1.0000
Total	100.00	100.00				

Element	Net Inte.	Bkgd Inte.	Inte. Error	P/B
ClK	83.37	29.22	1.43	2.85
CuK	18.44	10.74	3.43	1.72
ZrK	23.98	2.86	2.27	8.38

EDX spectrum of Cu-PM

Cu-OP-1

$ZrCl_4$ (602 mg, 2.58 mmol) and H_2O (61 µL, 3.4 mmol) were dissolved in 100 mL DMF while stirring. The solution was heated, and H_2bpydc (63 mg, 0.26 mmol), H_2bpdc (563 mg, 2.33 mmol), acetic acid (739 µL, 12.9 mmol) and $CuCl_2 \cdot H_2O$ (44 mg, 0.26 mmol) were added. A clear, green solution was obtained after a few minutes of stirring. The solution was kept at 95 °C for 4 days.

The solution was decanted off, and a green crystalline powder was recovered. The powder was then washed 3 times in 15 mL portions of anhydrous DMF and 3 times in 15 mL portions of 2-propanol, before it was dried in air at 60 °C.The dry powder was weighed and stored in a desiccator. The product weight was 159 mg, and the solvent fraction was assumed to be 44 %, the same as for **Cu-OP-2**. Thus the dry product weight was estimated to 88 mg and the final yield to 10 % ($Yield_{max}$: 921 mg).

This synthesis was done with the same ratio of reagents, although not always the same amounts, a total of 3 times, out of which 2 gave a crystalline product. The yields were 7 and 10 %.

Cu-OP-2

$ZrCl_4$ (602 mg, 2.58 mmol) and H_2O (61 µL, 3.4 mmol) were dissolved in 100 mL DMF while stirring. The solution was heated, and benzoic acid (1.58 g, 12.9 mmol), H_2bpydc (63 mg, 0.26 mmol), H_2bpdc (563 mg, 2.33 mmol) and $CuCl_2 \cdot H_2O$ (44 mg, 0.26 mmol) were added. A clear, green solution was obtained after a few minutes of stirring. The solution was kept at 95 °C for 4 days.

The solution was decanted off, and a green crystalline powder was recovered. The powder was then washed 3 times in 15 mL portions of anhydrous DMF and 3 times in 15 mL portions of 2-propanol, before it was dried in air at 60 °C. The dry powder was weighed and stored in a desiccator. The product weight was 699 mg, and the solvent fraction was found to be 44 % by evacuation. Thus the dry product weight was estimated to 389 mg and the final yield to 42 % ($Yield_{max}$: 921 mg).

This synthesis was done with the same ratio of reagents, although not always the same amounts, twice, out of which both gave a crystalline product. The yields were 18 and 42 %.

Adsorption data:

Starting point	3	
End point	12	
Slore	0,0020679	
Intercept	0,00000108	
Correlation coefficient	1	
Vm	483,33	[cm^3(STP) g^{-1}]
$a_{s,BET}$	2103,7	[m^2 g^{-1}]
C	1915,7	
Total pore volume (p/p_0=0.990)	0,8995	[cm^3 g^{-1}]
Average pore diameter	1,7103	[nm]

c:\edax32\genesis\genspc.spc

Label:

kV:25.0 Tilt:-0.2 Take-off:36.0 Det Type:SUTW+ Res:132 Amp.T:51.2

FS : 4247 Lsec : 50 11-Apr-2012 10:51:40

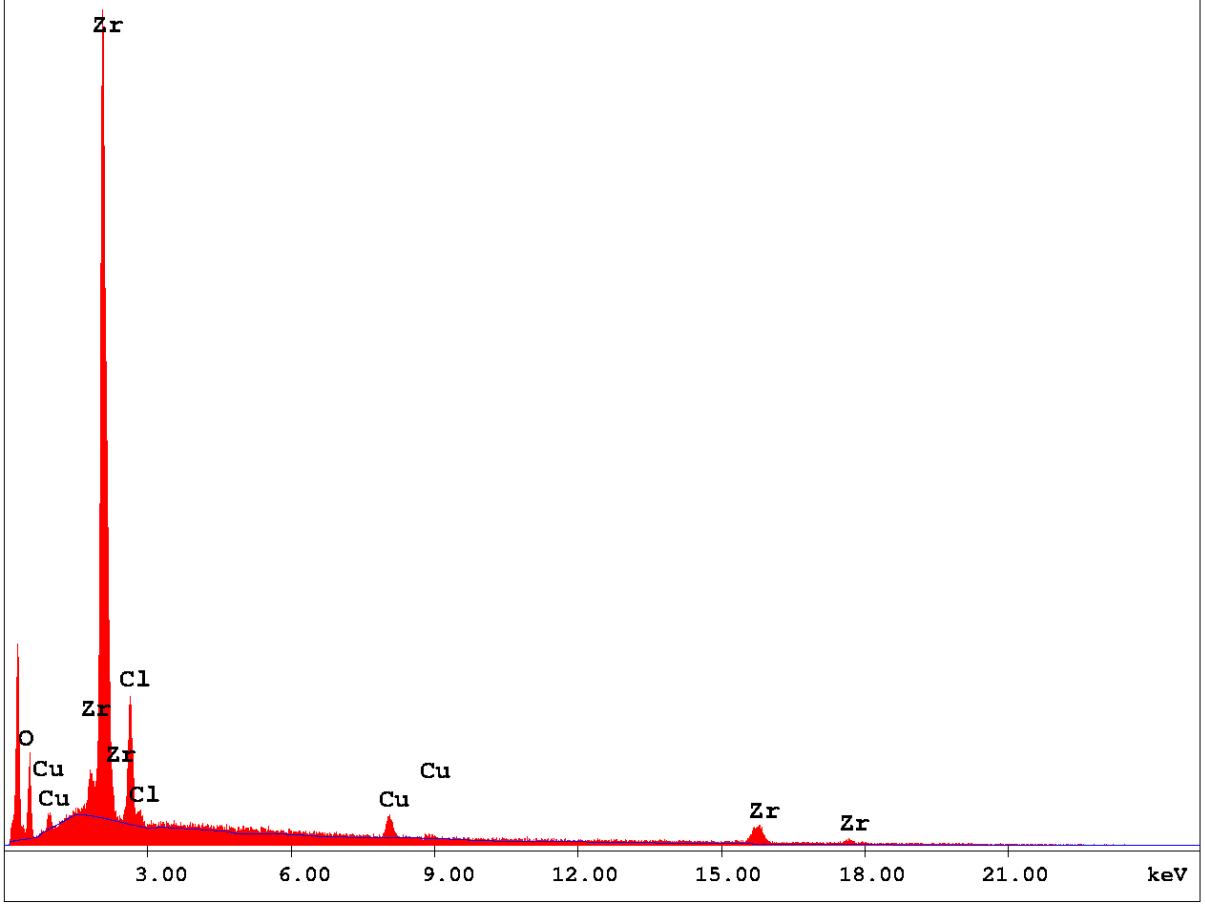

Element	Wt %	At %	K-Ratio	Z	A	F
O K	19.66	53.26	0.0279	1.1592	0.1225	1.0004
ClK	10.27	12.56	0.0447	1.0746	0.4052	1.0000
CuK	4.25	2.90	0.0404	0.9809	0.9691	1.0000
ZrK	65.82	31.28	0.5976	0.9069	1.0011	1.0000
Total	100.00	100.00				

Element	Net Inte.	Bkgd Inte.	Inte. Error	P/B
O K	47.38	5.38	2.28	8.81
ClK	108.42	23.42	1.63	4.63
CuK	27.18	12.34	3.75	2.20
ZrK	32.50	3.08	2.71	10.55

EDX spectrum of Cu-OP-2.

Cu-PS

300 mg UiO-67-bpy-2 (approximately 0.050 mmol bpy sites with a solvent loading of 41 %) was suspended in 15 mL 2-propanol in a 25 mL Erlenmeyer flask. $CuCl_2 \cdot H_2O$ (22 mg, 0.053 mmol) was added and dissolved under stirring. The suspension was left stirring overnight. A green powder was recovered, washed 3 times in 15 mL portions of 2-propanol and dried in air at 60 °C.

The dry powder was weighed and stored in a desiccator. The product weight was 214 mg, and the solvent fraction was found to be 53 % by evacuation. Thus the dry product weight was estimated to 100 mg and the final yield to 49 % ($Yield_{max}$: 207 mg). The low yield may be partly due to problems with powder recovery.

Adsorption data:

Starting point	1	
End point	9	
Slore	0,0020499	
Intercept	3,2699E-06	
Correlation coefficient	0,9999	
Vm	487,06	[cm^3(STP) g^{-1}]
$a_{s,BET}$	2119,9	[m^2 g^{-1}]
C	627,89	
Total pore volume (p/p_0=0.990)	1,1742	[cm^3 g^{-1}]
Average pore diameter	2,2156	[nm]

EDX has not been performed on these materials, but EXAFS confirms a high copper content.

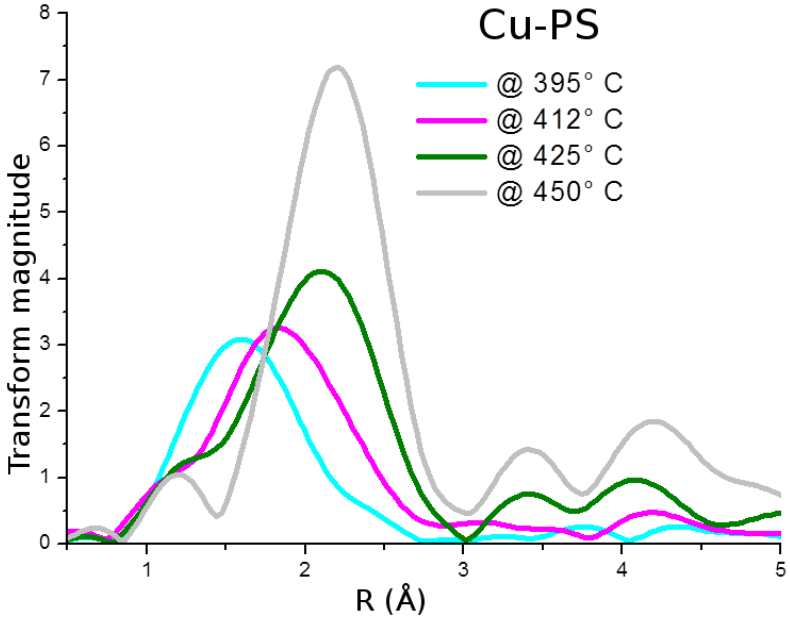

EXAFS spectra acquired while heating the sample. Cu-Cu contribution at 2.3 Å appears at 400°C.

UiO-67-Ru(bpy)$_3$ synthesis

$RuCl_3 \cdot 3H_2O$ (>98 %, Fluka) was used as received. [cis-Ru(bpy)$_2$]Cl_2 and [Ru(bpy)$_2$(H_2bpydc)]Cl_2 were synthesized as previously described.

Ru-PM

$ZrCl_4$ (181 mg, 0.775 mmol) and H_2O (18 µL, 1.0 mmol) were dissolved in 30 mL DMF while stirring. The solution was heated, and benzoic acid (473 mg, 3.87 mmol), H_2bpdc (169 mg, 0.697 mmol) and [Ru(bpy)$_2$(H_2bpydc)]Cl_2 (56 mg, 0.078 mmol) were added. A clear, dark red solution was obtained after a few minutes of stirring. The solution was kept at 95 °C for 4 days.

The solution was decanted off, and a brown crystalline powder was recovered. The powder was then washed 3 times in 15 mL portions of anhydrous DMF and 3 times in 15 mL portions of 2-propanol, before it was dried in air at 60 °C. The dry powder was weighed and stored in a desiccator. The product weight was 300 mg, and the solvent fraction was found to be 37 % by evacuation. Thus the dry product weight was estimated to 188 mg and the final yield to 68 % ($Yield_{max}$: 276 mg).

Adsorption data:

Starting point	23	
End point	40	
Slore	0,0019147	
Intercept	1,2938E-06	
Correlation coefficient	1	
Vm	521,92	[cm^3(STP) g^{-1}]
$a_{s,BET}$	2271,6	[m^2 g^{-1}]
C	1480,9	
Total pore volume (p/p_0=0.990)	0,9332	[cm^3 g^{-1}]
Average pore diameter	1,6433	[nm]

Ru-OP

Note: This was an attempt to make RuCl3-functionalized UiO-67, hence the absence of bpy in the synthesis. If the desired product was achieved, bpy was to be post-synthetically reacted with the already attached Ru atoms.

$ZrCl_4$ (602 mg, 2.58 mmol) and H_2O (61 µL, 3.4 mmol) were dissolved in 100 mL DMF while stirring. The solution was heated, and benzoic acid (1.58 g, 12.9 mmol), H_2bpydc (63 mg, 0.26 mmol), H_2bpdc (563 mg, 2.33 mmol) and $RuCl_3 \cdot xH_2O$ (58 mg, 0.258 mmol) were added. A very dark green solution was obtained immediately after addition of $RuCl_3 \cdot xH_2O$. The solution was kept at 95 °C for 4 days.

The solution was decanted off, and a greenish brown crystalline powder was recovered. The powder was then washed 3 times in 15 mL portions of anhydrous DMF and 3 times in 15 mL portions of 2-propanol, before it was dried in air at 60 °C. The dry powder was weighed and stored in a desiccator. The product weight was 254 mg, and the solvent fraction was found to be 39 % by evacuation. Thus the dry product weight was estimated to 156 mg and the final yield to 17 % ($Yield_{max}$: 921 mg).

Adsorption data:

Starting point	8	
End point	29	
Slore	0,0020737	
Intercept	1,2332E-06	
Correlation coefficient	0,9999	
Vm	481,95	[cm^3(STP) g^{-1}]
$a_{s,BET}$	2097,7	[m^2 g^{-1}]
C	1682,5	
Total pore volume (p/p_0=0.990)	1,2643	[cm^3 g^{-1}]
Average pore diameter	2,4108	[nm]

Ru-PS

300 mg UiO-67-bpy-1 (approximately 0.035 mmol bpy sites with a solvent loading of 42.5 %) was suspended in 15 mL anhydrous DMF in a 50 mL Erlenmeyer flask. [cis-$Ru(bpy)_2$]Cl_2 (24 mg, 0.050 mmol) was added and dissolved under stirring, abruptly changing the color of the solution from colorless to dark red. The suspension was heated to 100 °C and left overnight. A pink-brown powder was recovered, washed 3 times in 15 mL portions of 2-propanol and dried in air at 60 °C.

The dry powder was weighed and stored in a desiccator. The product weight was 206 mg, and the solvent fraction was found to be 26.6 % by evacuation. Thus the dry product weight was estimated to 151 mg and the final yield to 88 % ($Yield_{max}$: 173 mg).

Adsorption data:

Starting point	4	
End point	16	
Slore	0,0020819	
Intercept	7,5718E-07	
Correlation coefficient	1	
Vm	480,17	[cm^3(STP) g^{-1}]
$a_{s,BET}$	2089,9	[m^2 g^{-1}]
C	2750,5	
Total pore volume (p/p_0=0.990)	0,8622	[cm^3 g^{-1}]
Average pore diameter	1,6502	[nm]

Other functionalizations

Other functionalizations were made with the one-pot method, using 10 % molar equivalents of H_2bpydc and functionalization agent in the synthesis in respect to $ZrCl_4$.

$ZrCl_4$ (602 mg, 2.58 mmol) and H_2O (61 µL, 3.4 mmol) were dissolved in 100 mL DMF while stirring. The solution was heated, and benzoic acid (1.58 g, 12.9 mmol), H_2bpydc (63 mg, 0.26 mmol), H_2bpdc (563 mg, 2.33 mmol) and 0.258 mmols of functionalizing salt ($Fe(NO_3)_3 \cdot 9H_2O$, $CoCl_2 \cdot 6H_2O$, $NiCl_2 \cdot 6H_2O$, $RhCl_3 \cdot xH2O$, $Pd(NO_3)_2 \cdot 2H_2O$ and $IrCl_3 \cdot xH_2O$) were added. A clear solution was obtained after a few minutes of stirring. The solution was kept at 95 °C for 4 days.

The salts gave differently colored solutions and products:

Salt	Solution color	Product powder color
$Fe(NO_3)_3 \cdot 9H_2O$	Bleak yellow	White
$CoCl_2 \cdot 6H_2O$	Strong light blue	White
$NiCl_2 \cdot 6H_2O$	Green, turquoise	White
$RhCl_3 \cdot xH2O$	Orange	Orange
$Pd(NO_3)_2 \cdot 2H_2O$	Brownish yellow	Beige
$IrCl_3 \cdot xH_2O$	Deep red brown	Terracotta brown

The solution was decanted off, and a crystalline powder was recovered. The powder was then washed 3 times in 15 mL portions of anhydrous DMF and 3 times in 15 mL portions of 2-propanol, before it was dried in air at 60 °C. The dry powder was weighed and stored in a desiccator.

UiO-67 with 100 % H_2bpydc linker

The material was made with the one-pot method, using 10 % molar equivalents functionalization agent in the synthesis in respect to $ZrCl_4$.

$ZrCl_4$ (602 mg, 2.58 mmol) and H_2O (61 µL, 3.4 mmol) were dissolved in 100 mL DMF while stirring. The solution was heated, and benzoic acid (1.58 g, 12.9 mmol), H_2bpydc (631 mg, 2.58 mmol), and 0.258 mmols of functionalizing salt $CuCl_2 \cdot 2H_2O$, $RuCl_3 \cdot xH_2O$, $IrCl_3 \cdot xH_2O$, K_2PtCl_4 and K_2PtCl_6 were added. A clear solution was obtained after a several minutes of stirring. The solution was kept at 95 °C for 4 days.

Measuret BET surface areas:

Functionalization	**A_{BET}**
Blank, made without modulator	2473 m^2/g
Blank, made with 5 eq benzoic acid	2132 m^2/g
Blank, made with 5 eq acetic acid	2714 m^2/g
K_2PtCl_6, made with 5 eq benzoic acid	1033 m^2/g
$IrCl_3 \cdot xH_2O$, made with 5 eq benzoic acid	1918 m^2/g

UiO-70

After a diffraction pattern had been acquired, the first peak was assumed to be the [1 1 1] reflection, giving a unit cell size parameter of a = 30.19 Å. The structure was optimized using Universal force field[74] (Forcite software), and the diffraction pattern refined using Pawley refinement[75] (Reflex software). The final R_{wp} is 15.83%. This is a good result, considering that other phases were present in the pattern. Taking into account the precursors used, it is very unlikely that this assignment is wrong. Raw outputs of the methods follow here:

Structure:

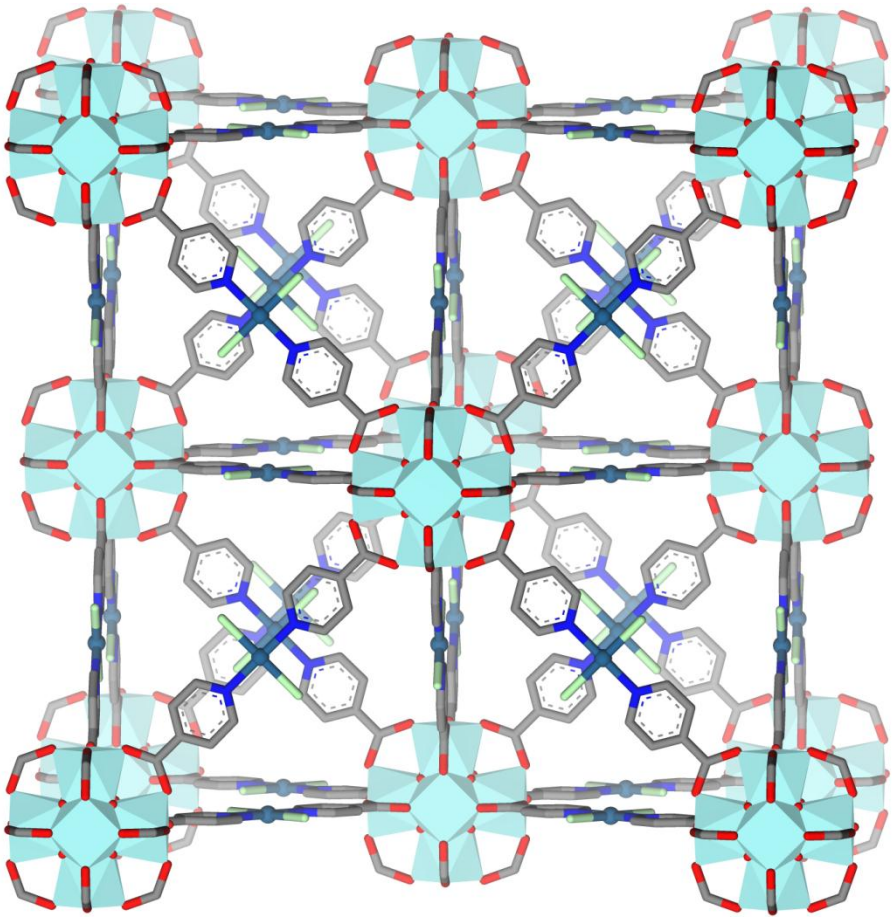

Unit cell parameters:

```
Space group: Fm-3m
a: 30.19 Å
```

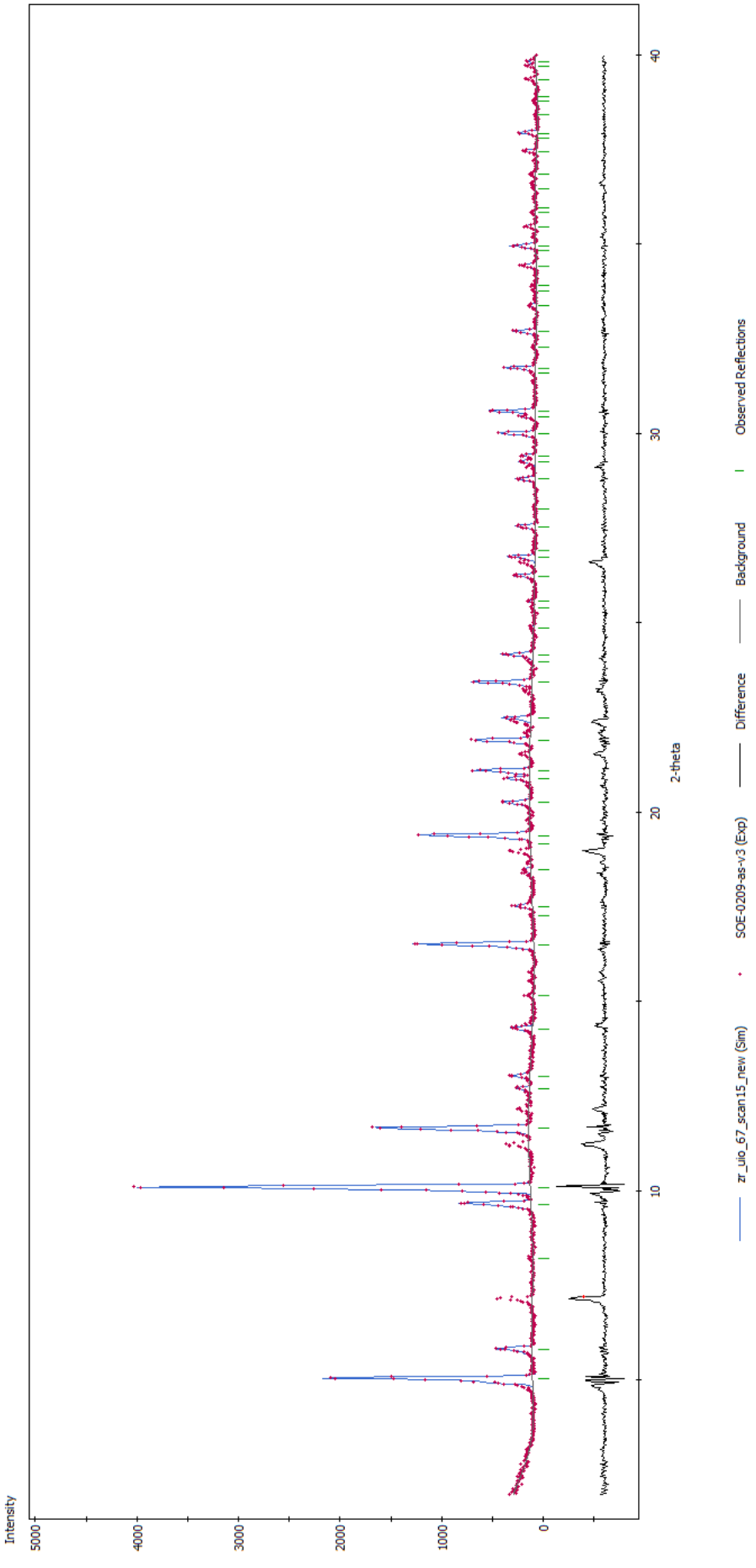

Diffraction pattern of UiO-70 along with refined pattern.

```
Forcite
-------
Task             : Geometry Optimization
Version          : 5.5
Build date       : Mar 22 2011
Host             : PH-3146
Threads          : Scalar
Operating system : Windows
Task started     : Wed Sep 21 13:51:14 2011

---- Geometry optimization parameters ----

Algorithm                       : Smart
Convergence tolerance:
  Energy                        : 0.001 kcal/mol
  Force                         : 0.5 kcal/mol/A
Maximum number of iterations    : 500
External pressure               : 0 GPa
Motion groups rigid             : NO
Optimize cell                   : NO

---- Energy parameters ----

Forcefield                      : Universal
Electrostatic terms:
  Summation method              : Ewald
  Accuracy                      : 0.001 kcal/mol
  Buffer width                  : 0.5 A

van der Waals terms:
  Summation method              : Ewald
  Accuracy                      : 0.001 kcal/mol
  Repulsive cutoff              : 6 A
  Buffer width                  : 0.5 A


---- Initial structure ----

Total enthalpy                  : 49676.231904 kcal/mol
  External pressure term        : 0.000000 kcal/mol
Total energy                    : 49676.231904 kcal/mol

Contributions to total energy (kcal/mol):
  Valence energy (diag. terms)  : 48222.733
    Bond                        :  3658.526
    Angle                       : 44554.832
    Torsion                     :     9.374
    Inversion                   :     0.000
  Valence energy (cross terms)  :     0.000
    Stretch-Stretch             :     0.000
    Stretch-Bend-Stretch        :     0.000
    Stretch-Torsion-Stretch     :     0.000
    Separated-Stretch-Stretch   :     0.000
    Torsion-Stretch             :     0.000
    Bend-Bend                   :     0.000
    Torsion-Bend-Bend           :     0.000
    Bend-Torsion-Bend           :     0.000
  Non-bond energy               :  1453.499
    Hydrogen bond               :     0.000
    van der Waals               :  1453.499
    Electrostatic               :     0.000
    3-Body                      :     0.000

rms force  : 8.614E+001 kcal/mol A
max force  : 3.659E+002 kcal/mol A

Cell parameters:    a:  30.190000 A    b:  30.190000 A    c:  30.190000 A
                alpha:  90.000 deg  beta:  90.000 deg gamma:  90.000 deg

---- Final structure ----
```

```
Total enthalpy                  : 44558.507866 kcal/mol
  External pressure term        : 0.000000 kcal/mol
Total energy                    : 44558.507866 kcal/mol

Contributions to total energy (kcal/mol):
  Valence energy (diag. terms)  : 43372.388
    Bond                        :   320.094
    Angle                       : 43042.919
    Torsion                     :     9.374
    Inversion                   :     0.000
  Valence energy (cross terms)  :     0.000
    Stretch-Stretch             :     0.000
    Stretch-Bend-Stretch        :     0.000
    Stretch-Torsion-Stretch     :     0.000
    Separated-Stretch-Stretch   :     0.000
    Torsion-Stretch             :     0.000
    Bend-Bend                   :     0.000
    Torsion-Bend-Bend           :     0.000
    Bend-Torsion-Bend           :     0.000
  Non-bond energy               :  1186.120
    Hydrogen bond               :     0.000
    van der Waals               :  1186.120
    Electrostatic               :     0.000
    3-Body                      :     0.000

rms force  : 6.824E-002 kcal/mol A
max force  : 1.723E-001 kcal/mol A

Cell parameters:    a:  30.190000 A    b:  30.190000 A    c:  30.190000 A
                alpha:  90.000 deg  beta:  90.000 deg gamma:  90.000 deg



Task terminated               : Wed Sep 21 13:51:19 2011
Total CPU time used by Forcite: 5 seconds (4.51s)

Termination status : Normal
```

MATERIALS STUDIO

Reflex Summary Report for Pawley Refinement of zr_uio_67_scan15_new

Final R_{wp}:	15.83%	Final R_p:	10.71%
Final R_{wp} (without background):	30.76%	Final CMACS:	2.38%

Setup

2θ Range (degrees):	2.00-40.00	Step Size (degrees):	0,021
Experiment:	SOE-0209-as-v3.xcd		
Excluded Regions:	-		
Number of Peaks:	95	Refined:	95

Radiation

Type:	X-ray	Source:	Copper
λ (Å):	1,540562	Monochromator:	None
Anom. Dispersion:	No	Polarization:	0,5

Lattice Parameters

Lattice Type:	Cubic	Space Group:	F 4/M -3 2/M

Parameter	Value	Refined?
a	30,19	No
b	30,19	No
c	30,19	No
α	90	No
β	90	No
γ	90	No

Pattern Parameters

Profile Function:	Gaussian		

FWHM

Parameter	Value	Refined?
U	0.13141 ± *0.01105*	Yes
V	-0.07503 ± *0.00816*	Yes
W	0.01908 ± *0.00065*	Yes

Line Shift

Instrument Geometry:	Bragg-Brentano		

Parameter	Value	Refined?
Zero Point	-0.96326 ± *0.00193*	Yes
Shift #1	0.95032 ± *0.00228*	Yes
Shift #2	-0.22937 ± *0.00412*	Yes

Asymmetry

Correction:	Berar-Baldinozzi	2θ Limit:	90

Parameter	Value	Refined?
P1	-3.70033 ± *0.09625*	Yes
P2	-0.93721 ± *0.02189*	Yes
P3	7.12422 ± *0.19198*	Yes
P4	1.81108 ± *0.04427*	Yes

Sample Parameters

Lattice Strain

Parameter	Value	Refined?
A	0.01101 ± *0.09552*	Yes
B	0.01101 ± *0.09552*	Yes
C	0.01101 ± *0.09552*	Yes

References

(1) Zhao, J.; Shi, D.; Cheng, H.; Chen, L.; Ma, P.; Niu, J. *Inorg. Chem. Commun.* **2010**, *13*, 822.
(2) Rappe, A. K.; Casewit, C. J.; Colwell, K. S.; Goddard, W. A., III; Skiff, W. M. *J. Am. Chem. Soc.* **1992**, *114*, 10024.
(3) Pawley, G. S. *J. Appl. Crystallogr.* **1981**, *14*, 357.